The Effect of Inflammatory Signalling on Sensory Neurone Excitability in the Dorsal Root Ganglia

Rebecca Lily Ellen Pope, MSci (Hons)

School of Life Sciences

University of Nottingham



Thesis submitted for the Degree of

Doctor of Philosophy

September 2025

Abstract

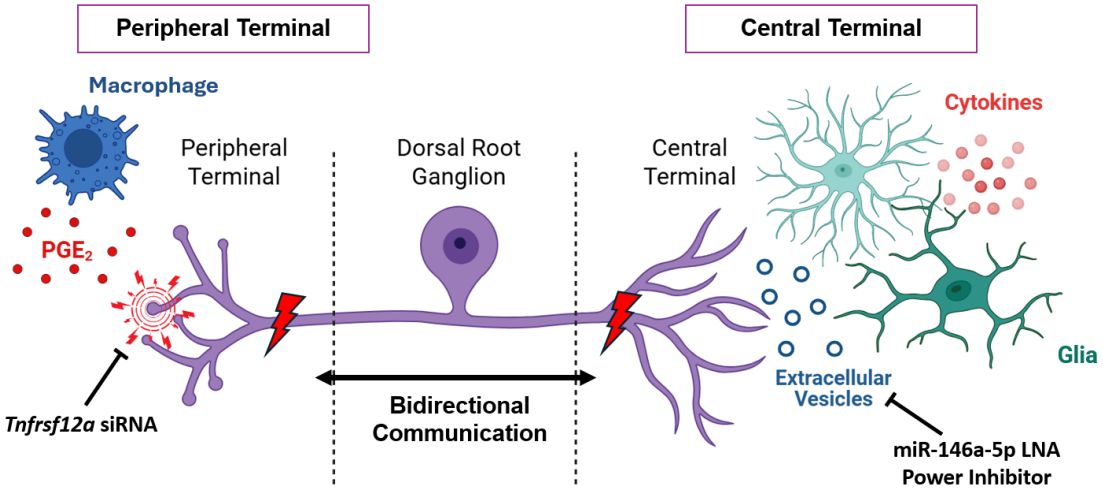
Persistent pain often arises from sensitisation of sensory neurones following injury or inflammation. This process is driven by complex interactions between immune cells, glia, and sensory neurones, yet the molecular mechanisms remain incompletely understood. This thesis explores how inflammatory cues at both the peripheral and central terminals of dorsal root ganglion (DRG) neurones contribute to sensitisation, focusing on the roles of prostaglandin E_2 (PGE_2), extracellular vesicles (EVs), and RNA.

Using compartmentalised microfluidic culture systems, I investigated how PGE_2 induces sensitisation when applied selectively to peripheral axons. Transcriptomic profiling of DRG neurones following PGE_2 stimulation revealed distinct region-specific dysregulation and identified select transcripts, including *Tnfrsf12a*, as novel candidates for the modulation of sensitisation. Functional assays confirmed *Tnfrsf12a*'s involvement in neuronal excitability.

To model the central terminal environment, spinal cord-derived mixed glial cultures were stimulated with pro-inflammatory cytokines, releasing EVs which were found to sensitise DRG neurones. Leveraging current knowledge about EV cargo in relevant model systems, I identified miRNAs reported to be enriched within EVs released by primary glial cells in response to inflammatory stimulation. This highlighted miR-146a-5p, miR-181a-5p and miR-142a-3p as key candidates. Functional experiments revealed that inhibiting miR-146a-5p prevented EV-induced neuronal sensitisation, indicating a causal role. Pathway analysis of predicted miR-146a-5p targets uncovered genes involved in anti-inflammatory processes that may be suppressed by miR-146a-5p.

Overall, this work highlights distinct mechanisms that underlie neuronal sensitisation across anatomically compartmentalised domains and identifies EV-derived

microRNAs as potent modulators of glia-neurone communication. These findings demonstrate how DRG neurones integrate signals within complex spatiotemporal landscapes that depend on local translation, intercellular signalling, and compartment-specific regulation. Together, they provide mechanistic insight into the pathogenesis of sustained pain and suggest new targets for therapeutic intervention.



Dedication

I dedicate this thesis, and the four years of hard work that led to it, to my wonderful Grandma, Frances Johnson. Her infectious fascination with the brain and boundless curiosity were the spark that ignited my passion for neuroscience. Watching lectures and reading New Scientist magazines together laid the foundation for everything I've pursued since. I miss you deeply, I love you dearly, and I wish you could be here to see this moment.

Acknowledgements

Firstly, I am incredibly thankful to Dr Federico Dajas-Bailador and Professor Gareth Hathway for their guidance and advice throughout my research journey. You have both truly helped me become a better, and more resilient, scientist.

I also gratefully acknowledge the Biotechnology and Biological Sciences Research Council's Doctoral Training Programme for funding this research.

I am thankful to Dr Asta Arendt-Tranholm for her contributions to the preliminary data, which laid the foundation for the first half of this thesis, and to Dr Rafael Fort for his expertise in bioinformatics.

I am profoundly grateful to Dr Alex Rathbone, whose wealth of knowledge, technical support, and willingness to act as a sounding board for every new idea greatly enriched this research. My sincere thanks also go to Dr Paula Jackson for introducing me to the lab, making me feel so welcome from the very beginning, and for sharing in my excitement over each new finding.

I would also like to acknowledge the invaluable emotional support, laughs, venting sessions, and encouragement that kept me afloat - especially Gareth Williams, who listened to more PhD-related moaning than anyone deserves - and also my girls Neave Smith, Hiya Deshpande, Dr Orla Canavan, Dr Anya Snary, and Dr Paula Jackson (again!). Their support was essential in sustaining me through the challenges of this work.

I am indebted to my family for their unwavering support at every stage and for always being there for me. I could not have completed this without you.

Finally, I am grateful to the team at Medicines Discovery Catapult, particularly Dr Eve Corrie and Dr Emma Jones, for being such an inspiring and supportive group to work with.

Publications and Commmunications that have derived from this work:

Publications

*Manuscript on BioxRiv encompassing Chapters 3 and 4 (*joint first author):*

Pope, Rebecca L*; Arendt-Tranholm, Asta*; Fort, Rafael Sebastian* et al. (2025). **Conserved Axonal Transcriptome Dynamics Underlie PGE_2-Induced Sensitisation and Identify Tnfrsf12a/Fn14 as a Regulator of Neuronal Excitability in DRG Neurons.**
doi: 10.1101/2025.09.02.673723

Posters and Presentations

- **2nd ISEV International Conference on Extracellular Vesicles in Nervous Systems (2025)**: Inflammatory Glial EVs: Key Mediators of Sensory Neurone Sensitisation.
- **NeuroBio UK (2024)**: Extracellular Vesicles as Drivers of Neuronal Sensitisation in Glia-Neurone Communication Mechanisms.
- **British Pain Society ASM (2024)**: Analysis of Changes in Axonal mRNA Transcriptomes and Activity of DRG Primary Neurones after PGE_2-Driven Sensitisation. **(Published Abstract)**
- **Advanced Pain Discovery Platform (2024)**: Analysis of Changes in Axonal mRNA Transcriptomes and Activity of DRG Primary Neurons After PGE_2-Driven Sensitisation.
- **Axon International Conference (2023)**: Axon-Driven Sensitisation of DRG Neurones Following Localised Exposure to Inflammatory Mediators.
- **British Pain Society ASM (2023)**: Local Processes in Sensory Neurone Sensitisation: Microfluidic Cell Culture Systems. **(Published Abstract and Invited Speaker)**
- **Advanced Pain Discovery Platform (2023)**: Microfluidic Cell Culture System to Investigate Localised Subcellular Processes Underlying Sensory Neurone Sensitisation by PGE_2.
- **UK Society for Extracellular Vesicles (2022)**: Role of Microglia Derived EVs in the Regulation of Sensory Neurone Excitability.

Contents

1 Introduction **1**

1.1 An Introduction to Pain . . . 2
1.2 Chronic Pain Epidemiology . . . 3
1.3 The Somatosensory Nervous System . . . 6
1.3.1 Primary Afferent Fibres . . . 6
1.3.2 Integration into the Spinal Cord . . . 21
1.3.3 Ascending Pathways . . . 22
1.3.4 Descending Control . . . 22
1.4 Acute Inflammation . . . 23
1.5 Chronic Inflammation . . . 24
1.6 Prostaglandin E_2 . . . 25
1.6.1 Knowledge Gaps in the Inflammatory Context . . . 31
1.7 TRPV1 and Capsaicin . . . 33
1.8 Glia-Neurone Communication . . . 36
1.9 *In vitro* Models for Investigating Pain Mechanisms . . . 38
1.9.1 Therapeutic Relevance . . . 41
1.9.2 Embryonic Neuronal Culture . . . 42
1.9.3 Postnatal Neuronal Culture . . . 43
1.9.4 Adult Neuronal Culture . . . 43
1.9.5 Assessing Excitability of *in vitro* Neurones . . . 44
1.10 Scope of the Thesis . . . 46

2 General Materials and Methods **48**

2.1 Animal Husbandry . . . 49
2.2 Dissection to Expose the Dorsal Root Ganglion . . . 49
2.3 Culture of Dorsal Root Ganglia . . . 50
2.3.1 Preparation for Cell Culture . . . 50
2.3.2 Dorsal Root Ganglion Extraction and Cell Dissociation . . . 53
2.3.3 Seeding of Dorsal Root Ganglion Neurones . . . 54
2.4 Calcium Imaging . . . 55
2.4.1 Loading of Calcium Indicator . . . 55

2.4.2 Imaging Protocol . . . 57
2.4.3 Calcium Imaging Analysis . . . 59
2.5 Brightfield Microscopy . . . 63
2.6 Immunocytochemistry . . . 63
2.6.1 Fixing Cells . . . 63
2.6.2 Washes and Incubations Prior to Staining . . . 64
2.6.3 Antibodies . . . 64
2.6.4 Imaging . . . 65
2.7 Statistical Analysis . . . 65

3 Prostaglandin-E_2 Induces Sensitisation of Sensory Neurone Axons and Cell Bodies 67

3.1 Introduction . . . 68
3.1.1 The Utility of *in vitro* Models to Investigate Inflammation . . . 68
3.1.2 Current PGE_2 Knowledge . . . 69
3.1.3 Unanswered Questions in PGE_2 Signalling . . . 70
3.1.4 Aims and Hypotheses . . . 71
3.2 Methods . . . 71
3.2.1 *In vitro* Neuronal Culture . . . 71
3.2.2 PGE_2 Treatment . . . 72
3.2.3 Calcium Imaging . . . 74
3.2.4 Immunocytochemistry . . . 75
3.2.5 Statistical Analysis . . . 75
3.3 Results . . . 76
3.3.1 Establishment of *in vitro* Models for Sensory Neurone Studies . . . 76
3.3.2 Stimulus Addition Generates Minimal Mechanical Pressure Activation 80
3.3.3 PGE_2 Incubation as a Model of Neuronal Sensitisation . . . 81
3.3.4 Axonal Incubation with PGE_2 Can Induce the Sensitisation of DRG Neurones . . . 82
3.3.5 PGE_2 Treatment Did Not Alter the Size Distribution of Axonal Capsaicin Respondents . . . 85
3.3.6 PGE_2's Effects on Neuronal Excitability Are Nociceptive Neurone-Specific . . . 88
3.3.7 PGE_2 Also Induces the Sensitisation of DRG Cell Bodies . . . 91
3.3.8 PGE_2 Treatment Did Not Alter the Size Distribution of Somal Capsaicin Respondents . . . 93
3.3.9 Overview of Sequential Axonal and Somal Stimulations . . . 95
3.3.10 EP_4 Receptors Were Upregulated in PGE_2-Treated Sensory Neurones 96
3.4 Discussion . . . 97
3.4.1 Summary of Key Findings . . . 97
3.4.2 Acute versus Prolonged Exposure in Inflammatory Models . . . 98
3.4.3 PGE_2-Induced Neuronal Sensitisation is Nociceptive Neurone-Specific 99

3.4.4 Constraints of Calcium Imaging . . . 102
3.4.5 EP_4 Mediates PGE_2-Induced Neuronal Sensitisation . . . 105
3.4.6 Retrograde Communication: A Novel Insight into PGE_2 Mechanisms 107
3.4.7 Chapter Conclusions . . . 110

4 *Tnfrsf12a* is Involved in Neuronal Excitability 112
4.1 Introduction . . . 113
4.1.1 The TWEAK receptor . . . 114
4.1.2 Uncovering RNA Dynamics Through Transcriptomics in the Nervous System . . . 115
4.1.3 Local Translation of mRNA . . . 116
4.1.4 Local Control of Excitability Through Spatially Restricted Gene Expression . . . 116
4.1.5 Aims and Hypotheses . . . 117
4.2 Methods . . . 118
4.2.1 DRG Neuronal Culture . . . 118
4.2.2 PGE_2 Treatment . . . 119
4.2.3 Transcript Knockdown Using siRNA . . . 119
4.2.4 RNA Extraction . . . 121
4.2.5 cDNA Synthesis . . . 122
4.2.6 Real-Time Quantitative-PCR . . . 123
4.2.7 Analysis of qPCR Data . . . 124
4.2.8 Transcriptomics and qPCR Validation - Methodological Comparison with Collaborator . . . 125
4.2.9 Bioinformatics and RNA Sequencing (RNA-Seq) . . . 126
4.2.10 Calcium Imaging . . . 128
4.2.11 Statistical Analysis . . . 129
4.3 Results . . . 130
4.3.1 Transcriptomic Changes in Subcellular Neuronal Compartments . . . 130
4.3.2 Transcripts are Differentially Regulated in the Axon Versus Soma Following PGE_2 Treatment. . . . 133
4.3.3 Pathway Analysis Reveals *Tnfrsf12a* is Involved in Multiple Processes 137
4.3.4 qPCR Confirms Effective *Tnfrsf12a* Transcript Silencing with siRNA . 138
4.3.5 Knockdown of *Tnfrsf12a* Lowers Sensory Neurone Excitation in Dissociated Cultures . . . 139
4.3.6 Targeted Axonal Knockdown of *Tnfrsf12a* Dampens Sensory Neurone Activity . . . 142
4.4 Discussion . . . 144
4.4.1 Summary of Key Findings . . . 144
4.4.2 siRNA Targeting *Tnfrsf12a* Reduced mRNA Levels . . . 145
4.4.3 *Tnfrsf12a*'s Effects were More Robust in Dissociated Cultures . . . 147
4.4.4 *Tnfrsf12a* and Pain . . . 148

4.4.5 *Tnfrsf12a* is Translated Locally in the Axon to Mediate Neuronal Inflammation and Sensitisation . . . 151
4.4.6 Developmental Conservation of TNFRSF12A-Mediated Sensitisation in Sensory Neurones . . . 155
4.4.7 Chapter Conclusions . . . 155

5 Glial-Derived Extracellular Vesicles Induce Neuronal Sensitisation via miR-146a-5p 158
5.1 Introduction . . . 159
5.1.1 Glial Modulation of Sensory Neurone Sensitisation . . . 159
5.1.2 Glial Extracellular Vesicles in Pain and Sensory Neurone Sensitisation 161
5.1.3 Recapitulating Reactive Glial States *in vitro* . . . 163
5.1.4 Characterisation of Extracellular Vesicles . . . 165
5.1.5 The Role of miRNAs in Glia-Neurone Bidirectional Communication . 166
5.1.6 Aims and Hypotheses . . . 168
5.2 Methods . . . 169
5.2.1 DRG Neuronal Culture . . . 169
5.2.2 Mixed Glial Culture . . . 169
5.2.3 Mixed Glial Culture Optimisation . . . 173
5.2.4 Brightfield Microscopy . . . 177
5.2.5 Immunocytochemistry . . . 177
5.2.6 Pro-inflammatory Stimulation with a Cytokine Cocktail . . . 178
5.2.7 Cell Lysate Collection . . . 179
5.2.8 Extracellular Vesicle Isolation . . . 180
5.2.9 Nanoparticle Tracking Analysis . . . 181
5.2.10 SDS-PAGE Gels to Determine Protein Elution Fractions . . . 182
5.2.11 Western Blotting to Identify Extracellular Vesicle Markers . . . 184
5.2.12 Application of Glial-Derived Extracellular Vesicles to DRG Neuronal Cultures . . . 185
5.2.13 Calcium Imaging in Microfluidic Chambers . . . 185
5.2.14 miRNA Power Inhibitors . . . 186
5.2.15 Pathway Enrichment Analysis . . . 188
5.2.16 Statistical Analysis . . . 189
5.3 Results . . . 189
5.3.1 Glial Cell Populations Are Heterogeneous . . . 189
5.3.2 Determination of Protein Fractions Following Size Exclusion Chromatography . . . 196
5.3.3 Extracellular Vesicle Concentrations Determined by Nanoparticle Tracking Analysis . . . 197
5.3.4 EV Markers Detected by Western Blot . . . 198
5.3.5 Functional Effects of Glial-Derived Extracellular Vesicles on Neuronal Sensitisation . . . 200

5.3.6 EV Functional Cargoes: Searching for miRNAs . . . 203
5.3.7 miR-142-3p is Not Involved in Sensory Neurone Sensitisation via Glial-Derived Extracellular Vesicles . . . 206
5.3.8 miR-181a-5p is Not Involved in Sensory Neurone Sensitisation via Glial-Derived Extracellular Vesicles . . . 208
5.3.9 miR-146a-5p Contributes to Sensory Neurone Sensitisation via Glial-Derived Extracellular Vesicles . . . 209
5.3.10 Downstream Targets of miR-146a-5p Differ Between Mouse and Human . . . 211
5.3.11 Gene Set Enrichment Analysis Identified Downstream Gene Targets Associated with Neurotransmission . . . 213
5.4 Discussion . . . 214
5.4.1 Summary of Key Findings . . . 214
5.4.2 Glia-Neurone Communication via EVs in Neuroinflammation . . . 214
5.4.3 Extracellular Vesicle Uptake and Characterisation . . . 216
5.4.4 miRNA-Mediated Sensitisation . . . 219
5.4.5 miR-146a-5p as a Central Mediator of Glial EV-Induced Sensitisation 220
5.4.6 Regulation of Neurotransmission-Associated Genes by miR-146a-5p 225
5.4.7 Select Downstream Targets of miR-146a-5p Are Involved in Anti-Inflammatory Processes and Decrease Neuronal Excitability . . . 226
5.4.8 Interspecies Variation . . . 228
5.4.9 Conclusions . . . 229

6 General Discussion and Future Work 231
6.1 Compartmentalised Mechanisms of Pain Sensitisation . . . 232
6.2 Spatially Distinct Transcriptomic Responses to PGE_2 . . . 233
6.3 Glial-Derived EVs Contribute to Central Terminal Sensitisation . . . 236
6.4 Considerations for Future Experimental Design . . . 238
6.4.1 Primary Neurone Cultures . . . 239
6.4.2 Embryonic Cultures . . . 239
6.4.3 Compartmentalised Microfluidic Cultures . . . 239
6.4.4 Calcium Imaging as a Functional Readout . . . 240
6.4.5 Retrograde vs Anterograde Signalling and Terminal Modelling . . . 241
6.5 Future Directions . . . 241
6.6 Thesis Conclusions . . . 244

7 Appendix 247

Figures

1.1 A Simplified Diagram of the Pain Pathway. 7
1.2 Sensory Neurone Structure. 8
1.3 Neuronal Action Potential. 11
1.4 Canonical miRNA Biogenesis and Gene Silencing Pathway. 17
1.5 Mechanism of siRNA-Mediated Gene Silencing. 19
1.6 Extracellular Vesicle Release and Uptake. 21
1.7 Synthesis Pathway of PGE_2. 26
1.8 The Interaction of PGE_2 at the Peripheral Terminal of the Sensory Neurone. 27
1.9 PGE_2 Mechanism of Action in Neurones. 28
1.10 Overview of the Action of PGE_2 Once Bound to a Sensory Neurone. 31
1.11 Calcium Imaging Mechanism. 45

2.1 Compartmentalised Microfluidic Chamber. 51
2.2 Boyden Chambers Were Used to Isolate Subcellular Compartments for RNA Extraction. 52
2.3 Calcium Imaging Dye Loading Protocol. 57
2.4 Calcium Imaging Methodology in Dissociated Cultures Versus Compartmentalised Microfluidic Chambers. 59
2.5 Calcium Imaging Analysis Step-by-Step Methodology. 62

3.1 Sensory Neurone Culture Methodologies. 73
3.2 Calcium Imaging Protocol for PGE_2 Sensitisation Experiments. 74
3.3 DRG Neurone Growth in Dissociated Culture. 77
3.4 Extent of Axon Growth Through Microgrooves into the Soma Compartment. 78
3.5 Brightfield Image of Dorsal Root Ganglion Neurones Cultured in Boyden Chambers. 79
3.6 Axons Grew Extensively from Explants in Culture. 80
3.7 Mechanical Flow Induced Smaller Calcium Transients Compared to Chemical Stimulation. 81
3.8 Calcium Response to 200 nM Capsaicin Stimulation of Dissociated Sensory Neurones Following PGE_2 Pre-Treatment. 82

3.9 Calcium Response to 100 nM Capsaicin Stimulation of Axon Terminals Following PGE_2 Pre-Treatment. . . . 83
3.10 Calcium Response to 200 nM Capsaicin Stimulation of Axon Terminals Following PGE_2 Pre-Treatment. . . . 84
3.11 Diameter Distribution of Cell Bodies Responding to Axonal Capsaicin Stimulation in Compartmentalised Microfluidic Chambers. . . . 87
3.12 Calcium Response to KCl Stimulation of Axons Following PGE_2 Pre-Treatment of Axon Terminals. . . . 89
3.13 Soma Diameter Distribution of DRG Neurones Responding to KCl Following PGE_2 Pre-Treatment of Axon Terminals. . . . 90
3.14 Calcium Response to 100 nM Capsaicin Stimulation of Somata Following PGE_2 Pre-Treatment of Axon Terminals. . . . 92
3.15 Calcium Response to 200 nM Capsaicin Stimulation of Axon Terminals Following PGE_2 Pre-Treatment. . . . 93
3.16 Diameter Distribution of Cell Bodies Responding to Somal Capsaicin Stimulation in Compartmentalised Microfluidic Chambers. . . . 95
3.17 Temporal Profile of DRG Neurone Responses to Axonal and Somal Stimuli. 96
3.18 EP_4 Expression was Increased in PGE_2-Treated Sensory Neurones. . . . 97
3.19 PGE_2-Induced Neuronal Sensitisation via Potentiation of TRPV1. . . . 102

4.1 PGE_2 Applied to the Axonal Terminal Sensitises Sensory Neurones. . . . 115
4.2 Protocol for PGE_2 Treatment in Boyden Chambers. . . . 119
4.3 siRNA Incubation Timeline. . . . 121
4.4 Calcium Imaging Stimulation Protocol. . . . 129
4.5 Analysis of Neurite Gene Expression in the Axon and Soma Compartments of E16.5 DRG Neurones. . . . 132
4.6 Transcriptomic Response to PGE_2 in Axonal and Somal Compartments of E16.5 DRG Neurones. . . . 134
4.7 Volcano Plot Demonstrating Transcriptomic Response to PGE_2 in Axonal and Somal Compartments of E16.5 DRG Neurones. . . . 135
4.8 Compartment-Specific Gene Ontology Enrichment Analysis of PGE_2-Stimulated E16.5 DRG Neurones. . . . 136
4.9 Cnetplot of Gene Ontology Biological Process Terms Associated with *Tnfrsf12a*. . . . 137
4.10 *Tnfrsf12a* Expression Exhibited a Progressive Decrease Following siRNA Treatment. . . . 139
4.11 Silencing *Tnfrsf12a* in Dissociated Cultures Reduced Neuronal Excitation. . 141
4.12 Silencing of *Tnfrsf12a* Specifically at the Sensory Neurone Axon Terminal Reduced Neuronal Excitability. . . . 143
4.13 Silencing of *Tnfrsf12a* at the Sensory Neurone Axon Terminal Showed a Trend to Reduce Neuronal Sensitisation. . . . 144

4.14 Silencing of *Tnfrsf12a* Specifically at the Sensory Neurone Axon Terminal Reduced Neuronal Excitability. 153

5.1 Bidirectional Communication Between Glia and Sensory Neurones via Extracellular Vesicles. 161
5.2 Protocol for the Culture of Mixed Glia from Embryonic Murine Spinal Cords. 171
5.3 Schematic for Glial Culture in Preparation for Co-Culture with DRG Sensory Neurones. 172
5.4 Schematic of DRG Addition for Co-Culture with Glia. 173
5.5 Brightfield Images of Microglia Isolated from Mixed Glial Culture. 175
5.6 Mixed Glial Culture Timeline. 179
5.7 Timeline of Extracellular Vesicle Addition to DRG Sensory Neurone Cultures. 185
5.8 Calcium Imaging Stimulation Protocol for Inverted Chambers. 186
5.9 Protocol for miRNA Inhibitor-EV Addition to DRG Cultures. 188
5.10 Different Glial Cell Growth Patterns Coexist in the Same Culture. 191
5.11 Immunocytochemistry of Mixed Glial Cultures Stained for Astrocytes and Microglia. 192
5.12 Quantification of $GFAP^+$ and $Iba1^+$ Cells. 193
5.13 Morphological Comparison of Control versus Cytokine-Treated Mixed Glial Cultures. 194
5.14 Representative Brightfield Images of Mixed Glia-DRG Co-Cultures. 195
5.15 Immunocytochemistry of Mixed Glia-DRG Co-Cultures. 196
5.16 SDS-PAGE Gels of Fractions Isolated by Size Exclusion Chromatography from Mixed Glia Cell Culture Medium. 197
5.17 Average Size Distribution of Particles Normalised to Cell Count. 198
5.18 Western Blot Analysis of EV Markers Across Fractions from Size Exclusion Chromatography, Concentrated Pooled Fractions, Flow-Through, and Whole-Cell Lysate. 199
5.19 Extracellular Vesicles, Derived from Glia Stimulated with Pro-Inflammatory Cytokines, Sensitised DRG Sensory Neurones. 201
5.20 Extracellular Vesicles from Activated Glia Drive Enhanced DRG Sensitisation Relative to Cytokine Exposure Alone. 202
5.21 Venn Diagram of Dysregulated miRNA Transcripts Within Extracellular Vesicles Derived from Primary Glial Cultures Following Pro-Inflammatory Treatments in the Literature. 203
5.22 Inhibition of miR-142a-3p Does Not Affect the Glial EV-Induced Sensory Neurone Sensitisation. 207
5.23 Inhibition of miR-181a-5p Does Not Affect the Glial EV-Induced Sensory Neurone Sensitisation. 209
5.24 Inhibition of miR-146a-5p Prevented the Glial EV-Induced Sensory Neurone Sensitisation. 210
5.25 The Central Terminal Mechanism of Glial EV-Induced Neuronal Sensitisation. 221

6.1 Bidirectional Modulation of Sensory Neurone Sensitisation via Peripheral and Central Terminals. 245

A1 Controls Lacking Primary Antibody for Immunocytochemistry of Mixed Glial Cultures. 249

A2 miRNAs Added Alone Did Not Affect Neuronal Excitability. 250

Tables

1.1 Estimated Sensory Neurone Subtype Identity by Soma Diameter at E16.5 in the Mouse DRG. . . . 10
1.2 EP Receptor Signalling and Role in Pain . . . 29

2.1 The Variations in DRG Seeding Protocols in Different Culture Formats. . . . 55
2.2 Primary Antibodies. . . . 65
2.3 General Secondary Antibodies. . . . 65

4.1 RNA Annealing Mix Reagents. . . . 123
4.2 Thermal Cycling Conditions for qPCR on the QuantStudio 5 Plate Reader. . . 124

5.1 Optimisation of Mixed Glial Culture. . . . 176
5.2 Composition of Resolving and Stacking Gels for SDS-PAGE. . . . 183
5.3 Antibodies Used for Western Blotting. . . . 184
5.4 Dysregulated miRNAs Identified in a Literature Search and their Known Functions. . . . 204
5.5 The Top 10 Genes Predicted to be Targeted by miR-146a-5p in Mouse Compared to Human. . . . 212
5.6 The Remaining Three Gene Targets of miR-146a-5p From the Top 10 In Humans. . . . 212
5.7 Biological Processes Predicted to be Targeted by miR-146a-5p. . . . 213

A1 siRNA Sequences Used for Knockdown. . . . 248
A2 Primers Used for Quantitative Real-Time PCR. . . . 248
A3 Primers Used for qPCR Validation of Transcriptomic Targets. . . . 248
A4 miRNA Power Inhibitor Sequences. . . . 249
A5 Expanded Biological Process Enrichment for miR-146a-5p Targets (Including Reference and Expected Counts). . . . 251

List of Abbreviations

AA	Arachidonic Acid
AGO2	Argonaute 2
ALIX	ALG-2-Interacting Protein X
ALS	Amyotrophic Lateral Sclerosis
AM	Acetoxymethyl
AMO	Anti-miRNA Oligonucleotide
APH	Aphidicolin
APS	Ammonium Persulfate
ATP	Adenosine Triphosphate
BBB	Blood-Brain Barrier
BSA	Bovine Serum Albumin
bp	Base Pairs
C1q	Complement Component 1q
cAMP	Cyclic Adenosine Monophosphate
$Ca_V3.2$	Voltage-Gated T-type Ca^{2+} Channel
CD11b	Cluster of Differentiation 11b
CGRP	Calcitonin Gene-Related Peptide
CNS	Central Nervous System
CNX	Calnexin
CTL	Control
CREB	cAMP Response Element-Binding Protein
CytoG EVs	EVs Derived From Cytokine-Treated Glia
DAPI	4',6-diamidino-2-phenylindole
dH_2O	Distilled Water
DIV	Day *in vitro*
DPBS	Dulbecco's Phosphate Buffered Saline
DRG	Dorsal Root Ganglion
DTT	Dithiothreitol

E16.5	Embryonic Day 16.5
ECL	Enhanced Chemiluminescence
ER	Endoplasmic Reticulum
ERK	Extracellular Signal-Regulated Kinase
EV	Extracellular Vesicle
EV CTL	Extracellular Vesicle Control
F	Fluorescence
FBS	Foetal Bovine Serum
FDR	False Discovery Rate
FLOT1	Flotillin-1
Fn14	Fibroblast Growth Factor-Inducible-14
FOV	Field of View
Fr	Fraction
GAB	Gel Application Buffer
GAPDH	Glyceraldehyde-3-Phosphate Dehydrogenase
GDNF	Glial-Derived Neurotrophic Factor
GDP	Guanosine Diphosphate
GO	Gene Ontology
GPCR	G-Protein Coupled Receptor
GSEA	Gene Set Enrichment Analysis
GTP	Guanosine Triphosphate
HBSS	Hank's Balanced Salt Solution
HCN	Hyperpolarisation-Activated Cyclic Nucleotide-Gated Channels
HK	Housekeeper
hsa	Homo sapien
IASP	The International Association for the Study of Pain
IB	Imaging Buffer
IB4	Isolectin B4

Iba1	Ionised Calcium-Binding Adapter Molecule 1
IL-1α	Interleukin-1α
IL-1β	Interleukin-1β
IP_3	Inositol Triphosphate
iPSC	Induced Pluripotent Stem Cells
K_{Ca}	Calcium-Activated Potassium Channel
KCC2	Potassium-Chloride Cotransporter 2
KCl	Potassium Chloride
L-15	Leibovitz L-15 Medium
LNA	Locked Nucleic Acid
MAPK	Mitogen-Activated Protein Kinase
MEA	Microelectrode Array
MFC	Microfluidic Chamber
miRNA	Micro Ribonucleic Acid
MISEV	Minimal Information for Studies of Extracellular Vesicles
mmu	Mus musculus
mRNA	Messenger Ribonucleic Acid
MVE	Multivesicular Endosome
MWCO	Molecular Weight Cut-Off
Na^+/K^+-ATPase	Sodium-Potassium Pump
NC	Negative Control
NF-κB	Nuclear Factor Kappa-Light-Chain-Enhancer of Activated B cells
NGF	Nerve Growth Factor
NICE	The National Institute for Health and Care Excellence
NKCC1	Sodium Potassium Chloride Cotransporter 1
NSAIDs	Non-Steroidal Anti-Inflammatory Drugs
NTA	Nanoparticle Tracking Analysis
Nunc	Nunclon™

OPC	Oligodendrocyte Progenitor Cell
$P2X_3$	P2X Purinoceptor 3
PAF	Primary Afferent Fibre
PAG	Periaqueductal Grey
PDL	Poly-D-Lysine
PDMS	Polydimethylsiloxane
PES	Polyethersulfone
PGE_2	Prostaglandin E_2
PI-PLC	Phosphoinositol-Phospholipase C
PIPS	Professional Internships for PhD Students
PKA	Protein Kinase A
PKC	Protein Kinase C
PLL	Poly-L-Lysine
PNS	Peripheral Nervous System
PT	Phosphorothioate
RAi	Ribonucleic Acid of Interest
RFU	Relative Fluorescent Units
RINs	RNA Integrity Numbers
RISC	RNA-Induced Silencing Complex
RNA	Ribonucleic Acid
RNAi	Ribonucleic Acid Interference
RNA-Seq	Ribonucleic Acid Sequencing
ROI	Region of Interest
rRNA	Ribosomal Ribonucleic Acid
RT	Room Temperature
RT-qPCR	Real-Time Quantitative Polymerase Chain Reaction
RVM	Rostral Ventral Medulla
sAHP	Slow Afterhyperpolarisation
SDS	Sodium Dodecyl Sulfate

SDS-PAGE	Sodium Dodecyl Sulfate-Polyacrylamide Gel Electrophoresis
SEC	Size Exclusion Chromatography
SGCs	Satellite Glial Cells
SHH	Sonic Hedgehog
siRNA	Small Interfering Ribonucleic Acid
SNL	Spinal Nerve Ligation
SSIV	SuperScript IV Reverse Transcriptase
STAT3	Signal Transducer and Activator of Transcription 3
STDEV	Standard Deviation
TEM	Transmission Electron Microscopy
TEMED	Tetramethylethylenediamine
TGS	Tris-Glycine-SDS
TLR	Toll-Like Receptor
TNF-α	Tumour Necrosis Factor-α
TNFRSF12A	Tumour Necrosis Factor Receptor Superfamily Member 12A
TMM	Trimmed Mean of M-Values
TrkA	Tropomyosin Receptor Kinase A
TRP	Transient Receptor Potential
TRPV1	Transient Receptor Potential Vanilloid-1
TWEAK	Tumour Necrosis Factor-Like Weak Inducer of Apoptosis
TWEAKR	Tumour Necrosis Factor-Like Weak Inducer of Apoptosis Receptor
UBE2	Ubiquitin-Conjugating Enzyme 2
UTC	Untreated Control
UTR	Untranslated Region
VGSC	Voltage-Gated Sodium Channel

Chapter 1

Introduction

1.1 An Introduction to Pain

Acute pain is an essential survival signal, as part of the body's protective mechanisms; hence, pain is highly conserved throughout evolution, from simple organisms, such as the nematode, through to *Drosophila* and to humans (Walters and Williams, 2019). Possessing both sensory and emotional aspects, pain is defined by The International Association for the Study of Pain (IASP) as "an unpleasant sensory and emotional experience associated with, or resembling that associated with, actual or potential tissue damage" (Raja et al., 2020).

Pain perception is an intricate, whole-body phenomenon, involving not only the peripheral and central nervous systems (PNS and CNS) but also contributions from the immune system and gut microbiome (Guo et al., 2019). The perception of pain can be divided into the sensory component, also referred to as nociception - "the neural process of encoding noxious stimuli" (Raja et al., 2020) - and the affective component, which represents our conscious awareness of the pain's unpleasantness. This emotional aspect shapes how we experience pain and drives protective behaviours. As such, pain is inherently subjective and personalised, influenced by an individual's life history; particularly experiences of early-life injury (Schwaller and Fitzgerald, 2014). It is this subjectivity that makes pain so challenging to treat.

While human studies are essential to understanding the full complexity of pain, preclinical research focuses on nociception which allows researchers to interrogate intracellular and intercellular mechanisms underlying neuronal excitability. There are several advantages to studying cellular models rather than whole animals, including reduced cost, lower ethical concerns, and greater experimental control. This makes cellular models particularly useful for high-throughput research, enabling the testing of multiple conditions and treatments in a controlled environment (Chrysostomidou, Cooper, and Weir, 2021).

Importantly, cellular systems, such as primary sensory neurone cultures and co-cultures with glia or other immune cells, can recapitulate key aspects of the nociceptive microenvironment, offering a reductionist system that is highly amenable to cellular and molecular manipulation, and therefore provides a powerful platform for dissecting pain mechanisms (Chrysostomidou, Cooper, and Weir, 2021). In the field of pain research, where plasticity and sensitisation involve tightly regulated, cell-specific interactions, these models provide a powerful means to link molecular perturbations with functional outcomes, such as changes in excitability or synaptic transmission (Bayat et al., 2021; Kimourtzis et al., 2024; Wang et al., 2021). Thus, cellular models not only complement *in vivo* approaches but also offer critical mechanistic insight that informs translational strategies and target validation.

1.2 Chronic Pain Epidemiology

When the mechanisms involved in sensory processing become dysregulated, acute pain may transition into a chronic pain state, persisting long after tissue healing has resolved. Chronic pain, clinically defined as pain lasting longer than three months, is maladaptive and severely impacts patients with conditions such as inflammatory diseases, neuropathic pain, and cancer (Treede et al., 2015). IASP has classified chronic pain conditions into seven categories, which include chronic primary pain, chronic cancer-related pain, chronic post-surgical or post-traumatic pain, and chronic neuropathic pain. These persistent pain conditions can arise from a variety of aetiologies, including inflammation or tissue damage, nervous system dysfunction (neuropathic pain), or idiopathically, such as with fibromyalgia (Treede et al., 2015).

An estimated 30% of the global population lives with chronic pain (Redpath et al., 2023), with prevalence varying widely between countries (Zimmer et al., 2022). In the UK, a 2017 NHS Digital survey reported that 34% of adults were living with chronic pain, with a higher prevalence among women (38%) than men (30%) (NHS Digital, 2017). The Global Burden of Disease Study 2013 identified chronic low

back pain as the principal source of years lived with disabilities, alongside other chronic conditions including osteoarthritis, migraine, chronic neck pain, and medication overuse headache (Rice, Smith, and Blyth, 2016). Despite its widespread impact, chronic pain is not immediately life threatening. Yet, its persistent nature can severely compromise quality of life and daily functioning (Redpath et al., 2023), while also imposing a heavy financial burden on healthcare systems and economies, contributing to lost productivity (Brewer and Baccei, 2020). For these reasons, many argue that chronic pain should be classed as a disease with its own clinical course (Goldberg and McGee, 2011; Raffaeli and Arnaudo, 2017), but this remains a contentious issue.

Chronic pain manifests in several forms, including hyperalgesia (an abnormally heightened sensitivity to painful stimuli), allodynia (pain in response to normally innocuous stimuli), and spontaneous pain. The mechanisms underlying these symptoms remain poorly understood, but both the PNS and CNS are implicated. In particular, dorsal root ganglion (DRG) neurones, which reside in the peripheral nervous system and project centrally into the spinal cord, become sensitised following peripheral injury. This process is believed to drive CNS changes and contribute to the transition from acute to chronic pain (St-Jacques and Ma, 2014).

For several decades, opioids such as morphine, have remained the gold-standard analgesics for treating acute and chronic pain, despite often providing only moderate to negligible improvement in pain relief in chronic pain patients, necessitating repeated dose escalation due to the development of opioid tolerance (Baron and McDonald, 2006). Their use is further hindered by debilitating, centrally mediated side-effects, including constipation, respiratory depression, nausea, opioid-induced hyperalgesia, and the potential for addiction (Mercadante, Arcuri, and Santoni, 2019; Reisine and Pasternak, 1996). Increasing opioid dosages to counteract tolerance can also induce or worsen opioid-induced hyperalgesia - a paradoxical pain hypersensitivity observed in both rodent models (Li, Angst, and Clark, 2001)

and patients undergoing opioid detoxification (Baron and McDonald, 2006). This phenomenon may further contribute to analgesic tolerance and is sometimes misdiagnosed as disease progression (Mercadante, Arcuri, and Santoni, 2019). The National Institute for Health and Care Excellence (NICE) no longer recommends the use of opioids, paracetamol, benzodiazepines, or non-steroidal anti-inflammatory drugs (NSAIDs) for treating chronic primary pain, citing a lack of evidence for their effectiveness and concerns over potential harm (NICE, 2021). Despite this, nearly a quarter of individuals with chronic pain in the UK are currently prescribed opioids (Clegg and Hughes, 2022).

Given these limitations, there is an urgent need to replace current analgesics with more effective pain management strategies. Despite promising results in preclinical models, many novel compounds have failed to meet clinical endpoints due to insufficient efficacy or unacceptable side-effects. Consequently, pharmaceutical companies have shown decreasing interest in developing new pain therapeutics (Colvin, Bull, and Hales, 2019).

To address this challenge, novel approaches are being explored, including the use of ribonucleic acid (RNA)-based technologies such as small interfering RNAs (siRNAs) and microRNA (miRNA) modulators, such as inhibitors and mimics. These tools enable the selective silencing or modulation of gene expression in pain-relevant pathways, often offering increased specificity compared to conventional small molecules. For example, siRNAs can be designed to inhibit the production of key ion channels or inflammatory mediators implicated in chronic pain (Kaur and Sharma, 2012; Luo et al., 2024), while miRNAs - either mimics or inhibitors - can be used to fine-tune complex regulatory networks involved in neuronal excitability and neuroinflammation (Ikuma et al., 2023; Zhang et al., 2023). Coupled with advances in targeted delivery systems, these RNA-based strategies hold promise for generating a new class of precision analgesics that address the underlying mechanisms of pain, rather than merely masking symptoms.

To improve chronic pain management, researchers must focus on understanding the intricate mechanisms driving pain initiation, the transition from acute to chronic pain, and the maintenance of a hypersensitive state. This requires investigating the pain pathway at multiple levels, from isolated *in vitro* models - examining the roles of dorsal root ganglion neurones and glial cells - to whole-animal *in vivo* studies that capture system-wide interactions (Berta et al., 2017). The shift toward mechanism-based, gene-targeted therapeutics represents a transformative direction for pain research and could reinvigorate innovation in a field that has long struggled with translational bottlenecks.

1.3 The Somatosensory Nervous System

The somatosensory nervous system is a highly integrative system, responsible for detecting, transducing, and transmitting information about external and internal stimuli (Yam et al., 2018). In the context of pain, noxious stimuli activate peripheral receptors, triggering electrical signals that travel along nociceptive primary afferent fibres (PAFs) to the spinal cord within the CNS. These signals are then relayed via ascending pathways to higher-order brain regions, including the somatosensory cortex, where pain perception occurs (Figure 1.1; Webb and Steeds, 2022).

1.3.1 Primary Afferent Fibres

PAFs - formed by sensory neurones (DRG neurones) - are the first-order neurones in the pain signalling pathway and play a crucial role in detecting noxious and innocuous stimuli. Their cell somata reside within the DRG, a structure that contains up to 15,000 neurones at limb-innervating segmental levels. Axons of these neurones fasciculate into roots, or nerves, containing fibres with varied functions and excitabilities (Esposito et al., 2019).

DRG neurones exhibit a distinctive pseudounipolar morphology, with a single axon that bifurcates into two processes: a peripheral (distal) branch that innervates tis-

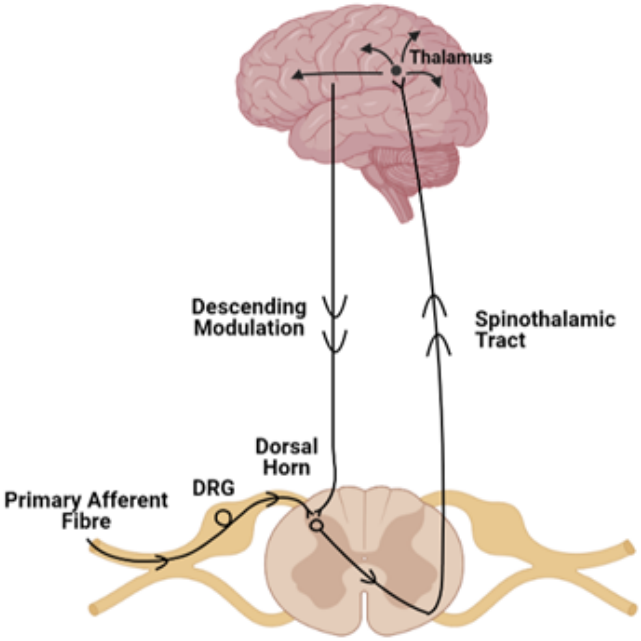


Figure 1.1. A Simplified Diagram of the Pain Pathway. Following activation of a primary afferent nociceptive fibre (DRG), an action potential travels along the fibre, entering the dorsal horn of the spinal cord. The DRG neurone synapses with a second order neurone, either an interneurone or a projection neurone, which travels via an ascending tract (such as the spinothalamic tract, to terminate in the thalamus), where information is relayed to other brain regions. Descending pathways modulate the excitability of the synapses within the dorsal horn. Arrows depict direction of action potential travel. Created using BioRender™.

sues to transduce sensory stimuli, and a central (proximal) branch that projects into the dorsal horn of the spinal cord to relay information along the pain pathway (Figure 1.2). To fulfil these roles, the axon must traverse long distances across diverse tissue environments, where terminal functionality is differentially regulated (Esposito et al., 2019). Far from being a passive "cable," the axon operates as a dynamic "motorway" - conducting electrical signals while actively transporting molecular cargo essential for local signalling and plasticity (Dalla Costa et al., 2021; Nagano and Araki, 2021).

DRG neurones are a heterogeneous population of neurones, ranging in diameter, function, and presence or absence of myelination. Myelination is produced by Schwann cells, a type of glial cell, which allow action potentials to be transduced at a greater velocity via saltatory conduction between nodes of Ranvier (described later in this section; Dubin and Patapoutian, 2010; Yam et al., 2018).

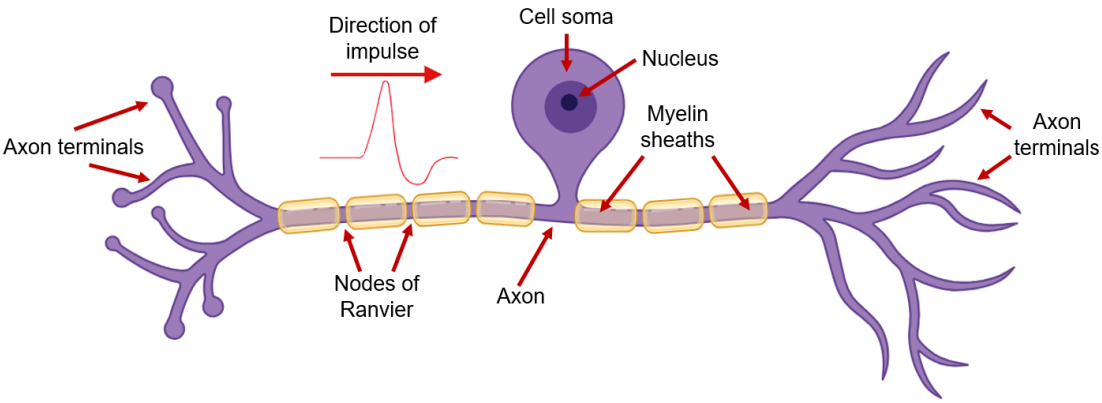


Figure 1.2. Sensory Neurone Structure. Neurones are highly polarised cells specialised for transmitting electrical impulses. Signals are received at the distal axon terminals and integrated at the cell soma. The axon conducts action potentials toward the proximal axon terminals, where neurotransmitters are released to propagate signals to target cells. In myelinated neurones, saltatory conduction between nodes of Ranvier greatly increases conduction velocity, an effect facilitated by insulating myelin sheaths. Created using BioRender™.

1.3.1.1 Sensory Neurone Subtypes and their Clinical Relevance

There have been many attempts to categorise sensory neurones, based on histological staining, myelination, conduction velocities, diameter, and protein markers. They have been generally classified into (Yam et al., 2018):

- Large, myelinated Aβ fibres which are low-threshold mechanosensory fibres, conducting signals relating to touch, pressure, and vibration. Axons terminate in laminae III and IV.
- Higher threshold, medium conduction velocity, thinly-myelinated Aδ fibres which transmit information relating to sharp, pricking pain which is perceived first. Axons terminate in laminae I, II, and V.
- Small, unmyelinated, polymodal C-fibres which conduct dull, aching, burning, or throbbing pain signals. Signals are transmitted more slowly and arrive after Aδ signals, with axons terminating in laminae I and II of the spinal cord. C-fibres are also involved in itch and temperature perception.

In addition, Aα sensory fibres originate from muscle spindle endings and Golgi

tendons, providing proprioceptive information; Aγ fibres innervate stretch fibres to regulate muscle spindle sensitivity; and B-fibres belong to the autonomic nervous system (Yam et al., 2018).

Based on rodent studies, C-fibres can be divided further into peptidergic and non-peptidergic, based on their mediator production and the expression of different receptors:

1. **Peptidergic C-fibres**: Release calcitonin gene-related peptide (CGRP) and substance P (SP), both of which contribute to pain hypersensitivity. Express TRPV1, tropomyosin receptor kinase A (TrkA), and μ-opioid receptors. Innervate both skin and deep tissue. Involved in nociception (Staedtler et al., 2024).

2. **Non-peptidergic C-fibres**: Contain low levels of neuropeptides and fewer TRPV1 and opioid receptors. Classically associated with innocuous mechanical sensation, with subsets contributing to itch processing (Staedtler et al., 2024).

Nociceptors, receptors located at the terminals of sensory neurones, can be activated by mechanical, thermal, or chemical stimuli (Webb and Steeds, 2022). Sensory neurones encode the location, intensity, and temporal profile of the noxious stimuli, ultimately driving pain perception. Understanding these nociceptive neurone subtypes may provide valuable insight into individual differences in pain perception and analgesic efficacy.

Axon and soma diameters are smaller in mice than in humans, and embryonic neurones are smaller still because these structures are still maturing. Based on previous developmental characterisations (Lechner et al., 2009), mouse neuronal soma diameters at embryonic day 16.5 (E16.5) can be stratified into <15 μm (small-diameter, likely C-fibres), 15-20 μm (intermediate, Aδ/larger C-fibre/immature Aβ), and >20 μm (large-diameter, presumptive Aβ) populations (Table 1.1).

Table 1.1. Estimated Sensory Neurone Subtype Identity by Soma Diameter at E16.5 in the Mouse DRG. The heterogeneous population of sensory neurones in the DRG can be categorised by their soma diameter. Embryonic neurones are still maturing so will have a smaller diameter than mature neurones. Based on classification by Lechner et al. (2009).

Size Bin	**Soma Diameter** (μm)	**Likely Subtype(s)**	**Notes**
Small	<15	C-fibres (TrkA$^+$)	Mostly unmyelinated neurones. Still differentiating at E16.5. Second pain, itch, temperature.
Medium	15-20	Aδ-like (maybe some immature Aβ and larger C-fibre)	Includes more mature TrkA$^+$ neurones and possibly low-threshold mechanoreceptors. Typically, the most responsive population at this stage. First pain, some light touch.
Large	>20	Aβ-like mechanoreceptors (TrkB$^+$), proprioceptors (TrkC$^+$)	Largest and earliest-born neurones. Likely represent functionally mature large-fibre populations. Touch, vibration, proprioception, pressure.

The heterogeneity in diameter, conduction velocity, and receptor expression underlies the differential responsiveness of DRG neurones to inflammatory mediators, providing a mechanistic basis for the selective modulation of pain signalling by molecules (Yin, Baillie, and Vetter, 2016).

1.3.1.2 Activation of Nociceptive Neurones

Nociceptive neurones remain electrically silent until a stimulus exceeds their activation threshold, at which point they generate all-or-nothing action potentials - rapid, transient changes in membrane potential that transmit signals along neurones to synapses (Dubin and Patapoutian, 2010). A neurone's electrical potential depends on the ratio of extracellular to intracellular ions and membrane permeability, regulated by ion channels (Yam et al., 2018).

Stimuli increase the membrane potential of a neurone from -70 mV to around +30 mV, opening voltage-gated sodium (Na^+) and calcium (Ca^{2+}) ion channels and trig-

gering an influx of Na^+ and Ca^{2+} ions from the extracellular space (Figure 1.3). This neuronal depolarisation permeabilises the membrane to extracellular Ca^{2+} ions and induces the release of Ca^{2+} from intracellular stores, such as the endoplasmic reticulum (Chen and Lui, 2023; Grider, Jessu, and Kabir, 2023).

Repolarisation, the return to baseline voltage, occurs when Na^+ channels inactivate and K^+ channels open, allowing K^+ efflux to reduce the positive charge. K^+ channels close more slowly than Na^+ channels, so the membrane briefly hyperpolarises below the resting potential (Figure 1.3). During this absolute refractory period, the neurone cannot fire another action potential. It is followed by a relative refractory period, during which a stronger stimulus is required to depolarise the neurone than usual because some Na^+ channels have recovered while K^+ channels remain open (Chen, 2023). Restoration of the resting potential is achieved by Na^+/K^+-ATPase (sodium-potassium pumps), which re-establish ionic gradients by removing Na^+ and importing K^+ (Grider, Jessu, and Kabir, 2023). This ensures the neurone is ready to initiate subsequent action potentials.

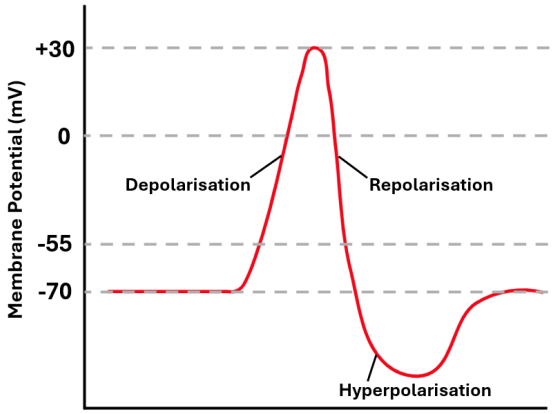


Figure 1.3. Neuronal Action Potential. Action potential generation begins with membrane depolarisation from -70 mV to +30 mV, opening voltage-gated Na^+ and Ca^{2+} channels and triggering ion influx. Intracellular Ca^{2+} release further amplifies this signal. Repolarisation occurs as Na^+ channels inactivate and K^+ channels open, causing K^+ efflux and membrane hyperpolarisation. This underlies the absolute and relative refractory periods. Resting potential is restored by Na^+/K^+-ATPase pumps to prepare the neurone for the next action potential.

Action potentials propagate along axons towards the terminals. In myelinated neurones, conduction occurs in a node-to-node manner, termed saltatory conduction.

Within myelinated regions, signals travel rapidly, while at the nodes of Ranvier clusters of ion channels depolarise the membrane above threshold to regenerate the signal. This mechanism markedly increases conduction velocity compared to unmyelinated axons, where each adjacent membrane segment must depolarise sequentially, producing a slower, continuous wave of activation (Grider, Jessu, and Kabir, 2023). Propagation speed depends on how far local depolarising currents spread before triggering the next segment, which is influenced by both membrane resistance and axonal diameter: wider axons have lower internal resistance and therefore faster conduction. Greater expression of voltage-gated sodium channels increases the available Na^+ current, resulting in a steeper upstroke and therefore faster depolarisation (Chen and Lui, 2023).

1.3.1.3 Sensitisation of Neurones

Peripheral Sensitisation

Repeated or intense noxious stimulation can lower the activation threshold, facilitating allodynia and hyperalgesia (Section 1.2; Latremoliere and Woolf, 2009). These hallmarks of peripheral sensitisation result from inflammatory mediators modulating ion channel activity, for example by increasing the conductance or expression of voltage-gated sodium and transient receptor potential (TRP) channels (Krames, 2014; Meng et al., 2016), thereby enhancing membrane excitability. This can lead to repetitive firing and spontaneous action potential generation, amplifying nociceptive input (Krames, 2014; Meng et al., 2016).

Central Sensitisation

At the central terminals, action potentials evoke neurotransmitter release that excites second-order neurones in the dorsal horn (Chen and Lui, 2023). Central sensitisation involves activity-dependent synaptic plasticity, including enhanced excitatory transmission, disinhibition, and increased postsynaptic responsiveness (Guo et al., 2019; Kim et al., 2012). Large low-threshold mechanoreceptors, normally

responsive only to innocuous stimuli, may be recruited to nociceptive signalling. Hyperalgesia can also arise in unaffected tissue, as pain is no longer coupled to peripheral input but to altered CNS neuronal properties (Latremoliere and Woolf, 2009). These adaptations lower the threshold for dorsal horn neurone activation and can sustain aberrant firing within central pain circuits.

Together, peripheral and central sensitisation increase the frequency, duration, and spatial spread of action potential activity, driving the progression from acute to chronic pain (Latremoliere and Woolf, 2009).

1.3.1.4 Voltage-Gated Sodium Channels

Voltage-gated sodium channels (VGSCs) are essential for action potential conduction; transport of sodium ions across the cell membrane alters the membrane potential of neurones. $Na_v1.7$, $Na_v1.8$, and $Na_v1.9$ are highly expressed on human nociceptive neurones and are involved in nociceptive signalling. Therefore, they are attractive peripheral analgesic targets (Osteen et al., 2025) - their inhibition reduces neuronal excitability and resultant pain behaviours in preclinical pain models (Dubin and Patapoutian, 2010), without affecting other essential biological processes (Osteen et al., 2025).

Suzetrigine (Journavx™), a $Na_v1.8$ inhibitor, was recently approved by the U.S. Food and Drug Administration for moderate to severe pain relief. By blocking $Na_v1.8$, the conduction of nociceptive action potentials is reduced, and thus pain signal transmission to the brain is decreased. As $Na_v1.8$ is selectively expressed in peripheral sensory neurones and largely absent from the CNS, $Na_v1.8$-targeted analgesia avoids many central side-effects associated with opioids (Osteen et al., 2025).

1.3.1.5 Local Translation

Neurones are highly complex and polarised cells that receive and integrate thousands of inputs from other neurones, glial cells, and diverse extracellular signals. To maintain function and support neurodevelopment, this vast information must be appropriately processed, transmitted, and stored (Holt, Martin, and Schuman, 2019). These functions rely on tightly regulated cellular mechanisms, including dynamic modifications of the neuronal proteome. Proteins within neurones act as sensors and effectors to coordinate processes such as synaptic pruning, synaptogenesis, and axon guidance (Holt, Martin, and Schuman, 2019).

In humans, DRG axons can extend up to one metre, making sensory neurones the longest cells in the body (Sörnmo and Laguna, 2005). Transport along an axon of a wide range of cargo has been recorded to vary between $\sim$0.5-1 μm per second (Maday et al., 2014). In a sensory neurone one metre in length - after the processing of a painful stimulus and coordination of a response - this rate of transport would take a minimum of 11.6 days to traffic a protein from the cell soma to its distal axon to exert a functional effect at the terminal. However, a response to a stimulus, involving the transport of a protein, is required within minutes (Holt, Martin, and Schuman, 2019). Relying solely on somatic transcription and subsequent protein transport would be inefficient for timely responses.

To support the extensive reach and spatiotemporal complexity of neuronal responses, sensory neurones possess complex machinery along the length of their axons, enabling the rapid transduction of sensory signals and adaptive responses to local environmental changes (Holt, Martin, and Schuman, 2019). Crucially, this extraordinary morphology necessitates the use of local axonal translation to meet the dynamic demands at each terminal. DRG neurones maintain a locally regulated pool of messenger RNAs (mRNAs) - single-stranded molecules of RNA that correspond to the genetic sequence of a gene - and the translational machinery within their axons, allowing site-specific protein synthesis in response to periph-

eral injury, inflammatory cues, or synaptic activity in the spinal cord (Gale et al., 2022).

The active transport of mRNAs along microtubules to specific subcellular compartments depends on signals within their 3' and 5' untranslated regions (UTRs; Tushev et al., 2018; Holt, Martin, and Schuman, 2019). While a substantial number of mRNAs have been identified in axons, the full extent of the mechanisms governing their localisation and translation - particularly across different subcellular domains of the axon - remains incompletely understood (Gumy et al., 2011).

Unlike the cell body, axons lack rough endoplasmic reticulum (ER), instead containing smooth ER tubules (Wu et al., 2017). Traditionally, these tubules were not thought to support translation; however, recent evidence suggests that the axonal ER can directly interact with ribosomes to facilitate local protein synthesis. Disruption of this interaction results in impaired protein production, altered ribosome distribution, and morphological defects in axons (Koppers et al., 2024). ER proteins, known for their involvement in mRNA translation, have also been found to be present within axons (Merianda et al., 2009).

Local translation supports adaptive plasticity at both axon terminals - enhancing receptor expression or cytoskeletal reorganisation peripherally and modulating synaptic strength and neurotransmitter release centrally. Such spatially restricted regulation is increasingly recognised as a key mechanism in pain modulation and chronic pain development (Gale et al., 2022).

Regulation of Local Translation

The spatial control of protein synthesis relies on distinct pools of RNA modulators within the local cytoplasm, including siRNAs, miRNAs, and RNA binding proteins (Bartel, 2004; Dalla Costa et al., 2021; Lucci et al., 2020; Mesquita-Ribeiro et al., 2021). By shaping the expression of proteins involved in cytoskeletal dynamics, receptor signalling, and ion channel function, these regulators contribute directly to

activity-dependent plasticity and to the maladaptive changes in excitability underlying inflammatory sensitisation (Gumy et al., 2011). The following sections outline the roles of miRNAs and siRNAs in post-transcriptional gene regulation.

miRNAs

miRNAs are small non-coding RNAs, approximately 22 nucleotides in length, that regulate gene expression post-transcriptionally (Prada et al., 2018). Acting alongside other small RNAs and protein factors, they shape the axonal proteome in an activity- and context-dependent manner (Dajas-Bailador et al., 2012; Koralewska et al., 2024; Lucci et al., 2020).

Primary miRNA (pri-miRNA) transcripts are produced by RNA polymerase II and are 5'-capped and 3'-polyadenylated (Potenza et al., 2017). The pri-miRNA is cleaved by Drosha to generate a stem-loop precursor (pre-miRNA), which is exported to the cytoplasm by Ran-GTP and Exportin-5 (Bartel, 2004). In the cytoplasm, Dicer processes the pre-miRNA into a mature duplex, one strand of which is incorporated into Argonaute 2 (AGO2) within the RNA-induced silencing complex (RISC). The RISC-miRNA complex then binds complementary sequences, typically in the 3' UTR of target mRNAs, to inhibit translation or promote mRNA degradation (Figure 1.4; Morel et al., 2013; Potenza et al., 2017).

This flexible regulatory mechanism allows subtle, graded control of protein synthesis and is highly conserved across evolution (Bartel, 2004). Because a single miRNA can target multiple mRNAs (Xu et al., 2020), they have become attractive tools for translational research, often overcoming species-specific barriers (Bartel, 2004).

Several miRNAs have been implicated in pain modulation, particularly in inflammatory states. Some promote sensitisation, such as miR-155 and miR-221, which inhibit suppressor of cytokine signalling 1 (SOCS1), driving neuroinflammation (Hassan et al., 2024; Morchio et al., 2023), and the miR-15/16 cluster, which acti-

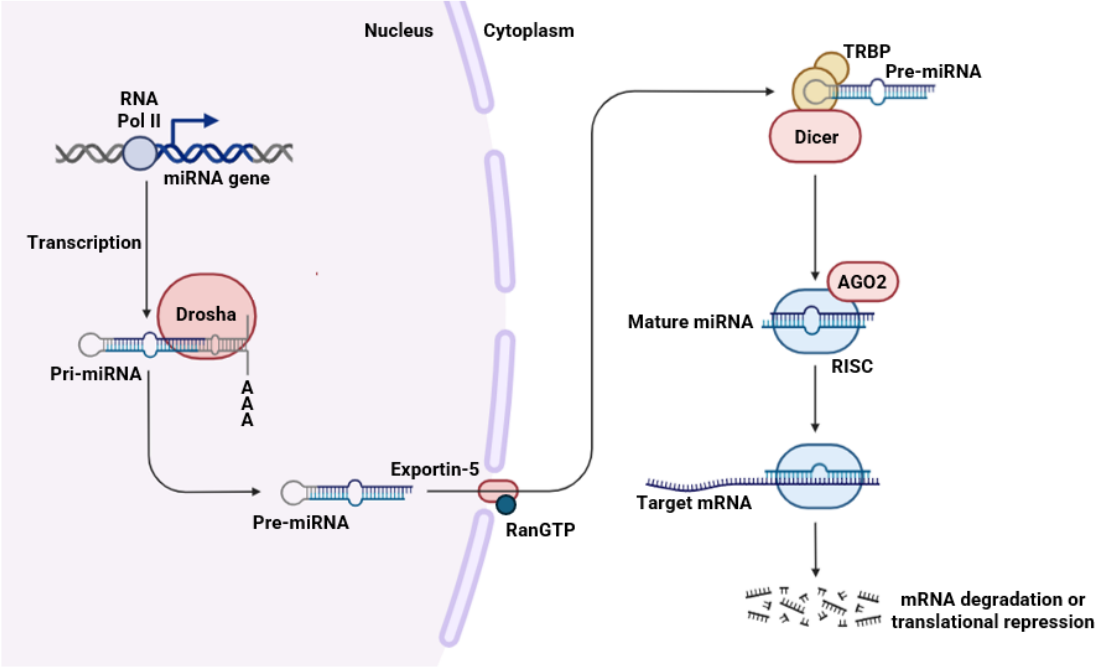


Figure 1.4. Canonical miRNA Biogenesis and Gene Silencing Pathway. The miRNA gene is transcribed by RNA polymerase II to produce a primary miRNA (pri-miRNA) transcript, which is typically capped and polyadenylated. This pri-miRNA is processed in the nucleus by the microprocessor complex containing Drosha, yielding a precursor miRNA (pre-miRNA). Pre-miRNA is then exported to the cytoplasm by Exportin-5 in a RanGTP-dependent manner. In the cytoplasm, Dicer, in complex with TRBP, cleaves the pre-miRNA into a mature miRNA duplex. One strand of the duplex is loaded into AGO2 to form the RNA-induced silencing complex (RISC). The RISC-miRNA complex then binds to target messenger RNAs (mRNAs), leading to either mRNA degradation or translational repression, depending on the degree of sequence complementarity. Adapted from a template on BioRender™.

vates inflammatory p38/NF-κB pathways by downregulating GRK2 (Morchio et al., 2023). Conversely, others exert protective effects: miR-223 is downregulated in neuropathic pain, leading to increased activation of MAPK (mitogen-activated protein kinase) signalling pathways (Morchio et al., 2023), while miR-146a-5p targets IRAK1 and TRAF6 in the TLR/NF-κB pathway, dampening inflammation and neuropathic pain, and is proposed as a regulator in osteoarthritic pain (Lu et al., 2015; Hassan et al., 2024).

Importantly, miRNAs are not confined to the soma. mRNAs, miRNAs, and other components of the post-transcriptional machinery are transported into axons - either bound directly to motor proteins or via an intermediary connection with RNA granules and vesicles - enabling spatially restricted repression of translation (Dalla

Costa et al., 2021). mRNAs and associated RNA regulatory factors are commonly sequestered in the axon, where they can be rapidly translated into proteins in response to local cues (Nagano and Araki, 2021). This is particularly significant in long-range neurones such as sensory neurones, where local control of the proteome supports axonal plasticity and responsiveness to extracellular cues (Holt, Martin, and Schuman, 2019).

siRNA

siRNAs are short double-stranded, non-coding RNA molecules, typically 19-21 nucleotides in length (Kaur and Sharma, 2012), that guide RISC to complementary mRNA sequences. Only recently have endogenous siRNAs been discovered in mammals and insects (Kaur and Sharma, 2012). Upon binding, RISC cleaves the target mRNA, leading to its degradation and subsequent suppression of protein translation - a process termed RNA interference (RNAi; Figure 1.5; Bartel, 2004). Gene knockdown using siRNA allows precise manipulation of gene expression, enabling researchers to dissect the functional contribution of individual transcripts in a cell type- or compartment-specific manner (Berta et al., 2017; Kaur and Sharma, 2012).

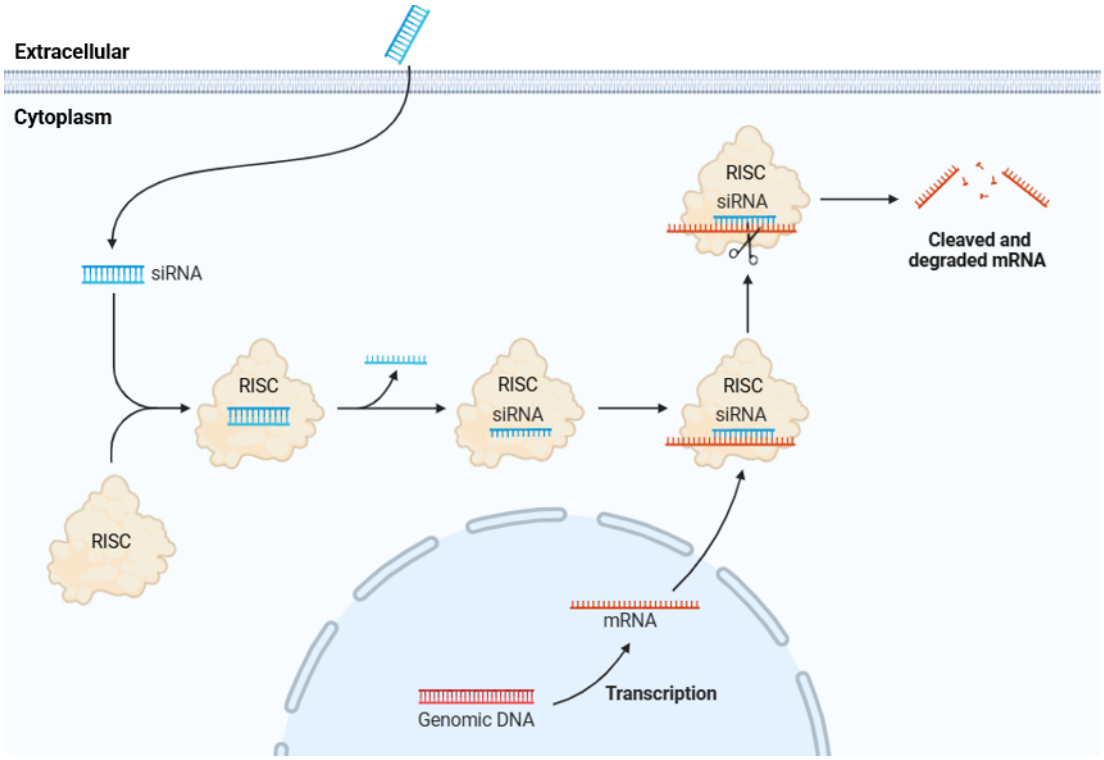


Figure 1.5. Mechanism of siRNA-Mediated Gene Silencing. siRNA is taken up by the recipient cell and incorporated into the RNA-induced silencing complex (RISC). The siRNA duplex is unwound, with the guide strand retained and the passenger strand typically degraded. The guide strand directs RISC to a complementary sequence within the target mRNA. Upon binding, RISC cleaves the mRNA, leading to its degradation and preventing translation, thereby silencing gene expression. Adapted from a BioRender™ template.

1.3.1.6 Extracellular Vesicles

According to the Minimal Information for Studies of Extracellular Vesicles 2023 (MISEV2023) guidelines, extracellular vesicles (EVs) are "particles released from cells, delimited by a lipid bilayer, and unable to replicate independently" due to the absence of a functional nucleus (Welsh et al., 2024). All cell types are thought to release EVs, but their mode of release, cargo, size, and abundance are highly dynamic and shaped by the local microenvironment (Welsh et al., 2024). First described in the 1970s, EVs have only recently been recognised as key mediators of intercellular communication and disease modulation (Ahmad et al., 2022). Their selective, receptor-mediated uptake and controlled release of bioactive cargo, combined with lower immunogenicity and embolic risk compared to cell or tissue transplantation, make EVs not only attractive therapeutic candidates but also compelling

mediators of cell-cell communication. In the context of neuronal signalling, this positions EVs as likely modulators of neuronal function, with potential relevance for targeted pain therapies (Ahmad et al., 2022; Suntres et al., 2013).

EVs arise via distinct cellular pathways. One involves endosomal maturation: plasma membrane invagination produces an early endosome, which matures into a multivesicular endosome (MVE) containing intraluminal vesicles (ILVs). MVEs may fuse with lysosomes for degradation or with the plasma membrane to release ILVs (exosomes) into the extracellular space via exocytosis (Figure 1.6; Teng and Fussenegger, 2021).

Alternatively, EVs may originate from direct outward budding of the plasma membrane through ectocytosis, producing vesicles often referred to as ectosomes or microvesicles. Once released, EVs can be internalised by recipient cells, such as sensory neurones, through diverse mechanisms, including endocytosis (clathrin-dependent, lipid raft-mediated, receptor-mediated), phagocytosis, or macropinocytosis (Figure 1.6; Teng and Fussenegger, 2021).

EVs transport diverse cargo, including proteins, lipids, and non-coding RNAs such as miRNAs, from donor to recipient cells, thereby modulating local translation in neighbouring cells (Chaudhuri et al., 2018). miRNAs within EVs regulate gene expression in recipient cells by binding complementary mRNA targets and repressing translation (Teng and Fussenegger, 2021). This intrinsic ability to deliver regulatory RNAs underlies the growing interest in EVs as therapeutic vectors (Suntres et al., 2013).

EVs from mesenchymal stromal cells, astrocytes, and microglia have shown neuroprotective effects in CNS injury and neuroinflammation (Ahmad et al., 2022; López-Cepeda et al., 2022; Peng et al., 2022; Xin et al., 2024 Zhu et al., 2025). In the PNS, sensory neurones are emerging as key EV targets, particularly under inflammatory conditions, where EVs can alter nociceptive neurone sensitivity

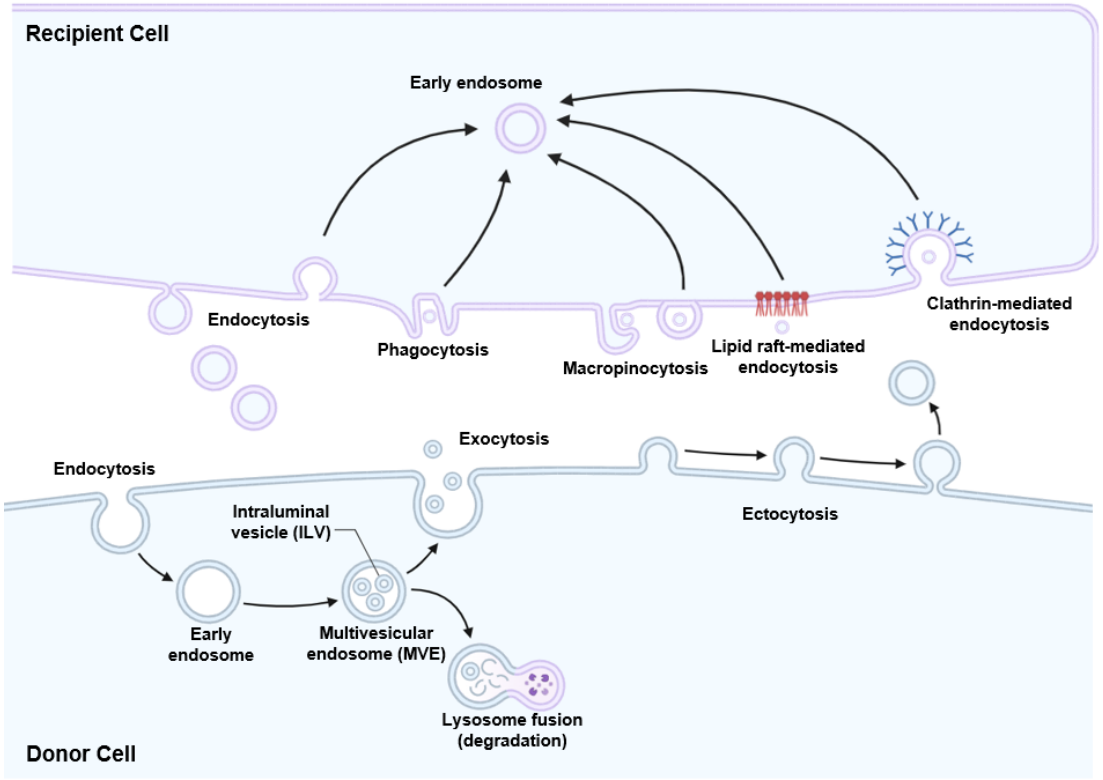


Figure 1.6. Extracellular Vesicle Release and Uptake. EVs are generated via two principal routes: invagination of the plasma membrane to form early endosomes, which mature into multivesicular endosomes (MVEs) containing intraluminal vesicles (ILVs); or direct budding from the plasma membrane (ectocytosis). MVEs may fuse with lysosomes for degradation, or with the plasma membrane to release ILVs into the extracellular space via exocytosis. Once released, EVs can be taken up by recipient cells through endocytosis (clathrin- or raft-mediated), phagocytosis, or macropinocytosis. Created using BioRender™.

and excitability. These dynamic processes enable the targeted transfer of bioactive molecules between cells, establishing EVs as central modulators of intercellular communication and promising tools for regenerative medicine (Ahmad et al., 2022).

1.3.2 Integration into the Spinal Cord

The spinal cord consists of ten cytoarchitectonic layers, known as the Rexed laminae. Nociceptive first-order neurones primarily terminate in the superficial dorsal horn, particularly laminae I and II, or in deeper lamina V (Rexed, 1952). Sensory neurones synapse onto interneurones and projection neurones, where their signals undergo complex modulation by local excitatory and inhibitory circuits. Rele-

vant second-order neurones include nociceptive-specific cells in lamina I and wide-dynamic-range neurones in lamina V, which respond to both noxious and innocuous input (Webb and Steeds, 2022). These cells integrate incoming signals, determining whether nociceptive input is amplified or suppressed, before ascending to higher-order brain regions. Maladaptive changes at this level, such as central sensitisation, can increase the excitability of second-order neurones, enhance synaptic efficacy, and weaken inhibitory control, which amplifies nociceptive transmission, broadens receptive fields, and contributes to the development and maintenance of chronic pain (Section 1.3.1.3; Latremoliere and Woolf, 2009; Webb and Steeds, 2022).

1.3.3 Ascending Pathways

Following signal integration, nociceptive information is relayed to the brain via ascending tracts, such as the spinothalamic tract, which conveys pain and temperature signals, and the spinoreticular tract, which influences autonomic reflexes and the emotional aspects of pain (Webb and Steeds, 2022). These tracts terminate in specific brain regions, including the somatosensory cortex, thalamus and amygdala, where pain is processed, interpreted, and emotionally contextualised (Yam et al., 2018). This processing enables the brain to localise the painful stimuli and adapt responses for future experiences.

1.3.4 Descending Control

Pain signals are further modulated by descending pathways originating in the brainstem and terminating in the dorsal horn. These pathways exert “top-down” control over nociceptive transmission, either inhibiting or facilitating pain signals, depending on physiological context. The periaqueductal gray (PAG) in the midbrain relays noxious information to the rostral ventromedial medulla (RVM), a critical hub for descending control (Staud, 2013).

Within the RVM, distinct populations of neurones - known as ‘on’, ‘off’, and ‘neutral’ cells - have been characterised based on their firing patterns in response to noxious stimulation. ‘On’ cells increase their firing prior to nociceptive reflexes and are associated with pain facilitation, whereas ‘off’ cells pause firing and are associated with the inhibition of pain. ‘Neutral’ cells show no consistent change in firing rate (Carlson et al., 2007). Through these cell types, the RVM can engage the endogenous opioidergic system to suppress pain perception. Monoamines such as noradrenaline and serotonin, released from descending fibres, also contribute to this modulation, although under certain conditions they may instead enhance nociceptive neurone excitability (Staud, 2013).

While the pain pathway is tightly regulated by excitatory and inhibitory mechanisms, it is also strongly influenced by inflammatory processes. Inflammation is crucial for protective nociceptive responses, but persistent inflammatory signalling can drive long-lasting sensitisation of the nervous system and contribute to chronic pain (Section 1.3.1.3). Dysfunction of descending inhibitory pathways may further exacerbate chronic pain, allowing pain to persist even after tissue damage has resolved (Latremoliere and Woolf, 2009). The following sections will examine how acute inflammation interacts with nociceptive pathways and how unresolved inflammation can promote chronic pain states.

1.4 Acute Inflammation

Acute inflammation is the immediate, adaptive immune response to tissue injury or infection. Following tissue damage, immune cells detect pathogen-associated and damage-associated molecular patterns (PAMPs and DAMPs), triggering the release of inflammatory mediators such as prostaglandins (Sekiguchi et al., 2013), serotonin (Su et al., 2016), adenosine (Taiwo and Levine, 1990), and cytokines, including tumour necrosis factor-α, interleukin-6, and interleukin-1β (TNF-α, IL-6, and IL-1β; Cheng, Xu, and Ma, 2022). These mediators induce vasodilation and increase vascular permeability, producing the classic cardinal signs of inflammation:

redness, heat, oedema, and pain (Kawahara et al., 2015).

Beyond their vascular effects, inflammatory mediators directly act on nociceptive neurones, particularly small-diameter fibres, to modulate pain sensitivity. Intense or repetitive noxious stimulation amplifies inflammatory mediator release (Latremoliere and Woolf, 2009). PGE_2, for example, lowers activation thresholds and enhances neuronal excitability (Sekiguchi et al., 2013), and in some cases can even induce spontaneous activity (Section 1.2; Aley and Levine, 1999). Such sensitisation ensures heightened pain perception during injury, promoting protective behaviours that prevent further tissue damage (Latremoliere and Woolf, 2009).

Normally, peripheral sensitisation resolves as the inflammatory response subsides, restoring nociceptive neurone function to baseline (Yao and Narumiya, 2019; Latremoliere and Woolf, 2009). However, if inflammation persists, prolonged exposure to inflammatory mediators can maintain nociceptive neurone hyperexcitability, increasing the risk of chronic pain and contributing to the transition to central sensitisation (Hehn, Baron, and Woolf, 2012).

1.5 Chronic Inflammation

As outlined in Section 1.2, when the biological mechanisms underlying pain become dysregulated, acute pain can transition into a chronic pain state that persists long after tissue healing has resolved. Chronic pain is heterogeneous in its origins, arising from inflammation, nervous system dysfunction, or idiopathically (Treede et al., 2015). Chronic inflammation represents one key driver of this transition, sustaining nociceptive neurone hyperexcitability and initiating maladaptive changes in the CNS that perpetuate pain, even in the absence of ongoing tissue damage (Latremoliere and Woolf, 2009).

Unlike acute inflammation, which resolves rapidly, chronic inflammation involves ongoing immune cell recruitment and tissue remodelling, sustained by persistent cytokine release - including TNF-α and IL-1β - from macrophages, lymphocytes,

and dendritic cells. These mediators prolong peripheral sensitisation by lowering nociceptive neurone activation thresholds and enhancing excitability. Additionally, they increase excitatory synaptic strength, creating a state of heightened neuronal responsiveness in the dorsal horn, while disrupting descending pain modulation, which reduces inhibitory control over spinal nociceptive transmission (Section 1.3.4). This loss of inhibitory tone further amplifies pain signalling and contributes to the persistence of chronic inflammatory pain. Their activation of glial cells in the spinal cord releases additional cytokines and trophic factors that exacerbate nociceptive transmission and hinder the resolution of sensitisation (Kim et al., 2012; Latremoliere and Woolf, 2009; Yam et al., 2018; Yao and Narumiya, 2019).

Persistent peripheral input and glial activation together drive central sensitisation, a neuroplastic state wherein prolonged nociceptive activity induces long-lasting changes in dorsal horn circuitry. Central sensitisation is characterised by increased membrane excitability, facilitation of synaptic efficacy, and disinhibition, enabling previously sub-threshold inputs to elicit action potentials. This leads to widespread and persistent hypersensitivity, including secondary hyperalgesia (pain extending beyond the initial injury site) and allodynia, and may involve recruitment of low-threshold Aβ fibres into pain pathways (Latremoliere and Woolf, 2009).

1.6 Prostaglandin E_2

Pro-inflammatory mediators - such as prostaglandins, cytokines, and ATP - act directly on sensory neurones to enhance their responsiveness, driving peripheral sensitisation. Sustained peripheral activation can subsequently trigger central sensitisation, contributing to the transition from acute to chronic pain (Moriyama et al., 2005; Latremoliere and Woolf, 2009). Among these mediators, prostaglandins are particularly influential, acting locally to modulate neuronal excitability during inflammation.

Prostaglandins are lipid mediators belonging to the eicosanoid family of oxygenated

C_{20} fatty acids, which includes PGE_2, PGD_2, PGF_2, PGI_2, and TXA_2 (Figure 1.7). They are synthesised from arachidonic acid (AA) by cyclooxygenase (COX) enzymes, which are expressed throughout the body (Kawahara et al., 2015). COX enzymes possess two catalytic sites: the cyclooxygenase site, which oxygenates AA to PGG_2, and the peroxidase site, which reduces PGG_2 to PGH_2. PGH_2 is an unstable intermediate that is rapidly converted by terminal synthases to generate the various prostaglandins and TXA_2 (Kawahara et al., 2015).

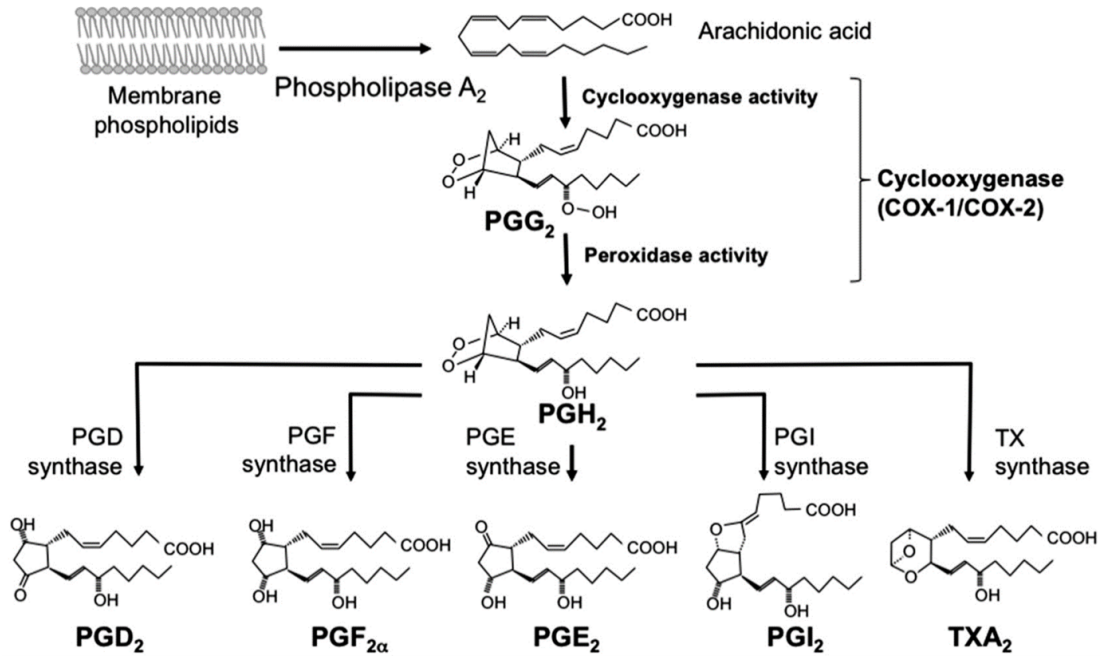


Figure 1.7. Synthesis Pathway of PGE_2. Arachidonic acid is released from membrane phospholipids by the action of phospholipase A_2. Cyclooxygenase enzymes convert arachidonic acid to the intermediate PGG_2, before peroxidase enzymes convert it to PGH_2. The relevant synthases synthesise the distinct prostanoids. Adapted from Kawahara et al., 2015.

Two COX isozymes catalyse this process: COX-1 and COX-2. While they share similar catalytic functions, they differ in regulation, tissue distribution, and activation kinetics. COX-1 preferentially converts AA at higher concentrations (>10 μM), which occur during acute injury or cellular damage, whereas COX-2 predominates at lower concentrations ($\leq$2.5 μM) and is the principal enzyme driving PGE_2 synthesis during sustained inflammation (Park, Pillinger, and Abramson, 2006). COX-2 selective inhibitors are widely used to treat inflammatory pain (e.g., arthritis and back pain), but their long-term utility is limited by cardiovascular and hepatic side

effects. Consequently, clinical guidelines recommend using NSAIDs at the lowest effective dose and for the shortest duration necessary (NICE, 2021).

PGE_2 is the most abundant and potent prostaglandin and plays a central role in inflammation and nociception. Its production is strongly upregulated during tissue injury or inflammation and can remain elevated in chronic inflammatory states (Ferreira, Moncada, and Vane, 1974; Vane et al., 1994). Acting locally on sensory neurones, it lowers their action potential threshold - primarily by modulating specific ion channels - and increases firing frequency, producing neuronal sensitisation and hyperalgesia (Figure 1.8; Kimourtzis et al., 2024).

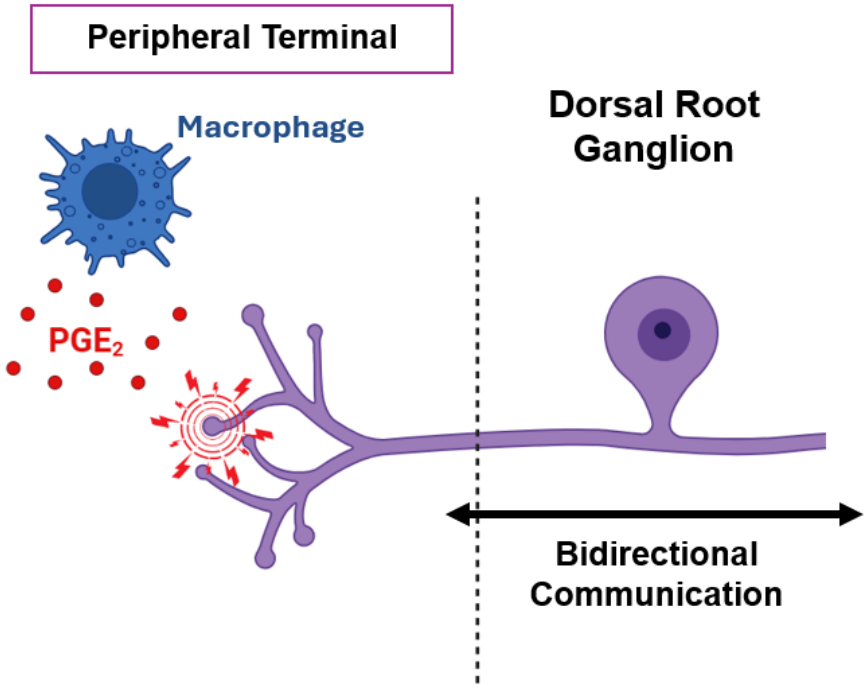


Figure 1.8. The Interaction of PGE_2 at the Peripheral Terminal of the Sensory Neurone. PGE_2 is released by local cells, such as macrophages, into the microenvironment following tissue injury by local cells. PGE_2 acts directly on sensory neurones to sensitise them. Created using BioRender™.

1.6.0.1 Prostaglandin E_2 Receptor Mechanisms

PGE_2 acts on nociceptive neurones through four G protein-coupled receptors (GPCRs): EP_1, EP_2, EP_3, and EP_4. Ligand binding induces a conformational change in these receptors, allowing them to engage heterotrimeric G proteins (Gs, Gi, or Gq). This

promotes the exchange of guanosine diphosphate (GDP) for guanosine triphosphate (GTP) in the Gα subunit, causing its dissociation from the G$\beta\gamma$ complex and initiating distinct downstream signalling cascades (Hilger, Masureel, and Kobilka, 2018).

EP receptor subtypes couple to different G proteins, resulting in divergent cellular effects (Figure 1.9). EP_1 couples to Gq, activating phosphoinositol-phospholipase C (PI-PLC), which generates inositol triphosphate (IP_3) to release Ca^{2+} from intracellular stores. EP_2 and EP_4 couple to Gs, stimulating adenylyl cyclase to elevate cyclic adenosine monophosphate (cAMP). In contrast, EP_3 predominantly couples to Gi, which inhibits adenylyl cyclase and suppresses cAMP production, though some isoforms can also couple to Gs or Gq (Biringer, 2012; Kawahara et al., 2015).

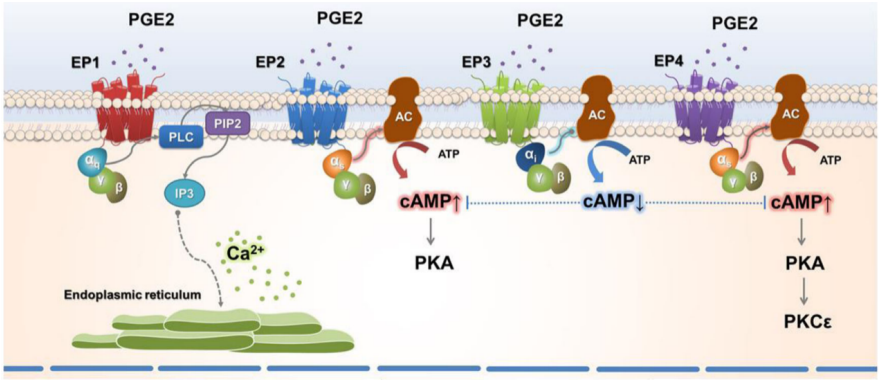


Figure 1.9. PGE_2 Mechanism of Action in Neurones. PGE_2 binds to the EP receptors on sensory neurone membranes. EP_1 receptor activation results in calcium release from intracellular stores, such as the endoplasmic reticulum, via IP_3 production. EP_2 and EP_4 binding results in cAMP production which triggers downstream phosphorylation of signalling proteins. EP_3 activation inhibits cAMP production, thereby decreasing downstream protein phosphorylation. Adapted from Jang, Kim, and Hwang (2020).

Each receptor subtype contributes differently to pain signalling. EP_1 has relatively low affinity for PGE_2 and is expressed in several tissues, including the CNS (Biringer, 2012). Its Gq-mediated rise in intracellular Ca^{2+} influences nociceptive neurone excitability and transcriptional activity and can also activate PKC to sensitise TRPV1 and other ion channels, promoting acute hyperalgesia (Ma et al., 2016). EP_3 is more widely distributed (notably in smooth muscle, kidney, endometrium,

and adipose tissue) and binds PGE_2 with high affinity. Through Gi-mediated inhibition of cAMP signalling, it modulates vascular permeability during acute inflammation (Biringer, 2012; Kawahara et al., 2015).

Although both EP_2 and EP_4 stimulate cAMP production, they differ in their signalling kinetics and downstream effects. EP_2 is relatively resistant to desensitisation, supporting sustained cAMP/PKA activity (Malty et al., 2016). EP_4, by contrast, undergoes rapid desensitisation and internalisation via β-arrestin, enabling additional PI3K/Akt and ERK signalling (Kawahara et al., 2015; Tsuge et al., 2019). These cascades enhance inflammatory cytokine production, neuronal plasticity, and nociceptive neurone sensitisation. EP_4 expression is also upregulated and externalised in DRG neurones during inflammation (St-Jacques and Ma, 2013).

The following table (Table 1.2) summarises the key signalling characteristics and pain-related roles of each EP receptor:

Table 1.2. EP Receptor Signalling and Role in Pain. Each EP receptor exhibits distinct G protein coupling, intracellular effects, and contributions to pain signalling.

Receptor	**PGE_2 Affinity**	**G protein**	**Intracellular Signalling**	**Pain Modulation**
EP_1	Low	Gq	↑ intracellular calcium	Generally pronociceptive
EP_2	Moderate	Gs	↑ cAMP, ↑ calcium	Pronociceptive, promotes sensitisation
EP_3	Highest	Gi (also Gs/Gq variants)	↓ cAMP (variant-dependent)	Mixed; some isoforms may be antinociceptive
EP_4	High	Gs	↑ cAMP, ↑ calcium	Pronociceptive; key in inflammatory pain

Pain signalling is most strongly associated with EP_1 and EP_4, while EP_3 contributes to vascular hyperpermeability and EP_2 has been implicated in joint pain (Morimoto et al., 2014; Kras, Dong, and Winkelstein, 2013). Activation of these

receptors modulates numerous ion channels that govern nociceptive neurone excitability (Figure 1.10). cAMP/PKA signalling enhances P2X purinoceptor 3 ($P2X_3$ receptor) and hyperpolarisation-activated cyclic nucleotide-gated (HCN) channel activity, facilitating cation influx and depolarisation. It also phosphorylates $Ca_V3.2$ (voltage-gated T-type Ca^{2+} channel), thereby increasing membrane excitability, and shifts the activation threshold of VGSCs to more hyperpolarised potentials, amplifying neuronal firing (Jang, Kim, and Hwang, 2020; Sekiguchi et al., 2013).

PGE_2 additionally disrupts inhibitory control by altering Cl^- homeostasis. Under physiological conditions, activation of $GABA_A$ and glycine receptors is inhibitory; however, PGE_2 reduces expression of the Cl^- exporter KCC2 while upregulating the Cl importer NKCC1. This leads to intracellular Cl^- accumulation, such that $GABA_A$ and glycine receptor activation becomes depolarising rather than hyperpolarising, thereby increasing excitability (Jang, Kim, and Hwang, 2020). It also suppresses the slow afterhyperpolarisation (sAHP; Section 1.3.1.2) mediated by Ca^{2+}-activated K^+ (K_{Ca}) channels - boosting firing frequency - and sensitises TRP channels including TRPA1, TRPV1, and TRPV4 (Jang, Kim, and Hwang, 2020).

Consistent with these cellular mechanisms, PGE_2 strongly promotes nociceptive neurone sensitisation *in vivo* and *in vitro*. Intraplantar PGE_2 injection evokes immediate nocifensive behaviour and sustained mechanical allodynia (Kassuya et al., 2007) and EP_4 antagonists have been found to reduce hyperalgesia (Jang, Kim, and Hwang, 2020; Nagahisa and Okumura, 2017). Electrophysiological recordings from isolated neurones (Lopshire and Nicol, 1997) and calcium imaging from DRG cultures demonstrate increased excitability (Kimourtzis et al., 2024; Wei et al., 2024), while chronic PGE_2 exposure stimulates the production of SP and CGRP in ganglion explants via EP_1/EP_4-PKA/PKC signalling (Ma, 2010). Mechanistically, PGE_2 sensitises TRPV1 responses in a PKC-dependent manner in HEK cells and mouse DRG neurones and also potentiates TRPV1 via EP_4-mediated PKA signalling (Moriyama et al., 2005). These pathways converge to enhance nociceptive

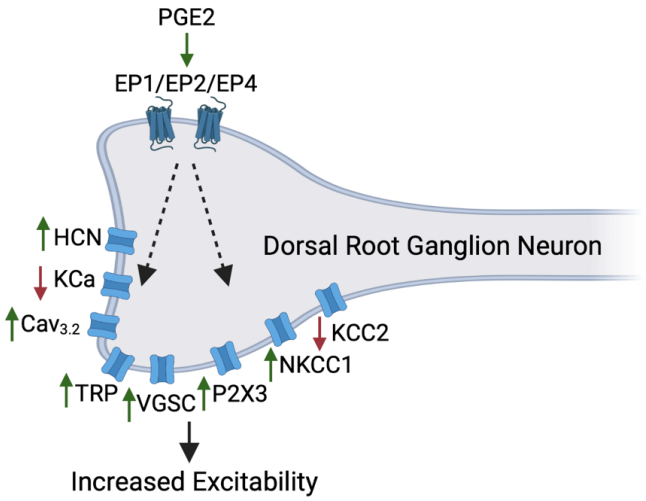


Figure 1.10. Overview of the Action of PGE_2 Once Bound to a Sensory Neurone. This schematic illustrates how PGE_2 signalling via EP receptors modulates ion channel activity to drive peripheral sensitisation - a key mechanism explored in Chapter 3. PGE_2 is released by immune cells during inflammation and acts directly on GPCRs, $EP_{1/2/4}$, on the surface of DRG neurones. The secondary messenger cascades activate a number of channels, including TRP, voltage-gated sodium channels, HCN, NKCC, $P2X_3$, $Ca_V3.2$, and inhibit K_{Ca} and KCC2 channels. This leads to peripheral sensitisation and can generate central sensitisation and chronic pain. Created using BioRender™.

neurone excitability and neuropeptide release. Indeed, antisense oligonucleotides targeting EP_3C (a splice variant) and EP_4 mRNA abolish PGE_2-stimulated cAMP production and block its ability to augment SP and CGRP release (Southall and Vasko, 2001), underscoring the functional relevance of EP receptor coupling to intracellular second messengers. Furthermore, PGE_2-induced thermal hyperalgesia and inflammatory nociceptive responses are significantly diminished in TRPV1- and EP_1-deficient mice, highlighting the necessity of these receptors for full behavioural expression of PGE_2-evoked pain (Moriyama et al., 2005).

1.6.1 Knowledge Gaps in the Inflammatory Context

To summarise, PGE_2 is a well-established mediator of pain that acts both directly and indirectly on primary sensory neurones. It excites nociceptive neurones and promotes the release of pro-nociceptive neuropeptides such as SP and CGRP, with EP_1 and EP_4 receptor activation significantly enhancing their expression (Ma, 2010). Beyond neuropeptide release, PGE_2 modulates the excitability of sen-

sory neurones by altering the activity and trafficking of key ion channels, including voltage-gated sodium channels and transient receptor potential (TRPV1) channels, which lowers the threshold for action potential generation (Malty et al., 2016; Jang, Kim, and Hwang, 2020). Through EP receptor engagement - particularly EP_4 - PGE_2 activates multiple intracellular signalling cascades, including PKA, PKC, PI3K/Akt, and ERK pathways, which collectively regulate ion channel phosphorylation, cytokine production, and gene transcription, contributing to both acute sensitisation and long-term changes in nociceptive responsiveness. These signalling pathways also drive EP_4 receptor externalisation in DRG neurones, amplifying nociceptive neurone responsiveness during inflammatory states (St-Jacques and Ma, 2013). Furthermore, PGE_2 can act in an autocrine and paracrine manner, influencing neighbouring neurones and glial cells, thereby coordinating a broader pro-nociceptive environment that underlies hyperalgesia and persistent pain.

Despite extensive characterisation of these mechanisms, key gaps remain. The transition from acute hyperalgesia to chronic pain, particularly in neuropathic and centrally sensitised states, is not fully understood. EP receptor crosstalk (e.g., EP_2/EP_4 with TRPV1) and the spatiotemporal dynamics of receptor activation across pain conditions require further investigation. Moreover, neuroimmune interactions involving spinal microglia and astrocytes, as well as epigenetic and transcriptional regulation of PGE_2 signalling, remain largely unexplored.

The compartmentalised architecture of sensory neurones introduces additional complexity at the subcellular level. Emerging evidence suggests that EP receptor-driven signalling may be spatially restricted to peripheral axons or terminals (Kimourtzis et al., 2024; Pope et al., 2025), where it could selectively enhance local TRPV1 sensitisation (Section 1.7) or translation of ion channel mRNAs. Post-transcriptional regulators, such as miRNAs, may further fine-tune these responses, yet their role in EP receptor signalling has not been systematically examined. Targeted siRNA approaches, as used in this thesis, offer a route to dissecting these

regulatory layers and identifying novel therapeutic targets within the EP receptor-TRPV1 axis.

1.7 TRPV1 and Capsaicin

TRPV1

The TRP channel family have emerged as a key group of ion channels involved in the transduction of thermal, mechanical, and chemical stimuli. Several TRP channels play pivotal roles in pain signalling including the heat-sensitive TRPV1, cool-activated TRPM8, and cold-responsive TRPA1, making them promising targets for analgesic development (Dubin and Patapoutian, 2010). These channels are primarily expressed in nociceptive sensory neurones and respond to distinct, yet sometimes overlapping, noxious cues (Saito and Saito, 2025).

Among them, transient receptor potential vanilloid 1 (TRPV1) is one of the most well-characterised. A non-selective cation channel expressed predominantly on sensory neurones, it plays a critical role in detecting and responding to thermal and chemical pain stimuli. TRPV1 is activated by capsaicin, noxious heat, acidic pH (protons), and a variety of endogenous lipids (Caterina et al., 1997) and is typically perceived as a burning pain - though it may also contribute to itch sensations under certain conditions (Willis, 2009).

Unlike other proteins that are restricted to specific subcellular regions, TRPV1 is ubiquitously distributed across the soma, axon, and peripheral terminals of sensory neurones (Tominaga et al., 1998). Developmentally, its expression is transiently widespread across both peptidergic and non-peptidergic sensory neurones but becomes predominantly peptidergic in adulthood (Cavanaugh et al., 2011). Unmyelinated, peptidergic C-fibres co-express CGRP and SP and are heavily implicated in peripheral sensitisation, a process exacerbated by inflammatory mediators such as PGE_2 (Moriyama et al., 2005) and nerve growth factor (NGF; Section 1.3.1.1; Ji et al., 2002). TRPV1 is also found on a subset of medium-diameter, thinly myelinated

Aδ fibres, further contributing to the transmission of noxious thermal and chemical signals (Cavanaugh et al., 2011).

Once activated, TRPV1 allows Na^+ and Ca^{2+} influx and the consequent depolarisation and action potential firing of nociceptive sensory neurones (Section 1.3.1.2). This triggers the release of glutamate and neuropeptides (CGRP and SP) at synapses with second-order neurones in the dorsal horn, thereby transmitting nociceptive signals to the brain. *In vivo*, local hypoesthesia (reduced sensitivity) occurs at the site of capsaicin injection due to desensitisation of $TRPV1^+$ afferents (Willis, 2009). In contrast, in the surrounding area, TRPV1 activation contributes to the development of inflammatory mechanical allodynia and hyperalgesia (Kim et al., 2012; Ma et al., 2016). Neuropeptide release promotes vasodilation, increased blood flow, and oedema - hallmarks of neurogenic inflammation (Yam et al., 2018).

During inflammation, multiple mediators, including PGE_2 and bradykinin, enhance TRPV1 activity and expression, increasing receptor density at the plasma membrane and amplifying nociceptive responses to capsaicin (Jang, Kim, and Hwang, 2020; Meng et al., 2016). PGE_2 plays a central role: its overproduction in injured tissues directly sensitises nociceptive fibres, enhances other pro-nociceptive signals, and promotes neuropeptide release, all of which act to potentiate TRPV1 (Jang, Kim, and Hwang, 2020). Supporting its functional relevance, TRPV1-deficient mice exhibit markedly reduced nociceptive behaviours and pain responses (Moriyama et al., 2005).

Mechanistically, after PGE_2 binds EP_4 and EP_1 receptors on sensory neurones, the subsequent release of SP and CGRP establishes a positive feedback loop that reinforces nociceptive signalling (Jang, Kim, and Hwang, 2020; Ma, 2010). These signalling pathways promote receptor trafficking of both EP_4 and TRPV1 to the plasma membrane, enhancing excitability and potentially contributing to chronic pain states (Ma et al., 2016; Ma and St-Jacques, 2018; St-Jacques and Ma, 2013).

TRPV1, itself, engages in a self-reinforcing loop that sustains sensitisation. Upon activation, calcium influx stimulates anandamide synthesis, providing endogenous ligand-driven reactivation (Stelt et al., 2005). Over longer timescales, TRPV1 activation upregulates genes that promote post-translational modifications - such as phosphorylation by PKA and PKC - that enhance channel gating and membrane localisation (Linley et al., 2010; Ma et al., 2016; Moriyama et al., 2005).

Together, this bidirectional interplay between inflammatory signalling and TRPV1 function represents a key mechanism underlying persistent pain states. It may also explain the sustained capsaicin hypersensitivity observed in inflammatory models.

Capsaicin

Capsaicin, the active component of chilli peppers, binds to TRPV1 to elicit a burning sensation and is widely used to probe nociceptive neurone excitability (Caterina et al., 1997). Notably, several species, including rabbits, chickens, tropical clawed frogs, and zebrafish, show reduced capsaicin sensitivity despite expressing TRPV1 orthologues, due to evolutionary divergence in the vanilloid binding domain that limits capsaicin-induced channel activation (Saito and Saito, 2025).

Capsaicin is extensively employed in both *in vitro* and *in vivo* models of pain. *In vivo*, it can be applied topically or injected into joints, soft tissue, or the spinal cord to rapidly induce acute pain behaviours via TRPV1 activation and sensory neurone depolarisation (Latremoliere and Woolf, 2009; Willis, 2009; Zhou et al., 2019). These responses often evolve into long-lasting hyperalgesia and allodynia. Repeated skin exposure not only triggers burning pain and primary hyperalgesia, but can also induce secondary hyperalgesia through central sensitisation mechanisms (Latremoliere and Woolf, 2009; Willis, 2009).

Paradoxically, prolonged TRPV1 activation can lead to desensitisation and even degeneration of TRPV1-expressing neurones (Lin et al., 2006; Stelt et al., 2005).

Sustained intracellular Ca^{2+} elevation, following repeated stimulation, underlies this effect, forming the mechanistic basis of capsaicin's analgesic potential. As a promising therapeutic agent for neuropathic pain, capsaicin is capable of selectively silencing hyperactive nociceptive neurones (Hehn, Baron, and Woolf, 2012).

1.8 Glia-Neurone Communication

Among the non-neuronal contributors to pain, glial cells - particularly astrocytes and microglia - play a crucial role. Once considered passive structural support or "glue", glia are now recognised as dynamic regulators of development, homeostasis, metabolism, and neurological disease across both the CNS and PNS (Kwon and Koh, 2020).

Glial cells play a central role in neuroinflammation and pain modulation. In response to injury or pathological stimuli, they become activated and adopt reactive phenotypes, characterised by the release of pro-inflammatory cytokines, chemokines, and bioactive molecules, such as ATP and prostaglandins (Ahmad et al., 2022; Baufeld et al., 2018; Cheng, Xu, and Ma, 2022; Souza et al., 2013). These mediators profoundly influence glia-neurone communication, altering neuronal excitability, synaptic strength, and plasticity (Cheng, Xu, and Ma, 2022). Thus, activated glia not only respond to neuronal activity but actively shape it, contributing to the initiation and maintenance of persistent pain states.

Microglia, the resident immune cells of the nervous system, respond rapidly to tissue damage. They detect environmental changes, remodel synapses, maintain myelin homeostasis, and defend against pathological insults (Zhan et al., 2014). Surface receptors such as toll-like receptors (TLRs) recognise PAMPs and DAMPs, triggering retraction of microglial processes and the adoption of an amoeboid morphology. Microglial migration and the release of inflammatory mediators including IL-1β, TNF-α, IL-6, and chemokines also occurs (Baufeld et al., 2018). These signals act on astrocytes and neurones, amplifying the inflammatory cascade. Mi-

crogliosis is characterised by upregulation of markers such as cluster of differentiation 11b (CD11b), CD68, and ionised calcium-binding adapter molecule 1 (Iba1; Ma et al., 2021; Roblain et al., 2021). If microglial activity is insufficient to clear pathological stimuli, they recruit astrocytes to mount a broader response (Liddelow et al., 2017).

Astrocytes provide essential support for neuronal homeostasis, including blood-brain barrier integrity, regulation of cerebral blood flow, metabolic support, synaptic modulation, and extracellular ion balance (Cheng, Xu, and Ma, 2022; Kwon and Koh, 2020). Inflammatory signals from microglia stimulate astrocytes to initiate secondary immune responses. Upon activation, astrocytes hypertrophy by reducing the number of processes and cross-sectional area, and they may form astroglial scars around sites of inflammation (Liddelow et al., 2017). They release cytokines (e.g., TNF-α, IL-1β), chemokines (e.g., CCL2, CXCL1), growth factors, and proteases that modulate microglial behaviour and enhance neuronal hypersensitivity (Cheng, Xu, and Ma, 2022). Markers such as glial fibrillary acidic protein (GFAP) are upregulated during astrogliosis (Ma et al., 2021).

Beyond classical soluble mediators, glial cells also communicate with neurones via EVs - lipid bilayer-bound particles that deliver proteins, lipids, and non-coding RNAs to recipient cells (Section 1.3.1.6; Ahmad et al., 2022). Recent studies show that glial-derived EVs are internalised by neurones and modulate their function, particularly under inflammatory conditions (Ahmad et al., 2022; Prada et al., 2018; Zhu et al., 2025). For example, activated glia release EVs enriched in inflammatory miRNAs that influence neuronal gene expression and excitability. These vesicles may serve as key mediators of neuroimmune crosstalk, contributing to nociceptive neurone sensitisation and persistent pain (Prada et al., 2018). However, the precise mechanisms by which glial EV cargo shapes sensory neurone plasticity remain incompletely defined.

Growing evidence highlights the importance of glial cells in modulating sensory

neurone excitability, both through classical inflammatory mediators and through EVs. In particular, glial-derived EVs carrying inflammatory cues, such as miRNAs, have emerged as potent regulators of neuronal function in pain (Morchio et al., 2023). Understanding how EV-mediated glia-neurone communication drives nociceptive neurone sensitisation is therefore essential, not only for advancing basic neurobiology but also for identifying novel therapeutic targets.

1.9 *In vitro* Models for Investigating Pain Mechanisms

Peripheral tissues are targeted by many diseases, often accompanied by inflammation and painful sensation. Sensory neurones are continuously exposed to a dynamic and frequently hostile microenvironment, encountering a wide array of signalling molecules, inflammatory mediators, and invading pathogens. This persistent exposure places them at the forefront of neuroimmune interactions, requiring them to actively modulate their function and maintain cellular integrity in response to environmental stressors (Dubin and Patapoutian, 2010). Understanding how sensory neurones adapt to these challenges is crucial for uncovering the mechanisms underlying pain processing.

As primary afferents form the initial stage of the pain pathway, *in vitro* sensory neurone cultures provide a tractable and highly informative platform for modelling nociception, encompassing both the cellular and molecular processes involved in the detection and transmission of noxious stimuli (Dubin and Patapoutian, 2010). These models offer several advantages over *in vivo* approaches: they are more cost-effective, reduce ethical concerns, and enable high-throughput experimentation (Chrysostomidou, Cooper, and Weir, 2021).

Compartmentalised Cell Culture Systems

A key advantage of *in vitro* systems is the ability to precisely manipulate the cellular environment (Tsantoulas et al., 2013). Inflammatory mediators can be applied directly to cultures to model sensitisation, with exposure protocols tailored to mimic

acute or chronic conditions (Kimourtzis et al., 2024; Malty et al., 2016; Pope et al., 2025). This flexibility is particularly valuable for investigating dynamic processes, such as hyperalgesic priming and prolonged sensitisation, which contribute to the transition from acute to chronic pain (Malty et al., 2016; Reichling and Levine, 2009).

Importantly, cultured primary sensory neurones retain key molecular features of nociceptive neurones, including the expression of ion channels and receptors such as TRPV1, TRPA1, TRPM8, and $P2X_3$ (Giorgi et al., 2023; Wang, Li, and Huang, 2007). Many nociceptive neurones are polymodal, capable of detecting mechanical, thermal, and chemical stimuli, making them highly relevant for mechanistic studies (Tominaga et al., 1998). This molecular diversity not only facilitates dissection of nociceptive signalling and plasticity but also highlights these neurones as promising targets for novel analgesic development (Amir, Michaelis, and Devor, 1999; Krames, 2014).

Dissociated DRG cultures have long provided a foundational platform for mechanistic studies. Advances in *in vitro* modelling - particularly the development of compartmentalised culture systems - have significantly expanded the ability to dissect subcellular processes in sensory neurones. These systems vary in complexity depending on the experimental aim. Commercially available microfluidic chambers, for instance, enable fluidic isolation between compartments, allowing selective stimulation or manipulation of axons, somata, or other cell types (Figure 2.1; Atmaramani et al., 2021; Kimourtzis et al., 2024; Lucci et al., 2020; Tsantoulas et al., 2013). Within these chambers, differential fluid volumes can sustain a chemotactic gradient, promoting axonal extension through microgrooves into the distal compartment (Atmaramani et al., 2021). Simpler configurations, such as Boyden chambers (also referred to as Twiss chambers or membrane inserts), offer physical separation and remain valuable for studying directional signalling and cell-cell interactions (Willis, 2009).

This spatial segregation is particularly relevant given the extreme anatomical polarity of DRG neurones, which possess some of the longest axons in the nervous system (Sörnmo and Laguna, 2005). Their somata reside in a distinct microenvironment from both peripheral and central terminals (Esposito et al., 2019). Microfluidic systems help recapitulate this anatomical separation, capturing a critical yet often overlooked feature of the pain pathway: the compartmentalised signalling landscape of DRG neurones (Kimourtzis et al., 2024; Tsantoulas et al., 2013).

System selection should be guided by the specific experimental question. As discussed in Section 1.3.1.5, the length and complexity of sensory neurone axons (Sörnmo and Laguna, 2005) necessitate local translation to coordinate rapid responses to microenvironmental changes (Holt, Martin, and Schuman, 2019). Compartmentalised chambers enable investigation of these spatially restricted processes by allowing targeted manipulation of one subcellular domain without perturbing the rest of the cell. For example, RNA interference or degradation strategies can be applied specifically to the axonal compartment to determine whether particular transcripts are required locally (Section 1.3.1.5; Gumy et al., 2011; Lucci et al., 2020; Mesquita-Ribeiro et al., 2021; Mesquita-Ribeiro, 2019).

Co-Culture

These systems also offer flexibility for co-culture approaches. Cells can be seeded into one compartment, and their interactions with other cell types observed as they extend processes or migrate through membranes or microgrooves into adjacent compartments (Giorgi et al., 2023; Tsantoulas et al., 2013). For instance, macrophages may actively migrate across physical barriers such as porous membranes or microchannels (Liu et al., 2025), while neurones extend axons through microgrooves into a separate compartment which could contain other cell types (Atmaramani et al., 2021; Tsantoulas et al., 2013). This set-up is particularly useful for modelling the local microenvironment of a specific neuronal domain. For example, the central terminal of a sensory neurone is likely to interact with a diverse range

of cells in the dorsal horn, including interneurones, projection neurones, and motor neurones, as well as non-neuronal cells such as astrocytes, microglia, endothelial cells, and infiltrating immune cells (Brewer and Baccei, 2020; Esposito et al., 2019). In addition to direct co-culture, conditioned media from other cell types (Ma et al., 2021; Varcianna et al., 2019) could also be applied compartmentally, providing an alternative means to study secreted factors and their compartment-specific effects.

1.9.1 Therapeutic Relevance

Nociceptive neurones are attractive therapeutic targets due to their essential role in initiating and maintaining pain states. They also have a unique anatomical position outside of the blood-brain barrier (BBB), which makes them accessible to systemically administered drugs without central side effects (Middleton et al., 2021). While targeting peripheral nociceptors can effectively reduce pain by preventing the initiation of central sensitisation, direct modulation of central terminals or spinal cord circuits may be required to reverse established central sensitisation. While peripheral nociceptors are readily accessible to systemically administered drugs, established central sensitisation - driven by changes at central terminals and spinal circuits - may require interventions that reach the CNS, such as intrathecal delivery or BBB-permeable compounds (Ho et al., 2020; Hua et al., 2005). Targeting peripheral input can also indirectly reduce central sensitisation by limiting ongoing nociceptive drive.

While much attention has been given to ion channels and signalling proteins in nociceptive processing, emerging evidence highlights the importance of post-transcriptional regulation, particularly by miRNAs, in driving nociceptive neuronal signalling during chronic pain (Morchio et al., 2023). These small non-coding RNAs fine-tune gene expression and may shape key processes such as sensitisation and synaptic remodelling (Boese et al., 2016; De Vito et al., 2022).

In vitro primary sensory neurone cultures are invaluable tools for dissecting the cellular and molecular mechanisms underpinning these processes. They have been widely used to study synapse formation, neurotransmitter release, ion channel activity, action potential generation, and axon development (Melli and Höke, 2009). By isolating neurones from the complex *in vivo* environment, these models allow for precise experimental control over extracellular cues (Owen and Egerton, 2012), facilitating the dissection of specific pathways involved in neurodevelopment, plasticity, and disease.

Sensory neurones can be cultured from embryonic, postnatal, or adult animals, using either explant or enzymatic dissociation methods (Owen and Egerton, 2012; Loreto and Gilley, 2020). The choice of donor age and culture technique depends on the experimental question: embryonic cultures offer higher yield and viability for developmental studies, while adult-derived cultures better model mature nociceptive responses and pain-related changes. Some culture ages may also require the addition of serum or trophic factors to support survival and growth, although these supplements can, themselves, modulate excitability and sensitise neurones (Owen and Egerton, 2012). Each approach has distinct advantages and must be tailored to the study's goals.

1.9.2 Embryonic Neuronal Culture

Embryonic neurones are typically easier to culture; a greater number of cells can be obtained per animal (Owen and Egerton, 2012) and the isolation process is more efficient compared to postnatal or adult tissue. Crucially, embryonic models are ideal for investigating neurodevelopmental processes such as synaptogenesis, pruning, and axonal pathfinding, as well as for studying peripheral neuropathies, neurodegenerative diseases, early-life neuropathologies, and drug screening (Melli and Höke, 2009). Embryonic DRG neurones are also particularly well-suited for use in compartmentalised microfluidic cultures due to their high cellular yield and robust axonal outgrowth, which are essential for achieving sufficient axon cross-

ing between compartments that require dense seeding for directional growth and chemotactic responsiveness. However, they rely on trophic factors, such as NGF, and display heterogeneity to a lesser degree (Owen and Egerton, 2012).

1.9.3 Postnatal Neuronal Culture

During the postnatal period, sensory neuronal circuitry and pain processing mechanisms continue to undergo significant maturation, particularly with respect to the development of descending modulatory systems that regulate nociceptive signalling (Hathway et al., 2009). Postnatal DRG neurones thus occupy an intermediate developmental state between embryonic and adult neurones, combining the higher cellular yield and culture viability of embryonic tissue with more functionally mature features characteristic of adult neurones (Owen and Egerton, 2012). This balance makes postnatal DRG cultures a valuable model for investigating developmental transitions in nociception and the progressive refinement of pain pathways.

1.9.4 Adult Neuronal Culture

For the investigation of pain mechanisms - particularly chronic and inflammatory pain, which predominantly affect adults (Goldberg and McGee, 2011) - it is ideal to culture DRG neurones from adult animals. These neurones originate from fully developed systems with refined sensory circuitry, offering greater translational relevance for modelling adult pathophysiology (Brewer and Baccei, 2020). However, their use is constrained by several practical limitations. Yields per animal are substantially lower, necessitating a greater number of animals to obtain sufficient cell numbers for experimentation. Moreover, the dissociation process is more labour-intensive due to increased connective tissue and myelination, often requiring additional enzymatic digestion, mechanical trituration, and post-dissociation purification steps to isolate viable neurones (Owen and Egerton, 2012).

Despite these challenges, both embryonic and adult DRG models offer distinct ad-

vantages. Demonstrating consistent findings across both systems may strengthen the validity and translational relevance of experimental outcomes, particularly when investigating age-dependent mechanisms of pain.

1.9.5 Assessing Excitability of *in vitro* Neurones

Assessing neuronal excitability is essential for understanding how sensory neurones encode stimuli and contribute to pathological pain mechanisms. Neuronal excitability in *in vitro* cultures can be measured in a variety of ways, including patch-clamping, microelectrode array (MEA), and by using fluorescent dyes. Patch-clamping involves applying a glass microelectrode to the plasma membrane of a cell, applying a known voltage or current to it and measuring the resultant current or voltage. Although useful for investigating cell dynamics, just one cell can be recorded from at one time. In microfluidic chamber studies, holes would need to be made in the material in order to access the cells, or additional open-channel devices would have to be purchased (Tsantoulas et al., 2013). Microelectrode arrays record the local field potentials within complex neuronal networks. Unfortunately, MEA provides a low signal-to-noise ratio, poor cell adhesion, and low spatial resolution (Ferrea et al., 2012; Lopes, Mateus, and Aguiar, 2018). Voltage dependent dye accumulation or exclusion from cells can be quantified, enabling spatiotemporal assessments of all cells within a field of view. These can be categorised into indirect dyes, which measure neuronal action potentials by measuring ion concentration changes (such as Ca^{2+} or Na^{+} ions), and direct dyes, which are plasma membrane-bound and therefore can respond directly to any membrane potential changes (Khadria, 2022).

Another widely used approach is calcium imaging - a microscopy technique that employs fluorescent dyes which increase in intensity upon binding Ca^{2+} ions. This method provides an indirect, yet sensitive, measure of neuronal activation, as intracellular calcium levels rise in response to depolarisation and receptor-mediated signalling (Figure 1.11). Calcium imaging also enables measurement of calcium

transients above and below action potential threshold with high spatial resolution (Bayat et al., 2021). Fluorescence intensity can be quantified within tissues, cells, or subcellular compartments to infer excitability. As outlined in Section 1.3.1.2, cellular activation triggers Ca^{2+} influx from the extracellular space and mobilises Ca^{2+} from intracellular stores such as the endoplasmic reticulum. Calcium signalling is particularly informative in neuronal systems due to its compartmental specificity and calcium's involvement in processes such as neurotransmitter release, gene expression, and synaptic plasticity (Mattson, 2007).

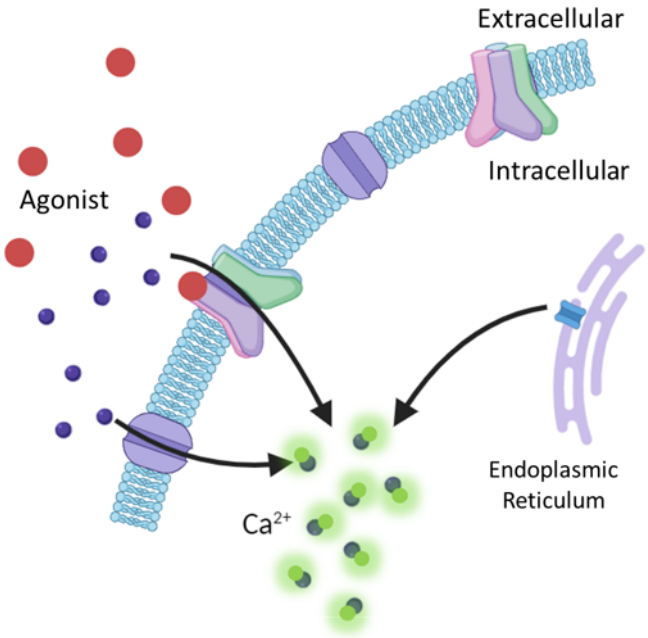


Figure 1.11. Calcium Imaging Mechanism. Calcium imaging is a microscopy technique used to measure neuronal excitability by detecting changes in intracellular calcium levels. When a neurone is activated, for example by the binding of an agonist, calcium ions (Ca^{2+}) enter the cell through voltage-gated calcium channels and ligand-gated receptors. Ca^{2+} is also released from intracellular stores, such as the endoplasmic reticulum. Calcium-sensitive fluorescent dyes bind to Ca^{2+} and emit fluorescence in proportion to the calcium concentration. The intensity of this fluorescence is measured over time, allowing quantification of neuronal activity. Created using BioRender™.

A wide range of calcium indicators are available, each with distinct properties such as excitation and emission wavelengths, calcium-binding affinities, and specificities. These indicators are selected based on the cell type, experimental conditions, and desired resolution of calcium dynamics. Fluorescent calcium dyes such as Fluo-4 and Fluo-5 increase their fluorescence intensity upon binding Ca^{2+}, en-

abling real-time monitoring of intracellular calcium fluctuations. Analogues including Fluo-5F, Fluo-5N, and Fluo-4FF possess lower calcium-binding affinities than Fluo-3 and Fluo-4, making them particularly suitable for detecting higher calcium concentrations (1 μM to 1 mM) that would otherwise saturate high-affinity indicators (Paredes et al., 2008; Thomas et al., 2000). These fluorescent dyes are all examples of single wavelength non-ratiometric dyes, but ratiometric indicators - which shift the peak wavelength of the excitation or emission curve following binding of calcium - can be calibrated more precisely, thereby minimising issues such as leakage of dye, photobleaching, and uneven loading. Examples include Fura-2 and Indo-1 (Paredes et al., 2008).

In this thesis, calcium imaging is used as an indirect measure to assess how inflammatory mediators, and extracellular vesicles alter sensory neurone excitability. Fluo-5F was chosen over Fura-2 for its lower Ca^{2+} affinity and higher brightness, making it better suited for detecting large, rapid calcium transients in live sensory neurones with high signal-to-noise and minimal technical complexity.

1.10 Scope of the Thesis

The work presented in this thesis investigates how inflammatory molecules contribute to the sensitisation of sensory neurones at the subcellular level and explores potential mRNA targets for modulating this process. Particular attention is given to the pro-inflammatory molecule PGE_2 at the peripheral terminal of sensory neurones and to the role of glial cells at the central terminal and their release of EVs, which may serve as vehicles for sensitising signals, including miRNAs. An overview of the experimental chapters is provided below:

Chapter 3 details the establishment and optimisation of *in vitro* models of sensory neurones, using both dissociated and compartmentalised culture systems. These models were used throughout the thesis to investigate axonal growth and neuronal excitability, the latter assessed via calcium imaging. Using these platforms,

PGE_2 was shown to sensitise distinct subcellular compartments of sensory neurones.

Chapter 4 investigates the molecular mechanisms underlying PGE_2-induced sensitisation. Our lab's recent transcriptomic analysis (RNA sequencing) was used to identify differentially expressed genes following PGE_2 treatment. *Tnfrsf12a* emerged as a key candidate transcript and was functionally validated using siRNA-mediated knockdown and calcium imaging to assess its role in sensitisation. Knockdown was confirmed by qPCR of the *Tnfrsf12a* transcript.

Chapter 5 focuses on the contribution of glial cells to sensory neurone sensitisation, with a spinal cord-derived mixed glial culture which was optimised and used to produce EVs under inflammatory conditions. Their functional impact on sensory neurone excitability was assessed, and miR-146a-5p was identified as a key inflammatory cargo. Inhibition of miR-146a-5p prevented EV-induced sensitisation, highlighting its potential as a therapeutic target.

Chapter 6 synthesises the thesis findings to highlight key mechanistic and translational insights. It contextualises how PGE_2 sensitises sensory neurones via compartment-specific signalling and *Tnfrsf12a*-mediated pathways, and how glial EVs - particularly containing miR-146a-5p - contribute to excitability. Together, these discoveries advance our understanding of neuroimmune modulation and identify novel therapeutic targets for pain.

Chapter 2

General Materials and Methods

2.1 Animal Husbandry

C57BL/6J mice (Charles River, UK) were bred and group-housed at the University of Nottingham, UK, in accordance with the Animals (Scientific Procedures) Act 1986/2012. Schedule 1 procedures were conducted according to the relevant guidelines for age and species. To adhere to the NC3R principles, all animal dissections and tissue collections were carefully planned to ensure maximal tissue was used, both from the pregnant dam and from the embryos (embryonic sex was not determined at the time of collection).

Due to temporary closure of our local animal facility in 2023, C57BL/6J mice were purchased from Charles River, UK, until early 2025. The long transport and associated stress appeared to affect neuronal viability and culture outcomes during this period, particularly in microfluidic experiments described in Chapter 4. Producing sufficient viable compartmentalised microfluidic chambers for these experiments required extended time, as many preps had to be discarded due to insufficient axon crossing or low cell viability. Consequently, fewer preparations were available, and with the usual number of researchers sharing them, this reduced the number of cells available per person. All procedures were conducted in accordance with relevant ethical guidelines.

2.2 Dissection to Expose the Dorsal Root Ganglion

Dissection tools were sterilised by soaking in 70% ethanol, followed by rinsing in Dulbecco's Phosphate Buffered Saline (DPBS) without calcium chloride and magnesium chloride (D8537, Sigma). At E16.5, embryos were obtained from pregnant dams. Decapitated embryos were positioned face-down, perpendicular to the dissector, with the caudal end oriented to the left. Using curved dissecting forceps to stabilise the embryo, a midline incision was made along the ventral surface using sprung scissors, extending from the neck to the caudal end. Care was taken to cut through the ribs without damaging the underlying spinal cord. The overlying skin

and muscle were gently retracted to expose the spinal cord. The spinal cord was then carefully removed in a single, continuous motion using forceps, starting caudally and peeling rostrally to reveal the DRGs. DRGs were individually extracted from the intervertebral foramina using fine forceps and placed into 3 mL Leibovitz's L-15 medium (1X, Gibco), taking care to minimise inclusion of meningeal tissue. For explant culture, DRG explants were kept at 4°C in L-15 until seeding (skip to Section 2.3.3).

2.3 Culture of Dorsal Root Ganglia

Protocols relating to preparation for cell culture, and cell culture itself, were performed aseptically within a class II cabinet.

2.3.1 Preparation for Cell Culture

Cell culture dishes were purchased sterile and cell culture treated. Before use, coverslips were soaked in 70% ethanol and left to airdry in a Class II cabinet overnight. Dishes, coverslips within dishes, and membrane inserts were coated with poly-L-lysine (PLL, Sigma P1524), at varying concentrations depending on the experimental system, the day before dissection:

- For compartmentalised microfluidic chambers (MFCs), 0.1 mg/mL PLL (diluted in sterile distilled water, dH_2O) was applied to each Nunclon™ dish (nunc, 35 mm, Thermo Fisher Scientific, 153710) or coverslip within a nunc.
- For Boyden chambers, 0.02 mg/mL PLL was used on nunc dishes, while 1 mg/mL PLL was applied to both the upper and lower surfaces of the porous membrane inserts to ensure adequate coating.
- For dissociated cultures, 0.02 mg/mL PLL was applied to dishes.
- For explant culture, 0.1 mg/mL PLL was applied to nunc dishes.

Dishes were incubated at 37°C for one-two hours, washed twice with dH_2O, and airdried overnight in a class II cabinet.

Compartmentalised Microfluidic Chambers

New two-channel, polydimethylsiloxane (PDMS) compartmentalised microfluidic chambers with a 150 μm microgroove barrier and a channel length of $\sim$22-23 mm (Figure 2.1; Xona Microfluidics®, SND150) were placed, channel side down, in a dish containing Hank's Balanced Salt Solution (HBSS, H9394, Sigma) and incubated at 37°C overnight. Chambers were washed twice with dH_2O and soaked in 70% ethanol, before they were left to dry in a Class II cabinet. Chambers that had previously been used were washed with 1% sodium dodecyl sulfate (SDS) in dH_2O overnight on a mechanical stirrer, the water replaced 4-6 times over the following days, before sonication for a few minutes in dH_2O and then in 70% ethanol. Microfluidic chambers were left to airdry in the Class II cabinet, used immediately, or stored sterilised in petri dishes and kept airtight with parafilm.

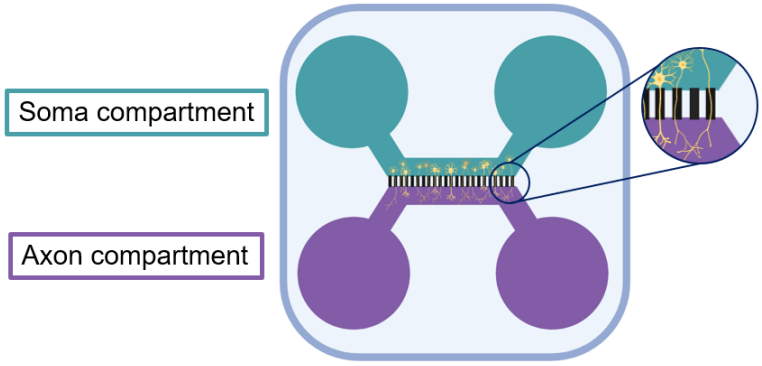


Figure 2.1. Compartmentalised Microfluidic Chamber. Compartmentalised microfluidic chambers, purchased from Xona Microfluidics®, were used to create two microenvironments for the axon terminals and cell somata to produce a more physiological *in vitro* model. Neurones cultured in compartmentalised microfluidic cultures have fluidically isolated axon terminals from their cell bodies to enable subcellular mechanistic investigations. Created using BioRender™.

One hour prior to seeding, compartmentalised microfluidic chambers were applied to nunc dishes (or coverslips in nunc dishes). 50 μL laminin (20 μg/mL, Sigma), diluted in high glucose DMEM (D6456, Sigma) was carefully applied to each channel of the chambers, to prevent the formation of air bubbles, and incubated at 37°C

for at least an hour before removal.

Boyden Chambers

In Boyden chambers (Figure 2.2), one hour prior to seeding, 500 μL of 20 μg/mL laminin (in DMEM) was applied to the centre of the nunc dish and above and below the porous membrane chamber insert. Dishes were incubated at 37°C for at least an hour before removal.

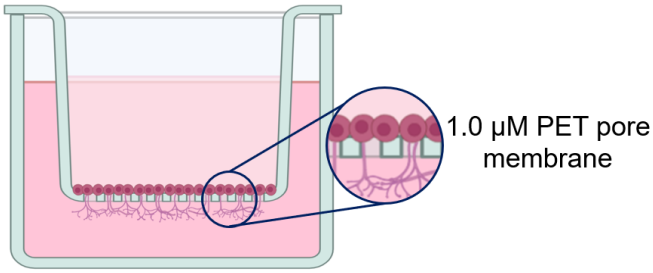


Figure 2.2. Boyden Chambers Were Used to Isolate Subcellular Compartments for RNA Extraction. DRG neurones were seeded on top of the porous membrane chamber insert and axons allowed to grow through the pores into the medium below. Axons could be axotomised and their RNA extracted, separate from their cell bodies. Created using BioRender™.

Dissociated Culture and Explants

For dissociated culture, 6-, 12- and 24-well plates (Costar®, Corning; CELLSTAR®, Greiner Bio-One), PDMS rings (fabricated in house, 11 mm diameter), or inverted chambers (8mm diameter wells) were used - if the microfluidic chamber channels had sheared, the chambers were repurposed by inverting them for use in small dissociated neuronal cultures. In this configuration, the compartmentalised channel was no longer functional, as the channel - normally located on the underside of the chamber - was positioned uppermost, resulting in discrete, non-connected wells rather than a compartmentalised system. Reusable PDMS rings and inverted chambers were sterilised and air-dried in the same manner as the microfluidic chambers.

One hour prior to seeding, PDMS rings or inverted chambers were applied to nunc dishes (or coverslips in nunc dishes). 20 μg/mL laminin (in DMEM) was applied to

the centre of the cell culture surface (volumes listed in Table 2.1) and incubated at 37°C for at least an hour before removal.

2.3.2 Dorsal Root Ganglion Extraction and Cell Dissociation

Once dissections were complete, the DRG explants were transferred via pipette to 3 mL 0.025% (w/v) trypsin (T9201, Sigma) in DPBS ($CaCl_2$/$MgCl_2$-free) and incubated for 20 minutes at 37°C. 5 mL 0.2% (w/v) collagenase type II solution (17101-015, Gibco) was prepared in DPBS ($CaCl_2$/$MgCl_2$-free), filter-sterilised using a 0.2 μm filter syringe (Starlab) and warmed to 37°C. Explants were transferred from trypsin into collagenase and incubated for 20 minutes at 37°C. DRG explants were removed from collagenase and added to 1 mL of resuspension medium (D6546 high glucose DMEM (Sigma), containing 10% (v/v) heat-inactivated foetal bovine serum (FBS, F9665, Sigma), 1% (v/v) glutaMAX™ (100X, Gibco) and 1% (v/v) Penicillin-Streptomycin (Sigma)), previously heated to 37°C.

Gentle mechanical disruption, using a pipette against the side of the Eppendorf tube, was used to dissociate aggregated cells and resuspend them in a homogeneous solution. After a five-minute centrifugation at 1000 x *g*, the supernatant was discarded and the cell pellet gently resuspended in the required volume of complete media (high glucose DMEM containing 1% (v/v) glutaMAX™, 2% (v/v) B27® supplement (50X, Gibco), 1% (v/v) Penicillin-Streptomycin, 50 ng/mL NGF 2.5S (Thermo Fisher Scientific), 50 ng/mL Glial-Derived Neurotrophic Factor (GDNF, Sigma) and 4 μM Aphidicolin (APH, Sigma)) for seeding. Complete media was supplemented with NGF and GDNF to promote neuronal proliferation and axonal outgrowth, and the DNA polymerase inhibitor APH to reduce the proliferation of non-neuronal cells (Mundy, Radio, and Freudenrich, 2010; Wu et al., 2021). Complete media - without NGF, GDNF, and APH - was stored at 4°C for up to three weeks. NGF, GDNF, and APH were added fresh to the required media volume on the day of use.

2.3.3 Seeding of Dorsal Root Ganglion Neurones

Compartmentalised Microfluidic Chambers

Laminin was removed immediately prior to seeding. To prevent cellular migration across the chamber and achieve fluidic isolation, 100 μL of DRG complete media was added to one side of the chamber to establish a hydrostatic gradient. On the opposite side, 10-15 DRGs (dissociated DRG explants not individual neurones) in 10 μL DRG complete media were seeded into the channel; most of the cell suspension was gently flushed into one end of the channel and the flow stopped by adding the remaining cell suspension to the other end of the channel. The same concentration of growth factors was maintained in media on both sides of the chamber. Media in the seeded compartment was topped up to 200 μL after a minimum of two hours. Fluidic isolation was reliably maintained by sustaining a volume imbalance between compartments and refreshing the cell medium every 48-72 hours. All treatments were applied to the axonal compartment, which was maintained at a lower volume than the somal compartment. As reported by Clark et al. (2018), molecular diffusion from lower- to higher-volume compartments did not occur until 96 hours, confirming that 24- and 48-hour treatments did not directly affect the cell somata.

Boyden Chambers

Following laminin removal, 25 DRGs were seeded in 100 μL DRG complete media on top of the porous membrane insert (Figure 2.2). Media was topped up to 1 mL 24 hours later and changed every 48-72 hours.

Dissociated Cultures

For dissociated cultures, DRG neurones were seeded in PDMS rings, in the wells of inverted MFCs, or 6-, 12- and 24-well plates. Cells were seeded in the centre of the wells, where the laminin coating had been applied - the number of DRGs

and the seeding volumes are listed in Table 2.1. Media volumes were topped up at least two hours post-seeding. Media was changed every 48-72 hours.

Explants

Explants were applied to 15 μL DRG complete media using forceps and media topped up the following day. Media was changed every 48-72 hours.

Table 2.1. The Variations in DRG Seeding Protocols in Different Culture Formats. Cells were cultured in compartmentalised microfluidic chambers and Boyden chambers, to maintain isolation of axon terminals from their cell bodies, or in various dissociated culture formats. Each required a different number of DRGs to be seeded for optimal growth, varying volumes of laminin and culture media.

Culture Format	**Volume of Laminin** (μL)	**Number of DRGs Seeded**	**Volume of Media DRGs Seeded In** (μL)	**Total Volume of Media** (μL)
Inverted chambers	10	1.5	20	100
PDMS rings	20	3	30	200
24-well plate	20	2	25	500
12-well plate	50	6	50	1500
6-well plate	100	20	100	2000
Microfluidic chamber	50 each channel	10-15	10	200 (plus 100 on other side)
Boyden chambers	500 above and below membrane	25	100	1000 above; 2000 below

2.4 Calcium Imaging

2.4.1 Loading of Calcium Indicator

Fluo-5F AM (F14222, Invitrogen™) is a single-wavelength, cell-permeant acetoxymethyl (AM) ester derivative of the calcium indicator Fluo-5. The AM ester groups facilitate membrane permeability, allowing intracellular loading of the dye. Fluo-5 has a lower binding affinity for intracellular calcium and, therefore, enables the detection of larger calcium transients (1 μM-1 mM), without saturating the fluorescent ligand response (Thermo Fisher Scientific, 2011). Using other dyes, such as Fluo-

4, would produce saturation within this range of detection (Paredes et al., 2008; Thomas et al., 2000).

454 μL of 20% Pluronic™-F127 in 20% DMSO (P3000MP, Invitrogen™) was added to 50 μg of Fluo-5F AM to produce a 100 μM stock and stored at -20°C in single-use aliquots. 1 μM Fluo-5F AM was created fresh on the day of the experiment by diluting 1 in 100 in imaging buffer (IB): 135 mM NaCl, 3 mM potassium chloride (KCl), 10 mM HEPES, 15 mM glucose in dH_2O, pH 7.4, and supplemented with 1 mM $MgSO_4$ and 2 mM $CaCl_2$ fresh for each experiment. The IB was maintained at pH 7.4 to mimic physiological extracellular conditions, ensuring normal neuronal responses to depolarisation with KCl and activation of TRPV1 by capsaicin. Due to extreme light-sensitivity, use of Fluo-5F AM was performed in red light conditions.

Compartmentalised Microfluidic Cultures

Cell culture media was removed from the somal side of compartmentalised microfluidic chambers, replaced with 100 μL 1 μM Fluo-5F AM, and incubated for 30 minutes at room temperature (RT; Figure 2.3A). Fluo-5F AM was removed and replaced with fresh 1X IB for a 30-minute de-esterification period; the AM ester group is cleaved from the Fluo-5, trapping it within the cell and enabling fluorescence upon binding of intracellular calcium (Lock, Parker, and Smith, 2015).

Before imaging, IB was removed from microfluidic devices. The nunc dishes containing the devices were directly mounted onto the microscope stage and a field of view within the somal compartment, close to the microgrooves, chosen as the image acquisition area.

Dissociated Cultures

Cell culture media was removed from the well and replaced with 100 μL 1 μM Fluo-5F AM and incubated for 30 minutes at RT (Figure 2.3B) before removal. 100 μL

IB was added for de-esterification for 30 minutes at RT and replaced with fresh IB prior to imaging. To account for dilution by IB present in the dish during imaging, the concentration of the stimulus added was adjusted accordingly. Nuncs were mounted directly on the stage and a field of view chosen close to the centre of the dish.

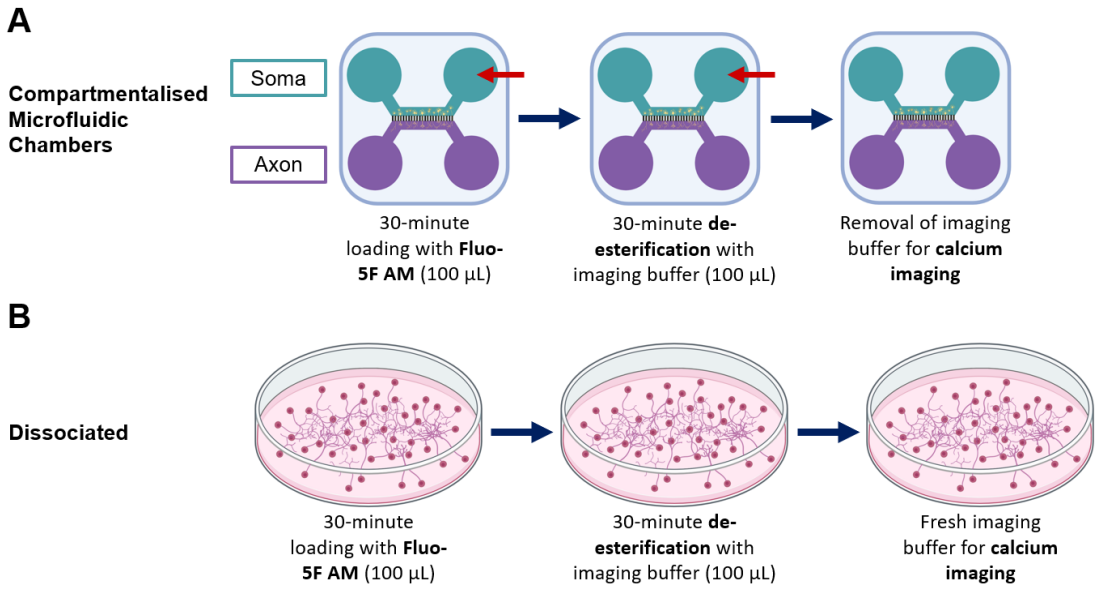


Figure 2.3. Calcium Imaging Dye Loading Protocol in Different Cell Culture Formats. **A -** Preparation for calcium imaging in compartmentalised microfluidic chambers. The fluorescent dye was added to the soma compartment of the chamber, before removal and replacement with imaging buffer to de-esterify the ester group in the dye. All imaging buffer was removed before imaging. Arrows indicate the compartment being manipulated. **B -** Preparation for calcium imaging in dissociated cultures. The fluorescent dye was incubated in the well, exposing cell somata and axon terminals, before removal and replacement with fresh imaging buffer for de-esterification of the dye. Imaging buffer was refreshed before imaging. Created using BioRender™.

2.4.2 Imaging Protocol

An Olympus IX70 Inverted tissue culture microscope (Olympus, Tokyo, Japan) was used to capture calcium transients, attached to a CoolLED pE excitation system (CoolLED Ltd., Andover, UK), PE-2 collimator, and an ORCA-R2 Hamamatsu Camera Controller C10600 (Hamamatsu Photonics, Hamamatsu City, Japan). Images were captured using the Multi-Acquisition function in Micro-Manager (MM-Studio Version 1.4.16), integrated with ImageJ. The imaging regimen consisted of acquiring fluorescent images at 470 nm excitation every 500 ms at 10x magnifi-

cation, with images saved as an image stack file. Exposure was set to 100 ms, binning to 2x2, the number of positions as 1, and the number of slices as 1.

Stimuli were reconstituted in IB: 100 nM or 200 nM capsaicin (M2028, Sigma) to activate nociceptive TRPV1$^+$ neurones, and 25 mM KCl to induce general neuronal depolarisation. Capsaicin is a nociceptive compound, which acts via TRPV1 receptors to generate an inflammatory response (Caterina et al., 1997). 100 nM and 200 nM capsaicin stimulations were selected because they are either side of the EC50 value for capsaicin's action on sensory neurones, previously reported by Lopshire and Nicol (1997).

Stimuli were gently applied using a pipette, either at the channel entrance of compartmentalised microfluidic chambers or directly onto dissociated cultures (Figure 2.4). The first stimulation time point was consistently set at 30 seconds into recording, allowing a stable baseline window (15 seconds) and accommodating minor manual timing variation (e.g., stimulation occurring a second or two early) without impacting baseline calculations. While automated delivery is conceptually possible, in practice aligning stimuli addition precisely with the channel entrance of a microfluidic chamber is challenging, so manual stimulation ensured accurate and reproducible stimulation. Axonal responses were always acquired first, with somal stimulation performed at the end of the assay to avoid desensitisation due to the larger Ca^{2+} influx typically observed upon direct somal stimulation (Bouskila and Bostock, 1998). A larger volume of stimulant was routinely applied to the somal compartment to ensure full exposure across the densely populated cell body region. In contrast, a smaller volume was used in the axonal compartment to minimise shearing of axons and to prevent dislodging of delicate neurites, while still achieving adequate coverage of the comparatively sparse axonal material. Coverage was visually confirmed under the microscope before proceeding with experiments.

Specific stimulation protocols and durations varied depending on the experimen-

tal question and are detailed in the relevant chapters. Calcium transients were recorded in cell somata, where the higher concentration of fluorescent indicators facilitates more reliable detection; although axonal signals can also be measured, they are typically less intense and more challenging to resolve.

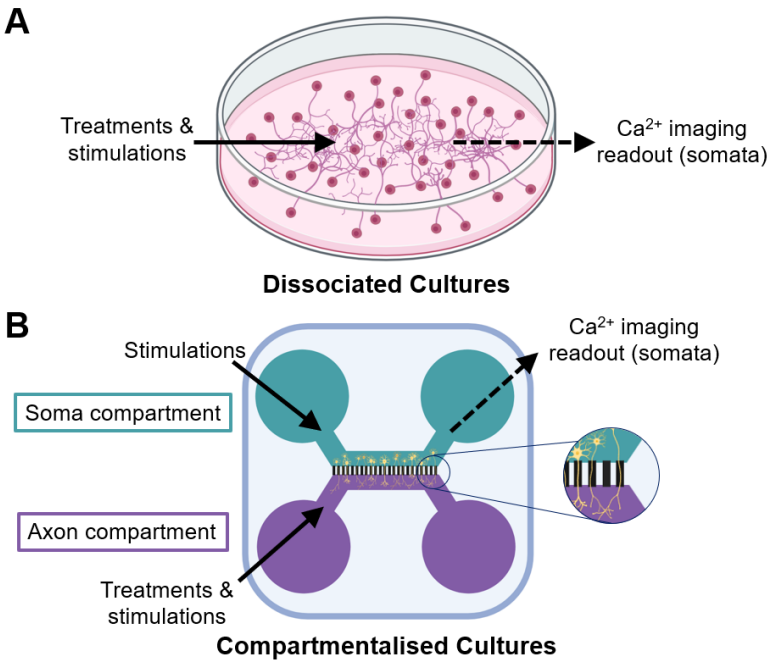


Figure 2.4. Calcium Imaging Methodology in Dissociated Cultures Versus Compartmentalised Microfluidic Chambers. A - In dissociated cultures, treatments and stimulations were added to the whole culture, interacting with axons and cell somata. Calcium transients were recorded from somata. **B -** In compartmentalised cultures, treatments were added to the axon compartment. Stimulations were applied to the channel entrance of soma and axon compartments. Calcium transients were measured in the cell somata. Created using BioRender™.

2.4.3 Calcium Imaging Analysis

Cells were selected as regions of interest on FIJI ImageJ (Fiji Is Just Image J, Version 1.54p, Schindelin et al., 2012) using the oval selection tool, and their area, mean, minimum and maximum fluorescence (mean grey intensity) measured at each of the time points (every 500 ms; Figure 2.5). Cultures were excluded from analysis if fewer than three cells exhibited fluorescence. In experiments using chambers, cases where fewer than three cells responded to the first axonal stimulation were interpreted as indicating a low number of axonal crossings. This suggested that such cultures were unlikely to have been adequately exposed to

pre-treatments, and therefore they were excluded from analysis for all subsequent stimulations. Experiments were included if they possessed at least two replicates for each treatment group.

Cells were selected as fluorescent responders to stimulations if their maximum relative fluorescent unit (RFU) value surpassed five standard deviations (STDEV) of their baseline. This thresholding step was used to exclude cells with unstable or spontaneous fluorescence, ensuring that only stimulus-evoked signals were quantified. Importantly, this approach does not bias selection toward high responders, as DRG neurones are normally quiescent and do not fluoresce spontaneously; rather, it reduces the likelihood of including false-positive signals in the analysis:

$$\text{Max RFU - Baseline} > 5 \text{ x STDEV of Baseline} \tag{2.1}$$

Peak responses were calculated by identifying the maximum fluorescence change for each individual cell and then averaging these values within each dish/culture. Calculating the peak from the population-averaged trace can underestimate the true response amplitudes, as asynchronous peak timings across cells reduce the apparent maximum. By quantifying peaks at the single-cell level before averaging, this approach accounted for temporal variability in cellular activation and provided a more accurate measure of response magnitude. This also means that the peaks of the averaged traces do not always appear directly comparable to those shown in the peak response graphs, but they contextualise the data by providing a more representative overall picture of the underlying cellular responses.

Fluorescence intensity, for each fluorescing cell, was normalised to baseline using basal readings recorded over 15 seconds prior to each stimulation. Fluorescence is expressed as $\triangle$F/F, where F is fluorescence intensity at a given time point (in RFU) and F_0 is baseline fluorescence intensity:

$$\frac{\Delta F}{F} = \frac{F - F_0}{F_0} \tag{2.2}$$

Following the averaging of peak responses for cells within a replicate, these values were then averaged within treatment groups. Changes in fluorescence were quantified as peak values plotted as bar charts, or spatiotemporal dynamics plotted over time (Figure 2.5).

Area under the curve was calculated on Microsoft Excel, where A is area, y_1 and y_2 are consecutive fluorescence values, and Δt is the time interval between measurements:

$$A = \frac{(y_1 + y_2)\Delta t}{2} \tag{2.3}$$

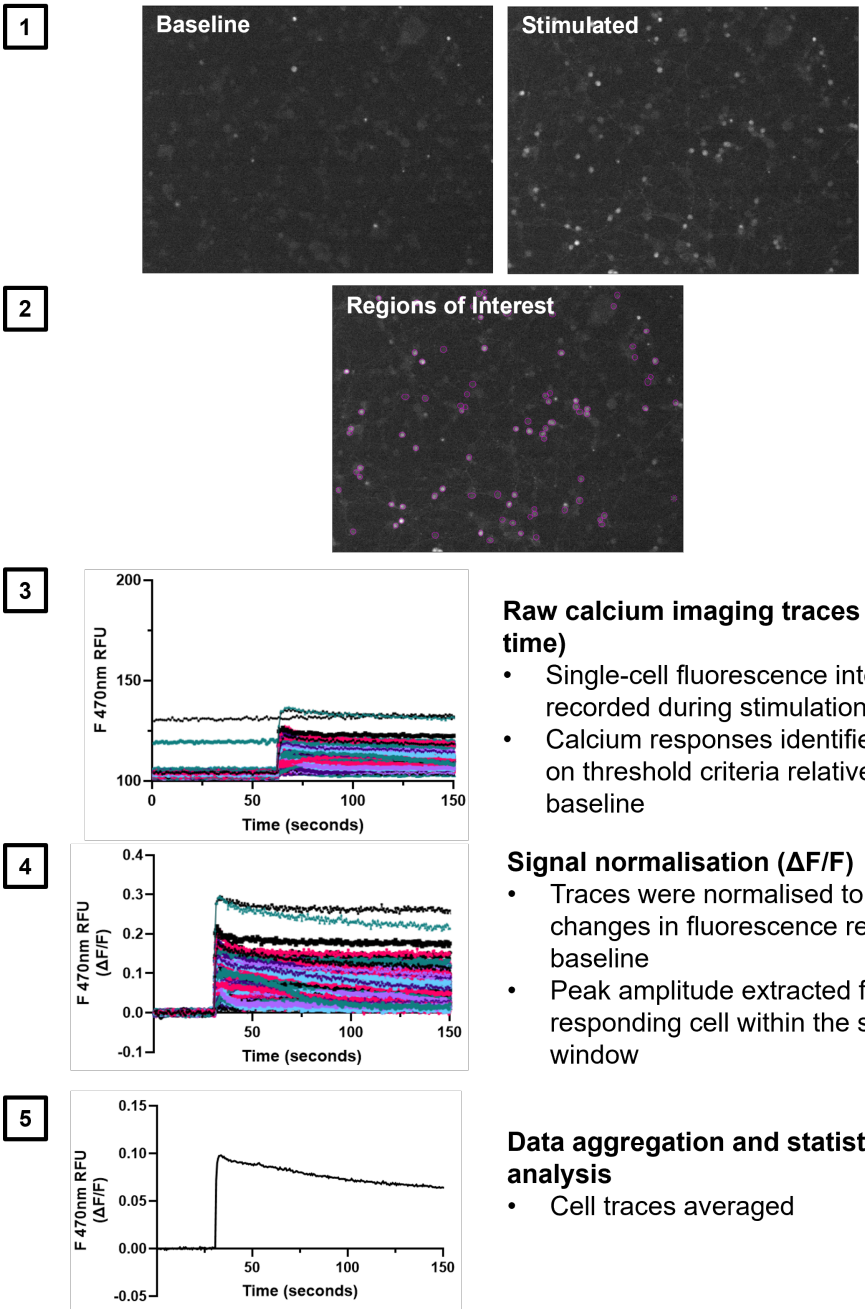


Figure 2.5. Calcium Imaging Analysis Step-by-Step Methodology. Calcium imaging stack files were opened in FIJI ImageJ (Schindelin et al., 2012). Regions of interest corresponding to individual cell somata were manually selected using the oval selection tool and saved as an RoiSet. Data were not plotted until the final stage of analysis, however, for illustrative purposes, representative single cell traces are shown at each stage of the analysis workflow in this diagram. Raw calcium imaging data for individual cells were baseline normalised by subtracting the mean baseline fluorescence (F_0) from the fluorescence value at each time point (ΔF), followed by division by the baseline value to generate $\Delta F/F$ traces. These normalised traces were used for all subsequent analyses. $\Delta F/F$ traces from individual cells within the same culture were averaged to generate a single trace per culture, representing a technical replicate. To combine data across cultures within the same treatment group, averaged traces were then averaged again to generate a biological replicate for statistical analysis. Individual peak values from single cells were also used to generate bar charts, allowing visualisation of the spread of responses within each treatment group.

Soma Diameter Analyses

To determine the percentage of neurones responding within different size categories, soma diameter was calculated from area measurements of DRG neurones that exhibited a stimulus-evoked response. Diameter bins were described in Section 1.3.1 (Table 1.1).

2.5 Brightfield Microscopy

Brightfield microscopy was performed using the Zeiss Axio Observer 10 (AX10; Zeiss, Germany) at 10x and 20x magnification. Images were taken using the Axiocam 305 mono digital camera, using Zeiss Zen Blue (Zen 2.6), and saved as CZI files. Scale bars were added on FIJI ImageJ (Schindelin et al., 2012) and exported as TIFF files.

2.6 Immunocytochemistry

2.6.1 Fixing Cells

Immunocytochemistry was used to visualise cell markers. At the experimental endpoint, compartmentalised microfluidic chambers, PDMS rings, or inverted chambers were gently prised away using forceps. Cells were incubated for 30 minutes at RT with 4% (w/v) paraformaldehyde solution (PFA, 10131580, Fisher Scientific) in 3.4% (w/v) sucrose, buffered with 1X DPBS (Dulbecco A, Thermo Fisher Scientific) and supplemented with 5 mM $MgCl_2$: to facilitate dissolution of PFA during preparation, 80 μL of 10 M NaOH was added and the solution was incubated at 55°C for 30-60 minutes until clear. Following addition of $MgCl_2$, transient cloudiness was resolved by drop-wise addition of $\sim$60 μL concentrated HCl to adjust to pH 7.4.

2.6.2 Washes and Incubations Prior to Staining

Cells were stored in 1X DPBS at 4°C until staining or immediately washed three times with 10 mM Glycine in DPBS for five minutes and then incubated in 10 mM Glycine (in DPBS)/0.2% (v/v) Triton® X-100 (Thermo Scientific) for 30 minutes at RT. Cells were washed with DPBS containing 0.1% (v/v) Triton® (DPBS/Triton) for five minutes three times, then incubated in 3% (w/v) bovine serum albumin (BSA, A7096, Sigma) in DPBS for 30 minutes at RT.

2.6.3 Antibodies

Primary antibody (Table 2.2) was diluted in 3% (w/v) BSA at the desired concentration and parafilm applied to the base of a dark humidified chamber. 50 μL of the antibody solution was added to the parafilm for each coverslip and the coverslip placed slowly cell-side down onto it. Cells were incubated in the humidified chamber at 4°C overnight.

Coverslips were washed three times in DPBS/Triton for five minutes. The appropriate secondary antibody (Table 2.3) was diluted in 3% (w/v) BSA at 1:300, along with 1:500 4',6-diamidino-2-phenylindole (DAPI), and 50 μL applied to each coverslip as before. Cells were incubated for two hours in a humidified chamber at RT. Coverslips were washed three times in DPBS/Triton for five minutes, once more with DPBS, and then mounted on slides with 15 μL Vectashield® Antifade Mounting Medium (H-1000-10, Vector Laboratories).

Anti-acetylated tubulin and anti-βIII tubulin were used to investigate neuronal structure and growth. Anti-EP4 identified the EP_4 PGE_2 receptor. Anti-GFAP and anti-Iba1 stained astrocytes and microglia, respectively.

Table 2.2. Primary Antibodies.

Primary Antibody	Dilution	Source	Provider	Reference Code
anti-acetylated tubulin	1:500	Mouse	Sigma-Aldrich	T7451
anti-βIII tubulin	1:300	Rabbit	Abcam	AB18207
anti-EP4	1:200	Rabbit	Bioss	BS-24918R
anti-GFAP (ASTRO6)	1:200	Mouse	Thermo Fisher	MA5-12023
anti-Iba1	1:200	Rabbit	Abcam	AB178847

Table 2.3. General Secondary Antibodies. All were purchased from Invitrogen™, apart from nuclear stain DAPI, which was obtained from Sigma-Aldrich.

Secondary Antibody	Dilution	Host Species	Fluor/Channel	Reference Code
anti-mouse IgG	1:300	Goat	568	A-11004
anti-mouse IgG	1:300	Goat	488	A11001
anti-rabbit IgG	1:300	Donkey	488	A-21206
anti-rabbit IgG	1:300	Goat	568	A11011
DAPI	1:500	N/A	405	D9542

2.6.4 Imaging

Fluorescent microscopy was performed using the Zeiss AX10 and Control Panel for Colibri 7 (423052-9751-000, Gottingen, Germany). Images were taken using the Axiocam 305 mono digital camera and exported as CZI files. Scale bars were added on FIJI ImageJ (Schindelin et al., 2012), and exported as TIFF files.

2.7 Statistical Analysis

Data were statistically analysed using GraphPad Prism 10. Normality was assessed using the Shapiro-Wilk test. For comparisons between two datasets, *t*-tests were used for parametric data, and Mann-Whitney U tests were used for non-parametric data. For comparisons against a normalised control value (e.g., RT-qPCR data where the control was set to one), one-sample *t*-tests were per-

formed. For three or more experimental groups, normal data were analysed using one-way ANOVA and Tukey's multiple comparison test of significance, and for non-parametric data, Kruskal-Wallis and Dunn's multiple comparison test of significance were employed. Significance was determined as $p < 0.05$. All data are presented as mean ± SEM.

Sample sizes were informed by pilot data and an a priori power calculation, which indicated that a minimum group size of $n = 3$ was sufficient to detect the expected effect size with 80% power at an α level of 0.05. Blinding was not used, as it was not practical to incorporate on a day-to-day basis. Biological replicates were defined as litters of mice derived from a single dam, while technical replicates were defined as individual chambers or dishes containing multiple neurones.

Chapter 3

Prostaglandin-E_2 Induces Sensitisation of Sensory Neurone Axons and Cell Bodies

3.1 Introduction

PGE_2 is a key inflammatory mediator that drives sensitisation of sensory neurones and contributes to pain hypersensitivity (Biringer, 2012; Ferreira, Moncada, and Vane, 1974; Jang et al., 2017; Kawahara et al., 2015; Kimourtzis et al., 2024; Ma et al., 2016; Malty et al., 2016; Moriyama et al., 2005; Southall and Vasko, 2001; St-Jacques and Ma, 2013; Vane et al., 1994; Wei et al., 2024). This chapter establishes the experimental models used throughout this thesis, and demonstrates PGE_2-induced sensitisation in dissociated DRG cultures and in compartmentalised systems, where axonal application produces both local and retrograde effects at the soma. In addition, it begins to explore underlying mechanisms, including the contribution of EP receptor subtypes and neurone subtype-specific responses.

3.1.1 The Utility of *in vitro* Models to Investigate Inflammation

In vitro models of sensory neurones are widely used to investigate the molecular mechanisms underlying inflammation and pain (Section 1.9). Their accessibility, ease of manipulation, and lower cost compared with *in vivo* approaches have made them central to pain research (Chrysostomidou, Cooper, and Weir, 2021). Inflammation is mediated by a diverse array of molecules and cell types (Linley et al., 2010), and the full impact of this complex process on neuronal function remains incompletely understood. Little is known about how inflammation affects distinct neuronal compartments, such as axon terminals versus cell somata or the axon, despite their importance for neuronal plasticity and pain chronification (Atmaramani et al., 2021; Clark et al., 2018; Giorgi et al., 2023; Tsantoulas et al., 2013).

Compartmentalised cell culture systems offer a way to address this problem. By fluidically isolating axon terminals from their somata, microfluidic platforms more closely replicate the cytoarchitecture of sensory neurones *in vivo*. This enables compartment-specific stimulation and readout, providing a powerful approach to

dissect the spatial dynamics of inflammatory sensitisation (Tsantoulas et al., 2013).

3.1.2 Current PGE_2 Knowledge

PGE_2 is a potent pro-inflammatory lipid mediator with a well-established role in inflammatory pain (Section 1.6; Jang, Kim, and Hwang, 2020; Kimourtzis et al., 2024). Following peripheral tissue damage, PGE_2 is synthesised downstream of COX-1/2 activation (Díaz-Muñoz et al., 2010) and released by immune cells (e.g., macrophages and neutrophils), fibroblasts, Schwann cells, and satellite glia (Jang, Kim, and Hwang, 2020).

The actions of PGE_2 are mediated via $EP_{1\text{-}4}$ GPCRs, whose downstream signalling varies by receptor subtype and cellular context (Table 1.2). In sensory neurones, PGE_2 enhances excitability through multiple mechanisms: it sensitises TRPV1 channels (Moriyama et al., 2005), modulates voltage-gated sodium currents (England, Bevan, and Docherty, 1996; Jang, Kim, and Hwang, 2020; Kimourtzis et al., 2024), facilitates purinergic $P2X_3$ signalling (Wang, Li, and Huang, 2007), and promotes store-operated calcium entry via Orai channels (Wei et al., 2024). Notably, PGE_2 preferentially enhances tetrodotoxin-resistant sodium currents, particularly those mediated by $Na_v1.8$, rather than tetrodotoxin-sensitive channels (Gold, Levine, and Correa, 1998). This selective modulation lowers the action potential threshold and supports sustained firing in nociceptive neurones.

PGE_2 signalling also enhances neurotransmitter release (Ma, 2010; Vasko, Campbell, and Waite, 1994) and amplifies immune responses (Tsuge et al., 2019). Collectively, these actions increase nociceptive neurone excitability and strengthen both peripheral input and central synaptic transmission, driving primary hyperalgesia and allodynia (Section 1.6.0.1; Kimourtzis et al., 2024; Moriyama et al., 2005; Wang, Li, and Huang, 2007) and contributing to central sensitisation (Latremoliere and Woolf, 2009). Notably, unlike many GPCR pathways, PGE_2 signalling resists desensitisation under chronic exposure, allowing sustained hypersensitivity during

prolonged inflammation (Malty et al., 2016).

The clinical relevance of this pathway is underscored by the widespread use of NSAIDs, which act by inhibiting COX-2-dependent PGE_2 synthesis. However, their limited efficacy and significant adverse effects (Section 1.6; Bindu, Mazumder, and Bandyopadhyay, 2020) highlight the need for more targeted approaches, informed by a detailed understanding of PGE_2 signalling in neurones.

3.1.3 Unanswered Questions in PGE_2 Signalling

Despite decades of study, key aspects of PGE_2 signalling remain poorly understood. Most *in vitro* studies have examined acute exposure, either as a stimulant during calcium imaging (Kimourtzis et al., 2024) or in short incubations prior to functional assays (Lopshire and Nicol, 1997; Zhou et al., 2019; Southall and Vasko, 2001; Stucky et al., 1996). Far less is known about how prolonged signalling drives persistent sensitisation (Malty et al., 2016; Ma and St-Jacques, 2018).

In addition, conventional dissociated cultures cannot resolve spatially distinct signalling. This is a major limitation given the compartmentalised architecture of sensory neurones (Atmaramani et al., 2021; Tsantoulas et al., 2013), where long peripheral axons transmit signals from sites of injury to the soma in the DRG and the central terminal within the spinal cord (Section 1.3.1; Esposito et al., 2019). Given that EP receptors are expressed on both axonal and somatic membranes (Moriyama et al., 2005; Southall and Vasko, 2001), this limitation also obscures potential compartment-specific mechanisms. Microfluidic studies have demonstrated that axonally restricted stimulation can evoke local depolarisation, initiate action potentials, and induce somatic calcium responses (Atmaramani et al., 2021; Clark et al., 2018; Kimourtzis et al., 2024; Tsantoulas et al., 2013). However, whether axonal PGE_2 receptor activation induces local translation, retrograde messaging, or other spatially distinct mechanisms of sensitisation remains an open question (Holt, Martin, and Schuman, 2019; Kaur and Sharma, 2012; Lucci et al., 2020).

3.1.4 Aims and Hypotheses

Hypotheses

I hypothesised that prolonged exposure (17 hours) to PGE_2 would sensitise sensory neurones, thereby providing a model of peripheral inflammation for mechanistic investigation. More specifically, I predicted that PGE_2 stimulation at axon terminals would induce local sensitisation capable of being retrogradely signalled to the soma, therefore modulating somatic responses.

Experimental Aims

To test these hypotheses, I aimed to:

- Culture embryonic mouse sensory neurones in compartmentalised systems, allowing fluidic isolation of axon terminals from their somata.
- Mimic prolonged peripheral insult by treating axonal compartments with PGE_2 overnight and assess whether this treatment could generate a model of neuroinflammatory sensitisation using calcium imaging.
- Investigate whether PGE_2-induced sensitisation at axon terminals could be communicated retrogradely to somata by stimulating the cell body directly during calcium imaging.

3.2 Methods

3.2.1 *In vitro* Neuronal Culture

E16.5 DRG sensory neurones were cultured in dissociated cultures or compartmentalised microfluidic cultures (Figure 3.1; Section 2.3.2 for methodology).

The initial experimentation and culture of DRG neurones, performed by Asta Arendt-Tranholm, was conducted in dissociated cultures within PDMS rings (Section 2.3.3;

Arendt-Tranholm, 2022). These experiments were used to establish the PGE_2-induced sensitisation model.

Subsequent subcellular investigations of PGE_2-induced neuronal sensitisation were performed in compartmentalised microfluidic chambers to ensure fluidic isolation of cell bodies from their axon terminals (Section 2.3.3).

3.2.2 PGE_2 Treatment

DRG sensory neurones were exposed to pro-inflammatory PGE_2 for a prolonged incubation time (17-24 hours) to induce an *in vitro* model of neuronal sensitisation.

Dissociated Cultures

PGE_2 (Cayman Chemical), was purged with gaseous nitrogen before resuspension in DPBS ($CaCl_2$/$MgCl_2$-free) to generate a 10 mM stock which was stored at -80°C. To maintain a consistent concentration of 10 μm, PGE_2 was diluted to its final working concentration in DRG complete media (Section 2.3.2 for components) and administered to DRG sensory neurones (day *in vitro* 7, DIV7) every two hours over a 24-hour period due to its instability and to produce a prolonged pro-inflammatory environment (Figure 3.1A). This was achieved without full media replacement, ensuring sustained exposure while minimising disturbance to the cells. An identical volume of DPBS ($CaCl_2$/$MgCl_2$-free) was used as a vehicle control and added to DRG neurones in the same manner as with PGE_2 every two hours for 24 hours.

Compartmentalised Microfluidic Cultures

A more stable form of PGE_2 was used for subsequent work in compartmentalised microfluidic chambers. 10 mg/mL 16,16-dimethyl prostaglandin E_2 (Tocris), dissolved in methyl acetate, was purged with gaseous nitrogen to evaporate the solvent. A 100 mM stock solution was established through reconstitution in dimethyl

sulfoxide (DMSO, D4540 Sigma) and stored at -80°C for up to six months.

DRGs were cultured until DIV6 to ensure extensive axon crossing through the microgrooves to the axon compartment; Clark et al. (2018) have demonstrated that, by DIV5, approximately 55 $\pm$ 5% of neurones have a projecting axon that reaches the axonal compartment and by DIV7 this increases to 76 $\pm$ 3%. On the experimental day (DIV6), a 10 mM solution was established through dilution in DPBS ($CaCl_2$/$MgCl_2$-free), before a final working concentration of 10 μM was obtained fresh by diluting in DRG complete media. 100 μL of the PGE_2-media solution was applied to the axon compartment of microfluidic chambers. 200 μL DRG complete media, without PGE_2, was added to the soma-enriched compartment (Figure 3.1B).

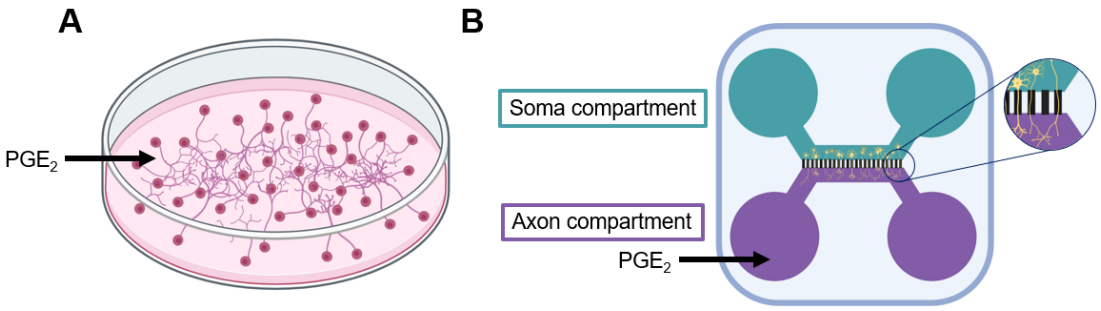


Figure 3.1. Sensory Neurone Culture Methodologies. A - In dissociated cultures, neurones were seeded in the centre of the well and allowed to interact and network freely. PGE_2 was applied directly to the culture media, interacting with the 'whole cell'. **B -** In compartmentalised microfluidic cultures, cells were seeded in one compartment of the chamber (soma-enriched compartment) to project through the microgrooves to the axon compartment. PGE_2 pre-treatments were applied to the axon compartment. Created using BioRender™.

For a vehicle control, DMSO was diluted 1 in 10 in DPBS ($CaCl_2$/$MgCl_2$-free), then 1:1000 in DRG complete medium (1:10 000 DMSO) and applied to cultures in a volume matched to that used for PGE_2 treatment. 200 μL DRG complete media was added to the soma-enriched compartment. Cultures were returned to the incubator for 17 hours until calcium imaging was performed.

PGE_2, applied to the axonal compartment, did not diffuse into the soma-enriched compartment due to the higher volume maintained there relative to the axonal com-

partment, as discussed in Section 2.3.3.

3.2.3 Calcium Imaging

Calcium imaging was performed to determine whether PGE_2 treatment had altered neuronal excitability. The imaging set-up and parameters are described in Section 2.4.

In dissociated cultures, neurones were stimulated with 30 μL 200 nM capsaicin 30 seconds into recording and imaged for a total of eight minutes (Figure 3.2A).

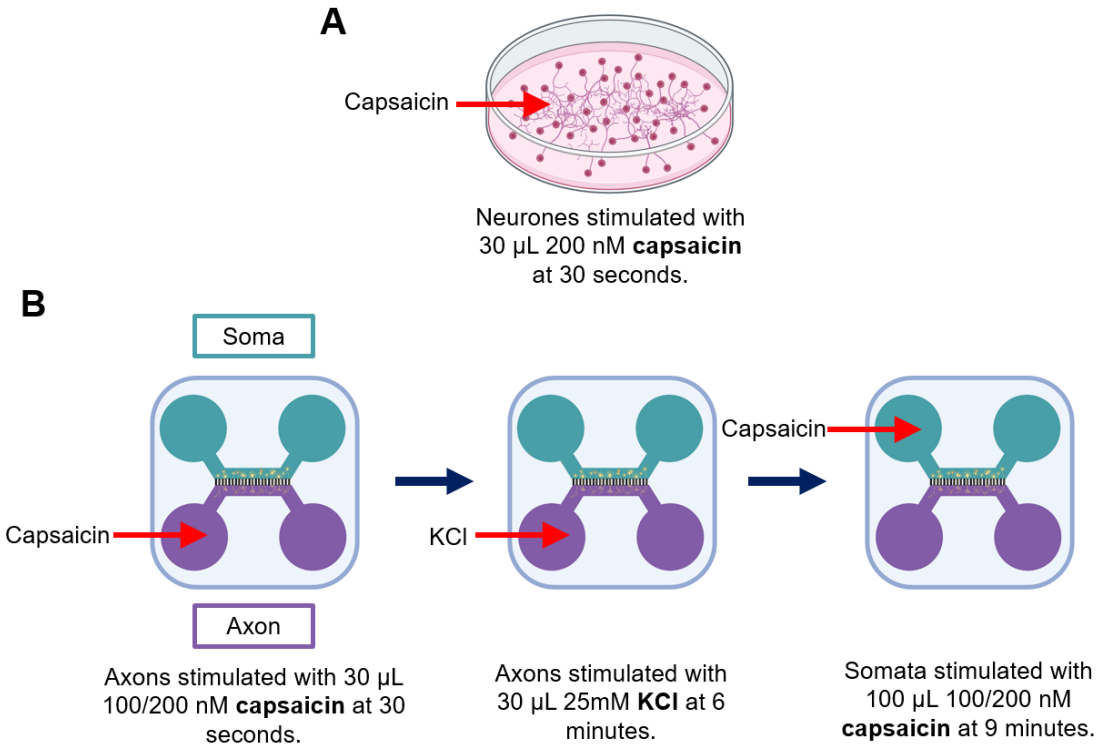


Figure 3.2. Calcium Imaging Protocol for PGE_2 Sensitisation Experiments. A - Neurones grown in dissociated cultures received one 30 μL 200 nM stimulation 30 seconds into recording. **B -** For neurones grown in compartmentalised microfluidic chambers, the stimulation regimen was as follows: 30 μL 100/200 nM capsaicin to the axon compartment after 30 seconds, 30 μL 25 mM KCl to the axon compartment six minutes into recording, and 100 μL 100/200 nM capsaicin to the soma compartment at nine minutes. New baselines were taken before each stimulation was applied. Created using BioRender™.

In compartmentalised microfluidic cultures, stimuli were applied as follows: 30 μL 100/200 nM capsaicin to the axon terminals 30 seconds into recording; 30 μL 25 mM KCl to the axonal compartment at six minutes (to allow time for recovery from

the initial capsaicin stimulus); 100 μL 100/200 nM capsaicin to the soma-enriched side at nine minutes (Figure 3.2B). New baselines were calculated before each stimulation.

For mechanical flow control experiments, 30 μL of fresh 1X IB was applied to the axonal compartment of compartmentalised microfluidic chambers.

Calcium Imaging Analysis

The analysis of calcium imaging datasets are described in Sections 2.4.3 and 2.7. While Asta Arendt-Tranholm performed the experiments on dissociated whole-cell cultures, I carried out those involving microfluidic chambers. I was responsible for the analysis and organisation of all calcium imaging data.

3.2.4 Immunocytochemistry

Cell fixation, immunocytochemistry, and imaging at 20x were performed as described in Section 2.6. A pilot study was conducted to quantify EP_4 receptor levels in PGE_2-treated cells relative to vehicle controls (antibodies in Tables 2.2 and 2.3). DAPI staining was used to identify the nuclei of cell bodies, while acetylated tubulin was used to visualise neuronal processes.

Three images were taken at random per replicate. Total EP_4 labelling was calculated by measuring the area occupied by the signal and multiplying it by the average pixel intensity. DAPI counts were performed manually. A custom-built macro was devised to automatically threshold and generate measurements of area occupied by EP_4 receptor labelling and mean grey intensity on FIJI ImageJ (Schindelin et al., 2012).

3.2.5 Statistical Analysis

Statistical analyses were conducted according to the methods outlined in Chapter 2 (Section 2.7). For the experiments in this chapter, two-tailed *t*-tests were used

for comparisons between two groups, and two-way ANOVAs with post-hoc tests were used for multiple group comparisons, as appropriate. A p-value < 0.05 was considered statistically significant.

3.3 Results

3.3.1 Establishment of *in vitro* Models for Sensory Neurone Studies

Four distinct *in vitro* culture systems were established and validated for sensory neurone studies, each yielding reproducible morphological and experimental outcomes under defined conditions: dissociated cultures, compartmentalised microfluidic chambers, Boyden chambers, and DRG explants.

Dissociated Cultures

Dissociated cultures were reliably established with minimal cell numbers and allowed experimental manipulation as early as two hours after seeding. By DIV3, extensive neurite outgrowth was consistently observed (Figure 3.3), making them particularly useful for studying early axon outgrowth before the axonal network had fully developed (Figure 3.3C). RNA extracted from these cultures reflected whole-cell content due to the shared physico-chemical environment of axons and somata, limiting subcellular resolution but enabling rapid screening of treatment effects. Both pre-treatment and stimulation protocols lacked spatial resolution, resulting in calcium imaging readouts that captured whole-cell responses. As such, dissociated cultures were well-suited to initial experiments aimed at determining whether an effect is present, prior to transitioning to more complex culture systems. However, they were less appropriate for dissecting detailed spatiotemporal or subcellular mechanisms.

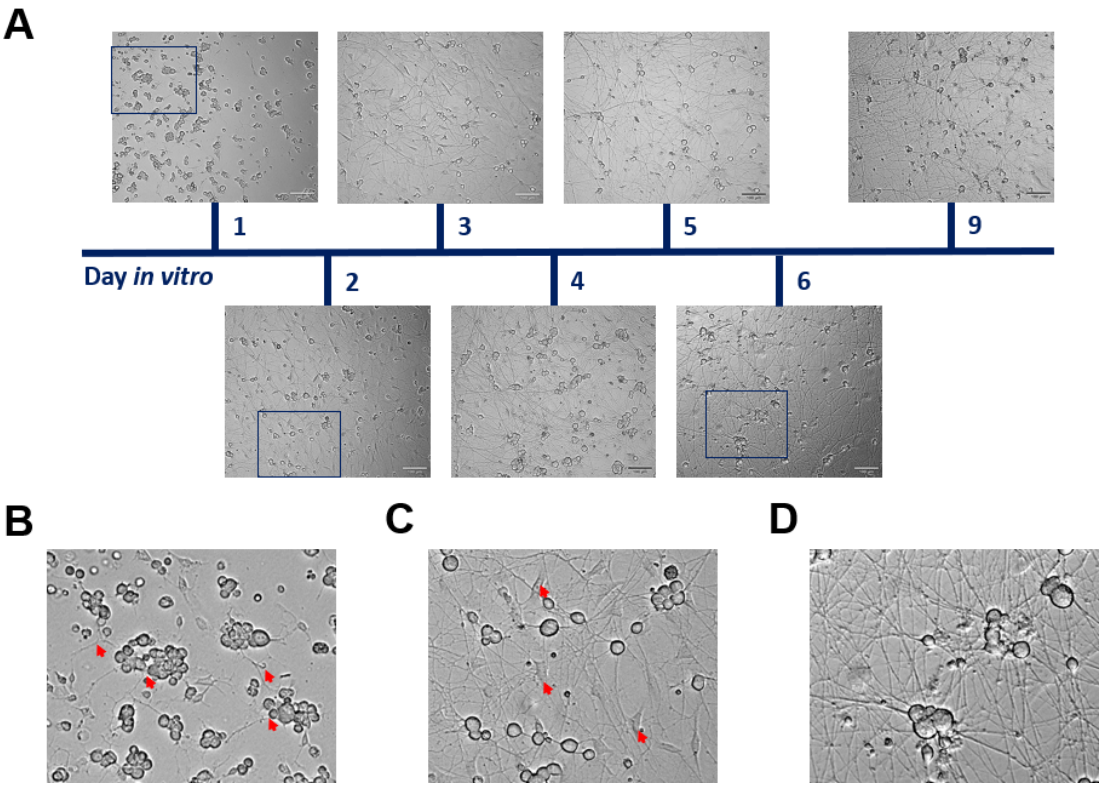


Figure 3.3. DRG Neurone Growth in Dissociated Culture. A - Timeline of brightfield images from DIV1 (day of seeding) to DIV9. **B-D -** Boxed regions of the brightfield images were selected and digitally enlarged to better visualise neurite outgrowth and network formation. **B -** Arrows depict where neurones began to project processes from DIV1. **C -** By DIV3, extensive neuronal networks were evident, with some non-neuronal cells persisting in culture, indicated by arrows. **D -** Dense neuronal networks were present by DIV6. Images acquired at 10x magnification. Scale bars: 100 μm.

Compartmentalised Microfluidic Cultures

Compartmentalised microfluidic chambers enabled fluidic isolation of axons from somata, permitting region-specific stimulation and sampling. Although axonal projections through microgrooves were evident by DIV3, sufficient extension for experimental manipulation required at least five days in culture (Figure 3.4). RNA extraction from isolated axons was feasible but required pooling material from multiple chambers, limiting throughput and increasing technical burden.

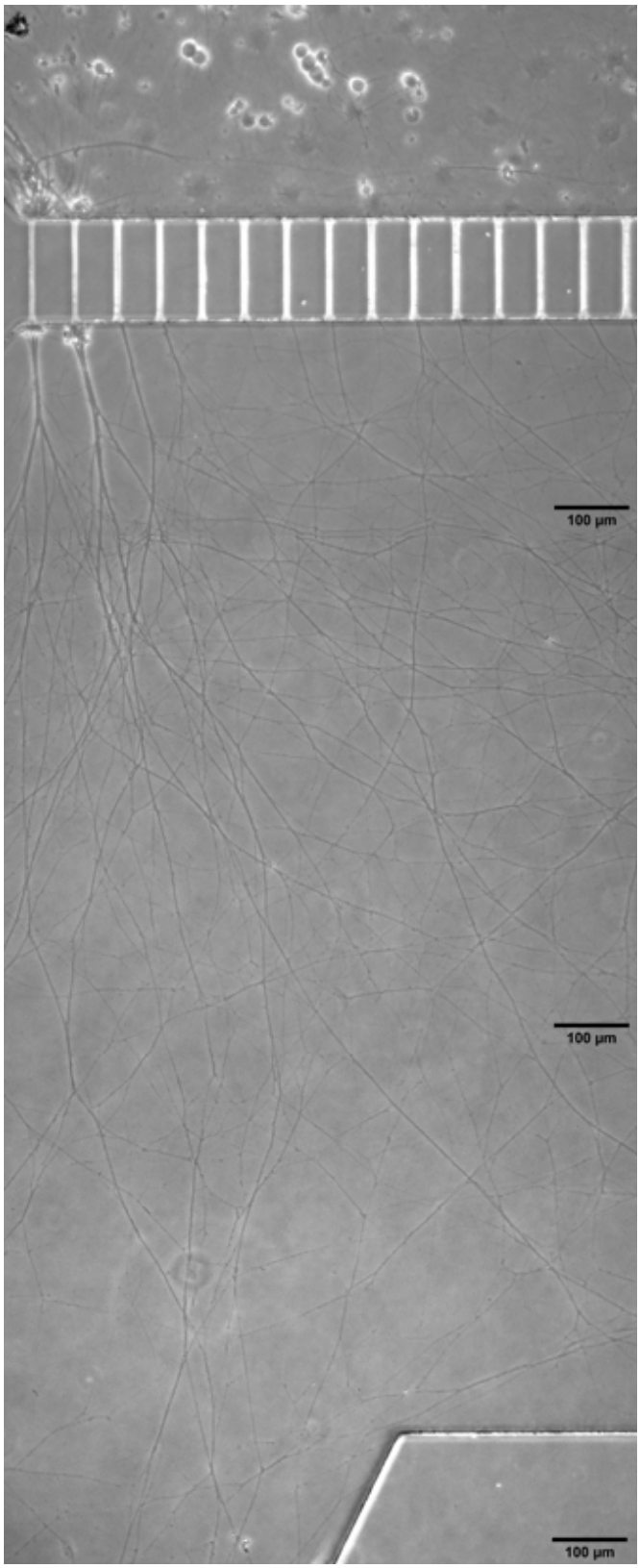


Figure 3.4. Extent of Axon Growth Through Microgrooves into the Soma Compartment. Stitched brightfield images of dorsal root ganglion sensory neurones in compartmentalised microfluidic chambers taken at DIV6. Axons extended extensively from the soma compartment to the axonal compartment. Images acquired at 10x magnification. Scale bars: 100 μm.

Boyden Chambers

Boyden chambers supported high-density cultures and enabled scalable axonal RNA isolation, although fluidic isolation was not achievable in this system. Axons reliably extended through the porous membrane, and RNA could be extracted following axotomy (Figure 3.5), proving suitable for transcriptomic profiling of axonal compartments.

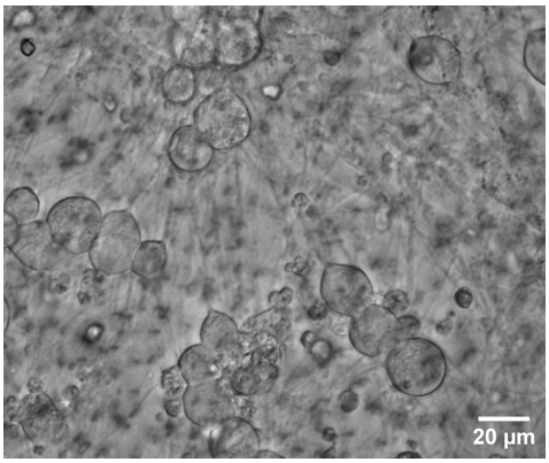


Figure 3.5. Brightfield Image of Dorsal Root Ganglion Neurones Cultured in Boyden Chambers. Image taken above the membrane insert, upon which the cells were seeded. Axons grew densely and extended through to the compartment below via the 1 μm pores. Image acquired at 20x magnification. Scale bar: 20 μm.

Explant Culture

Explants maintained native satellite glial populations and supported robust radial axon extension (Figure 3.6). While less compatible with calcium imaging or precise pharmacological control, this model would enable qualitative assessment of neurone-glia interactions and axonal degeneration under more physiological conditions.

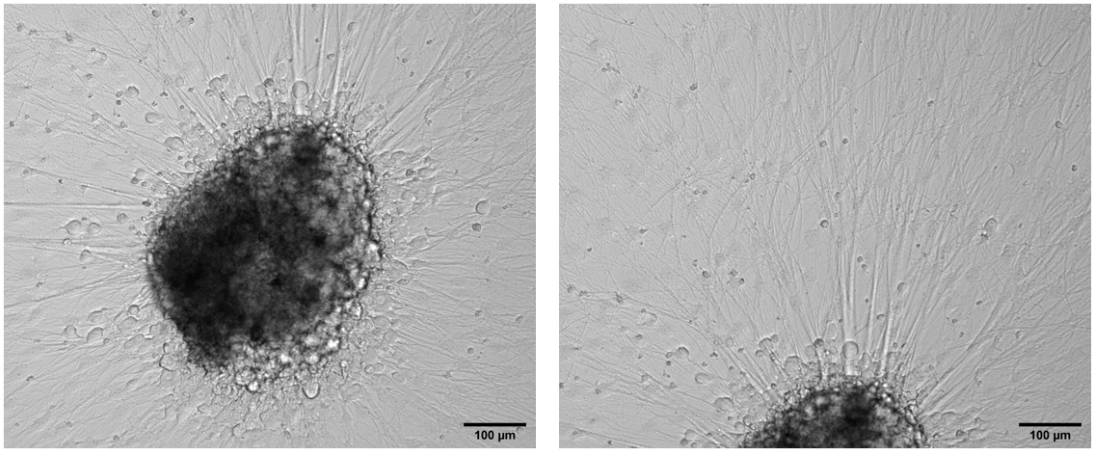


Figure 3.6. Axons Grew Extensively from Explants in Culture. Brightfield images of dorsal root ganglion explants at DIV5. Axons extended extensively from the explant in multiple directions and focal planes. Images acquired at 10x magnification. Scale bar: 100 μm.

3.3.2 Stimulus Addition Generates Minimal Mechanical Pressure Activation

To account for potential mechanically-induced responses during stimulant application, mechanical flow controls were performed specifically in microfluidic chambers, which contain channels that exaggerate fluid flow over axons. In these conditions, IB alone was added to the axonal compartment, and calcium transients were recorded in the corresponding cell somata. This mechanical stimulation elicited a detectable response, though the average fluorescence intensity of calcium transients was much lower than those evoked by chemical stimulation.

On average, the response to IB alone was approximately one-third smaller than the response to KCl applied subsequently to the same axons (Figure 3.7B), and was similarly reduced compared to capsaicin-induced responses measured in separate, unstimulated chambers (Figure 3.7A). Overall, it was concluded that its contribution was minor and should be consistent across different experimental replicates and conditions, with the relative ratio between mechanical and chemical responses expected to remain stable.

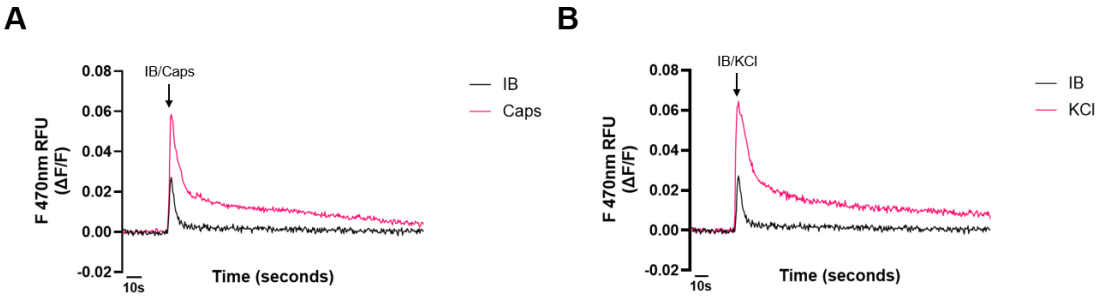


Figure 3.7. Mechanical Flow Induced Smaller Calcium Transients Compared to Chemical Stimulation. A - Averaged calcium trace (ΔF/F) from DRG neurones showing the somatic response to capsaicin applied to the axonal compartment. Compared to capsaicin-evoked responses, mechanical flow (imaging buffer alone) in separate chambers elicited calcium transients of reduced magnitude (∼one-third lower). **B -** Averaged calcium trace (ΔF/F) from DRG neurones showing somatic responses to sequential axonal application of imaging buffer followed by KCl within the same microfluidic chambers. The calcium transient evoked by imaging buffer alone was smaller, approximately one-third the magnitude of the subsequent KCl-induced response in the same cells.
N = 1 biological replicate; *n* = 2 chambers per treatment group; 4-16 cells analysed per chamber. Abbreviations: IB - imaging buffer; Caps - capsaicin.

3.3.3 PGE_2 Incubation as a Model of Neuronal Sensitisation

Previous experimental work in our lab sought to investigate the effect of a 24-hour treatment of 10 μM PGE_2 on sensory neurone excitability in dissociated cultures (Figure 3.8A), with the aim of producing an *in vitro* model of neuronal sensitisation.

PGE_2 significantly increased the response to 200 nM capsaicin by enhancing the level of calcium transients in cell somata during calcium imaging ($p = 0.0228$, *t*-test, Figure 3.8B-C). Although an increase was also observed when the prolonged response was analysed as area under the curve, this was not significantly increased compared to control (Figure 3.8D).

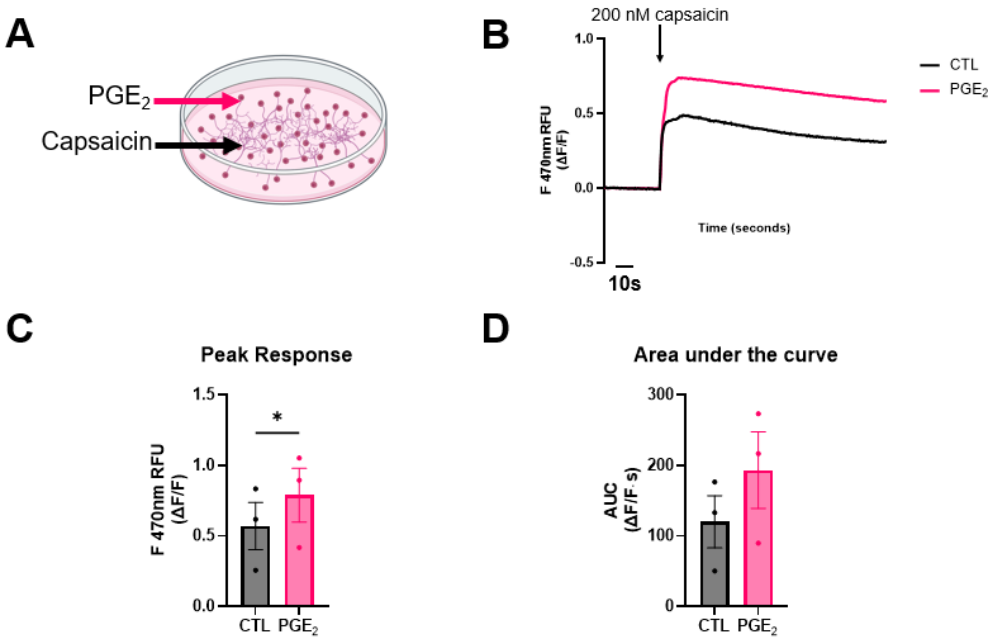


Figure 3.8. Calcium Response to 200 nM Capsaicin Stimulation of Dissociated Sensory Neurones Following PGE_2 Pre-Treatment. A - DRG sensory neurones were cultured in PDMS rings for seven days before treatment with 10 μM PGE_2 for 24 hours. During calcium imaging, capsaicin was applied to the whole-cell culture and the calcium response measured as fluorescence intensity in the somata of neurones. Created using BioRender™. **B -** Average calcium trace (ΔF/F) in response to 200 nM capsaicin. Neurones pre-treated with PGE_2 demonstrated a greater fluorescence intensity in response. **C -** Neurones pre-treated with PGE_2 demonstrated a significantly increased peak of calcium transients (ΔF/F, mean ± SEM), relative to controls (p = 0.0228, t-test). **D -** The area under the curve of calcium traces (peak to 100 seconds; mean ± SEM) showed a trend to increase in the PGE_2 group but was not significant (t-test).
Experiment performed by Asta Arendt-Tranholm, data analysis and arrangement performed by me. N = 3 biological replicates; $n \geq$ 2 technical replicates per experiment; 5-14 cells per replicate. $p < 0.05$ was considered statistically significant.

3.3.4 Axonal Incubation with PGE_2 Can Induce the Sensitisation of DRG Neurones

To dissect the subcellular mechanism of PGE_2-induced neuronal sensitisation, DRG neurones were cultured in compartmentalised microfluidic chambers and isolated axons were treated with PGE_2 for 17 hours before calcium imaging was performed.

100 nM Capsaicin Preliminary Experiments

In preliminary experiments, application of 100 nM capsaicin to axon terminals of

PGE_2 pre-treated cultures did not produce a heightened calcium response in cell somata relative to vehicle control, suggesting that the capsaicin concentration was insufficient to produce sensitisation effects (*t*-test; Figure 3.9). Therefore, 200 nM capsaicin was used in all subsequent experiments to robustly stimulate TRPV1-expressing axons and reveal functional sensitisation.

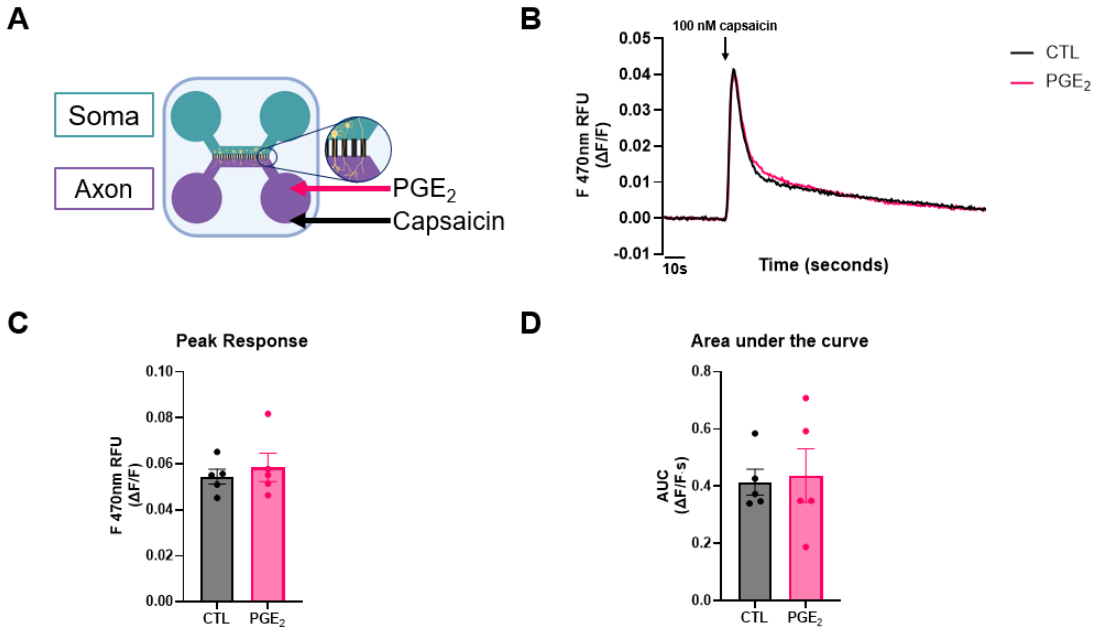


Figure 3.9. Calcium Response to 100 nM Capsaicin Stimulation of Axon Terminals Following PGE_2 Pre-Treatment. A - DRG sensory neurones were cultured in compartmentalised microfluidic chambers for six days before the axon-enriched compartment was treated with PGE_2 for 17 hours. During calcium imaging, 100 nM capsaicin was applied to the axon compartment and the calcium response measured as fluorescence intensity in the somata of corresponding axons. Created using BioRender™. **B -** Averaged calcium trace (ΔF/F) in response to 30 μL of 100 nM capsaicin applied to the axon terminals. There were no differences in response between PGE_2-treated cells and controls. **C -** Neurones pre-treated with PGE_2 demonstrated a similar level of calcium transients as controls (ΔF/F, mean ± SEM; *t*-test). **D -** The area under the curve of calcium traces (peak to 50 seconds; mean ± SEM) was not increased between control and PGE_2 pre-treated neurones (*t*-test). N = 5 biological replicates; $n \geq 2$ technical replicates per experiment; 4-35 cells per replicate. $p < 0.05$ was considered statistically significant.

200 nM Capsaicin Experiments

Stimulation of the axonal compartment with 200 nM capsaicin induced a characteristic transient increase in calcium in cell somata (Figure 3.10B; Bouskila and Bostock, 1998; Tsantoulas et al., 2013), without causing desensitisation or toxicity.

In cultures with axons treated with PGE_2 for 17 hours, significantly greater calcium transients were exhibited in their cell somata following axon stimulation with capsaicin, compared to control cells (Figure 3.10C; p = 0.0024, t-test), indicating that neuronal sensitisation had occurred. The area under the curve of the calcium trace was also significantly increased in PGE_2-treated chambers (Figure 3.10D; p = 0.0049, t-test).

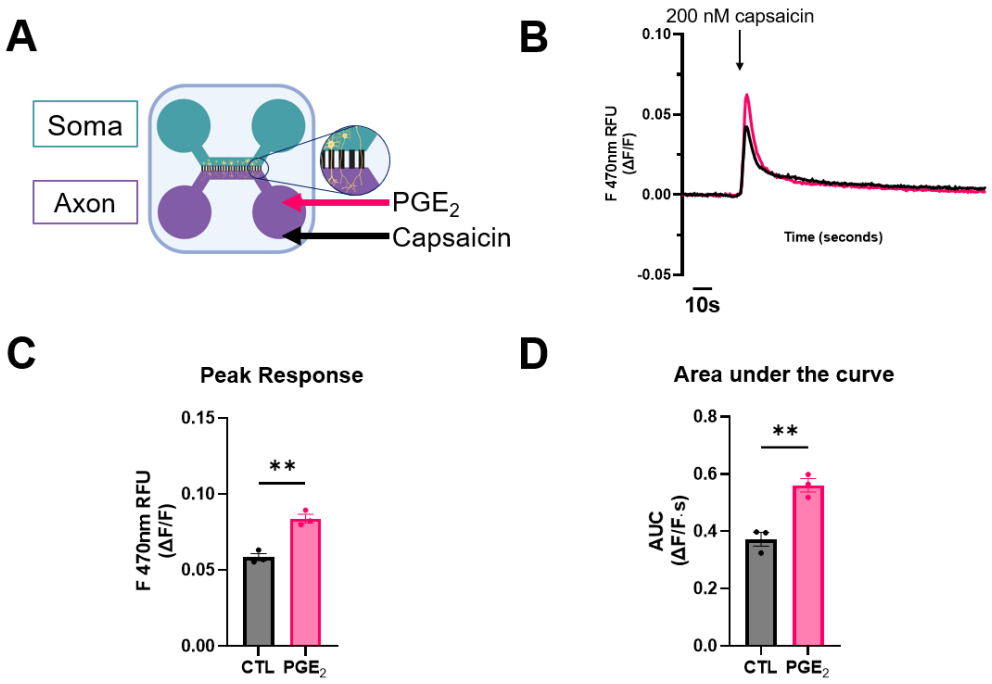


Figure 3.10. Calcium Response to 200 nM Capsaicin Stimulation of Axon Terminals Following PGE_2 Pre-Treatment. A - DRG sensory neurones were cultured in compartmentalised microfluidic chambers for six days before the axon-enriched compartment was treated with PGE_2 for 17 hours. During calcium imaging, capsaicin was applied to the axon compartment and the calcium response measured as fluorescence intensity in the cell bodies of corresponding axons. Created using BioRender™. **B -** Averaged calcium trace (ΔF/F) in response to 30 μL of 200 nM capsaicin applied to the axon terminals. Neurones pre-treated with PGE_2 demonstrated a greater fluorescence intensity in response. **C -** Neurones pre-treated with PGE_2 demonstrated a significant increase in calcium transients (ΔF/F, mean ± SEM) in their cell bodies, relative to controls (p = 0.0024, t-test). **D -** The area under the curve of calcium traces (peak to 50 seconds; mean ± SEM) was significantly increased in the PGE_2 pre-treated neurones, relative to controls (p = 0.0049, t-test).
N = 3 biological replicates; $n \geq 2$ technical replicates per experiment; 5-28 cells per technical replicate. $p < 0.05$ was considered statistically significant.

3.3.5 PGE_2 Treatment Did Not Alter the Size Distribution of Axonal Capsaicin Respondents

DRG *in vitro* cultures contain a heterogeneous population of sensory neurones and have been classified here as: small diameter cell bodies, likely representing nociceptive C-fibres (<15 μm), medium diameter cell bodies, from Aδ nociceptive neurones and some larger C-fibres (15-20 μm), and large diameter Aβ mechanoreceptors and proprioceptors (>20 μm), in accordance with Lechner et al. (2009) (Table 1.1; Section 1.3.1).

To determine whether axonal PGE_2 treatment affected the size distribution of capsaicin-responsive (200 nM) nociceptive neurones, soma diameters of neurones that responded to capsaicin - applied to their axon terminals during calcium imaging - were compared. There were no significant differences in cell size distribution of capsaicin respondents between control and PGE_2-treated populations, with the majority of neurones under 20 μm.

There was a significant main effect of soma diameter on the proportion of cells responding to capsaicin ($F(2, 34) = 10.65$, $p = 0.0003$, two-way ANOVA), indicating that the likelihood of a neurone responding depended on its diameter class. However, there was no significant main effect of treatment group ($F(1, 17) = 0.05607$, $p = 0.8156$) and no significant interaction between treatment group and neurone diameters ($F(2, 34) = 1.098$, $p = 0.3450$), suggesting that PGE_2 treatment did not alter the pattern of diameter-dependent responses. There was no significant variation between technical replicates ($p > 0.9999$).

Post-hoc testing confirmed that there were no significant differences in the number of neurones responding to capsaicin between treatment groups within any diameter bin: <15 μm (mean difference = 8.17, $p = 0.3268$, Tukey's post-hoc test), 15-20 μm (mean difference = -11.97, $p = 0.1532$), or >20 μm (mean difference = 3.796, $p = 0.6474$). However, there was a non-significant trend toward a greater number of

medium-diameter neurones and fewer small-diameter neurones in the PGE_2 group relative to control.

In control neurones, there were no significant differences between the number of neurones responding to capsaicin between any soma diameter bins. In the PGE_2 group, there were significantly more medium-diameter neurones than both small- ($p = 0.0287$) and large-diameter neurones ($p = 0.0006$; Figure 3.11B). These findings reinforce the main effect of neurone diameter observed in the ANOVA and suggest that, while neurone diameter influences the proportion of neurones responding to capsaicin, PGE_2 treatment does not significantly change this distribution.

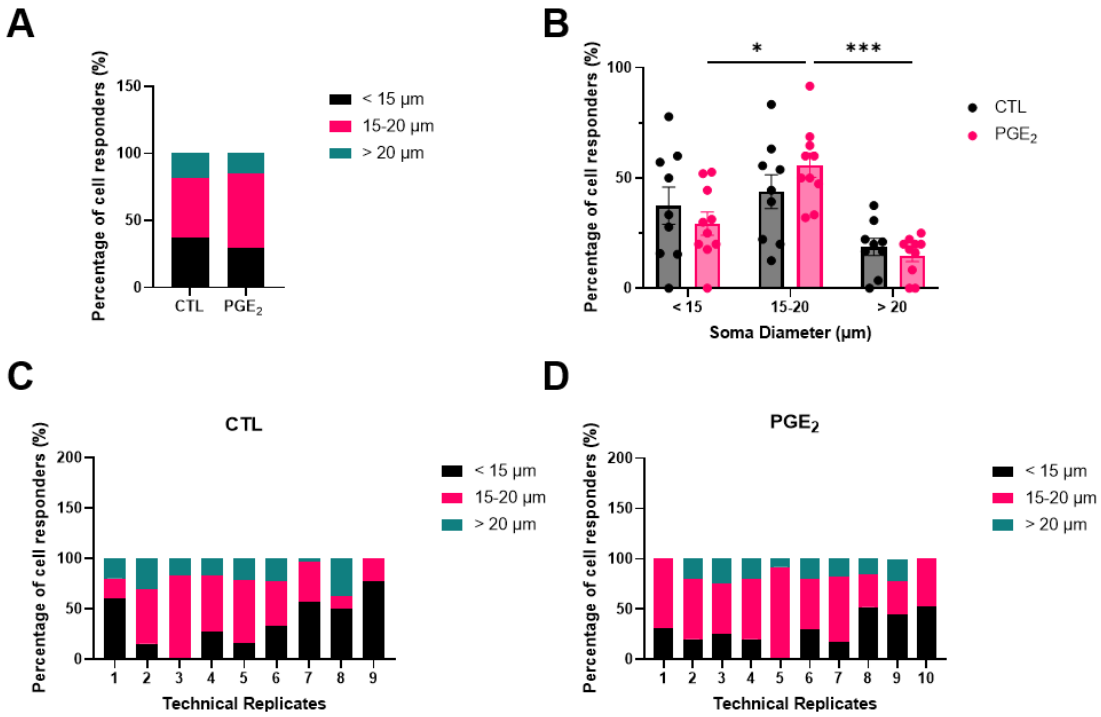


Figure 3.11. Diameter Distribution of Cell Bodies Responding to Axonal Capsaicin Stimulation in Compartmentalised Microfluidic Chambers. A - Percentage distribution of soma diameters for DRG neurones that responded to 200 nM capsaicin applied to the axonal compartment. In both control and PGE_2-treated cultures, the majority of responsive neurones were 15-20 μm in diameter. Small-diameter neurones (<15 μm) made up an average of 37.5% of capsaicin responders, medium-diameter (15-20 μm) an average of 43.8%, and large-diameter (>20μm) 18.7% in the control group. Small-diameter neurones (<15 μm) made up an average of 29.3% of capsaicin responders, medium-diameter (15-20 μm) an average of 55.8%, and large-diameter (>20μm) 14.9% in the PGE_2 group. **B -** A significant main effect of soma diameter on capsaicin response was revealed ($F(2, 34) = 10.65$, $p = 0.0003$, two-way ANOVA; mean ± SEM), but no significant effect of treatment ($F(1, 17) = 0.05607$, $p = 0.8156$) and no interaction between the two ($F(2, 34) = 1.098$, $p = 0.345$). There was no significant variation between technical replicates ($p > 0.9999$). There were no significant differences in the number of responders between treatment groups across any diameter bin: <15 μm ($p = 0.3268$, Tukey's post-hoc test), 15-20 μm ($p = 0.1532$), or >20 μm ($p = 0.647$), though a non-significant trend was observed toward more medium-diameter and fewer small-diameter responders in the PGE_2 group, relative to control. Within-group comparisons showed a significantly greater number of medium-diameter responders than small- ($p = 0.0287$) or large-diameter ($p = 0.0006$) responders in the PGE_2-treated group, but not in controls. These findings suggest that, while neurone diameter influences responsivity to capsaicin, PGE_2 treatment does not significantly alter this distribution. **C -** Percentage distribution of soma diameters for DRG neurones that responded to capsaicin within replicates in the control group. **D -** Percentage distribution of soma diameters for DRG neurones that responded within replicates to capsaicin in the PGE_2 group.

$N = 3$ biological replicates. $n = 9$ technical replicates in the control group; 5-25 cells per replicate. $n = 10$ technical replicates in the PGE_2 group; 6-28 cells per replicate. $p < 0.05$ was considered statistically significant.

3.3.6 PGE_2's Effects on Neuronal Excitability Are Nociceptive Neurone-Specific

To assess whether PGE_2 altered neuronal excitability globally - rather than selectively affecting nociceptive neurones - KCl, a depolarising agent, was used. Six minutes into recording, 30 μL of 25 mM KCl was delivered to the axon terminals (Figure 3.12A). Calcium transients in the somata of PGE_2-treated neurones did not differ from controls (Figure 3.12B and D; *t*-test). However, analysis of peak responses, independent of trace peak timing, revealed a trend toward increased calcium signals in the PGE_2 group compared to controls, though this did not reach significance (*t*-test; Figure 3.12C).

To investigate whether PGE_2 treatment influenced the size distribution of neurones responsive to general depolarisation, soma diameter was analysed for DRG neurones responding to the axonally-applied KCl stimulation (following a previous stimulation with capsaicin). There were no differences in cell size distribution of capsaicin respondents between control and PGE_2-treated populations, and neurones were mostly <20 μm, as with the axonal capsaicin stimulation.

There was a significant main effect of neurone diameter on the percentage of responders ($F(2, 30) = 18.94$, $p < 0.0001$, two-way ANOVA), indicating that the number of responders varied by size class. However, there was no significant main effect of treatment ($F(1, 15) = 3.427$, $p = 0.0839$) and no significant interaction between diameter and treatment group ($F(2, 30) = 0.4908$, $p = 0.6169$), suggesting that PGE_2 did not significantly alter the diameter distribution of KCl-responsive neurones.

As with the axonal capsaicin dataset, post-hoc analysis confirmed that there were no significant differences between control and PGE_2 groups for any diameter bin: <15 μm (mean difference = 3.567, $p = 0.6805$), 15-20 μm (mean difference = -8.492, $p = 0.3291$), or >20 μm (mean difference = 4.924, $p = 0.5701$). Within

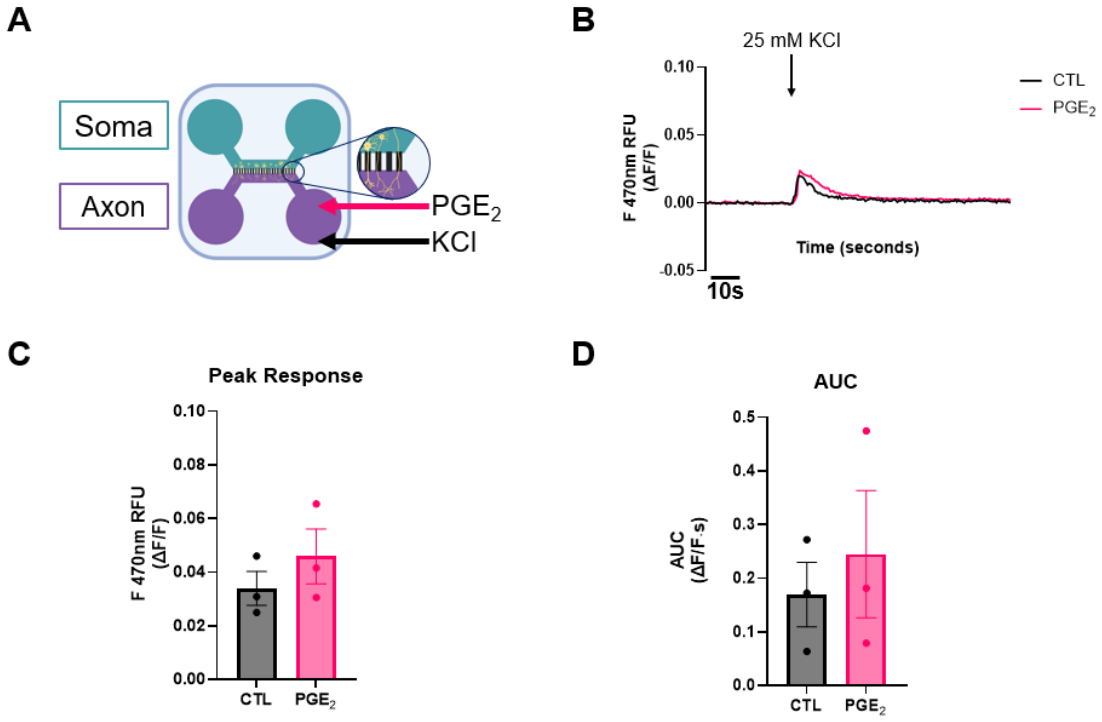


Figure 3.12. Calcium Response to KCl Stimulation of Axons Following PGE_2 Pre-Treatment of Axon Terminals. A - DRG sensory neurones were cultured in compartmentalised microfluidic chambers for six days, then the axonal compartment was treated with PGE_2 for 17 hours. During calcium imaging, 30 μL of 25 mM KCl was applied to the axon compartment, and calcium responses were measured as changes in fluorescence intensity in the corresponding cell bodies. Created using BioRender™. **B -** Averaged calcium traces (ΔF/F) in response to 30 μL of 25 mM KCl. PGE_2-pretreated neurones showed similar transients to controls. **C -** Peak calcium responses (ΔF/F, mean ± SEM; *t*-test) showed a trend toward an increase after PGE_2 pre-treatment but was not statistically significant (*t*-test). **D -** The area under the curve of calcium traces (peak to 50 seconds) was not statistically increased following PGE_2 treatment (mean ± SEM; *t*-test).
N = 3 biological replicates; $n \geq 2$ technical replicates; 3-22 cells per technical replicate. $p < 0.05$ was considered statistically significant.

each treatment group, response percentages differed significantly across diameter bins. In both control and PGE_2 conditions, significantly more medium-diameter neurones responded to KCl compared to large-diameter (CTL: $p = 0.0041$; PGE_2: $p < 0.0001$; Figure 3.13B). The percentage of small-diameter responders was significantly lower than medium-diameter responders in the PGE_2 group (mean difference = -37.48, $p = 0.0027$), but not in control. These data indicate that PGE_2 does not significantly alter the overall pattern of size-dependent responsiveness to KCl.

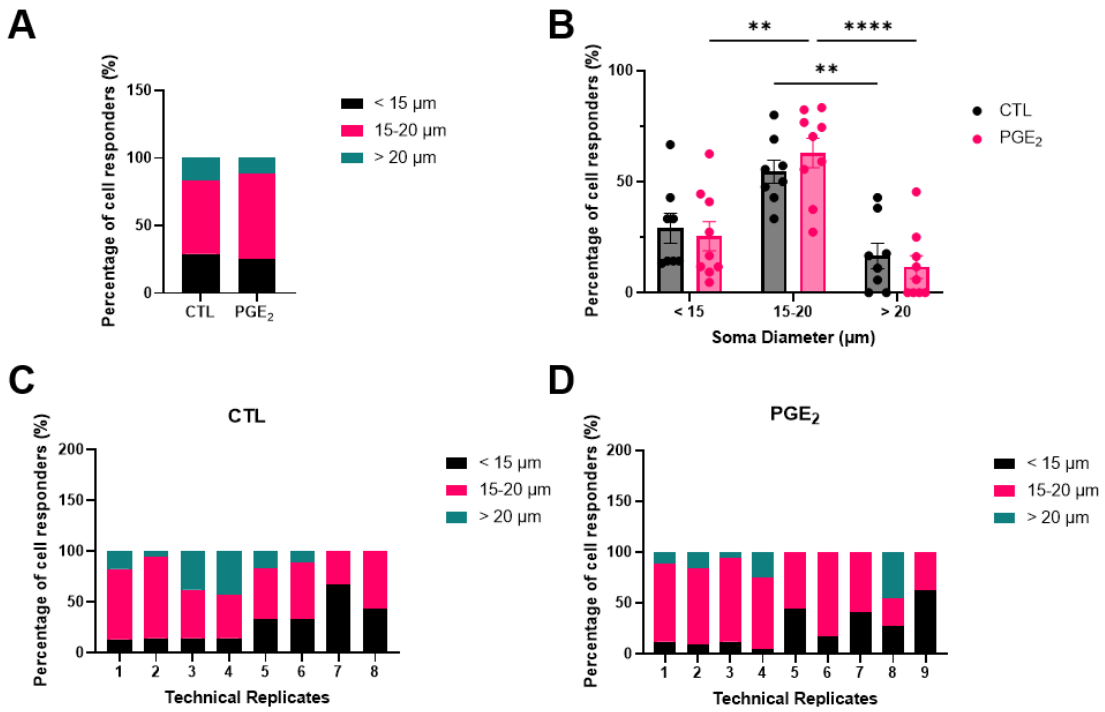


Figure 3.13. Soma Diameter Distribution of DRG Neurones Responding to KCl Following PGE_2 Pre-Treatment of Axon Terminals. A - Percentage distribution of soma diameters for DRG neurones that responded to 25 mM KCl applied to the axonal compartment. In both control and PGE_2-treated cultures, the majority of responsive neurones were 15-20 μm in diameter. Small-diameter neurones (<15 μm) made up an average of 29% of KCl responders, medium-diameter (15-20 μm) an average of 54.4%, and large-diameter (>20μm) 16.5% in the control group. Small-diameter neurones (<15 μm) made up an average of 25.5% of KCl responders, medium-diameter (15-20 μm) an average of 62.9%, and large-diameter (>20μm) 11.6% in the PGE_2 group. **B -** A significant main effect of soma diameter on KCl response was revealed ($F(2, 30) = 18.94$, $p < 0.0001$, two-way ANOVA; mean ± SEM), but no significant effect of treatment ($F(1, 15) = 3.427$, $p = 0.0839$) and no interaction between the two ($F(2, 30) = 0.4908$, $p = 0.6169$). There was no significant variation between technical replicates ($p > 0.9999$). Post-hoc analysis found no significant differences in the number of responders between treatment groups across any diameter bin: <15 μm ($p = 0.6805$, Tukey's post-hoc test), 15-20 μm ($p = 0.3291$), or >20 μm ($p = 0.5701$), though a non-significant trend was observed toward more medium-diameter and fewer small- and large-diameter responders in the PGE_2 group, relative to control. Within-group comparisons showed a significantly greater number of medium-diameter responders than small- ($p = 0.0027$) or large-diameter ($p < 0.0001$) responders in the PGE_2-treated group, but only between medium- and large-diameter neurones in controls ($p = 0.0041$). These findings suggest that while neurone diameter influences KCl responsiveness, PGE_2 treatment does not significantly alter this distribution. **C -** Percentage distribution of soma diameters for DRG neurones that responded to KCl in the control group. **D -** Percentage distribution of soma diameters for DRG neurones that responded to KCl in the PGE_2 group. $N = 3$ biological replicates. $n = 9$ technical replicates in the control group; 3-18 cells per replicate. $n = 11$ technical replicates in the PGE_2 group; 5-22 cells per replicate. $p < 0.05$ was considered statistically significant.

3.3.7 PGE_2 Also Induces the Sensitisation of DRG Cell Bodies

The third and final stimulation, 100 μL 200 nM capsaicin, was applied to the soma-enriched compartment.

100 nM Capsaicin Preliminary Experiments

As with axon stimulation, prior to 200 nM experiments, a lower concentration of capsaicin (100 nM) was also tested in the soma-enriched compartment (Figure 3.14). The trace was characteristically longer in duration for somata stimulation (Figure 3.14B; Bouskila and Bostock, 1998). In cultures where axons had been pre-treated with PGE_2, 100 nM capsaicin evoked a significantly elevated calcium response to somata stimulation compared to controls (p = 0.0396, t-test; Figure 3.14C), although this increase was not statistically significant for the area under the curve of the calcium trace (Figure 3.14D; t-test). This suggested a potential threshold effect that became more robustly detectable at higher concentrations, prompting the use of 200 nM capsaicin in all final experiments.

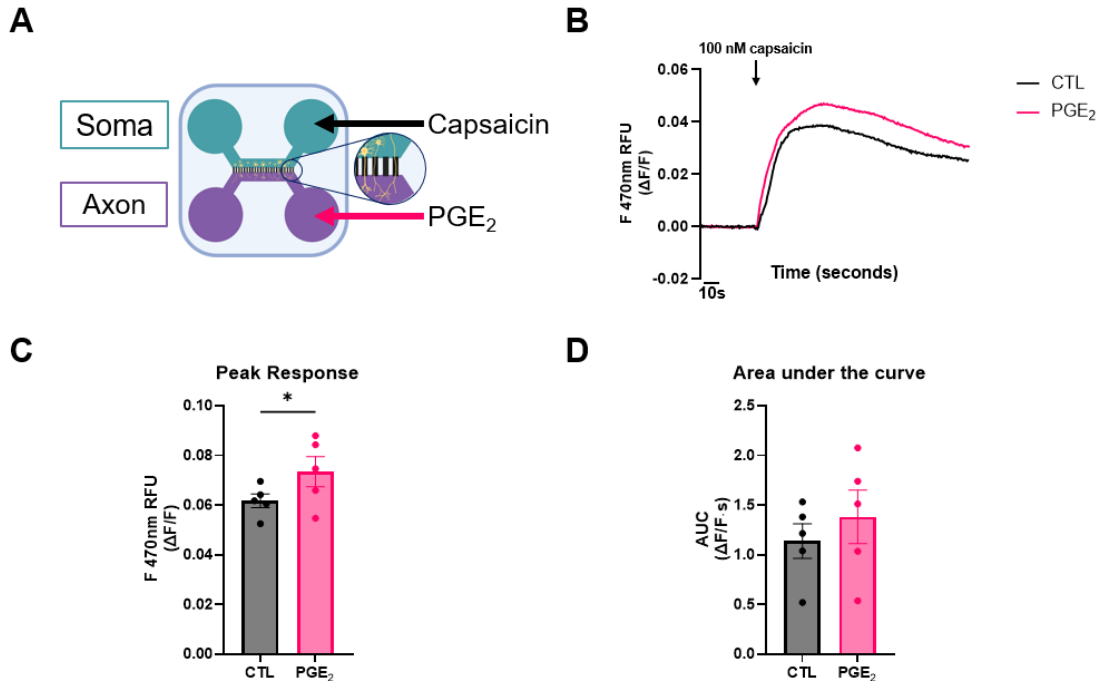


Figure 3.14. Calcium Response to 100 nM Capsaicin Stimulation of Somata Following PGE_2 Pre-Treatment of Axon Terminals. A - DRG sensory neurones were cultured in compartmentalised microfluidic chambers for six days before the axon-enriched compartment was treated with PGE_2 for 17 hours. During calcium imaging, 100 nM capsaicin was applied to the soma compartment, and calcium responses were measured as changes in fluorescence intensity in the corresponding cell bodies. Created using BioRender™. **B -** Averaged calcium traces ($\Delta F/F$) showing the response to 100 μL of 100 nM capsaicin applied to neuronal somata. Neurones pre-treated with PGE_2 exhibited greater calcium transients compared to controls. **C -** Peak calcium responses ($\Delta F/F$, mean ± SEM) were increased in PGE_2 pre-treated neurones relative to controls (p = 0.0396, t-test). **D -** The area under the curve of calcium traces (peak to 60 seconds; mean ± SEM) was increased in PGE_2 pre-treated neurones compared to controls, but this was not significant (t-test). N = 6 biological replicates; $n = \geq 2$ technical replicates; 5-70 cells per technical replicate. $p < 0.05$ was considered statistically significant.

200 nM Capsaicin Experiments

As with 100 nM capsaicin, stimulation of the soma-enriched compartment with 200 nM capsaicin produced a longer lasting change in calcium transients than an axon stimulation (Figure 3.15B). Cultures with axons treated with PGE_2 for 17 hours (Figure 3.15A) exhibited significantly greater calcium transients in their cell somata following direct 200 nM capsaicin stimulation, compared to control cells (p = 0.0435, t-test; Figure 3.15C). The area under the curve of the calcium trace was not significantly increased in PGE_2-treated chambers (Figure 3.15D; t-test) relative

to control, but showed a trend to increase.

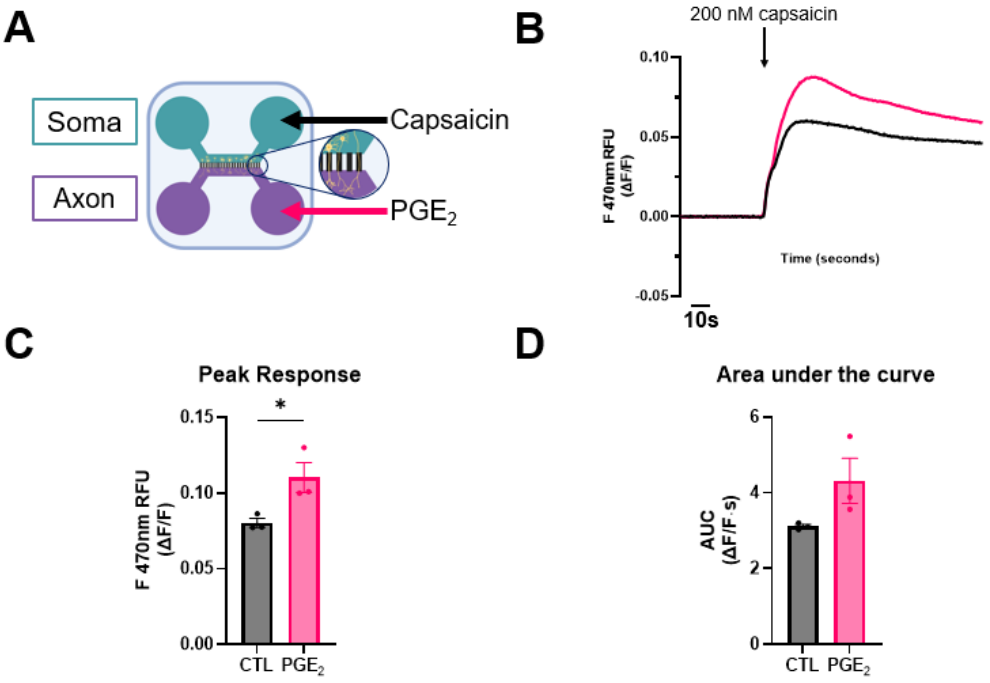


Figure 3.15. Calcium Response to 200 nM Capsaicin Stimulation of Axon Terminals Following PGE_2 Pre-Treatment. A - DRG sensory neurones were cultured in compartmentalised microfluidic chambers for six days before the axon-enriched compartment was treated with PGE_2 for 17 hours. During calcium imaging, 200 nM capsaicin was applied to the soma-enriched compartment and the calcium response measured as fluorescence intensity in cell bodies. Created using BioRender™. **B -** Averaged calcium trace (ΔF/F) in response to 100 μL of 200 nM capsaicin applied to the cell somata. Neurones pre-treated with PGE_2 demonstrated a greater fluorescence intensity in response. **C -** Neurones pre-treated with PGE_2 exhibited a significant increase in calcium transients (ΔF/F, mean ± SEM) in their cell bodies, relative to controls (p = 0.0435, t-test). **D -** The area under the curve of calcium traces (peak to 100 seconds; mean ± SEM) was not significantly changed between treatment groups, but showed a trend to increase (t-test).
N = 3 biological replicates; $n \geq 2$ technical replicates; 21-70 cells per replicate. $p < 0.05$ was considered statistically significant.

3.3.8 PGE_2 Treatment Did Not Alter the Size Distribution of Somal Capsaicin Respondents

To assess whether the soma diameter of neurones responsive to somally-applied capsaicin (200 nM) differed between treatment conditions, neurones were grouped into diameter bins. Within each treatment group, the proportion of neurones responding to capsaicin varied significantly across diameter classes. However, no significant differences were observed between treatment groups. The majority of

responsive neurones fell within the 15-20 μm diameter range.

There was a strong main effect of diameter on capsaicin response ($F(2, 36) = 33.13$, $p < 0.0001$, two-way ANOVA), accounting for 64.69% of total variation (Figure 3.16B). In contrast, treatment with PGE_2 had no significant overall effect on the somal diameter of capsaicin respondents ($F(1, 18) = 1.237$, $p = 0.2806$), and there was no significant interaction between diameter and treatment ($F(2, 36) = 0.1781$, $p = 0.8376$), suggesting that the pattern of diameter-dependent responsiveness was preserved regardless of treatment. There was also no significant variation between technical replicates ($F(18, 36) = 0.0004$, $p > 0.9999$), confirming high reproducibility of the assay.

Post-hoc analysis revealed that neurones with diameters of 15-20 μm comprised significantly more of the capsaicin respondents than both smaller (<15 μm) and larger (>20 μm) diameter neurones under both control and PGE_2 conditions (all $p < 0.0001$). No significant differences in capsaicin responses were observed between control and PGE_2-treated groups within any diameter category (<15 μm: $p = 0.9897$; 15-20 μm: $p = 0.5871$; >20 μm: $p = 0.6288$, Tukey's post-hoc test).

Taken together, these results indicate that capsaicin responsiveness in the cell soma is strongly diameter-dependent, with intermediate-sized neurones (15-20 μm) making up the majority of responders, and that PGE_2 treatment does not alter this diameter-response profile.

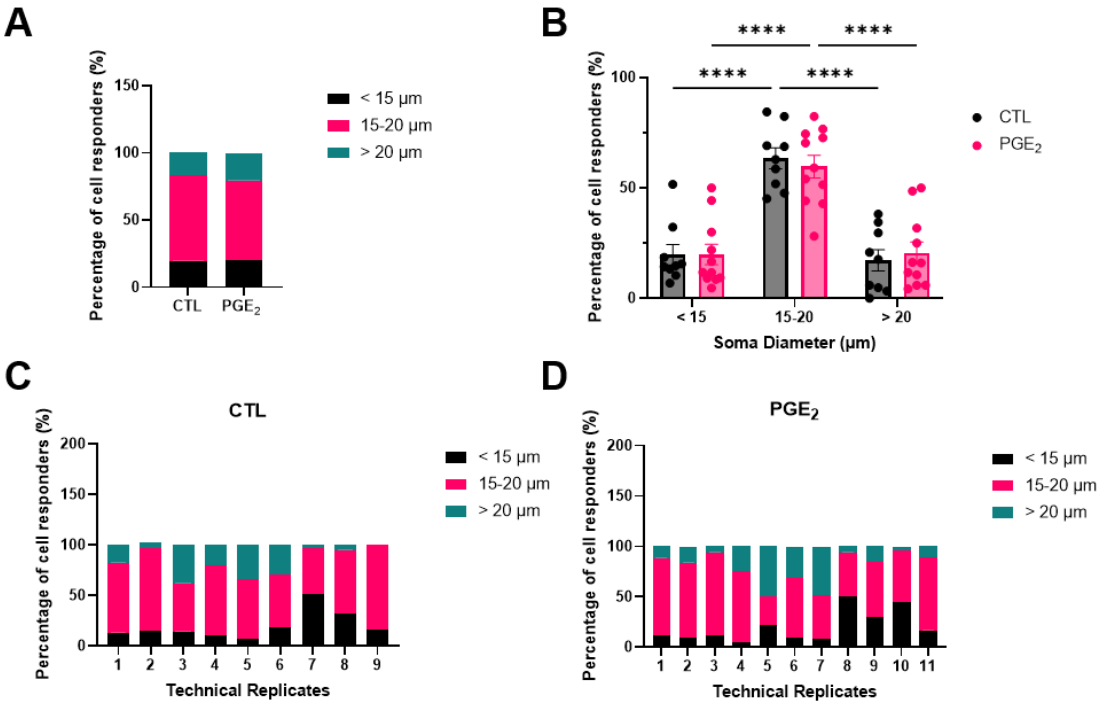


Figure 3.16. Diameter Distribution of Cell Bodies Responding to Somal Capsaicin Stimulation in Compartmentalised Microfluidic Chambers. A - Percentage of capsaicin responders in control and PGE_2-treated cultures. In both treatment groups, respondents were predominantly 15-20 μm in diameter (78.9% in control, 77.7% in treated), with the second most common cell size <15 μm (19.7% in control, 19.8% in treated). The PGE_2-treated group had 2.5% respondents which were >20 μm in diameter, whereas the control group had 1.6%. **B -** Percentage of capsaicin respondents compared between treatment group and diameter. Capsaicin responsivity varied significantly with cell diameter ($p <$ 0.0001, two-way ANOVA; mean ± SEM), with intermediate-sized neurones (15-20 μm) responding in the greatest numbers. 15-20 μm neurones responded significantly more often than both smaller and larger cells in both treatment groups ($p < 0.0001$, Tukey's post-hoc test). No significant differences in capsaicin responders were detected between control and PGE_2 conditions within any diameter group. Technical replicates showed no significant variability ($p > 0.9999$), confirming assay reproducibility. **C -** Distribution of soma diameters of capsaicin-responsive cells in each chamber of the control group. **D -** Distribution of soma diameters of capsaicin-responsive cells in each chamber of the PGE_2 group.
$N = 3$ biological replicates. $n = 9$ technical replicates in the control group; 21-70 cells per replicate. $n = 11$ technical replicates in the PGE_2 group; 22-70 cells per replicate. $p < 0.05$ was considered statistically significant.

3.3.9 Overview of Sequential Axonal and Somal Stimulations

To summarise the sequential application of all stimuli discussed above and provide a reference for the timing and relative magnitude of responses, a full calcium trace is shown in Figure 3.17. This trace represents neurones that responded to the initial 200 nM axonal capsaicin stimulation, some of which subsequently responded

to 25 mM axonal KCl and/or 200 nM somal capsaicin. Axons were stimulated sequentially with 200 nM capsaicin, 25 mM KCl, and finally somata were stimulated with 200 nM capsaicin. This integrated trace illustrates the temporal profile of calcium responses across all experimental conditions described above and provides a visual summary of neuronal responsiveness within the same cells. While calcium responses in this integrated trace were not formally quantified for KCl or somal capsaicin, the fluorescence intensity appears greater in PGE_2-treated neurones compared to controls for each stimulus, consistent with the sensitisation effects described in the individual analyses above.

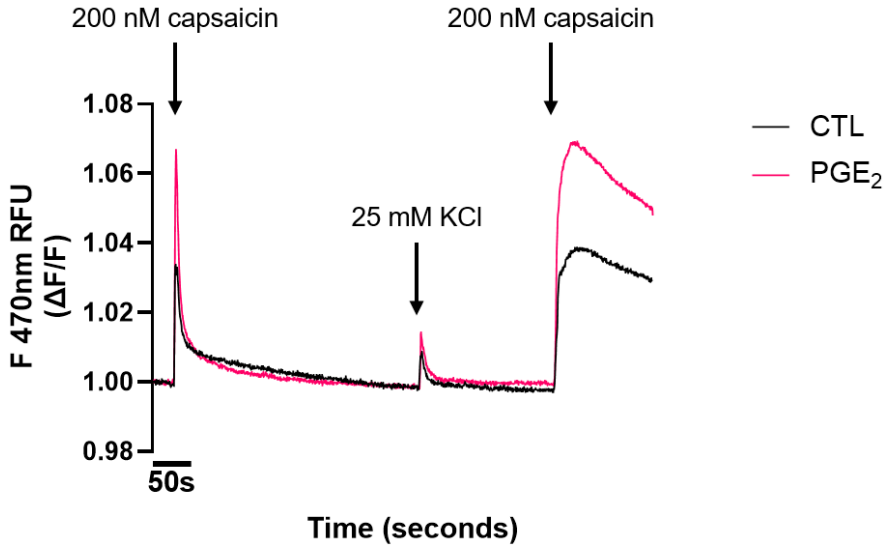


Figure 3.17. Temporal Profile of DRG Neurone Responses to Axonal and Somal Stimuli. DRG sensory neurones were cultured in compartmentalised microfluidic chambers for six days before the axonal compartment was treated with PGE_2 for 17 hours. During calcium imaging, the calcium response was measured as fluorescence intensity in cell bodies. Calcium trace (ΔF/F) in response to 30 μL of 200 nM capsaicin applied to axons 30 seconds into recording, 30 μL 25 mM KCl applied to axons six minutes into recording, and 100 μL 200 nM capsaicin applied to cell somata nine minutes into recording. This trace represents neurones that responded to the initial 200 nM axonal capsaicin stimulation, some of which responded to subsequent stimulation.

3.3.10 EP_4 Receptors Were Upregulated in PGE_2-Treated Sensory Neurones

To assess EP_4 receptor levels following PGE_2 treatment, a pilot study was performed, quantifying three images per technical replicate. EP_4 protein levels were

significantly upregulated in the PGE_2-treated neurones (Figure 3.18A): total EP_4 receptor labelling was significantly increased (p = 0.0095, t-test; Figure 3.18B), as was EP_4 receptor labelling after normalisation to the number of $DAPI^+$ nuclei (p = 0.0024, t-test; Figure 3.18C).

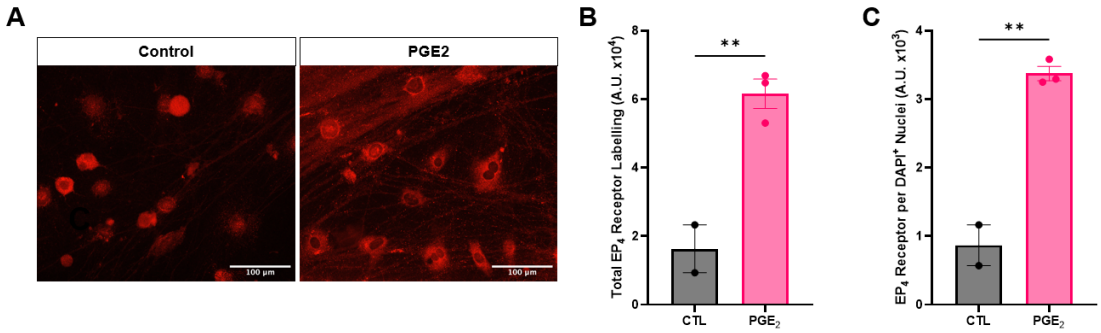


Figure 3.18. EP_4 Expression was Increased in PGE_2-Treated Sensory Neurones. A - EP_4 staining in control and PGE_2-treated cells. Scale bar 100 μm. **B -** Total EP_4 receptor labelling was increased in the PGE_2 treatment group relative to control (p = 0.0095, t-test). **C -** EP_4 receptor labelling normalised to the number of $DAPI^+$ nuclei was significantly heightened compared to control (p = 0.0024, t-test). Data shown as mean ± SEM.
One biological replicate was performed, with each technical replicate representing the quantification of three images.

3.4 Discussion

3.4.1 Summary of Key Findings

In this chapter, I have demonstrated that the potent pro-inflammatory mediator PGE_2 induced a robust and spatially dynamic state of sensitisation in DRG neurones. In dissociated cultures, widespread and prolonged PGE_2 exposure sensitised the entire neurone, whereas in compartmentalised microfluidic systems, targeted axonal application, to mimic a peripheral insult, was sufficient to evoke sensitisation, by stimulating at the site of incubation and retrogradely at the soma, both determined by calcium transient measurement in the soma. These findings confirm that sustained PGE_2 signalling alone is capable of driving sensitisation across neuronal compartments, a process relevant to chronic inflammatory pain.

3.4.2 Acute versus Prolonged Exposure in Inflammatory Models

To capture the dynamics of prolonged inflammation, I examined how sustained PGE_2 exposure might influence neurones more broadly, as well as how it might act locally at axon terminals. Most previous studies investigating PGE_2-induced sensitisation have relied on acute exposure models *in vitro* and *in vivo* (typically < one hour; Gu, Kwong, and Lee, 2003; Kimourtzis et al., 2024; Lopshire and Nicol, 1997; Moriyama et al., 2005; Rangwani, 2018; Southall and Vasko, 2001; St-Jacques and Ma, 2013; Vasko, Campbell, and Waite, 1994; Wei et al., 2024). In contrast, my extended 17-hour exposure paradigm aimed to more closely resemble chronic inflammatory conditions, such as those modelled by complete Freund's adjuvant injection (as summarised by Jang, Kim, and Hwang (2020); St-Jacques and Ma, 2013) which maintain elevated COX-2 for a sustained period, and therefore PGE_2 levels. This suggests that the model used here may capture additional plasticity mechanisms that are overlooked in short-term assays.

Here, calcium imaging was used to assess excitability, stimulating with 200 nM capsaicin, a TRPV1-selective nociceptive agonist (Caterina et al., 1997). In dissociated cultures, where all cellular compartments are uniformly exposed to treatments, PGE_2 induced a pronounced sensitisation, evident as enhanced capsaicin-evoked calcium responses (Results Section 3.3.3; Pope et al., 2025; Arendt-Tranholm, 2022). This aligns with reports of increased responses to calcium following PGE_2 treatment in rat vagal sensory neurones (Gu, Kwong, and Lee, 2003), mouse DRG neurones (Wei et al., 2024), and rat DRG neurones (Lopshire and Nicol, 1997), although these studies did not employ capsaicin stimulation. Consistent with my findings, Moriyama et al. (2005) demonstrated PGE_2-enhanced capsaicin-activated currents using whole-cell patch clamp. However, dissociated culture systems, used in the vast majority of DRG studies, lack the spatial resolution required to study compartment-specific signalling (Atmaramani et al., 2021).

To address this, I then used microfluidic chambers that allow fluidic isolation of axons from their somata (Atmaramani et al., 2021), hypothesising that PGE_2 applied locally to the axon terminals would induce local molecular changes within the axon to communicate sensitisation to the soma. While one possibility was that sensitisation could arise purely through local mechanisms at the terminals (e.g., receptor upregulation), localised PGE_2 application induced significant sensitisation to capsaicin, not only at the terminals, but also at the soma. This was a somewhat surprising result, indicating that sensitisation signals can propagate retrogradely from the periphery to the cell body, extending beyond a purely local effect. Kimourtzis et al. (2024) previously demonstrated retrograde propagation of sensitisation to the soma by applying PGE_2 acutely to axons in microfluidic chambers, which led to immediate repetitive neuronal firing in the soma after axonal stimulation with KCl. Importantly, they did not stimulate the somata directly as shown here, only assessing the effects of axonal activation. In addition, their study focused on acute exposure ($\leq$1 h), whereas the 17-hour exposure, here, in theory models prolonged inflammation, more closely approximating pathological pain states. Nevertheless, this cannot be considered truly "chronic", as many *in vivo* models sustain inflammation for several days (Jang, Kim, and Hwang, 2020), and patients may experience inflammatory pain for months or years (Treede et al., 2015). Thus, the experimental design of the work here represents an intermediate time-frame that captures plasticity mechanisms beyond acute receptor signalling, yet precedes the long-term structural changes associated with chronic pain.

3.4.3 PGE_2-Induced Neuronal Sensitisation is Nociceptive Neurone-Specific

Notably, in this model, the spatially restricted treatment did not significantly affect general excitability when assessed with KCl, which depolarises neuronal membranes in a receptor-independent manner and therefore provides a measure of broad neuronal responsiveness - although, this could be due to low statistical

power. Cell size distribution of KCl responders was also unaffected by PGE_2, although a trend toward an increased proportion of medium-diameter neurone responders was observed, consistent with previous findings by Stucky et al. (1996) and supporting a model of selective nociceptive neurone sensitisation. In non-selective assays like KCl stimulation, such subtle changes may be masked by the responses of large-diameter, low-threshold mechanoreceptors not targeted by PGE_2. This could be contested, however, as some groups have demonstrated PGE_2-induced sensitisation to general depolarisation with KCl (Gu, Kwong, and Lee, 2003; Kimourtzis et al., 2024; Rangwani, 2018). In further support of my findings, preferential action of PGE_2 on small-diameter C-fibre and medium-diameter Aδ fibres that express EP receptors and TRPV1 has been demonstrated before (Cavanaugh et al., 2011; Joseph and Levine, 2010; Lin et al., 2006; St-Jacques and Ma, 2014). Thus, PGE_2 likely modulates excitability predominantly in a subtype-specific manner, rather than producing a global increase across all sensory neurones.

As discussed in Section 1.7, activation of TRPV1 on nociceptive neurones induces an influx of Ca^{2+} into the cytoplasm (Willis, 2009), detected in the experiments, here, as increased fluorescence of the calcium-sensitive dye Fluo-5. This PGE_2-induced sensitisation likely reflects enhanced TRPV1 function through its potentiation of phosphorylation-dependent sensitisation (Figure 3.19; Moriyama et al., 2005), as well as by promoting receptor trafficking and insertion into the plasma membrane and, in some contexts, *de novo* protein synthesis (Ma et al., 2016). Previous studies have demonstrated that EP receptors are present in $TRPV1^+$ nociceptive subpopulations, predominantly in smaller-diameter neurones (Moriyama et al., 2005). In dorsal root ganglia, non-peptidergic nociceptors tend to bind IB4 ($IB4^+$) whereas peptidergic nociceptors typically do not ($IB4^-$), reflecting widely used phenotypic classifications in sensory neurones. Hyperalgesic priming induced by PGE_2 has been reported to be restricted to $IB4^+$ nociceptors, as ablation of these cells eliminated prolonged hyperalgesia in priming paradigms, implying

a key role for this subpopulation in plasticity triggered by inflammatory mediators (Joseph and Levine, 2010). However, PGE_2 can also directly sensitise broader nociceptive neurone populations; for example, it primes intermediate-size neurones for subsequent responses to noxious stimuli (Stucky et al., 1996), aligning with our observation of a slight increase in the recruitment of medium-diameter fibres following axonal PGE_2 exposure.

These observations reinforce that capsaicin responsiveness is largely determined by soma diameter, with smaller C-fibre and medium Aδ neurones exhibiting the highest likelihood of response. While PGE_2 treatment did not significantly alter the overall size distribution of capsaicin-responsive neurones, the trend toward increased medium-diameter recruitment aligns with previous reports that PGE_2 can subtly sensitise intermediate nociceptive neurones without recruiting entirely new functional classes (Stucky et al., 1996). This supports a model in which PGE_2 modulates excitability in a subtype-specific manner, targeting nociceptive neurones expressing EP receptors and TRPV1, rather than producing a global increase across all sensory neurones.

Importantly, I observed the functional effect, not only by stimulating the axon itself, but also by directly stimulating the soma following PGE_2 incubation at the terminal. While previous microfluidic studies have demonstrated that depolarisation at distal axons can propagate signals to the soma (Clark et al., 2018), such retrograde communication had not been tested in the context of PGE_2-induced sensitisation (Kimourtzis et al., 2024). This indicates the involvement of a mechanism by which terminal sensitisation can influence somatic responses. One possible pathway may involve local translation of axonal transcripts, with newly synthesised proteins or downstream messengers influencing neuronal signalling processes (Dalla Costa et al., 2021; Lucci et al., 2020).

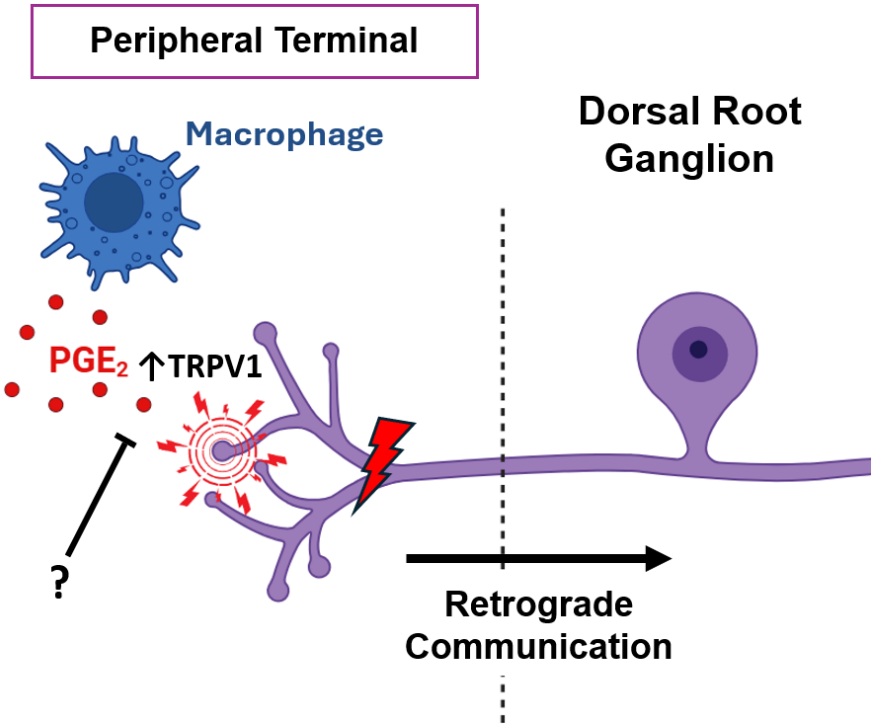


Figure 3.19. PGE_2-Induced Neuronal Sensitisation via Potentiation of TRPV1. PGE_2, released by local immune cells such as macrophages following tissue injury, was applied to axon terminals of sensory neurones cultured in compartmentalised microfluidic devices. Calcium imaging revealed sensitisation, both locally at the axon terminal and retrogradely at the soma, indicating the presence of an axon-initiated inflammatory signal. Sensitisation appeared to be capsaicin- (TRPV1-) dependent (not elicited by KCl), suggesting potentiation of TRPV1 as the underlying mechanism. Created with BioRender™.

To further confirm the role of TRPV1 in this model of sensitisation, immunocytochemistry could be used to assess changes in its expression. However, as previous studies have already demonstrated increased receptor density under inflammatory conditions (Ma et al., 2016; Moriyama et al., 2005), functional assays were prioritised in the present work. Nonetheless, repeating these experiments in TRPV1 knockout cells and/or rodent models would provide additional mechanistic validation.

3.4.4 Constraints of Calcium Imaging

Mechanical Flow

The force of stimulant addition has the potential to generate a neuronal response

by modulating ion channel activity, affecting our Ca^{2+} readout during calcium imaging. Specifically, mechanical stimulation, such as fluid flow, has been shown to enhance N-type calcium currents (involved in neurotransmitter release) while suppressing T-type currents in sensory neurones (crucial for sensing pain, touch, and temperature), thereby altering calcium influx (Bouskila and Bostock, 1998). Such changes would be expected to manifest as increased calcium transients and thus elevated fluorescence intensity during imaging.

In MFCs, the geometry of the device causes applied stimuli to be funnelled through narrow channels, potentially increasing shear stress or pressure at the cell surface. This greater mechanical force could inadvertently activate mechanosensitive channels or pressure-sensitive receptors, thereby generating calcium transients independent of specific ligand-receptor interaction. This phenomenon has been previously observed in cultured DRG neurones, where directed fluid flow alone was sufficient to modulate calcium channel activity (Bouskila and Bostock, 1998), supporting the importance of acknowledging mechanical variables in calcium imaging studies. However, the calcium transients evoked in response to imaging buffer, applied as a mechanical flow control in the work presented here, were minimal compared to chemical stimulation.

Repeated Stimulation

Multiple stimulations were necessary to collect comparable responses to different agonists from the same set of sensory neurones across their subcellular compartments. A key limitation of this approach, however, is the time required for intracellular calcium levels to return to baseline before a subsequent stimulation can be measured accurately. For example, in rat DRG neurones, recovery of ryanodine-sensitive calcium stores following depletion can take approximately two to seven minutes, depending on the extent of post-depletion overshoot (Usachev and Thayer, 1999). Similarly, *in vivo* calcium imaging protocols of sensory neurones recommend waiting at least five minutes between successive stimulations to

allow for sufficient recovery (Shannonhouse et al., 2023). In contrast, Clark et al. (2018) demonstrated that repeated KCl depolarisations delivered to axon terminals at five-minute intervals evoked highly reproducible calcium responses in the soma, with minimal baseline drift and only a small proportion of neurones exhibiting tachyphylaxis. This confirms that sequential stimulation of the same cells across compartments is feasible in microfluidic cultures and suitable for assessing functional responses, although recovery kinetics still constrain the minimum interval between stimulations. In an ideal scenario, a 10 minute imaging break would have been performed between stimulations, but this duration was not feasible within the constraints of a single continuous imaging experiment and would necessitate a return to cell culture conditions with growth supplements in between stimulations. This approach would also not guarantee measurement from the same cell bodies. Alternatively, a live-cell incubator could be used to maintain optimal conditions during imaging; however, such equipment was not available in our laboratory.

As a result, it remains uncertain whether cells responding to a second or third stimulation - such as KCl following capsaicin (which elicited calcium responses to a lesser degree than expected), or somatic capsaicin following both KCl and an initial capsaicin addition - were responding in the same manner as they would have if naïve. Prior stimulation may have altered excitability, desensitised receptor populations, or induced refractory states that confound interpretation (Grider, Jessu, and Kabir, 2023; Linley et al., 2010; Shannonhouse et al., 2023). While this limitation is inherent to sequential stimulation protocols, it must be explicitly acknowledged when evaluating these results.

Impact of Stimulation Volume and Regional Sensitivity

Additionally, differences in the number of responsive cells between axonal and somatic stimulation can be influenced by both biological and analytical factors. Although the same cells were imaged across compartments, only those that responded to a given stimulus were included in the analysis. As demonstrated by

Clark et al. (2018), sensory neurone terminals and somata can exhibit different sensitivities to the same agonist in microfluidic cultures, meaning that the subset of cells classified as responders may differ depending on whether axons or somata are stimulated. In addition, differences in stimulus volume applied to each compartment can affect the number of cells exposed to sufficient agonist concentrations, with larger volumes (as applied to the cell somata) increasing the likelihood of capturing more responders within the imaging field, despite sensitivity differences. Consequently, observed discrepancies in responder counts may reflect a combination of genuine compartment-specific sensitivity and differences in stimulus exposure, rather than technical limitations alone. Any comparisons of responder numbers across compartments should therefore be made with caution.

3.4.5 EP_4 Mediates PGE_2-Induced Neuronal Sensitisation

The findings here raise an important mechanistic question: which PGE_2 receptor subtypes are responsible for the observed retrograde sensitisation? PGE_2 signals via four EP receptors ($EP_{1\text{-}4}$), all expressed in sensory neurones (Oida et al., 1995) and coupled to distinct intracellular pathways. Identifying the receptor(s) engaged in axonal signalling is critical for targeting compartment-specific mechanisms underlying pain.

Within this work, a pilot immunocytochemistry study was performed to quantify the levels of EP_4 following PGE_2 treatment. EP_4 antibody binding was significantly increased, suggesting EP_4 upregulation and its role in the PGE_2-induced neuronal sensitisation in this chapter. Increased protein levels could be due to increased receptor externalisation or *de novo* EP_4 protein synthesis (Ma et al., 2016; St-Jacques and Ma, 2013). EP_4 receptor externalisation to the plasma membrane has previously been observed in peripheral sensory neurones following PGE_2 exposure (St-Jacques and Ma, 2013), increasing receptor availability and facilitating axonal signalling. *In vivo*, PGE_2-EP_4 signalling has also been shown to potentiate nociceptive responses by enhancing peripheral excitability and engaging voltage-

gated sodium channels in sensory neurones during acute inflammation (Jang et al., 2017). This trafficking could potentiate retrograde communication by enhancing the capacity of distal axonal EP_4 receptors to activate downstream cAMP/PKA pathways that influence somatic excitability. In further support of this, the persistent spiking activity observed following acute axonal treatment with PGE_2 was been found to be mediated by EP_4-PKA and $Na_v1.8$ signalling (Kimourtzis et al., 2024).

Other studies have demonstrated that peripheral EP_1 receptors, but not central EP_1, play an essential role in PGE_2-induced pain sensitisation (Johansson, Narumiya, and Zeilhofer, 2011). Inhibition or loss of EP_1 decreases nociceptive signalling, thermal hyperalgesia, and inflammatory pain (Moriyama et al., 2005; Johansson, Narumiya, and Zeilhofer, 2011). PGE_2 enhances TRPV1-mediated responses via EP_1 receptors in a largely PKC-dependent manner (Moriyama et al., 2005), while EP_4 stimulates adenylyl cyclase, increasing cAMP and activating PKA-dependent sensitisation (covered in more detail in Section 1.6.0.1; Biringer, 2012).

While PGE_2 sensitisation has been found to be dependent on EP_4-mediated PKA activation (Moriyama et al., 2005), prolonged exposure ($\geq$ 12 hours) leads to desensitisation of this pathway. Nonetheless, sensitisation persists via alternative signalling involving EP_2, EP_3, and EP_4 (Malty et al., 2016). This suggests a mechanistic shift during chronic inflammation, wherein persistent excitability is maintained despite attenuation of canonical second messenger signalling. The findings here support this model; prolonged PGE_2 exposure enhanced TRPV1-mediated responses without increasing general excitability, suggesting receptor- and compartment-specific modulation. This aligns with other chronic pain models using sustained IL-6 or NGF exposure (Atmaramani et al., 2021; Tsantoulas et al., 2013), reinforcing the physiological relevance of this design.

Together, these data extend earlier observations that PGE_2 enhances TRPV1 via EP_4- and EP_1-linked pathways (Moriyama et al., 2005). While both EP_1 and EP_4

receptors are strong candidates for mediating this PGE_2-induced nociceptive neurone sensitisation, the available evidence - which supports EP_4's involvement (Kimourtzis et al., 2024; Lin et al., 2006; Southall and Vasko, 2001; St-Jacques and Ma, 2014; St-Jacques and Ma, 2013), the reported weak PGE_2-EP_1 binding (Biringer, 2012), and the preliminary evidence of EP_4 upregulation - suggests a predominant role for the EP_4/cAMP/PKA pathway as a key mediator of retrograde signalling in this model. I have now demonstrated that activation of these mechanisms, exclusively at the axon, is sufficient to induce retrograde sensitisation, with important implications for understanding peripheral contributions to chronic pain.

Future work combining single-cell transcriptomics with alternative functional assays could further clarify the contributions of each EP receptor subtype across distinct nociceptive neurone classes in retrograde sensitisation. EP_4 could represent a valuable therapeutic entry point to selectively target peripherally initiated pain signalling, potentially avoiding NSAID-associated systemic side-effects (NICE, 2021). Indeed, grapiprant - a selective EP_4 antagonist - has been approved for veterinary use in dogs with osteoarthritis and been shown to effectively alleviate pain and inflammation, with a favourable safety profile (Nagahisa and Okumura, 2017). These findings underscore the translational potential of EP_4 antagonism in pain management and reinforce its candidacy as a targeted, peripheral pain therapy.

3.4.6 Retrograde Communication: A Novel Insight into PGE_2 Mechanisms

Peripheral sensitisation by PGE_2 is well established *in vivo* - lowering nociceptive neurone thresholds to thermal and mechanical stimuli (Chen, Tanner, and Levine, 1999; Minami et al., 1999; Woolf and Ma, 2007) and inducing primary hyperalgesia (Chen, Tanner, and Levine, 1999, Minami et al., 1999, Woolf and Ma, 2007). Despite previous studies demonstrating that PGE_2 can sensitise sensory neurones *in*

vitro, most have examined the effects on the soma by applying PGE_2 globally (Lopshire and Nicol, 1997; Southall and Vasko, 2001; Stucky et al., 1996; Zhou et al., 2019) - direct evidence for axon-to-soma signalling as a contributor to sensitisation is limited. The use of compartmentalised microfluidic chambers, here, isolates the axonal compartment, allowing the dissection of directionality in the signalling response. This adds a critical spatial dimension to existing models of inflammatory pain and supports the emerging view that axons are active integrators of signalling, not merely passive conductors (Clark et al., 2018; Gale et al., 2022; Holt, Martin, and Schuman, 2019).

The data in this chapter demonstrate that PGE_2, when applied exclusively to sensory neurone axon terminals, is sufficient to induce retrograde sensitisation at the soma. As mentioned in Section 3.4.2, Kimourtzis et al. (2024) began to address this by acutely applying PGE_2 to axons in microfluidic chambers, while Clark et al. (2018) demonstrated that depolarisation of distal axons can propagate signals to the soma. Taken together, our studies provide direct evidence for retrograde communication from the periphery to the cell body, supporting a model in which spatially confined axonal signalling can influence upstream neuronal excitability. Traditionally, peripheral inflammation has been viewed as a local phenomenon that lowers nociceptive neurone thresholds. However, together, our data suggest that peripheral signals can initiate intracellular changes in the axon that propagate to the soma and may influence central terminals (Dalla Costa et al., 2021), potentially contributing to central sensitisation via enhanced neurotransmission at the synapse (Ma, 2010). Although second-order spinal neurones were not examined, these findings indicate the possibility that axonally initiated retrograde signalling could influence synaptic output at the central terminal, thereby linking peripheral inflammation to central pain processing (Latremoliere and Woolf, 2009).

Retrograde signalling has been well documented in sensory neurones. Examples include NGF binding to TrkA receptors and forming retrogradely transported

signalling endosomes (Cui et al., 2007); cAMP response element-binding protein (CREB) local synthesis in the axon and retrograde transport to the nucleus to promote neuronal survival (Cox et al., 2008); and injury-induced axonal cues that trigger transcriptional programmes in the soma (Ben-Yaakov et al., 2012; Hanz et al., 2003; Kar et al., 2013). The exact mechanism underlying PGE_2-induced retrograde communication remains unclear, but several possibilities warrant investigation in future work:

- **Retrograde transport of signalling endosomes**, similar to NGF-TrkA complexes and CREB (Cox et al., 2008; Cui et al., 2007; Dalla Costa et al., 2021), potentially carrying activated EP receptors, RNAs, or downstream effectors to the soma.

- **Local translation of axonally enriched mRNAs**, resulting in proteins that modulate somatic excitability or transcription-dependent signalling cascades, such as importin $\beta 1$ and signal transducer and activator of transcription 3 (STAT3; Ben-Yaakov et al., 2012; Dalla Costa et al., 2021; Hanz et al., 2003; Kar et al., 2013)

- **Diffusible second messengers**, such as Ca^{2+} or cAMP, which may propagate through the axon to influence somatic signalling (Kimourtzis et al., 2024).

Retrograde transport, local translation, and diffusible messengers represent non-mutually-exclusive pathways by which axonally initiated signals could influence somatic excitability. In the following chapter, local translation is explored as a candidate mechanism through transcriptomic profiling and targeted siRNA knockdown of axonally regulated transcripts.

3.4.7 Chapter Conclusions

I hypothesised that neurones exposed to PGE_2 for an extended period would demonstrate neuronal sensitisation. To do this I assessed excitability during calcium imaging with 200 nM capsaicin, a TRPV1-selective agonist. In dissociated cultures, where all cellular compartments are exposed, PGE_2 induced a pronounced sensitisation, demonstrated by increased capsaicin-evoked calcium responses (Section 3.3.3, Pope et al., 2025; Arendt-Tranholm, 2022). To improve spatial resolution and distinguish compartment-specific signalling, PGE_2 exposure was restricted to axon terminals. Peripheral axonal stimulation by PGE_2 was sufficient to induce sustained sensitisation in sensory neurone axons and somata, providing direct evidence for retrograde communication from the periphery to the soma and highlighting a spatially directed mechanism of neuronal modulation. These effects were evident in TRPV1-expressing nociceptive neurones, implicating subtype-and modality-specific signalling pathways likely involving EP_4. This expands our understanding of how compartmentalised signalling contributes to pain plasticity. Future work could repeat these experiments in adult DRG neurones.

Microfluidic culture systems enabled precise spatial separation of axonal and somatic compartments (Atmaramani et al., 2021), allowing us to interrogate not just whether sensitisation occurs, but where it is initiated. These findings reframe the axon as an active signalling hub in the transition from acute to chronic pain, challenging soma-centric models. They also reinforce the need for spatially resolved experimental approaches to understand mechanisms underlying chronic inflammatory pain and to identify compartment-specific therapeutic targets. This approach should improve the translational relevance to *in vivo* rodent research and subsequent clinical studies. However, such systems cannot fully recapitulate the intact environment, which involves immune cell recruitment, vascular changes, and connectivity with second-order spinal neurones. *In vivo*, peripheral sensitisation of this kind would be expected to increase neurotransmission at central terminals, pro-

moting spinal plasticity and central sensitisation, both of which are hallmarks of chronic pain (Latremoliere and Woolf, 2009).

In the following chapter, I build on these findings by investigating the mechanisms underlying retrograde sensitisation. Specifically, I test whether local translation of axonal mRNAs contributes to the initiation of somatic excitability changes. Using compartment-specific RNA sequencing and siRNA knockdown, I aim to identify spatially regulated transcripts that are both locally translated and functionally required for persistent sensitisation. This approach offers the potential to uncover novel, spatially targeted therapeutic strategies for chronic pain.

Chapter 4

Tnfrsf12a is Involved in Neuronal Excitability

4.1 Introduction

Inflammation induces profound molecular changes in sensory neurones that increase excitability and drive persistent pain (Latremoliere and Woolf, 2009; Tsantoulas et al., 2013). These changes are mediated not only by transcriptional reprogramming in the soma, but also by local signalling and protein synthesis within peripheral axons, which can rapidly modify neuronal responsiveness to inflammatory mediators (Gale et al., 2022; Holt, Martin, and Schuman, 2019; Kar et al., 2013). Identifying inflammation-responsive genes that are enriched in axons, and that have established links to immune signalling pathways, is therefore critical for understanding mechanisms of nociceptor sensitisation.

Using compartmentalised sensory neurone cultures, this chapter aimed to identify candidate mediators of inflammatory sensitisation that are selectively regulated within axons following PGE_2 exposure. Transcriptomic profiling of axonal and somatic compartments revealed a subset of inflammation-associated mRNAs that were preferentially upregulated in axons. Among these, *Tnfrsf12a* emerged as a strong candidate due to its known role in pro-inflammatory signalling, its reported expression in sensory neurones, and its potential to link neuroimmune activation with changes in neuronal excitability (Burkly, Michaelson, and Zheng, 2011; Huang et al., 2025; Tanabe et al., 2003).

This chapter therefore investigates the role of tumour necrosis factor receptor superfamily member 12A (TNFRSF12A), also known as fibroblast growth factor-inducible 14 (Fn14) or the receptor for tumour necrosis factor-like weak inducer of apoptosis (TWEAK), in mediating a sensitised neuronal state. I combine axon versus soma transcriptomic analysis following PGE_2 treatment with targeted siRNA knockdown of *Tnfrsf12a* to test the hypothesis that local translation of *Tnfrsf12a*in axons contributes to inflammatory sensitisation.

4.1.1 The TWEAK receptor

TNFRSF12A is a member of the tumour necrosis factor receptor superfamily and serves as the primary receptor for TWEAK. Activation of TNFRSF12A initiates NF-κB and MAPK signalling cascades that drive the expression of pro-inflammatory cytokines and chemokines (Winkles, 2008). Importantly, TNFRSF12A is expressed by a broad range of cell types relevant to pain and inflammation, including immune cells such as monocytes and macrophages, endothelial cells, astrocytes, and neurones (Nazeri et al., 2014). This widespread expression positions TNFRSF12A as a key mediator of neurone-glia and neuroimmune interactions.

Consistent with this role, TNFRSF12A expression is upregulated in both peripheral and central nervous system tissues following injury and inflammation (Burkly, Michaelson, and Zheng, 2011; Huang et al., 2025; Tanabe et al., 2003). TNFRSF12A signalling has been implicated in a range of inflammatory and pathological conditions, including arthritis, inflammatory bowel disease, multiple sclerosis, and cancer (Chen et al., 2025b; Nazeri et al., 2014), highlighting its function as part of a multifunctional pro-inflammatory pathway.

Within sensory neurones specifically, TNFRSF12A has been linked to cell survival, neurite outgrowth, and inflammatory diseases (Nazeri et al., 2014; Tanabe et al., 2003). Despite this, its potential role in regulating nociceptor excitability at the subcellular level remains poorly defined. Given its strong association with inflammatory signalling pathways, and its axonal upregulation following PGE_2 exposure identified here, TNFRSF12A represents a biologically plausible mediator of neuronal sensitisation. It may act downstream of PGE_2-triggered inflammatory cascades to modulate axonal signalling and excitability (Figure 4.1).

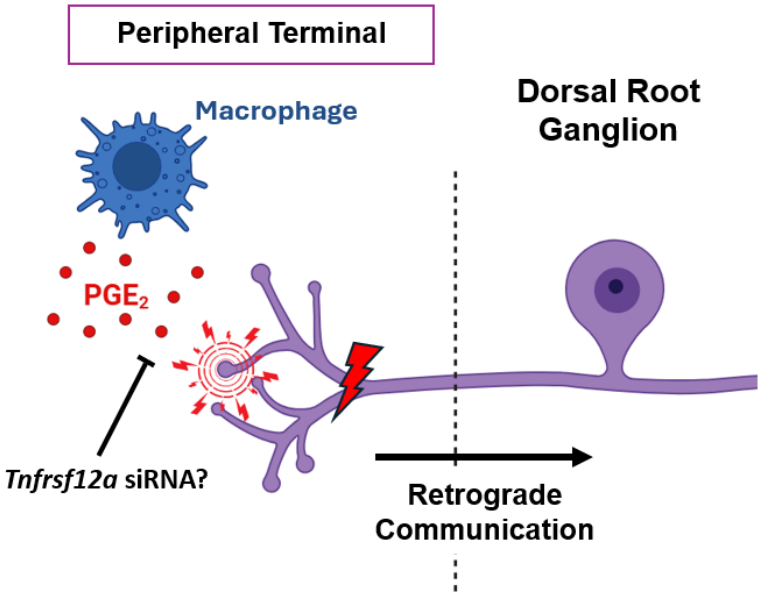


Figure 4.1. PGE_2 Applied to the Axonal Terminal Sensitises Sensory Neurones. Macrophages are amongst the cells that produce PGE_2 in the local environment of the sensory neurone peripheral terminal. PGE_2 binds to its receptors on DRGs and induces neuronal sensitisation. The mechanisms by which this occurs are not fully explored but could involve TNFRSF12A - silencing *Tnfrsf12a* with siRNA may inhibit sensitisation. Created using BioRender™.

4.1.2 Uncovering RNA Dynamics Through Transcriptomics in the Nervous System

RNA is the key intermediary between the genome and the proteome, carrying the instructions that determine cellular structure and behaviour (Section 1.3.1.5). Transcriptomics has transformed our ability to profile gene expression across tissues, developmental stages, and experimental conditions (Christopher et al., 2022). In the context of pain and nociception, these approaches not only reveal how mRNA abundance shifts in response to injury and inflammation, but also reveal the wider dynamics of RNA biology, including alternative splicing, RNA editing, and non-coding RNAs (Kringel and Lötsch, 2025; Wang et al., 2021).

In the nervous system, transcriptomics has identified molecular signatures underlying cell-specific functions, plasticity, and pathology (Kringel and Lötsch, 2025). Beyond whole-cell analyses, spatially resolved transcriptomics can reveal differences

in RNA localisation within individual cells (Fazal and Chang, 2019; Christopher et al., 2022) - a feature of particular importance in neurones due to their extreme compartmentalisation, and especially in sensory neurones given their length (Holt, Martin, and Schuman, 2019; Sasaki, 2020; Sörnmo and Laguna, 2005).

4.1.3 Local Translation of mRNA

Although local translation occurs in many cell types, its physiological importance is most evident in neurones due to their polarity and compartmentalised structure (Sasaki, 2020). While most mRNAs are transcribed in the nucleus and translated in the soma, many transcripts are transported to distal compartments, such as axons and terminals, where they can be locally translated in response to external stimuli. This allows rapid, spatially restricted protein synthesis, supporting processes such as synaptic plasticity, axonal regeneration, and sensory processing, without relying on long-range transport from the soma (Section 1.3.1.5; Holt, Martin, and Schuman, 2019; Willis and Twiss, 2011).

In nociceptive neurones, axonal translation has been implicated in injury-induced sensitisation and chronic pain (Gale et al., 2022). Compartmentalised RNA sequencing has revealed distinct axonal transcriptomes, highlighting that neurones maintain local regulatory mechanisms capable of responding dynamically to inflammatory mediators (Christopher et al., 2022; Sasaki, 2020; Tushev et al., 2018).

4.1.4 Local Control of Excitability Through Spatially Restricted Gene Expression

While transcriptomics provides powerful insights, it does not directly establish functional relevance. To address this, targeted molecular approaches such as siRNA knockdown are required (Kaur and Sharma, 2012). As described in Section 1.3.1.5, siRNAs are short, double-stranded RNA molecules that degrade complementary mRNAs, thereby preventing protein translation. They provide a precise way to

manipulate gene expression and probe molecular function (Kaur and Sharma, 2012). In neuronal physiology, siRNAs can be spatially restricted using microfluidic cultures, enabling axon-specific gene silencing while leaving somata unaffected (Hengst et al., 2006). This is especially valuable for studying local translation as a mechanism of neuronal plasticity and sensitisation.

4.1.5 Aims and Hypotheses

Hypotheses

I hypothesised that axonal enrichment of *Tnfrsf12a* reflects its local translation in response to inflammatory stimuli and that this translation contributes to neuronal sensitisation. Specifically, I predicted that selective axonal knockdown of *Tnfrsf12a* would attenuate increases in excitability.

Experimental Aims

To test this hypothesis, I aimed to:

- Measure neuronal excitability in dissociated DRG cultures following global *Tnfrsf12a* siRNA knockdown using calcium imaging.
- Measure neuronal excitability in compartmentalised cultures following axon-restricted *Tnfrsf12a* siRNA knockdown.
- Verify siRNA knockdown efficiency by real-time quantitative polymerase chain reaction (RT-qPCR).

The transcriptomic data presented in this chapter were originally generated as part of a collaborative project. Boyden chamber cultures and RNA extraction for transcriptomics were performed by Asta Arendt-Tranholm, with RNA sequencing subsequently carried out by an external provider (Arendt-Tranholm, 2022). These data are used here with full attribution to inform and contextualise the siRNA-mediated gene knockdown studies carried out in this thesis. All siRNA treatments, dissoci-

ated experiments, microfluidic chamber experiments, functional analyses, subsequent RNA extractions and RT-qPCRs were performed by me.

Bioinformatic analysis, including differential gene expression and gene set enrichment, was conducted by Rafael Fort (Pope et al., 2025).

4.2 Methods

4.2.1 DRG Neuronal Culture

Culture for Functional Assessment

E16.5 DRG neurones were cultured, as previously described in Section 2.3.2. For functional assessment of siRNA addition, neurones were cultured in dissociated cultures in PDMS rings or in compartmentalised cultures in microfluidic chambers. DRGs were cultured for five days before treatment.

Experiments in this chapter were affected by the closure of our animal unit for an extended period - refer to Section 2.1 for more details.

Culture for RT-qPCR and Transcriptomics

For confirmation of mRNA knockdown following siRNA treatment (RT-qPCR), 6-well plates with 20 DRGs (post-dissociation) per well were cultured (Section 2.3.2).

For RNA-sequencing and transcriptomics, 25 E16.5 DRGs were seeded post-dissociation in nuncs with a modified Boyden chamber (1 μM porous tissue culture membrane inserts, Costar) by Arendt-Tranholm (2022), adapting a protocol from Unsain et al. (2014) (Figure 2.2; Section 2.3.2). Axons grew through the membrane, remaining isolated from their cell body but, unlike in compartmentalised microfluidic chambers, there was no fluidic isolation (Willis and Twiss, 2011). Despite this disadvantage, and in order to produce a suitable RNA yield for transcriptomics to be performed, Boyden chambers were ideal because many more cells could be seeded in these chambers (Willis and Twiss, 2011).

For comparison, DRG explants were also isolated from adult 8-week-old C57BL/6 mice and kept on ice in HBSS (Arendt-Tranholm, 2022). In brief, tissue was sequentially digested with collagenase A, collagenase D with papain, and an enzyme T solution containing trypsin inhibitor and BSA, with incubation at 37℃ and gentle mechanical dissociation. The resulting cell suspension was filtered through a 70 μm strainer, centrifuged, and resuspended in L-15 media supplemented with FBS, Pen/Strep, 5-Fluoro-2'-deoxyuridine to limit non-neuronal growth, and NGF to support axonal growth. Dissociated DRG neurones were then seeded into porous membrane inserts for culture. For more detailed methodology, refer to Arendt-Tranholm (2022).

4.2.2 PGE_2 Treatment

As described in Section 3.2.2, neurones were treated with 10 μM PGE_2. PGE_2 was applied to both the axonal and somatic compartments of the Boyden chamber to ensure uniform exposure across the membrane barrier (Figure 4.2).

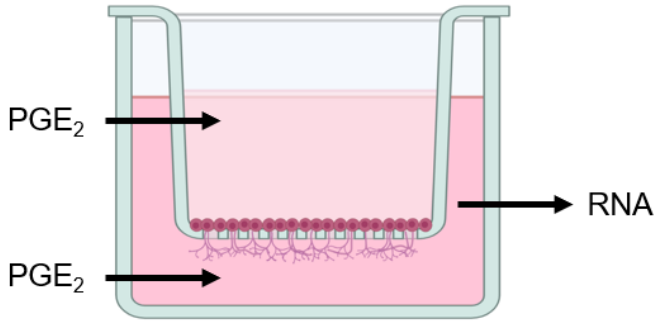


Figure 4.2. Protocol for PGE_2 Treatment in Boyden Chambers. In Boyden chambers, cells were seeded onto the membrane and allowed to project their axons through the pores into the media below. PGE_2 was applied both to the cell soma and axon compartments. This model was used for RNA extraction. Created using BioRender™.

4.2.3 Transcript Knockdown Using siRNA

A SMARTPool of four siRNAs targeting murine *Tnfrsf12a* mRNA (Accell, Horizon Biosciences) was used as a single reagent to enhance potency and specificity. A non-targeting siRNA pool (Accell Non-Targeting Control Pool, Horizon Biosciences)

was selected as a control to account for non-sequence-specific effects (sequences in Appendix, Table A1).

Preparation of siRNA

For both the target and non-targeting control siRNA, tubes were briefly centrifuged to ensure the contents were at the bottom. The 5 nmol pellet was dissolved in 50 μL HyClone water (Cytiva) to produce a stock concentration of 100 μM. After gently pipetting up and down three-five times, tubes were sealed and placed on a roller mixer at RT for 30 minutes to ensure complete dissolution. Aliquots were stored at -20°C.

siRNA Treatment Protocol

Before use, target and control siRNA were further diluted in DRG complete media to a working concentration of 1 μM.

For calcium imaging, 1 μM siRNA, or 1 μM non-targeting control siRNA was added to whole-cell dissociated cultures, or to the axon compartment of compartmentalised microfluidic chambers, at DIV5 for 48 hours (Figure 4.3A). An untreated control condition involving a media change was also included.

For RNA extraction, DRG neurones were cultured in 6-well plates until DIV5, at which point 1 μM *Tnfrsf12a* siRNA or 1 μM non-targeting control siRNA was added to the culture media. RNA was extracted at 24 and 48 hours post-treatment to assess mRNA knockdown efficiency (Figure 4.3B).

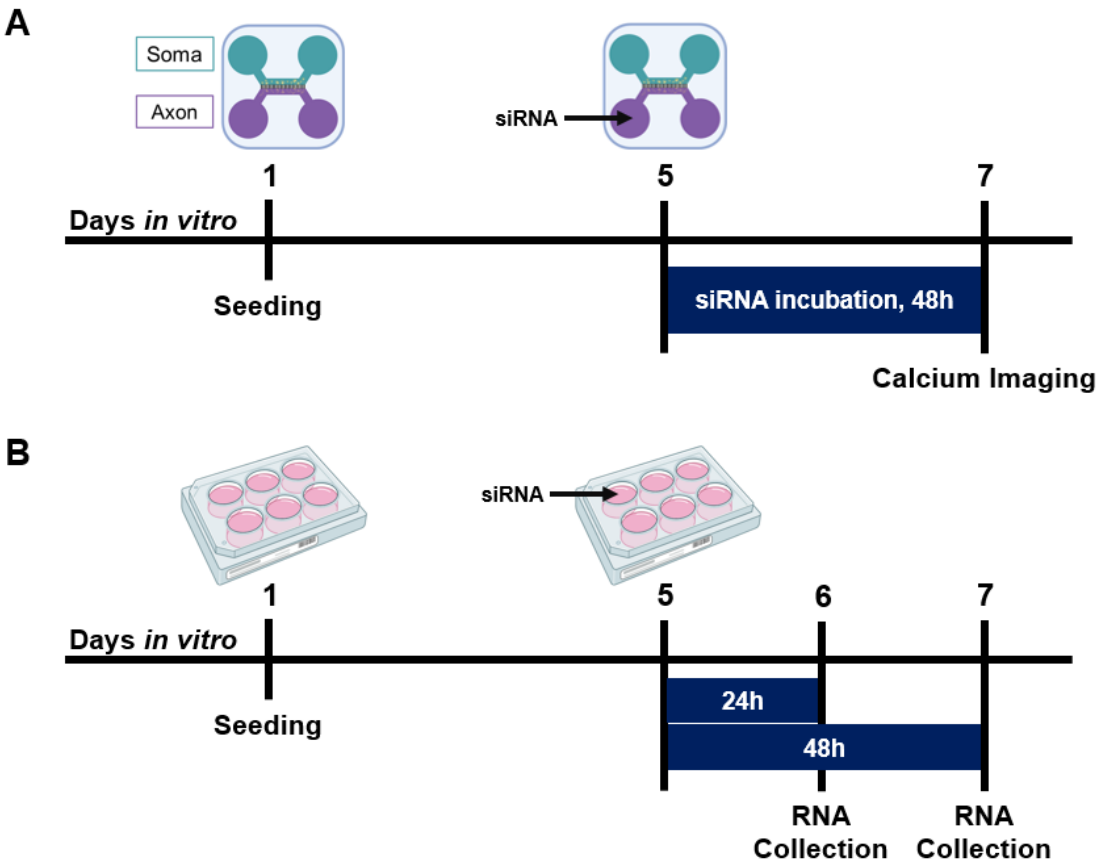


Figure 4.3. siRNA Incubation Timeline. DRGs were cultured for five days before media was replaced with fresh media supplemented with 1 μM of *Tnfrsf12a* siRNA, siRNA non-targeting control, or given a sham media change. **A -** Calcium imaging was performed 48 hours after axon terminal treatment to assess neuronal excitability in cells cultured within microfluidic chambers. **B -** RNA was collected from 6-well plates at two time points: 24 hours post-treatment (subset of wells) and 48 hours post-treatment (remaining wells). Figure created using BioRender™.

4.2.4 RNA Extraction

As described in Section 4.2.1, RNA extraction from DRG neurones was conducted using 6-well plates to enable sufficient RNA yield. For each treatment group, one well was used to minimise the siRNA volume.

On DIV5, DRG neurones were treated with either 1 μM siRNA or 1 μM siRNA non-targeting control, as described in Section 4.2.3. On DIV6 and DIV7, wells were gently washed with DPBS ($CaCl_2$/$MgCl_2$-free) to remove residual media prior to RNA extraction, corresponding to 24 and 48 hours post-siRNA treatment. 500 μL of TRIzol® Reagent (15596026, Invitrogen™) was added and the cells were

scraped to release them into the reagent. Cells in TRIzol® were frozen at -20°C until the next stage was performed.

RNA extraction was undertaken as per manufacturer's instructions, in brief:

After thawing, chloroform was added to each sample at 0.2 mL per 1 mL TRIzol® and the tubes shaken vigorously for 15 seconds. A three-minute incubation was performed at RT, prior to centrifugation at 12,000 x *g* for 15 minutes at 4°C to form three distinct layers. The colourless, upper aqueous phase, containing the RNA, was carefully transferred to a new tube, without disturbing the lower levels which contained DNA and protein.

Isopropanol (100%) was added at 0.5 mL per 1 mL TRIzol® to the aqueous phase, mixed by inverting the tubes, and incubated at RT for 10 minutes. The samples were centrifuged for 10 minutes at 4°C and the supernatant discarded. The pellet was washed with 75% ethanol at 1 mL per 1 mL TRIzol®, briefly vortexed, and centrifuged at 7,500 x *g* for five minutes at 4°C.

The supernatant was carefully removed and discarded, and the RNA pellet air-dried, before resuspension in 10 μL RNase-free water (low volume due to suspected low RNA yields). The resuspended RNA was incubated on a heat block at 60°C for 10-15 minutes and the RNA quality determined on the NanoDrop 2000 spectrophotometer (Thermo Fisher Scientific, USA) by assessing absorbance at 260 nm (Becker et al., 2010). A 260/280 ratio close to two was deemed acceptable.

4.2.5 cDNA Synthesis

cDNA synthesis was performed using SuperScript™ IV (SSIV) Reverse Transcriptase (Invitrogen™), following the manufacturer's protocol. The reaction mix (formulation in Table 4.1) was combined on ice, mixed, and briefly centrifuged. The RNA-primer mix was heated to 65°C for five minutes using the thermocycler (Ep-

pendorf Mastercycler 5333) to allow primers to attach, and then cooled to 4°C for one minute.

Table 4.1. RNA Annealing Mix Reagents.

Component	Volume
50 μM Oligo d(T)20 primer	1 μL
40 mM dNTP mix (10 mM each)	1 μL
Template RNA - 100ng	up to 11μL
DEPC-treated or nuclease-free water	to 13 μL

The 5X SSIV Buffer was pre-warmed to room temperature and briefly vortexed. The following components were combined in a reaction tube per sample (making up slightly more than the required volumes): 4 μL 5x SSIV Buffer, 1 μL 100 mM dithiothreitol (DTT), 1 μL RNaseOUT™ Recombinant RNase Inhibitor (Invitrogen™), 1 μL SSIV Reverse Transcriptase (200 U/μL). The tube was mixed and briefly centrifuged.

7 μL of the reaction mix was added to each tube of annealed RNA. The reaction mix was incubated at 50°C for 10 minutes and then inactivated at 80°C for 10 minutes, using the thermocycler. The cDNA was stored at -20°C overnight.

4.2.6 Real-Time Quantitative-PCR

To measure the expression level of *Tnfrsf12a* RNA, RT-qPCR was conducted. Candidate genes were assessed as potential reference genes, with glyceraldehyde-3-phosphate dehydrogenase (*Gapdh*) and ubiquitin-conjugating enzyme E2 (*Ube2*) found to be the most stably expressed.

cDNA and the forward and reverse primers were thawed on ice. The PCR reaction mix was prepared on ice for each primer set, scaled to the required volume for the number of wells, and mixed thoroughly. For each well of a 96-well QuantStudio™ qPCR plate (Starlab), the reaction mix contained: 5 μL PowerUp™ SYBR™ Green Master Mix (2X, Applied Biosystems), 3.6 μL RNase-free H_2O, and 0.4 μL of 10 μM

forward and reverse primers (listed in Appendix Table A2). 1 μL of the appropriate DNA template was added to each well, then the PCR plate was sealed with an optical adhesive cover (ThermalSeal® RT2RR™ Sealing Films, Excel Scientific), smoothing it down with an applicator. The plate was centrifuged for four minutes at 5,000 x *g* at 4°C. If any bubbles remained, the wells were gently flicked and centrifuged again briefly at the same speed.

The plate was placed into the QuantStudio™ 5 Real-Time PCR System (Applied Biosystems) and the fast cycling mode selected with the stages listed in Table 4.2:

Table 4.2. Thermal Cycling Conditions for qPCR on the QuantStudio 5 Plate Reader.

Step	Temperature/Time	Cycles
UDG activation	50°C for 2 min	1
Dual-Lock™ DNA polymerase activation	95°C for 2 min	1
Denaturation	95°C for 1 sec	40
Annealing/extension	60°C for 30 sec	

4.2.7 Analysis of qPCR Data

Expression patterns of *Tnfrsf12a* mRNA were normalised to the geometric mean of the internal housekeepers (HK), *Gapdh* and *Ube2*, and compared between treatment groups: *Tnfrsf12a* siRNA and siRNA control, using the comparative Ct method ($2^{-\Delta\Delta Ct}$) (Livak and Schmittgen, 2001).

The fold change of the expression of RNA (Ribonucleic acid of interest, RAi) in the target sample, relative to control, is defined by the following equation:

$$\Delta\Delta Ct = (Ct_{RAi} - Ct_{HK})_{Target} - (Ct_{RAi} - Ct_{HK})_{siRNAControl} \quad (4.1)$$

As 2^0 = 1, the expression of the RAi in control conditions is close to one.

4.2.8 Transcriptomics and qPCR Validation - Methodological Comparison with Collaborator

To identify transcripts of interest from PGE_2-induced sensitisation, bulk RNA sequencing and qPCR validation were conducted previously on a cohort of E16.5 and 8-week-old DRG neuronal cultures grown in Boyden chambers (Arendt-Tranholm, 2022). DRG neurones were treated with 10 μM PGE_2 in both the axon and somal compartments of the Boyden chamber at DIV6 (Section 4.2.2). While key steps were conceptually similar to those employed in the current study - including the use of TRIzol™ Reagent for RNA extraction and SYBR™-based qPCR for transcript quantification - important methodological distinctions are noted below. These reflect slight procedural differences rather than fundamental changes, and are not expected to impact the interpretation of results. Nonetheless, they are included here for clarity and transparency.

RNA Extraction

In both cases, TRIzol™ Reagent was used to lyse cells and isolate RNA; however, the collaborator used 1 mL TRIzol™ per sample and collected RNA separately from soma and axonal compartments within compartmentalised Boyden chambers, in contrast to the pooled well-based extraction performed in this study. Their protocol additionally included the use of RNase-free DNA LoBind® tubes to minimise RNA loss, and GlycoBlue™ as a coprecipitant to aid in RNA pellet visibility and yield. A further GTC precipitation step was added to enhance RNA purity. RNA pellets were eluted in a larger volume (30 μL) and stored at either -20°C or -80°C depending on downstream use.

While both protocols relied on NanoDrop 2000 spectrophotometry for RNA quantification, the collaborator also assessed RNA integrity using Agilent TapeStation electrophoresis, calculating RNA Integrity Numbers (RINs) and 28S/18S ratios to confirm suitability for sequencing.

cDNA Synthesis

In the current study, reverse transcription was conducted using the SuperScript™ IV Reverse Transcriptase Kit with oligo$(dT)_{20}$ primers, whereas the collaborator used the SuperScript™ III CellsDirect cDNA Synthesis Kit with random hexamer primers. Incubation conditions and reaction mixes were kit-specific, but both approaches followed manufacturer-recommended protocols and aimed to generate high quality first-strand cDNA.

Real-Time Quantitative PCR

Both datasets utilised RT-qPCR to validate RNA expression, though the reagents and equipment differed slightly. In this study, reactions were run on a QuantStudio™ qPCR system using PowerUp™ SYBR™ Green Master Mix, while the collaborator used the GoTaq qPCR Master Mix (Promega) and conducted amplification on a QIAGEN Rotor-Gene Q platform.

Reaction volumes and thermal cycling profiles were optimised for each system. Despite these procedural differences studies normalised gene expression to housekeepers using the comparative Ct method ($2^{-\Delta\Delta Ct}$) as described by Livak and Schmittgen (2001). Primers for overlapping target genes - such as *Tnfrsf12a* - were independently validated in each study and are detailed in Appendix Tables A2 and A3.

4.2.9 Bioinformatics and RNA Sequencing (RNA-Seq)

The RNA sequencing data presented here were originally generated and analysed by Arendt-Tranholm (2022) but were not analysed in this manner until a joint publication was produced (Pope et al., 2025). The data are used in this chapter with full attribution to provide context for downstream experimental work conducted in this thesis. These foundational data informed gene selection and the rationale for siRNA-mediated knockdown studies.

In brief, library preparation included DNase treatment followed by either ribosomal RNA (rRNA) depletion (for embryonic DRG neurones) or polyA selection (for adult DRG neurones). Embryonic DRG samples underwent paired-end 150 base pairs (bp) sequencing using the Illumina HiSeq platform (GeneWiz, Azenta Life Sciences), while adult DRG samples were sequenced as single-end 75 bp reads on the Illumina NextSeq 500 (University of Texas at Dallas Genome Core). All samples had RINs above 7.

Sequencing quality was assessed using FastQC. Reads were aligned to the GENCODE GRCm38 mouse genome using the STAR aligner with GENCODE vM25 reference annotation. HTSeq was used to generate gene-level count data, and filtering was applied to retain only protein-coding, non-mitochondrial genes.

On average, embryonic DRG neurones yielded 28,442,101 ± 12,577,154 reads, and adult DRG neurones yielded 32,947,254 ± 5,322,518 reads, with respective genome mapping rates of 85.1% ± 11.2 and 98.4% ± 0.2. Gene expression data were normalised using the Trimmed Mean of M-values (TMM) method. Differential expression analysis was performed using the edgeR algorithm via the SARTools pipeline in RStudio, with a threshold of counts per million ≥ 1 applied for inclusion in downstream analyses. Full methodological details are available in Pope et al. (2025).

Gene Set Enrichment Analysis

To investigate functional gene expression patterns, Gene Set Enrichment Analysis (GSEA) was performed by Rafael Fort using the gseGO function from the clusterProfiler R package (Version 4.8.2), focusing on Gene Ontology (GO) categories: Biological Process, Molecular Function, and Cellular Component. Genes were ranked by $\log_2$ fold change and terms with an adjusted p-value < 0.05 were considered significant.

All transcriptomic data visualisations were produced in R (version 4.3) using the

clusterProfiler, enrichplot, ggplot2, and gplots packages (the latter used for heatmap.2). Hierarchical clustering was performed using Euclidean distance and Ward's linkage method.

While the transcriptomic and validation experiments were not conducted as part of this thesis, the results informed gene selection and interpretation of downstream siRNA knockdown targets in my study.

4.2.10 Calcium Imaging

As with the previous chapter's experiments, calcium imaging preparation and parameters are described in Section 2.4. The imaging regimen was modified, with changes to the number of frames acquired and the total duration of imaging to suit the experimental requirements described here.

Dissociated Cultures

Before imaging, IB, used for de-esterification of Fluo-5F AM, was replaced with 100 μL fresh IB. After 30 seconds imaging, 30.5 μL 850 nM capsaicin was added to the inverted chamber well (final concentration 200 nM). The neurones were imaged for a total of 3 minutes 20 seconds (400 images, one every 500 ms). IB was removed and replaced with fresh IB immediately after cessation of recording.

After seven minutes, in which time the next two wells were imaged, the next imaging cycle was started. Thirty seconds into recording, 24.8 μL 131 mM KCl was added to the inverted chamber well (final concentration 25 mM) and imaged for a total of 3 minutes 20 seconds (Figure 4.4B).

Compartmentalised Microfluidic Chambers

Before imaging, IB was removed from the soma and axon compartment of the chambers. After 30 seconds recording, 30 μL 200 nM capsaicin was applied to axon terminals and then at five minutes, 100 μL 25 mM KCl was applied to the

soma-enriched compartment (Figure 4.4A). Somata were imaged for 11 minutes 15 seconds (960 images, one every 500 ms).

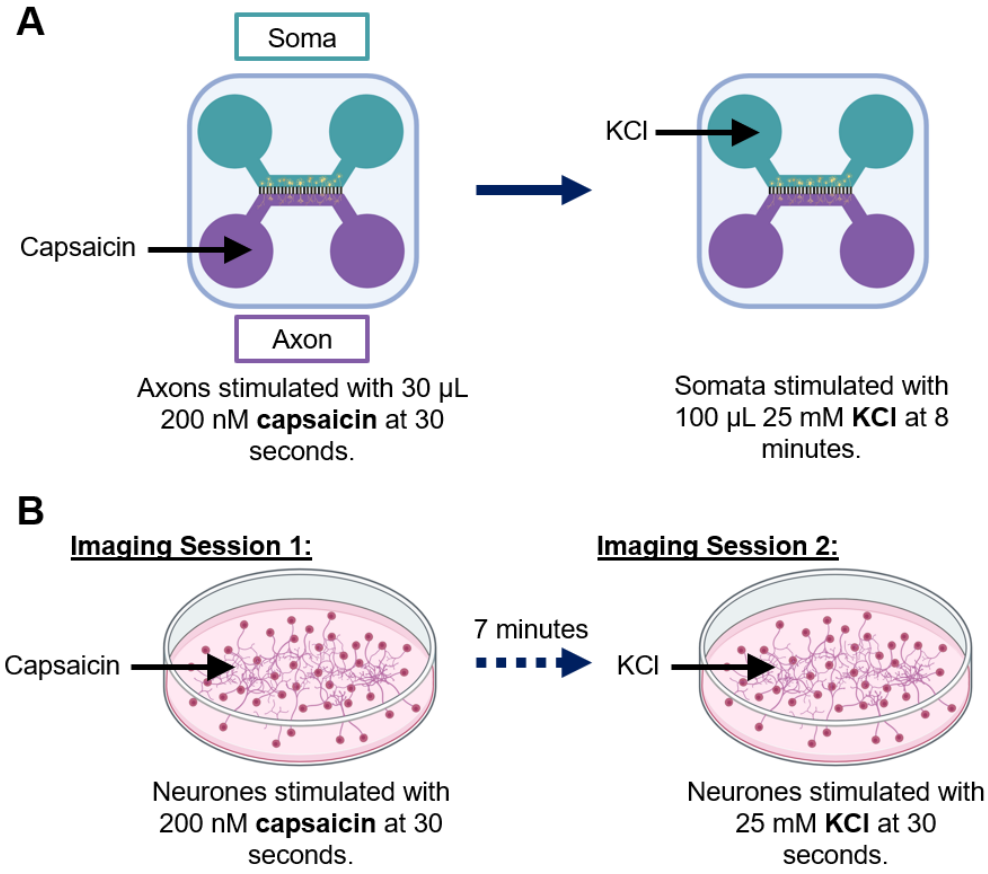


Figure 4.4. Calcium Imaging Stimulation Protocol. A - In compartmentalised microfluidic chambers, after 30 seconds the axon compartment was stimulated with 30 μL 200 nM capsaicin and then at eight minutes with 100 μL 25 mM KCl. **B -** In dissociated cultures, neurones were stimulated with 200 nM capsaicin at 30 seconds. After imaging, there was a seven-minute break until the second round of imaging, stimulating with 25 mM KCl 30 seconds into recording. Created using BioRender™.

Analysis was performed as previously described in Section 2.4.3.

4.2.11 Statistical Analysis

Statistical analyses were conducted according to the methods outlined in Chapter 2 (Section 2.7). For the experiments in this chapter, one-way ANOVAs (or Kruskal-Wallis tests for non-parametric data) with post-hoc tests were used for multiple group comparisons, as appropriate. For comparisons against a normalised control

value (e.g., RT-qPCR data where the control was set to one), one-sample *t*-tests were performed. A p value < 0.05 was considered statistically significant.

4.3 Results

4.3.1 Transcriptomic Changes in Subcellular Neuronal Compartments

To investigate localised transcriptomic changes at both the somatic and axonal levels, we cultured DRG neurones using a modified Boyden chamber system, physically separating axons from their cell somata. For embryonic DRG neurones, approximately 85% of sequencing reads successfully mapped to the mouse genome, indicating high-quality data.

To validate the cellular composition of our samples, we assessed the expression of established cell-type-specific marker genes within the RNA-seq datasets. This included five markers for Schwann cells, 12 for satellite glial cells, five for immune cells, such as macrophages, and 11 for DRG neurones, based on prior single-cell transcriptomic profiling of the DRG (Liang et al., 2020; Ray et al., 2018; Wangzhou et al., 2020; Zeisel et al., 2018).

Somatic transcriptomes from E16.5 cultures demonstrated strong enrichment for DRG neuronal markers, with comparatively low expression of glial and immune markers, confirming that the cultures are predominantly neuronal and thus suitable for transcriptomic analysis of DRG neurone populations (Pope et al., 2025).

In contrast, transcriptomes derived from the axonal compartment displayed a more diverse expression pattern, including some non-neuronal markers. While this might superficially suggest low-level contamination, the absence of corresponding signals in the soma samples from the same cultures argues against this. Rather, these findings likely reflect the unique molecular identity and functional specialisation of the axonal compartment, which may not conform to canonical cell-type

expression profiles.

To explore this further, we examined the expression of a panel of genes, conserved across species and neuronal types, which were previously reported to be enriched in neurite-specific transcriptomes (Kügelgen and Chekulaeva, 2020). Strikingly, all selected neurite markers were robustly expressed in our axonal datasets, supporting the conclusion that these transcriptomes represent bona fide axonal RNA content. This also raises the possibility of a conserved molecular signature within axons that spans different neuronal subtypes (Figure 4.5).

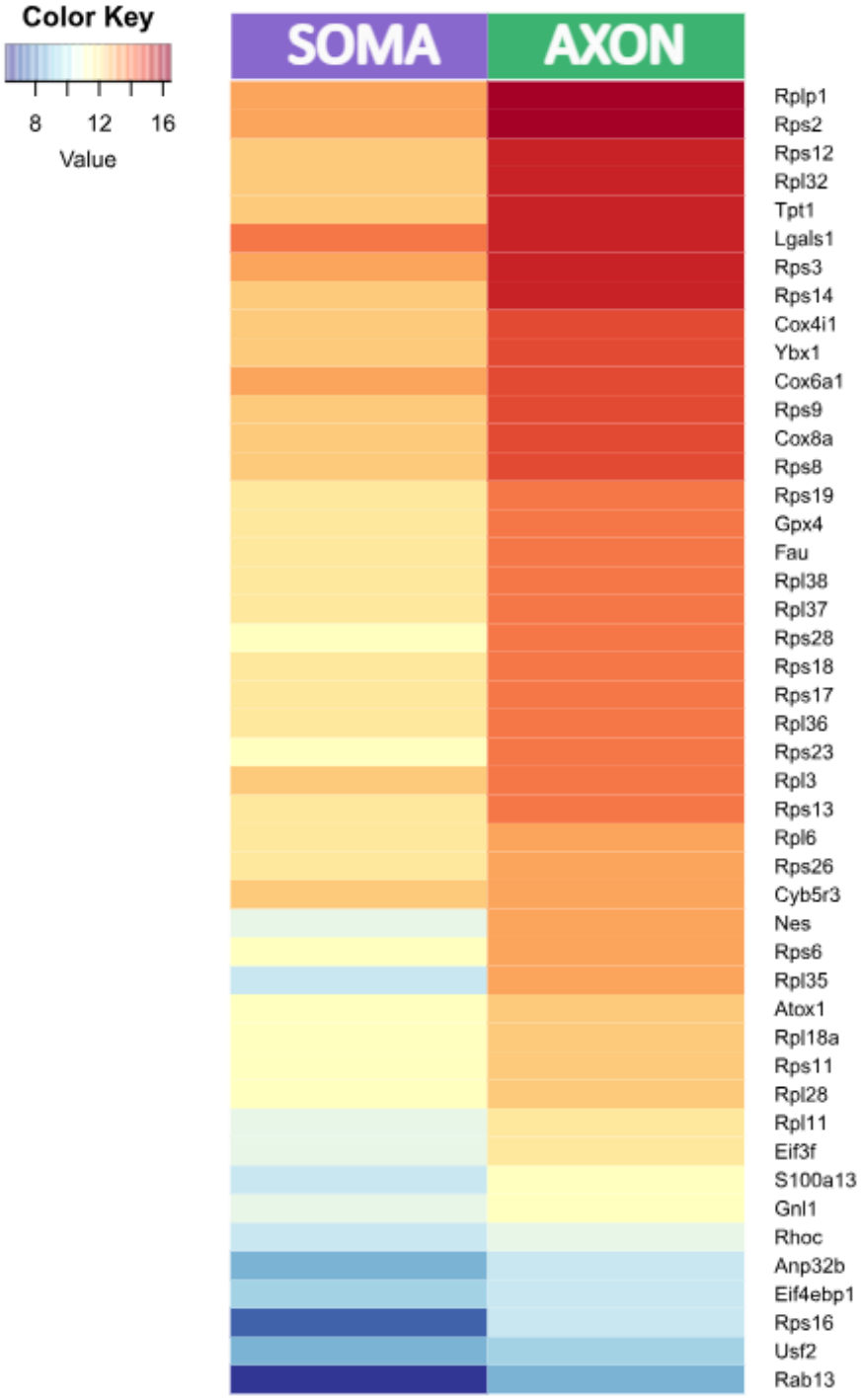


Figure 4.5. Analysis of Neurite Gene Expression in the Axon and Soma Compartments of E16.5 DRG Neurones. Heatmap of neurite marker genes (Z-score of $\log_2$ normalised counts) as defined in Kügelgen and Chekulaeva (2020) ordered by decreasing abundance in the axon relative to the soma. Hierarchical clustering distance was measured by Euclidean and Ward clustering algorithms. Figure produced by Rafael Fort from data collected by Asta Arendt-Tranholm.

4.3.2 Transcripts are Differentially Regulated in the Axon Versus Soma Following PGE_2 Treatment.

Recognising the growing importance of subcellular transcriptomes in regulating neuronal function, the effects of PGE_2 exposure on the axonal and somatic RNA profiles of DRG neurones were examined. Several of the identified axonal marker transcripts (Figure 4.5) exhibited distinct, compartment-specific changes in expression following PGE_2 treatment. Notably, these transcripts were downregulated in axons and concurrently upregulated in the soma, relative to controls (Figure 4.6). This opposing regulation suggests potential redistribution, or altered trafficking, of mRNAs in response to inflammatory signalling, possibly reflecting a dynamic reorganisation of the local transcriptome to support adaptive responses such as sensitisation or injury-like changes.

Hierarchical clustering of the transcriptomic data further supported this compartmental distinction. The primary separation in the heatmap corresponded to axonal versus somatic origin, with PGE_2 treatment introducing a secondary layer of clustering (Figure 4.6). This pattern reinforces the molecular compartmentalisation of DRG neurones and the existence of a functionally distinct axonal transcriptome.

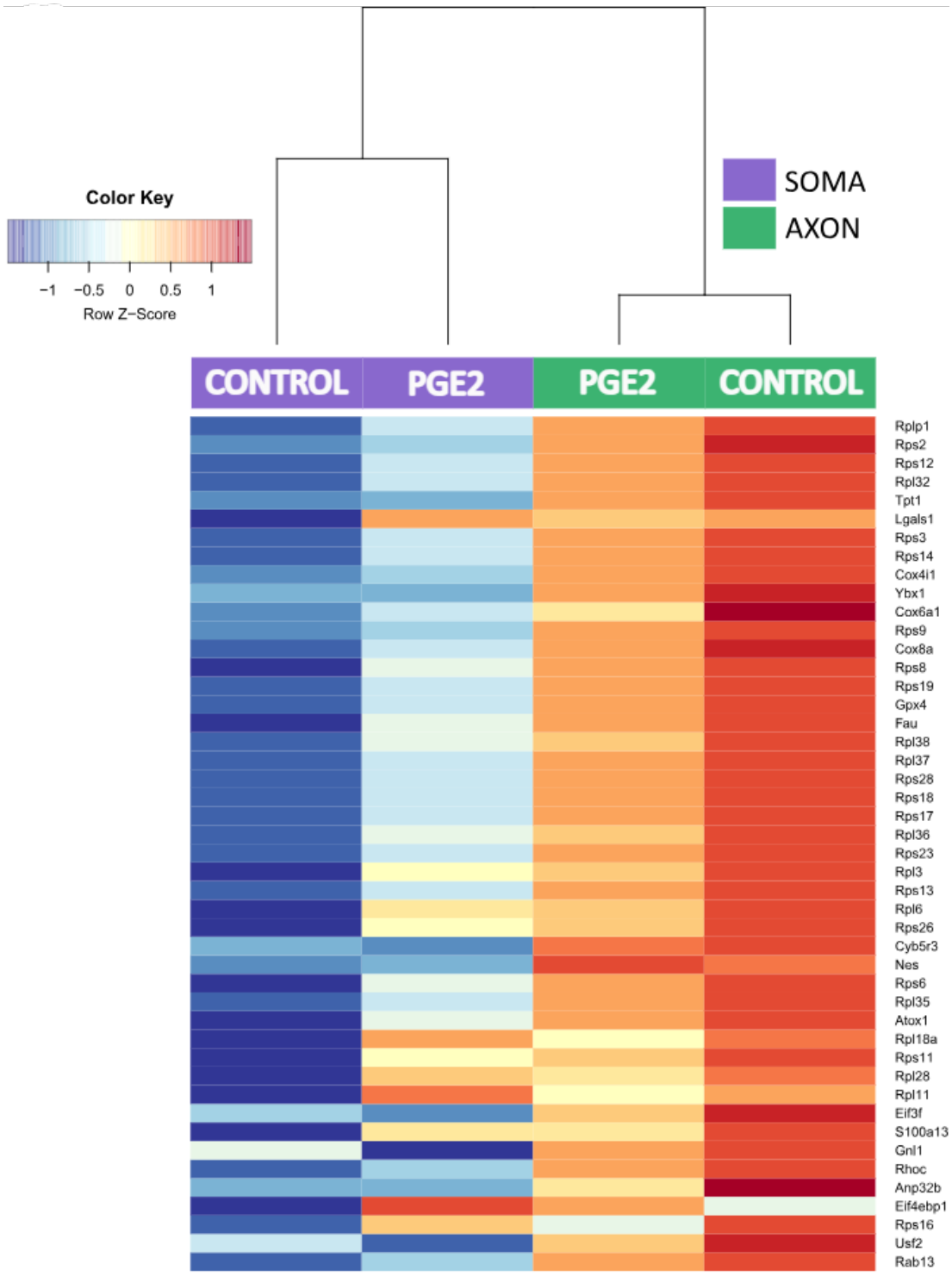


Figure 4.6. Transcriptomic Response to PGE_2 in Axonal and Somal Compartments of E16.5 DRG Neurones. A - Heatmap of neurite marker genes (as defined by Kügelgen and Chekulaeva (2020)) comparing soma and axon compartments following PGE_2 exposure (Z-score of $\log_2$ normalised counts). Hierarchical clustering distance was measured by Euclidean and Ward clustering algorithms. Figure produced by Rafael Fort from data collected by Asta Arendt-Tranholm.

Beyond changes in known axonal markers, PGE_2 stimulation induced broader transcriptomic alterations in embryonic DRG cultures, with numerous genes significantly up- or downregulated in both the soma and axon relative to their respective control conditions (Figure 4.7). Enrichment analysis revealed that pathways associated with translation and mitochondrial energy metabolism were upregulated in the soma following PGE_2 treatment, but were comparatively under-represented in the axonal PGE_2 dataset when analysed relative to axonal controls (Figure 4.8). Importantly, this reflects a relative shift in axonal transcript composition rather than a global suppression of axonal translational capacity.

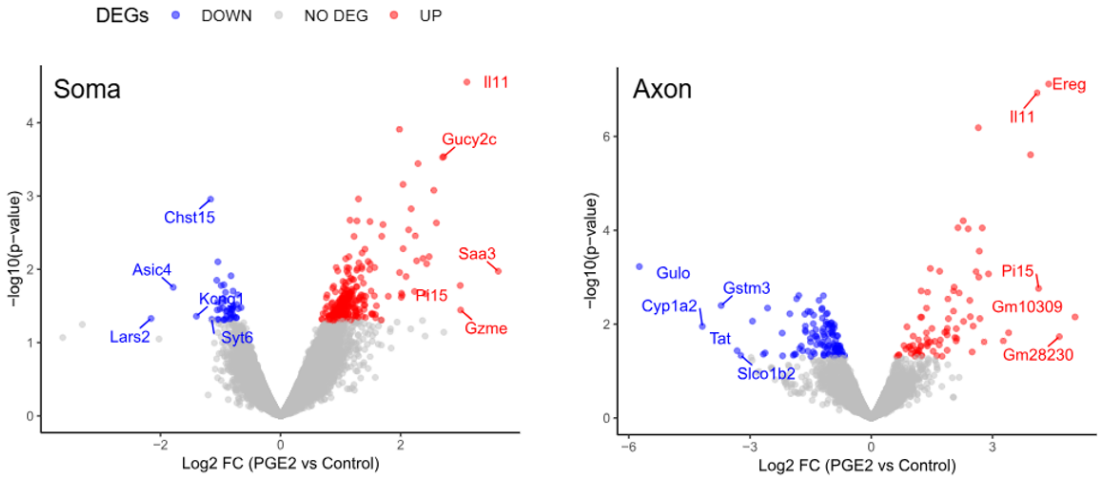


Figure 4.7. Volcano Plot Demonstrating Transcriptomic Response to PGE_2 in Axonal and Somal Compartments of E16.5 DRG Neurones. Volcano plots showing differential gene expression between PGE_2-treated and control conditions in the soma and axon. Genes with a $\log_2$ fold change greater than |0.58| and a p-value < 0.05 are highlighted in colour; with the top five upregulated (red) and downregulated genes (blue) labelled. Figure produced by Rafael Fort from data collected by Asta Arendt-Tranholm.

In contrast, the axonal transcriptome following PGE_2 exposure showed increased enrichment of genes associated with receptor and ligand activity, cytokine activity, inflammatory responses, and extracellular matrix organisation (Figure 4.8). This pattern suggests that PGE_2 drives a functional reprogramming of the axonal transcriptome away from metabolic and housekeeping pathways towards signalling and inflammatory processes. Such a shift is consistent with the axon acting as an active site of local inflammatory signalling, in which PGE_2-induced sensitisation is supported by selective local translation of signalling molecules, rather than a global increase in mitochondrial or translational pathways.

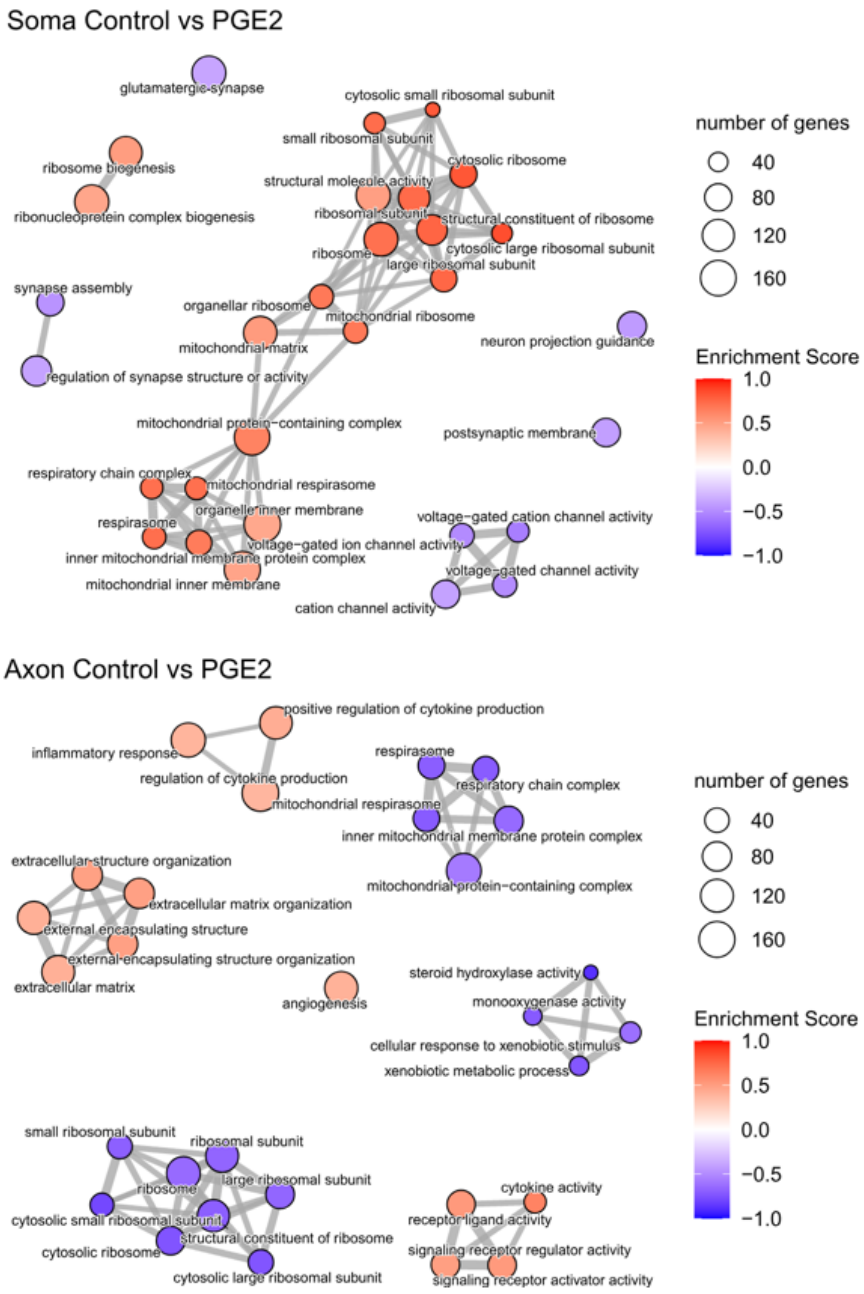


Figure 4.8. Compartment-Specific Gene Ontology Enrichment Analysis of PGE_2-Stimulated E16.5 DRG Neurones. emapplots of the top 30 significantly enriched (p-adjusted value < 0.05) GO Biological Process terms from the GSEA analysis comparing PGE_2 vs control for soma and axon. Circle size represents the number of genes associated with each term, with red denoting upregulation and blue indicating downregulation in the PGE_2 condition, relative to control. In the cell soma, PGE_2-treated neurones exhibited greater activation of cellular processes involved in protein synthesis (red), such as ribosomal and mitochondrial functioning, and less activation of restructuring of neuronal networks (blue), such as synapse assembly and voltage-gated channel activity, than control neurones. In PGE_2-treated axons, there was greater activation of cellular processes involved in inflammation, cellular organisation and signalling, such as cytokine production, extracellular structure organisation and ligand activity, and less activation of mechanisms with a role in translation and mitochondrial functioning, such as ribosome-related processes and mitochondrial protein complexes. Figure produced by Rafael Fort from data collected by Asta Arendt-Tranholm.

4.3.3 Pathway Analysis Reveals *Tnfrsf12a* is Involved in Multiple Processes

Notably, *Tnfrsf12a* was one of only four genes (*Tnfrsf12a*, *Thbs*, *Gpx1*, and *Cx3cl1*) found to be enriched across the major pathways identified in the analysis. Pathway analysis indicated that *Tnfrsf12a* is involved in several key biological processes, including angiogenesis, apoptotic signalling, and wound healing - each essential for maintaining cellular integrity and responding to injury (Figure 4.9).

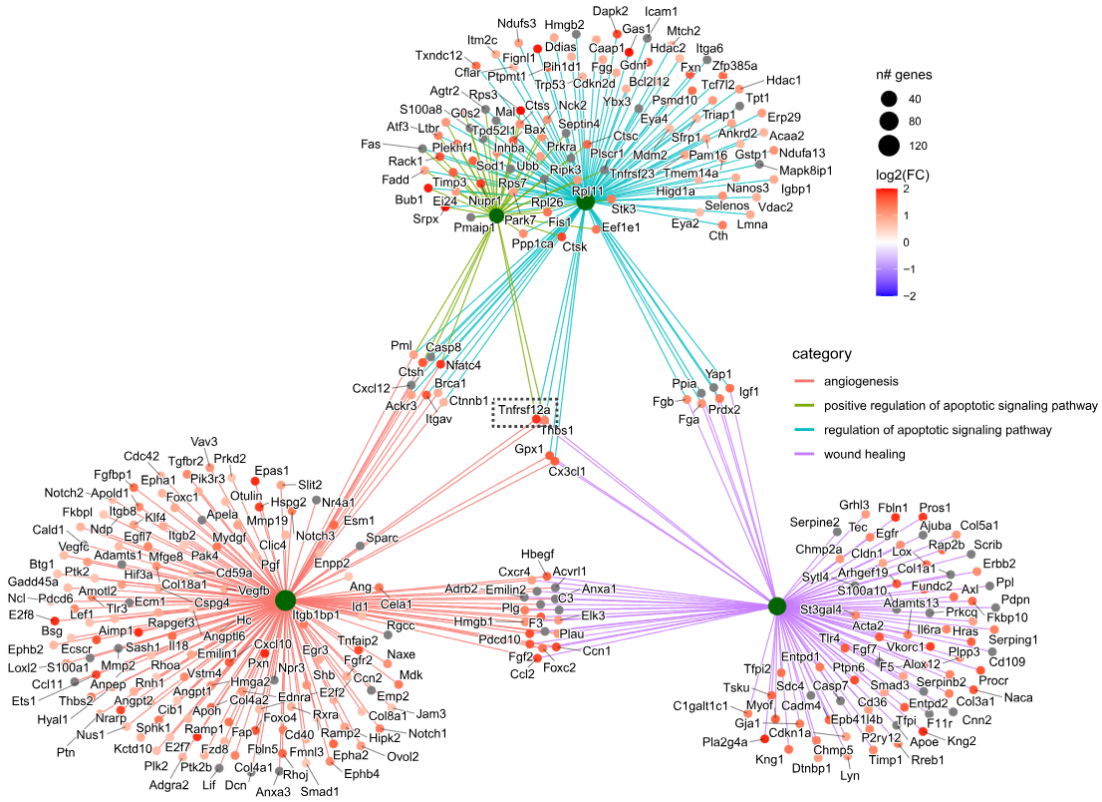


Figure 4.9. Cnetplot of Gene Ontology Biological Process Terms Associated with *Tnfrsf12a*. *Tnfrsf12a* is significantly increased following exposure to PGE_2 in E16.5 axons. Node colour represents log_2 fold change (axon vs soma), with each category representing a GO term, and connecting line colours matching the associated category and GO term. Figure produced by Rafael Fort from data collected by Asta Arendt-Tranholm.

4.3.4 qPCR Confirms Effective *Tnfrsf12a* Transcript Silencing with siRNA

qPCR was used to quantify *Tnfrsf12a* mRNA levels in dissociated DRG neurones 24 and 48 hours after addition of *Tnfrsf12a* siRNA. Expression was normalised to the geometric mean of the housekeeping genes, *Gapdh* and *Ube2*, and quantified using the $2^{(-\Delta\Delta Ct)}$ method. *Tnfrsf12a* levels in the siRNA-treated group were compared to those in the control (non-targeting siRNA).

At 24 hours, across three independent replicates, *Tnfrsf12a* expression showed a modest reduction. Fold change expression levels were reduced to 0.76 ± 0.11 relative to control (set to 1; Figure 4.10A), signalling a decrease of 24%. Log_2-transformed values likewise indicated a trend toward downregulation (mean = -0.44 ± 0.22) but this was not statistically significant (one-sample *t*-test versus siRNA CTL set to 0; Figure 4.10B).

By 48 hours, *Tnfrsf12a* expression had decreased further to 0.61 ± 0.11 relative to control, approaching but not reaching statistical significance ($p = 0.07$, one-sample *t*-test; Figure 4.10A), indicating a mean decrease of 39%. The log_2-transformed fold change values also showed a more pronounced reduction (mean = -0.75 ± 0.24, $p = 0.09$; Figure 4.10B).

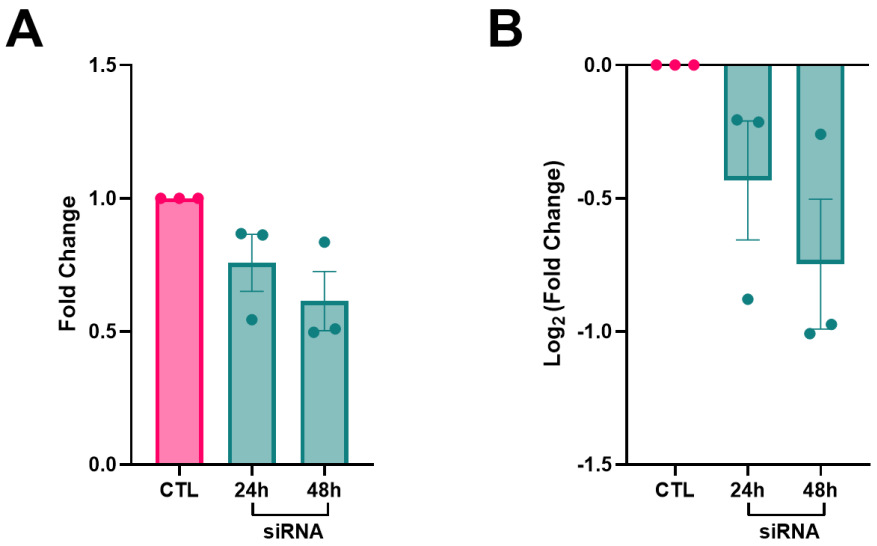


Figure 4.10. *Tnfrsf12a* Expression Exhibited a Progressive Decrease Following siRNA Treatment. A - At 24 hours, fold change in *Tnfrsf12a* expression was reduced to 0.76 ± 0.10 (relative to control, set to 1), but without significant difference. By 48 hours, expression decreased further to 0.61 ± 0.11 relative to control, approaching but not reaching significance (p = 0.07, one-sample t-test). **B –** Log_2-transformed fold change values at 24 hours showed a consistent but non-significant trend toward downregulation (mean = -0.44 ± 0.22). At 48 hours, log_2-transformed values indicated a more pronounced reduction (mean = -0.75 ± 0.24), again not quite statistically significant (one-sample t-test vs 0, p = 0.09).
N = 3 biological replicates. Data represent mean ± SEM. CTL - siRNA non-targeting control.

4.3.5 Knockdown of *Tnfrsf12a* Lowers Sensory Neurone Excitation in Dissociated Cultures

To investigate the broad functional relevance of TNFRSF12A in E16.5 sensory neurones, *Tnfrsf12a*-targeting siRNA or non-targeting control siRNA (siRNA CTL) was applied to dissociated DRG cultures for 48 hours (Figure 4.11A). Neuronal excitability was subsequently assessed using calcium imaging in response to depolarising stimuli. An untreated media change alone (UTC) was included as an additional control condition.

Knockdown of *Tnfrsf12a* in the whole-cell neuronal cultures significantly reduced the excitability of DRG sensory neurones in response to 200 nM capsaicin, relative to the siRNA CTL and UTC (Figure 4.11B), suggesting that *Tnfrsf12a* has a poten-

tial role in neuronal excitability. Peak calcium responses were compared between siRNA-treated neurones, siRNA CTL, and UTC, with a significant difference found between groups (p = 0.0159, Kruskal-Wallis test). Post-hoc analyses revealed that the significant difference was a decrease in calcium transients in siRNA-treated groups relative to the primary control group (siRNA CTL; p = 0.0243, Dunn's post-hoc test; Figure 4.11C).

The area under the curve of the averaged siRNA trace was significantly reduced compared to siRNA CTL and UTC (Figure 4.11D): there was a significant difference among group means ($F(2, 9) = 10.08$, p = 0.0050, R^2 = 0.6913, one-way ANOVA), with post-hoc analyses identifying a marked decrease in the area under the curve for siRNA-treated cells versus siRNA CTL (p = 0.0137, Tukey's post-hoc test) and siRNA versus UTC (p = 0.0068).

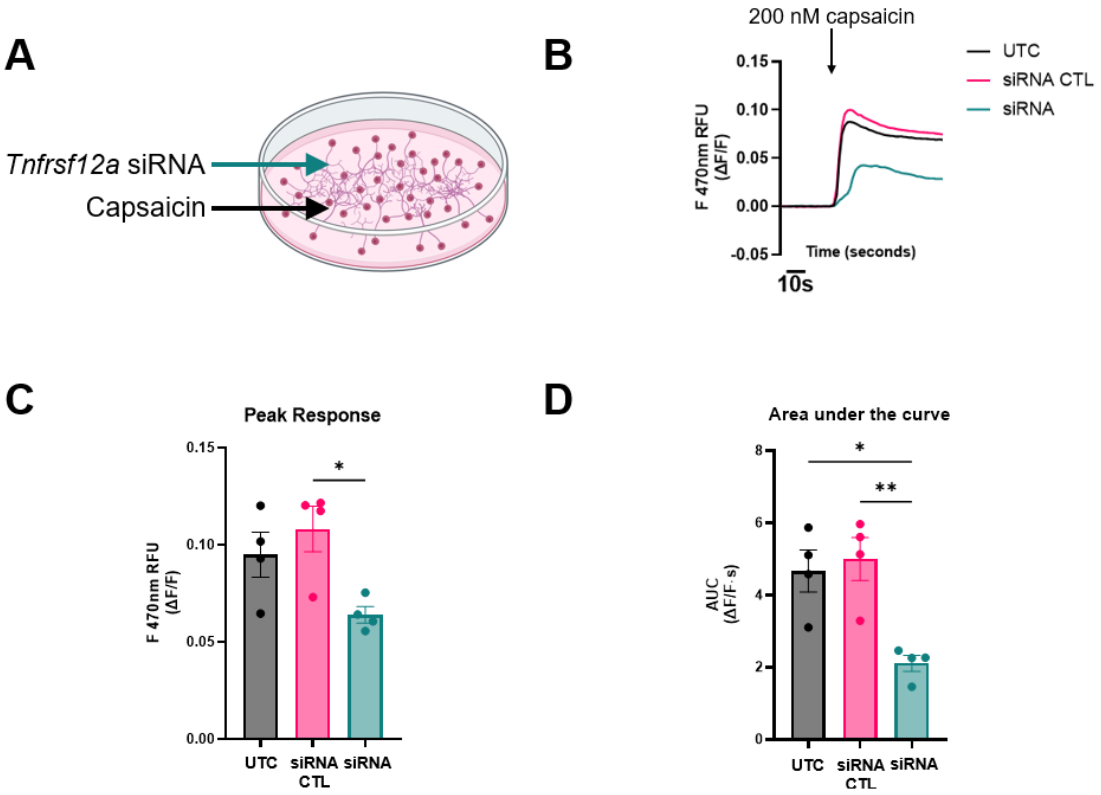


Figure 4.11. Silencing *Tnfrsf12a* in Dissociated Cultures Reduced Neuronal Excitation. A - siRNA targeting *Tnfrsf12a* mRNA was applied to dissociated cultures of DRG sensory neurones for 48 hours. Calcium imaging was performed, stimulating with 200 nM capsaicin, and the calcium transients in the cell somata measured. **B -** Averaged ΔF/F Ca^{2+} trace in response to capsaicin. The peak and duration of siRNA-treated neurones was reduced. **C -** The ΔF/F peak response of siRNA-treated neurones was reduced relative to siRNA CTL (p = 0.0243, Dunn's post-hoc test; mean ± SEM) and showed a trend to decrease relative to UTC. **D -** The area under the curve for the siRNA calcium trace (peak to 100 seconds; mean ± SEM) demonstrated a significant decrease versus siRNA CTL and UTC (p = 0.0137 and p = 0.0068, respectively, one-way ANOVA).
N = 4 biological replicates; n = 2 technical replicates; 3-70 cells per replicate. $p < 0.05$ was considered statistically significant.

Global knockdown of *Tnfrsf12a* in dissociated DRG cultures reduced neuronal excitability. To further dissect the underlying subcellular mechanism, targeted knockdown of the transcript in the axon alone was required to determine its specific contribution at the site.

4.3.6 Targeted Axonal Knockdown of *Tnfrsf12a* Dampens Sensory Neurone Activity

To assess the functional role of TNFRSF12A specifically in the axons of sensory neurones, *Tnfrsf12a* siRNA or siRNA control was selectively applied to the axonal compartment of compartmentalised microfluidic cultures for 48 hours (Figure 4.12A). Neuronal excitability was then evaluated using calcium imaging. A media change alone (UTC) was included as an additional control condition.

Selective axonal knockdown of *Tnfrsf12a* markedly dampened DRG neurone excitability when 200 nM capsaicin was delivered to the axonal compartment (Figure 4.12B). Peak calcium responses were lower than those recorded in both the non-targeting siRNA CTL and the UTC (Figure 4.12C), indicating that *Tnfrsf12a* is involved in excitability and may contribute to inflammatory sensitisation. Statistics supported this: peak calcium responses were compared between the three treatment groups, with a significant difference found between them (p = 0.0278, Friedman test). Post-hoc analyses revealed that there was a significant decrease in calcium transients in the siRNA-treated group compared to UTC (p = 0.0429, Dunn's post-hoc test), but only a trend to decrease relative to the siRNA CTL.

The area under the curve of the averaged siRNA trace was not significantly reduced compared to the siRNA CTL or UTC groups (Figure 4.12D; one-way ANOVA and Tukey's post-hoc test). This is likely because the trace appeared less smooth and peaked more variably than in dissociated cultures (Figure 4.12B). This variability likely reflects lower signal-to-noise ratios in axonal compartments, reduced numbers of responsive axons, and technical factors specific to the microfluidic set-up, such as spatial gradients in stimulus delivery.

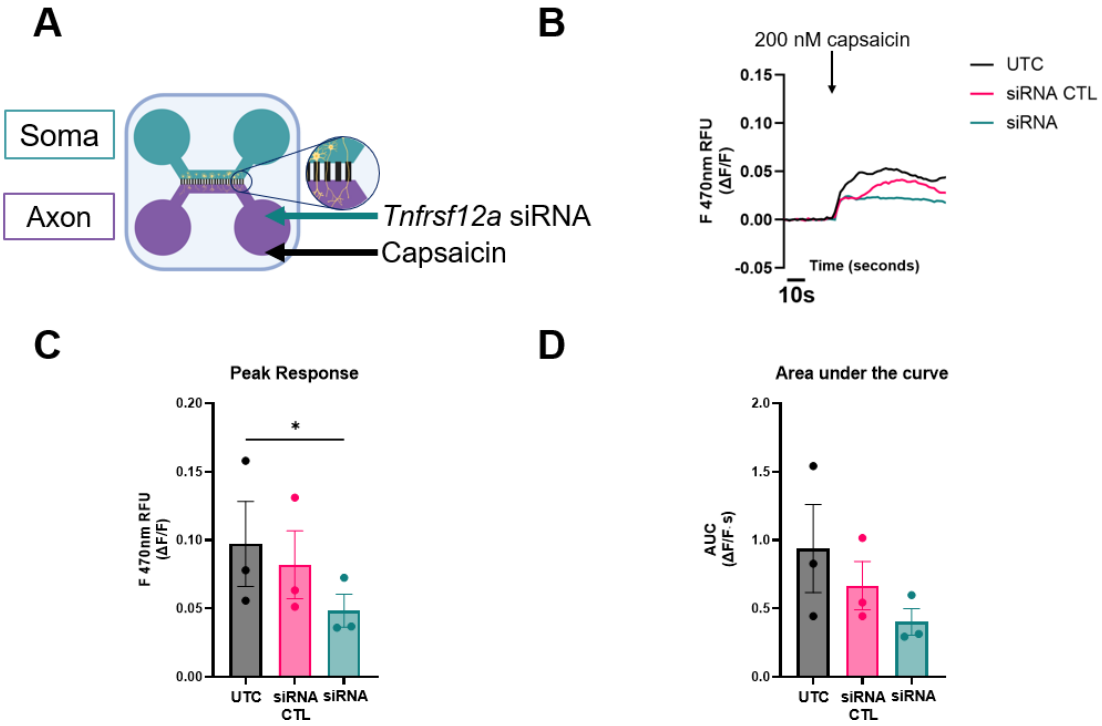


Figure 4.12. Silencing of *Tnfrsf12a* Specifically at the Sensory Neurone Axon Terminal Reduced Neuronal Excitability. **A -** siRNA targeting *Tnfrsf12a* mRNA was applied locally to the axon compartment within microfluidic chambers, enabling selective knockdown at the axon terminal. Calcium imaging was performed, stimulating axons with 200 nM capsaicin, and the calcium transients in the cell somata measured. **B -** Averaged ΔF/F Ca^{2+} trace in response to capsaicin applied axonally. The profile of the calcium response was decreased in the siRNA-treated cells, relative to siRNA CTL and UTC. **C -** The peak calcium response was significantly reduced in siRNA-treated cells relative to UTC (p = 0.0429, Friedman test; mean ± SEM), with a trend to decrease compared to siRNA CTL. **D -** The area under the curve (peak to 50 seconds) for the siRNA calcium trace demonstrated a trend to decrease versus siRNA CTL and UTC but was not significant (Tukey's post-hoc test; mean ± SEM).
N = 3 biological replicates; n $\geq$ 2 technical replicates; 3-40 cells per replicate. $p < 0.05$ was considered statistically significant.

Five minutes into calcium imaging - following initial capsaicin stimulation at 30 seconds - the soma-enriched compartment was stimulated with 100 μL 25 mM KCl to assess general neuronal depolarisation via calcium transients recorded in the cell bodies (Figure 4.13A).

Knockdown of *Tnfrsf12a* in the axonal compartment produced a trend toward reduced neuronal excitability in response to KCl, relative to both siRNA control and UTC conditions (Figure 4.13B-D). Further replicates are required to perform statistical analyses.

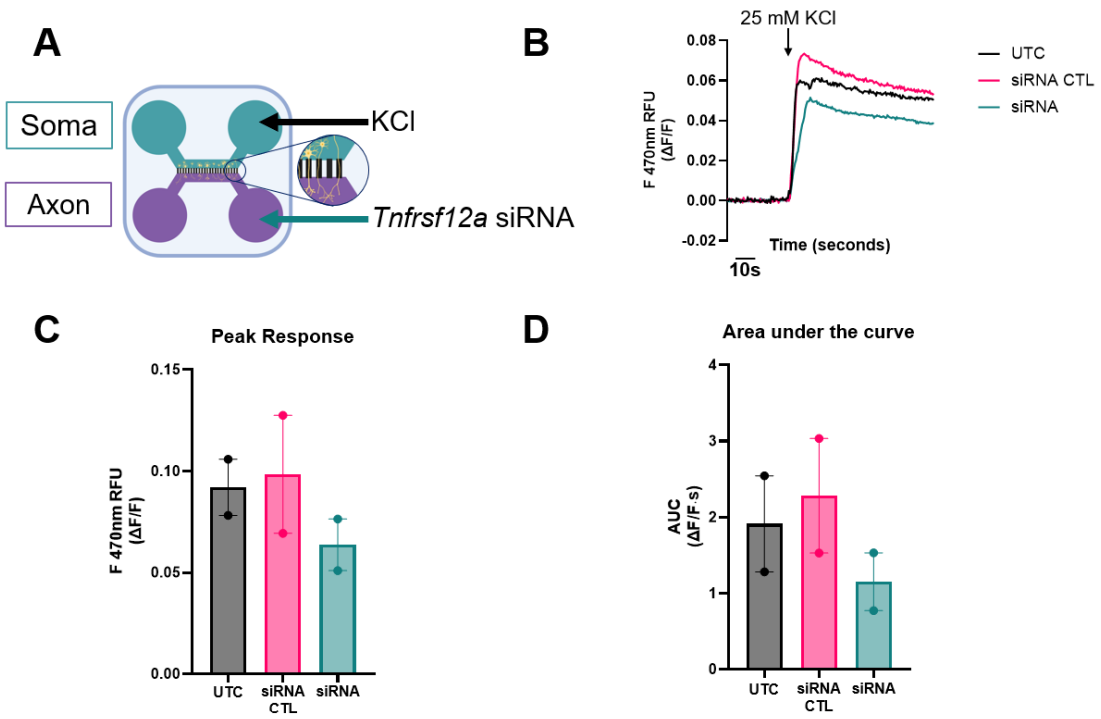


Figure 4.13. Silencing of *Tnfrsf12a* at the Sensory Neurone Axon Terminal Showed a Trend to Reduce Neuronal Sensitisation. A - siRNA targeting *Tnfrsf12a* mRNA was applied locally to the axon compartment within microfluidic chambers, enabling selective knockdown at the axon terminal. 100 μL 25 mM KCl was applied to the soma-enriched compartment during calcium imaging and the calcium transient response in the cell somata measured. **B -** Averaged ΔF/F Ca^{2+} response to KCl. Evoked transients were decreased in the siRNA-treated group relative to siRNA CTL and UTC. **C -** The peak calcium response (ΔF/F; mean ± SEM) showed a trend to reduce in siRNA-treated cells relative to siRNA CTL and UTC. **D -** The area under the curve (mean ± SEM) for the siRNA calcium trace demonstrated a trend to decrease versus siRNA CTL and UTC.
N = 2 biological replicates; n $\geq$ 2 technical replicates; 4-44 cells per replicate.

4.4 Discussion

4.4.1 Summary of Key Findings

To investigate the transcriptional changes underlying PGE_2-induced sensory neurone sensitisation, we performed subcellular transcriptomics on embryonic DRG neurones in compartmentalised cultures (Pope et al., 2025; Arendt-Tranholm, 2022). The differential regulation of transcripts in the axon versus soma following PGE_2 supports the concept of axonal local translation (Holt, Martin, and Schuman, 2019; Lucci et al., 2020; Sasaki, 2020) and its involvement in inflammation (Gumy et al., 2011; Ji et al., 2002). These experiments revealed that although many transcripts

were upregulated, select mRNA were increased after applying strict analytical parameters. There was a marked upregulation of *Tnfrsf12a* mRNA in the axonal compartment following PGE_2 exposure. Although initially described as a fibroblast growth factor-inducible gene, TNFRSF12A (Fn14) is now recognised as an inducible receptor expressed in diverse cell types, including neurones, glia (Potrovita et al., 2004), endothelial cells, and immune cells (Burkly, Michaelson, and Zheng, 2011), particularly under inflammatory conditions.

In this chapter, I functionally validated these findings using siRNA-mediated knockdown of *Tnfrsf12a* in both dissociated DRG cultures and microfluidic chambers. Silencing *Tnfrsf12a* reduced sensory neurone excitability, supporting a pro-excitability and potentially pro-sensitising role. Importantly, the microfluidic model allowed selective manipulation of axon terminals, enabling us to propose a local, translation-dependent role for *Tnfrsf12a* at peripheral terminals. This level of subcellular resolution would be difficult to achieve using standard *in vitro* or *in vivo* systems.

4.4.2 siRNA Targeting *Tnfrsf12a* Reduced mRNA Levels

In the previous chapter, it was shown that peripheral PGE_2 application, mimicking its release during inflammation, increased excitability locally in the axon but also in the cell soma - identified by increased calcium transients in response to stimulation - indicating a retrograde signalling mechanism. I hypothesised that this involved local translational processes. Consistent with this, *Tnfrsf12a* was enriched in axons following pro-inflammatory PGE_2 treatment. This extends previous findings which demonstrated *Tnfrsf12a* mRNA and TNFRSF12A protein enrichment in whole DRG after injury (Huang et al., 2019), and *Tnfrsf12a* upregulation following stress and injury (Inta et al., 2008; Potrovita et al., 2004; Tanabe et al., 2003). Its expression is also particularly sensitive to pro-inflammatory cytokines such as IL-1β and TNF-α (Burkly, Michaelson, and Zheng, 2011; Chen et al., 2025a; Samidurai et al., 2020) - cytokines that are readily released at the site of injury, further proposing an inflammatory role.

The approach in this chapter revealed that enrichment occurs specifically in axons, where local translation could directly contribute to excitability. Using siRNA, I showed that reducing *Tnfrsf12a* expression (over 48 hours) lowered neuronal responses to capsaicin in both dissociated and compartmentalised cultures, where stimulation was solely applied to axons. RT-qPCR confirmed knockdown efficiency (24% at 24 hours, 39% at 48 hours). Although the manufacturer (Dharmacon™, Horizon Discovery) recommended a 96-hour incubation for optimal silencing, achieving this in primary sensory neurones cultured in compartmentalised microfluidic systems is challenging, as to ensure that fluidic isolation is maintained, more frequent media changes were required (Clark et al., 2018). The cells were already at a relatively advanced stage to ensure adequate axon crossing prior to siRNA transfection, which was followed by a 48-hour incubation. Alternatively, replacing the media with a fresh dose of siRNA would introduce uncertainty regarding the amount already internalised by the cells, making it difficult to maintain an accurate effective siRNA concentration. However, extending the incubation by an additional 24 hours might have been beneficial, providing extra time for more complete knockdown.

Ideally, mRNA knockdown would have been confirmed in axons directly, but RNA isolation from subcellular compartments is highly resource-, cost-, and labour-intensive. It is also important to note that mRNA levels do not always reflect protein abundance due to post-transcriptional regulation (Vogel and Marcotte, 2012). Protein suppression was not quantified in these investigations, therefore this could limit our interpretation; it cannot be definitively stated that functional changes were due to reduced receptor levels, as indirect effects could also be involved. The use of non-targeting controls and spatially restricted siRNA application help mitigate the risk of off-target or indirect effects, although they cannot be excluded. Notably, siRNA applied to distal axons has been shown to produce compartment-specific knockdown without affecting transcript levels in the soma, suggesting that retrograde transport of siRNA is minimal or absent (Hengst et al., 2006). Future studies

should include immunostaining or Western blot to assess TNFRSF12A protein-level suppression.

It is important to note that the levels of TWEAK ligand were not assessed in this model. However, previous studies have shown that functional consequences of TNFRSF12A upregulation may occur independently of changes in TWEAK levels. For instance, in DRG neurones, TNFRSF12A expression is strongly induced following axotomy, whereas TWEAK ligand expression remains unchanged (Tanabe et al., 2003). These findings suggest that receptor upregulation alone can be sufficient to alter downstream signalling, likely due to increased receptor availability for baseline ligand activity or ligand-independent signalling mechanisms.

4.4.3 *Tnfrsf12a*'s Effects were More Robust in Dissociated Cultures

Notably, the effect of siRNA-mediated *Tnfrsf12a* knockdown on neuronal excitability was more robust in dissociated cultures than in microfluidic chambers. In dissociated cultures, significant reductions were observed in both peak calcium responses and area under the curve when comparing siRNA-treated cells to both siRNA non-targeting control and untreated control groups.

In contrast, in microfluidic chambers, significant reductions were only observed when comparing the untreated control group to siRNA-treated cells; the difference between siRNA control and siRNA-treated cells did not reach significance, despite a trend toward decreased excitability following siRNA treatment. This discrepancy may reflect several factors. First, axonal knockdown in microfluidics specifically targets the peripheral terminal, whereas dissociated culture knockdown is global, potentially amplifying the magnitude of effect. Second, differences in baseline variability - arising from lower numbers of axons crossing compartments than the number of cells targeted in dissociated cultures - and potentially reduced transfection efficiency at the axonal terminal may limit statistical power. Furthermore, 48 hours

may be adequate time for whole-cell cultures to take up sufficient levels of siRNA, but might not be for cells grown in chambers: axons might take up less siRNA than somata due to differences in endocytic capacity, membrane composition, or accessibility of the transfection reagent, even if total surface area is comparable.

Furthermore, calcium traces from microfluidic experiments were less smooth and exhibited greater temporal variability than those from dissociated cultures. This likely reflects a combination of factors, including the smaller number of responsive axons and technical limitations in stimulus diffusion or imaging access. Additionally, some late upward deflections in the traces may represent network or secondary activation effects: asynchronous responses among neighbouring axons, or residual local connectivity, could cause certain neurones to activate slightly later, producing delayed calcium increases that are less apparent in larger, more homogeneous dissociated populations. These considerations underscore the challenges of interpreting subcellular calcium imaging data and highlight the difficulty of resolving subtle functional changes in compartments like axons. Together, these factors likely contribute to the smaller and more variable knockdown effect observed in microfluidic cultures. Importantly, the fact that axonal knockdown alone produced a significant reduction compared to untreated cells supports a functionally relevant role for *Tnfrsf12a* at the axon. Additional studies investigating $\geq$ 72-hour siRNA incubations would be useful to provide more significant *Tnfrsf12a* knockdown and elucidate its role further.

4.4.4 *Tnfrsf12a* and Pain

By adding complementary siRNA targeting *Tnfrsf12a* to DRG cultures, I have demonstrated that the transcript contributes functionally to neuronal excitability; a 48-hour siRNA-mediated knockdown reduced sensory neurone excitability in response to capsaicin, in both dissociated and compartmentalised cultures.

Our findings reveal a novel role for *Tnfrsf12a* in regulating sensory neurone ex-

citability *in vitro*, expanding on the limited but growing body of evidence implicating TNFRSF12A in pain. To date, only two studies have examined its role in nociceptive processing, both conducted *in vivo* (Huang et al., 2019; Huang et al., 2025). Huang et al. (2019) demonstrated that *Tnfrsf12a* expression increased ipsilaterally in neuropathic pain models and that knockdown of the transcript attenuated mechanical and thermal hypersensitivity. Furthermore, intrathecal administration of *Tnfrsf12a* into naïve mice was sufficient to induce pain behaviours, directly implicating TNFRSF12A in nociceptive signalling. These findings support our proposition that TNFRSF12A contributes to peripheral sensitisation.

More recently, *Tnfrsf12a* was identified as a key effector of thalamic sensitisation in a model of central post-stroke pain. Following thalamic haemorrhage, neuronal expression of the cytidine acetyltransferase NAT10 was upregulated, leading to modification of *Tnfrsf12a* mRNA which enhanced its stability and translation. This post-transcriptional upregulation of TNFRSF12A activated the NF-κB signalling cascade, evidenced by increased nuclear translocation of p65, and contributed to sustained nociceptive hypersensitivity (Huang et al., 2025). Our findings support and extend these *in vivo* results by demonstrating that *Tnfrsf12a* knockdown reduces neuronal excitability, a hallmark of neuroinflammation and peripheral sensitisation in sensory neurones, suggesting a pro-nociceptive role for TNFRSF12A signalling. Importantly, its involvement in both central and peripheral inflammatory processes highlights TNFRSF12A as a convergent mediator of neuroinflammation and sensitisation across compartments (Burkly et al., 2007; Huang et al., 2019; Huang et al., 2025; Tanabe et al., 2003). This dual role strengthens its candidacy as a therapeutic target for modulating pain at multiple levels of the nervous system.

While the precise mechanism remains to be fully elucidated, TNFRSF12A is a well-characterised activator of the NF-κB and MAPK pathways. Both pathways have been implicated in pain and inflammation (Ji et al., 2002; Luo et al., 2024;

Potrovita et al., 2004; Zhang et al., 2020). NF-κB is a transcription factor that controls genes encoding inflammatory cytokines and nociceptive mediators, and therefore plays a crucial role in the onset of neuropathic pain (Xu, Fan, and Shao, 2025). Upon TWEAK binding, TNFRSF12A recruits TRAF2 (and cIAP1), leading to IκBα activation by kinases, including NF-κB inducing kinase, and the production of p52 (Blanco-Colio, 2014). This promotes transcription of pro-inflammatory genes such as *Ptgs2*, *Tnf*, and *Ccl2*, which contribute to nociceptive neurone sensitisation (Maqbool et al., 2013). In parallel, MAPK signalling, which involves ERK, p38, and sometimes JNK (Ji et al., 2002; Xu, Fan, and Shao, 2025), plays an important role in neuronal plasticity and peripheral sensitisation (Ji et al., 2002), by regulating ion channel activity, gene transcription, and long-term changes in sensory neurone excitability. In further support of this, inhibiting NF-κB action alleviates neuropathic pain and neuronal inflammation (Huang et al., 2019). Here, NF-κB and MAPK pathway involvement was not investigated; in future work, live reporters of their activity could be used to confirm their activation.

Although siRNA-mediated knockdown was performed under basal conditions, this allowed us to isolate the contribution of axonal *Tnfrsf12a* to neuronal excitability independent of exogenous inflammatory stimuli. Since our transcriptomic data show that PGE_2 upregulates *Tnfrsf12a*, it is likely that TNFRSF12A exerts an even more pronounced effect during inflammation. Future studies could test whether axonal knockdown of *Tnfrsf12a* attenuates PGE_2-induced hyperexcitability, directly linking its local translation to inflammatory sensitisation.

Together, these findings establish that axonal TNFRSF12A plays a direct, likely translation-dependent role in neuronal excitability. Along with our findings, the two *in vivo* pain studies position TNFRSF12A as a key driver of sensitisation across both peripheral and central pain states and highlight novel epitranscriptomic regulation via NAT10.

4.4.5 *Tnfrsf12a* is Translated Locally in the Axon to Mediate Neuronal Inflammation and Sensitisation

The identification of *Tnfrsf12a* as an axonally enriched and inflammation-regulated transcript supports the idea that axonal mRNA pools are not merely passive reservoirs but actively contribute to the local regulation of sensory function. In addition, axon-specific knockdown, via fluidically isolated siRNA application (Hengst et al., 2006), suggested that *Tnfrsf12a* can exert functional effects at the axonal compartment, independent of direct somatic input, consistent with its local translation. These findings are supported by our discovery of ribosomal proteins in the axon, which are involved in local translation, and the differential expression of mRNA transcripts between axonal and somatic compartments (Pope et al., 2025). This highlights the capacity for spatially restricted protein synthesis in axons; a concept that has previously been shown by other groups (Gale et al., 2022; Gumy et al., 2011; Holt, Martin, and Schuman, 2019; Koppers et al., 2024; Merianda et al., 2009; Tushev et al., 2018; Willis and Twiss, 2011). Such local translation enables neurones to rapidly adapt to microenvironmental stimuli without requiring input from the soma.

Similarly to the previous chapter, I wanted to investigate potential retrograde communication of neuronal sensitisation to the cell somata. To test this, the cell somata were stimulated with KCl: there was a trend toward reduced neuronal excitability following axonal *Tnfrsf12a* knockdown, but the study was underpowered. This may still reflect a genuine biological effect, but further experiments are required. Importantly, KCl is a non-selective depolarising agent that activates all excitable neurones by altering membrane potential (Kimourtzis et al., 2024), rather than targeting nociceptive-specific pathways like capsaicin does (Cavanaugh et al., 2011). As discussed in the previous chapter's discussion (Section 3.4.3), any dampening of excitability in nociceptive neurone subpopulations may have been diluted by unaffected responses in non-nociceptive cells, indicating a nociceptive-specific ef-

fect. Moreover, because KCl-induced depolarisation does not rely on transducer channels (e.g., TRPV1), it may be less sensitive to modulatory effects exerted by TNFRSF12A at the peripheral terminal. This distinction underscores the importance of using stimulus-specific readouts when probing mechanisms of sensitisation and further supports the idea that TNFRSF12A's role is particularly relevant in nociceptive-specific inflammatory signalling.

This also points towards TNFRSF12A's downstream effects impacting TRPV1 activity specifically; TRPV1's augmentation during inflammation is known to occur via its phosphorylation, its trafficking to the membrane, and transcriptional upregulation (Figure 4.14; Jang, Kim, and Hwang, 2020; Moriyama et al., 2005). This is enhanced by NF-κB and MAPK signalling (discussed further in the following section; Ji et al., 2002; Luo et al., 2024; Zhang et al., 2020), both of which are activated by TNFRSF12A (Huang et al., 2025; Liu et al., 2025), suggesting an indirect potentiation of TRPV1 activity. In support of this, mRNA levels of *Trpv1* have been found to significantly increase following chronic constriction injury (Wang et al., 2020), as have levels of *Tnfrsf12a* (Huang et al., 2019). However, single-cell datasets have demonstrated some heterogeneity in the regulation of *Trpv1* levels, implying inter-model variation (Ji et al., 2002; Wang et al., 2021). Other channel expression levels and functions could be modified by MAPK signalling, such as $Na_v1.8$ and $P2X_3$ (Xu, Fan, and Shao, 2025), giving rise to enhanced calcium signalling in response to stimulation. To the best of our knowledge, TNFRSF12A has not yet been linked to the regulation of TRPV1.

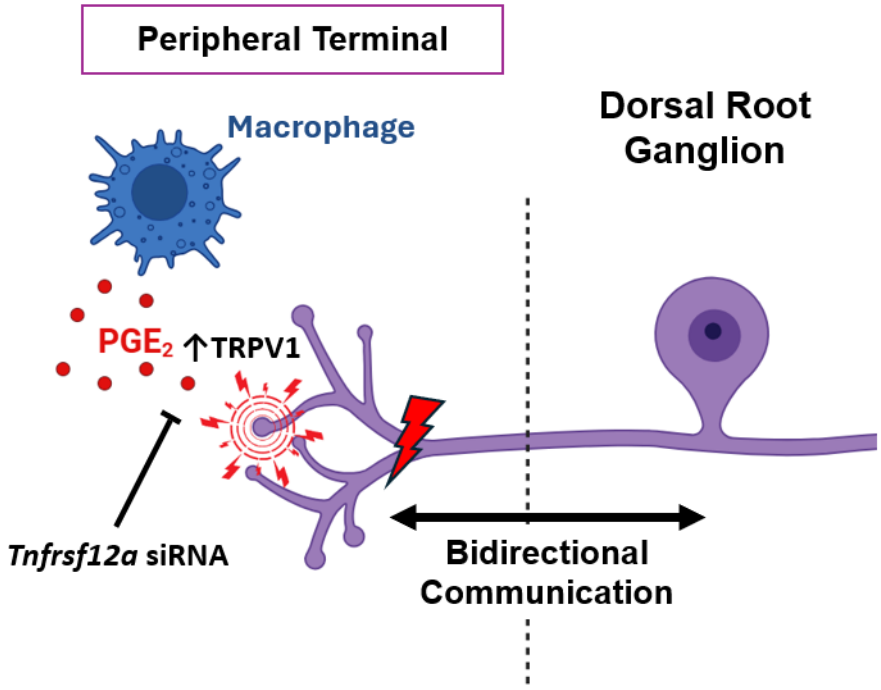


Figure 4.14. Silencing of *Tnfrsf12a* Specifically at the Sensory Neurone Axon Terminal Reduced Neuronal Excitability. siRNA targeting *Tnfrsf12a* mRNA was applied locally within compartmentalised microfluidic chambers, enabling selective knockdown at the axon terminal. Neuronal excitability was assessed using calcium imaging and was found to be reduced following 48-hour incubation with siRNA. These findings indicate that axonal translation of *Tnfrsf12a* is functionally relevant in mediating excitability in sensory neurones, potentially via indirect upregulation of TRPV1 activity. Created using BioRender™.

Comparable mechanisms of retrograde communication following local translation have been demonstrated in other systems and were discussed briefly in Section 3.4.6. For example, CREB is locally synthesised in axons in response to NGF and then retrogradely transported to the nucleus, where it promotes neuronal survival (Cox et al., 2008). Similarly, repression of miR-26a in axons triggers local synthesis of GSK3β, which is subsequently transported to the soma where it impacts axonal growth (Lucci et al., 2020). Axonal injury has also been shown to induce local synthesis of importin β1 and STAT3, both of which undergo retrograde transport to the nucleus to mediate transcriptional responses (Hanz et al., 2003; Ben-Yaakov et al., 2012). This precedent supports a model in which *Tnfrsf12a* is locally translated in the axon to mediate peripheral sensitisation and potentially initiate signalling cascades that influence synapses and central neuronal excitability. The differen-

tial regulation of signalling pathways between the soma and axon highlights the capacity of neurones to dynamically prioritise localised responses to their microenvironment. This spatial specificity enables efficient adaptation to environmental stimuli - such as inflammation or injury - by selectively enhancing processes like local protein synthesis, excitability modulation, or cytoskeletal remodelling, while downregulating energy-intensive global responses (Gale et al., 2022).

Disruption of *Tnfrsf12a* expression likely interferes with both transcriptional and post-translational mechanisms of sensitisation, consistent with our observation of reduced calcium responses. Additionally, the localisation of *Tnfrsf12a* mRNA to the axon suggests that local translation at peripheral terminals may also contribute to stimulus-response coupling, potentially via cytoskeletal remodelling, membrane protein dynamics, and inflammatory pathway activation (Chen et al., 2025a; Huang et al., 2019; Willis and Twiss, 2011). Taken together, these data propose a model in which TNFRSF12A acts as a sensitisation hub, linking inflammatory signalling to neuronal hyperexcitability, and support the therapeutic potential of targeting *Tnfrsf12a* in chronic pain.

These findings position TNFRSF12A as a central mediator of pain sensitisation in both peripheral and central models. Its regulation by NAT10-mediated RNA acetylation introduces a novel epitranscriptomic mechanism in the context of central post-stroke pain (Huang et al., 2025) and suggests that targeting either TNFRSF12A or NAT10 may offer a promising therapeutic strategy. Alternatively, local translation of TNFRSF12A at the axon terminal may alter membrane signalling dynamics or cytoskeletal organisation (Sasaki, 2020), thereby influencing stimulus-response coupling. Thus, TNFRSF12A is likely to integrate transcriptional, translational, and inflammatory signals to modulate sensory neurone excitability in pain.

4.4.6 Developmental Conservation of TNFRSF12A-Mediated Sensitisation in Sensory Neurones

Our investigations were performed in embryonic sensory neurones, despite the immaturity of neuronal networks and transcriptome differences (Gumy et al., 2011; Lechner et al., 2009). However, in our transcriptomic investigations, we found that 75% of the transcripts upregulated in eight-week-old mouse cultures following PGE_2 treatment were also upregulated in embryonic cultures (Pope et al., 2025). This justified the use of embryonic DRG neurones, alongside their relative ease of subcellular manipulation (as discussed in Section 1.9.2), for functional investigations. Importantly, the mechanisms we describe are likely to be conserved in mature systems - TNFRSF12A is upregulated in adult pain models (Inta et al., 2008; Potrovita et al., 2004; Tanabe et al., 2003) and shows conserved expression patterns across species (Zheng and Burkly, 2008), suggesting translational relevance. Nonetheless, future studies using adult or human sensory neurones would help validate the applicability of these findings to clinical pain states. Therapeutically, targeting *Tnfrsf12a* or its downstream effectors - such as NF-κB - could offer a peripherally acting strategy for pain modulation, without the side-effects commonly associated with pain management medication. This is particularly compelling given that *Tnfrsf12a* exhibits low basal expression in most non-neuronal tissues, with levels rising markedly only in response to injury or inflammation (Burkly, Michaelson, and Zheng, 2011; Burkly, 2014; Liu et al., 2025).

4.4.7 Chapter Conclusions

Using compartmentalised cultures of embryonic DRG neurones, subcellular transcriptomic analysis revealed differential gene regulation in axons versus somata following PGE_2 treatment, supporting the concept of local axonal translation in inflammatory sensitisation. Among the selectively upregulated transcripts, *Tnfrsf12a* showed marked enrichment in the axonal compartment. Functional validation via

siRNA knockdown demonstrated that silencing *Tnfrsf12a* reduced neuronal excitability, implicating TNFRSF12A as a pro-sensitising, inflammation-associated receptor. Microfluidic models enabled targeted axonal manipulation, reinforcing the idea that axons are dynamic sites of transcript regulation and protein synthesis. These findings position *Tnfrsf12a* as a locally translated effector of peripheral sensitisation.

While the investigations detailed in the first two results chapters have advanced our understanding of peripheral sensitisation, particularly the modulatory roles of PGE_2 and *Tnfrsf12a* at the terminal endings of sensory neurones, they also underscore the complexity of nociceptive signalling. Peripheral inputs do not act in isolation; rather, they initiate and modulate a cascade of events that extend centrally, particularly within the spinal cord dorsal horn, where pain signals are integrated, amplified, or suppressed (Webb and Steeds, 2022). The transition from peripheral to central sensitisation is a key step in the development of chronic pain, yet the mechanisms underpinning this process remain incompletely understood.

Recent evidence has highlighted the crucial influence of non-neuronal cells, particularly glia, in modulating central nociceptive processing. Among the diverse modes of glia-neurone communication, extracellular vesicles have emerged as potent mediators capable of altering neuronal function, structure, and excitability (Ahmad et al., 2022; Prada et al., 2018; Zhu et al., 2025). These vesicles carry a complex cargo of proteins, lipids, and nucleic acids, and can induce long-lasting changes in neuronal behaviour, including sensitisation (Ahmad et al., 2022).

Given the demonstrated capacity of PGE_2 and *Tnfrsf12a* to modulate peripheral nociceptive neurone sensitivity, I hypothesised that parallel, or complementary, modulatory influences might be exerted at the central terminal, potentially contributing to pain amplification via distinct mechanisms. The focus was therefore shifted to the interaction between glial-derived EVs and the central terminals of sensory neurones, with the aim of identifying novel, targetable pathways involved in EV-induced

sensitisation. This shift acknowledges the broader neuroimmune context of pain, wherein glial cells may exert complementary or even synergistic effects on nociceptive neurone sensitisation, both peripherally and centrally.

Chapter 5

Glial-Derived Extracellular Vesicles Induce Neuronal Sensitisation via miR-146a-5p

5.1 Introduction

Glial cells are key regulators of neuroinflammation, releasing extracellular vesicles that can modulate neuronal function and contribute to pain hypersensitivity (Ahmad et al., 2022; Zhu et al., 2025). This chapter describes the optimisation of spinal cord-derived mixed glial cultures to provide a physiologically relevant source of EVs, their collection and characterisation, and subsequent application to DRG neurones. EVs released from cytokine-stimulated glia were sufficient to induce neuronal sensitisation, an effect rescued by miRNA inhibition. Pathway analysis of predicted miRNA targets was then used to begin defining the molecular mechanisms underlying this glia-neurone communication.

5.1.1 Glial Modulation of Sensory Neurone Sensitisation

Sensitisation of sensory neurones is a fundamental process in the initiation, maintenance, and resolution of pain (Latremoliere and Woolf, 2009; Yao and Narumiya, 2019). While transient sensitisation is adaptive and protective, chronic sensory neurone sensitisation becomes maladaptive and contributes to persistent pain (Latremoliere and Woolf, 2009). This sensitisation is not only mediated by changes intrinsic to the neurone - including altered expression and activity of ion channels such as voltage-gated sodium and calcium channels - but also by extrinsic factors within the local microenvironment, such as the release of inflammatory factors by neighbouring cells (Krames, 2015). A wide array of molecular mediators, derived from a broad range of cellular sources, can influence neuronal excitability (Latremoliere and Woolf, 2009); however, the full complexity of these mechanisms remains incompletely understood.

Glial cells, both in the PNS and CNS, are increasingly acknowledged as key participants in neuroinflammation and the modulation of pain signalling. Bidirectional communication between glia and neurones is exerted via multiple mechanisms, including the release of mediators into the extracellular space, direct physical contact

and guidance via cell adhesion molecules, and secretomes (Section 1.8; Ahmad et al., 2022; Krames, 2014). Within the secretome system, EVs are one important mediator involved in cell-cell communication (Figure 5.1; Peng et al., 2022).

Microglia, astrocytes, and neurones form an interdependent triad within the CNS, engaging in continuous bidirectional communication to maintain homeostasis and coordinate responses to injury (Ahmad et al., 2022). This dynamic interplay is particularly relevant at sites where central terminals of DRG neurones project into the spinal cord, integrating peripheral sensory input with central immune and glial signalling. Under physiological conditions, astrocytes regulate extracellular ion balance, remove excess neurotransmitters such as glutamate, and release neurotrophic factors that support neuronal survival (Kwon and Koh, 2020). Microglia survey the microenvironment and remove debris through phagocytosis, while also releasing growth factors that promote repair (Baufeld et al., 2018; Zhan et al., 2014). Neurones influence both astrocyte and microglial activity through neurotransmitter release, membrane-bound ligands, and EV-mediated transfer of regulatory molecules (Ahmad et al., 2022).

During neuroinflammation, this homeostatic relationship shifts. Activated microglia release cytokines (e.g., TNF-α, IL-1β, IL-6), chemokines, and reactive oxygen/nitrogen species that can directly enhance neuronal excitability or prime astrocytes toward a reactive phenotype (Baufeld et al., 2018). Reactive astrocytes, in turn, secrete pro-inflammatory mediators, alter glutamate transporter expression, and modulate synaptic activity, which can prolong or amplify nociceptive signalling (Cheng, Xu, and Ma, 2022). Both glial types can release EVs containing proteins, lipids, and non-coding RNAs that alter neuronal gene expression, ion channel activity, and synaptic organisation (Figure 5.1; Ahmad et al., 2022). Conversely, stressed or hyperactive neurones can signal back to glia via ATP (Ma et al., 2021), chemokines like fractalkine (Souza et al., 2013), or EV cargo (Ma et al., 2024), to either promote glial activation or attempt to restore homeostasis.

This continuous feedback loop means that pathological changes in one cell type can propagate through the network, sustaining sensitisation even after the initial trigger has resolved. Understanding these reciprocal interactions, particularly the EV-mediated component, is essential for modelling the glial contribution to chronic sensory neurone sensitisation.

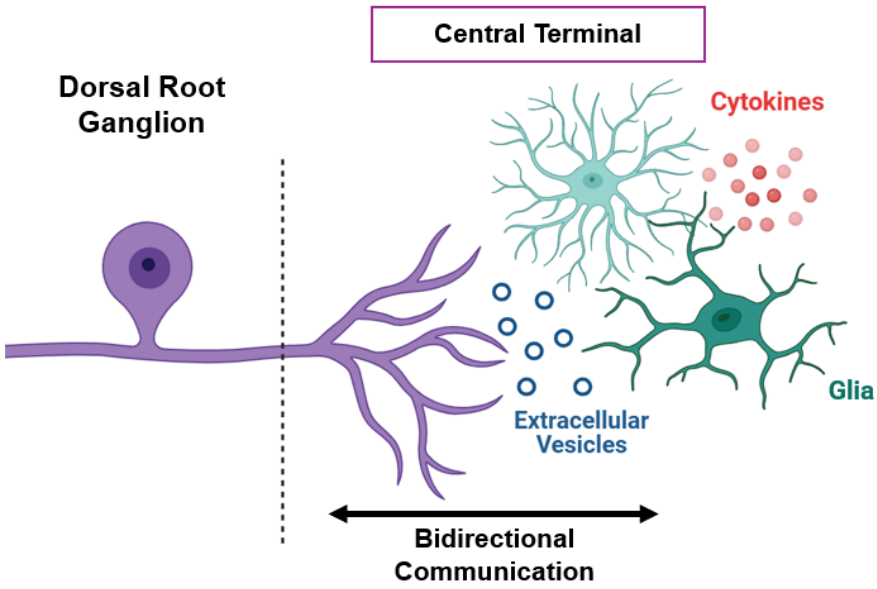


Figure 5.1. Bidirectional Communication Between Glia and Sensory Neurones via Extracellular Vesicles. Glial cells release EVs in response to stimulation by pro-inflammatory cytokines. These EVs can be taken up by sensory neurones, modulating neuronal function. Conversely, sensory neurones also release EVs capable of influencing glial activity, highlighting a bidirectional mode of communication between these cell types during inflammation. Created using BioRender™.

5.1.2 Glial Extracellular Vesicles in Pain and Sensory Neurone Sensitisation

An expanding body of evidence indicates that glial-derived EVs are active drivers of pain hypersensitivity and neuronal sensitisation. In neuropathic pain conditions, neuroinflammation and oxidative stress are associated with activation of microglia and astrocytes within the spinal dorsal horn (You et al., 2025). Spinal cord injury models demonstrate increased expression of microglial activation markers, alongside dysregulation of non-coding RNAs in lipopolysaccharide-stimulated microglial cultures, suggesting that transcriptional and post-transcriptional mechanisms con-

tribute to sustained microglial reactivity (You et al., 2025).

Studies investigating spinal nerve ligation (SNL)-induced neuropathic pain have shown that microglia-derived EVs contribute to nociceptive processing: EVs shed from microglia were increased in the cerebrospinal fluid and dorsal horn following SNL, and injection of these vesicles reduced paw withdrawal threshold and paw withdrawal latency in naïve rats. EV exposure also increased the amplitude and frequency of spontaneous excitatory postsynaptic currents, indicating enhanced excitatory transmission. Vesicle shedding was linked to activation of the neuroinflammatory P2X7-p38 pathway, and vesicles were enriched in IL-1β, with inhibition of IL-1β reversing behavioural hypersensitivity (Li et al., 2017).

Peripheral glial populations also release EVs with pronociceptive properties. Oxaliplatin activated cultured satellite glial cells (SGCs) and increased exosome secretion, while conditioned SGC-derived exosomes induced mechanical hypersensitivity when administered intrathecally to naïve mice. These exosomes exerted pronociceptive effects on DRG neurones and extensively altered miRNA cargo, including the differential expression of miR-142a-3p and miR-181a-5p (Zhao et al., 2023).

Astrocyte-derived EVs can exert context-dependent effects on neuroinflammatory signalling. During central sensitisation, reactive astrocytes can release EVs which suppress microglial activation and attenuate neuroinflammation, indicating that EVs can also convey anti-inflammatory signals (Han et al., 2022). In contrast, in models of morphine tolerance, astrocyte-derived EVs display elevated sonic hedgehog (SHH) protein, which activates SHH signalling via primary cilia on astrocytes, and inhibition of EV release prevents the development of morphine tolerance *in vivo* (Ma, Kutchy, and Hu, 2021).

Microglial EVs have additionally been linked to synaptic dysfunction and reduced cognition associated with pain. In postoperative pain models, surgery induced

microglial activation, neuronal degeneration, and loss of synapse-associated proteins within the hippocampus, accompanied by increased NF-κB phosphorylation and IL-1β expression in neurones. EVs derived from polarised microglia promoted synaptic loss, neuronal degeneration, and memory impairment even in the absence of surgery, and EVs enriched in IL-1R1 were shown to drive postoperative cognitive dysfunction by regulating neuronal inflammation (Qi et al., 2023). Complementary work identified miR-124-3p as a microglial EV-associated regulator of inflammatory responses, autophagy, and apoptosis. Postoperative pain reduced miR-124-3p levels in microglial EVs, while overexpression or stereotactic delivery of exogenous microglial miR-124-3p suppressed polarisation, reduced microglial proliferation, and alleviated cognitive impairment (Kong et al., 2024).

Importantly, as mentioned previously, EV-mediated communication in pain is bidirectional. DRG neurone-derived exosomes, isolated from mice subjected to SNL, exacerbated neuropathic pain behaviours when injected into recipient animals, lowering mechanical thresholds and enhancing thermal and cold sensitivity. These neurone-derived EVs promoted BV2 microglial activation via miR-16-5p, demonstrating that sensory neurones can actively regulate microglial inflammatory states through EV release (Xing et al., 2024).

Finally, emerging clinical evidence supports the relevance of glial EVs in human inflammatory disease. Children with juvenile idiopathic arthritis exhibited increased levels of astrocyte-derived EVs and the astrocytic protein S100β in plasma, with EV abundance correlating with disease activity (Berntson et al., 2024).

5.1.3 Recapitulating Reactive Glial States *in vitro*

Studying glia-neurone interactions at the central terminals of DRG neurones is best achieved using spinal cord-derived glial populations. To better investigate the complex glial environment present *in vivo*, mixed glial cultures can be utilised. Unlike isolated astrocyte or microglial cultures, mixed glia retain essential intercellular in-

teractions that shape inflammatory signalling and extracellular vesicle composition (Ahmad et al., 2022). This offers a more physiologically relevant model for studying glia to neurone communication. In the specific context of sensory neurone-glia interactions, it is particularly important to use glia derived from the spinal cord, as glia originating from different regions of the CNS exhibit distinct functional properties and secretome compositions that would not interact with sensory neurones *in vivo*, as summarised by Xuan et al. (2019). For instance, spinal cord glia are the first to show heightened inflammatory and injury-related responses and play key roles in modulating neuronal signalling in sensory pathways (Clarke et al., 2019). By contrast, cortical glia are especially important during development where they are contribute to synapse formation and refinement, and they also play central roles in plasticity, neurodegenerative disease, and chronic inflammation (Fiorin and Espírito Santo, 2025). Despite regional differences, cortical glia are frequently used in place of spinal glia, even when spinal-specific phenotypes would be more appropriate (e.g., Liu et al., 2015; Xu, Gou, and Dong, 2010), largely due to the higher yield of glial cells from cortical tissue.

To model the glial response to inflammatory conditions that may occur *in vivo* at the central terminal of DRG neurones, glial cultures can be stimulated with a combination of pro-inflammatory cytokines: TNF-α, interleukin-1α (IL-1α), and complement component 1q (C1q). This cocktail has been shown to induce a pro-inflammatory phenotype in both astrocytes (Liddelow et al., 2017) and microglia (Kong et al., 2019; Silverman et al., 2016), but it remains an approximation and simplification of the inflammatory milieu encountered *in vivo*.

TNF-α and IL-1α are classical pro-inflammatory cytokines that promote the release of additional inflammatory mediators. TNF-α is a pleiotropic cytokine that activates glial cells via TNF receptors, whereas IL-1α, a potent pro-inflammatory molecule, binds to the IL-1 receptor. Both lead to downstream activation of pro-inflammatory NF-κB (Kong et al., 2019) and MAPK pathways (Meng et al., 2016; Petersen et

al., 2005). In microglia, TNF-α promotes reactivity, increases levels of inflammatory *Tnf*, *Il1b*, and *Nos2* mRNAs and the production of other pro-inflammatory cytokines, including autocrine-stimulated release of TNF-α (Brás et al., 2020), generating a pro-inflammatory feedback loop. Astrocytes also become reactive, secrete chemokines such as CXCL10, increase blood-brain barrier permeability, and reduce synaptic support (Lawrence et al., 2023; Liddelow et al., 2017). In comparison, IL-1α acts as a potent pro-inflammatory signal, increasing levels of numerous pro-inflammatory molecules, including COX-2, IL-6, TNF-α, and CCL2 (affecting PGE_2 levels, relevant to Chapter 3; Liu and Quan, 2018; Yao and Narumiya, 2019). It also promotes astrocytic hypertrophy and facilitates immune cell infiltration by stimulating CXCL10 secretion (Liddelow et al., 2017).

C1q, together with TNF-α and IL-1α, induces a neurotoxic A1 astrocyte phenotype, characterised by the downregulation of genes that normally support neuronal survival and synaptogenesis, and the upregulation of pro-inflammatory and cytotoxic programmes. In this state, astrocytes actively secrete factors that damage neurones and oligodendrocytes, rather than providing trophic or synaptic support. C1q is a key driver of microglial reactivity, with reactive astrocytes in turn promoting increased C1q expression in microglia, reinforcing neuroinflammatory feedback loops. More broadly, transcriptomic studies link C1q-associated glial reactivity to activation of inflammatory pathways such as NF-κB and JAK-STAT, consistent with its role in amplifying neurodegenerative processes (Zhang et al., 2023). Together, this cytokine trio acts synergistically to convert quiescent glia into a highly reactive state (Liddelow et al., 2017), altering production of inflammatory mediators and EVs, thereby modelling key features of neuroinflammatory environments that may contribute to chronic pain.

5.1.4 Characterisation of Extracellular Vesicles

To explore EV-mediated mechanisms in detail, precise and accurate characterisation of EVs is essential - it is required of researchers to adhere to field-wide

standards to ensure rigour and reproducibility. The MISEV guidelines provide key recommendations to standardise extracellular vesicle research and improve transparency (Welsh et al., 2024). These guidelines cover EV nomenclature, collection, storage, use, EV structure, and specific markers to identify (for more detail on EVs, see Section 1.3.1.6).

To characterise EV samples, researchers must assess particle size distribution and concentration using techniques such as nanoparticle tracking analysis (NTA), transmission or cryogenic electron microscopy (TEM/cryo-EM), or flow cytometry. Confirmation of EV identity and purity involves detecting characteristic transmembrane (e.g., CD63 and CD9) and cytosolic (e.g., ALIX and TSG101) proteins, while ensuring minimal contamination from proteins such as calnexin (endoplasmic reticulum), apolipoproteins, or other co-isolated secreted proteins. EM-based approaches are also recommended for visualising EV morphology. To demonstrate EV uptake by recipient cells, fluorescent labelling combined with flow cytometry or confocal microscopy can also be used (Welsh et al., 2024). These criteria informed the experimental design and validation steps described in this chapter.

5.1.5 The Role of miRNAs in Glia-Neurone Bidirectional Communication

It is now well-established that glia and neurones engage in complex, bidirectional communication that shapes neuronal excitability, homeostasis, and pathology (Ahmad et al., 2022). A growing body of evidence shows that EVs are key mediators of this dialogue, acting as shuttles for regulatory molecules including miRNAs. While glia and miRNAs have been individually implicated in pain (see Sections 1.8 and 1.3.1.5, respectively), research into the specific contribution of glial-derived, EV-contained miRNAs to sensory neurone sensitisation is in its infancy.

Astrocyte- and microglia-derived EVs can profoundly modulate neuronal function. For instance, microglial EVs carrying miR-146a-5p can be taken up by neurones,

where they suppress synaptic genes such as *Syt1* and *Nlg1*, leading to synaptic dysfunction and reduced dendritic spine density (Prada et al., 2018). Astrocyte-derived EVs can be both neuroprotective and deleterious depending on their activation state: EVs from homeostatic astrocytes attenuate microglial activation and promote axonal growth, while reactive astrocyte EVs exacerbate inflammation and impair functional recovery after injury (Zhu et al., 2025). Furthermore, astrocyte EV cargo is altered in various disease states, such as amyotrophic lateral sclerosis (ALS) - miR-155-5p and miR-494-3p dysregulation contributing to motor neurone degeneration (Marton et al., 2023; Varcianna et al., 2019) - and Alzheimer's disease; for example, with miR-206-3p and human acidic fibroblast growth factor-modulated EVs (Peng et al., 2022).

Conversely, neurone-to-glia signalling via EVs is also critical and often overlooked. Neurone-derived EVs can be taken up by astrocytes and microglia both *in vitro* and *in vivo* (Ma et al., 2024; Men et al., 2019; Morel et al., 2013). For example, miR-181c-5p-enriched EVs from epileptogenic neurones reduce GLT-1 expression in astrocytes *in vitro* and *in vivo*, impairing glutamate uptake and enhancing seizure susceptibility (Ma et al., 2024). Likewise, Morel et al. (2013) showed that neurone-derived EVs containing miR-124a can increase GLT-1 protein in astrocytes, *in vitro* and *in vivo* highlighting a mechanism of neuronal regulation of astrocytic glutamate clearance, which may be involved in the pathology of ALS. In the context of brain injury, neuronal EVs enriched in miR-100-5p were shown to activate microglia via NF-κB signalling (Xin et al., 2024), while in Alzheimer's disease, small neurone-derived EVs from patients induced elevated IL-6 expression in microglia, likely mediated by let-7e (Durur et al., 2022).

Together, these findings point to a dynamic and bidirectional EV-mediated regulatory axis, in which miRNAs function not only as cell-intrinsic gene regulators but also as intercellular signalling molecules capable of reshaping the glial-neuronal environment. However, the role of glial-derived EVs in sensory neurone sensiti-

sation, and particularly the contribution of EV-associated miRNAs, remains underexplored.

To investigate the role of a specific miRNA, a range of molecular strategies have been developed to manipulate miRNA levels. These include overexpression using vector-based systems and various inhibitory approaches. Among the most established tools for miRNA knockdown are antisense oligonucleotides, also known as anti-miRNA oligonucleotides (AMOs), which bind specifically to the mature miRNA sequence to block its function. Over time, AMOs have been refined into chemically modified forms to improve stability and efficacy - most notably 2'-O-methyl, 2'-O-methoxyethyl, and locked nucleic acid (LNA) oligonucleotides - often incorporating a phosphorothioate (PT) backbone for enhanced resistance to nuclease degradation. LNA-modified AMOs offer high binding affinity, improved mismatch discrimination, and favourable pharmacokinetic properties, including low toxicity and high metabolic stability, making them suitable for both *in vitro* and *in vivo* use. The substitution of non-bridging oxygen atoms with sulphur in the PS backbone further enhances serum stability and cellular uptake (Liu, Sall, and Yang, 2008).

5.1.6 Aims and Hypotheses

Hypotheses

I proposed a conceptual model in which glial-derived EVs act as molecular conduits of inflammation-induced plasticity at the central terminals of sensory neurones. Specifically, I hypothesised that EVs released from glial cells in an inflamed state could encode and deliver pro-nociceptive signals, reshaping the transcriptional and excitability landscape of sensory neurones in ways that contribute to peripheral, and potentially central, sensitisation. Within this framework, I further posited that non-coding RNAs - particularly miRNAs - embedded within these vesicles may serve as key molecular agents, orchestrating sustained changes in gene expression and neuronal responsiveness.

Experimental Aims

To explore these hypotheses, I sought to:

- Assess whether EVs, derived from mixed glia, sensitise DRG neurones using calcium imaging as a readout of neuronal excitability.
- Identify candidate miRNAs involved in EV-induced sensitisation through targeted literature review and test their function using miRNA inhibitors.

5.2 Methods

5.2.1 DRG Neuronal Culture

E16.5 DRG neurones were cultured, as previously described in Section 2.3.2, in dissociated cultures in inverted chambers (Section 2.3.1 for details).

If co-culturing with mixed glia, upon glial confluence in one side of compartmentalised microfluidic chambers, E16.5 DRG sensory neurones were seeded into the other compartment, according to the usual protocol described in Section 2.3.2. Laminin coating was applied only to the DRG compartment.

5.2.2 Mixed Glial Culture

To reconstruct the complex microenvironment of the dorsal horn, a primary spinal cord-derived mixed glial culture was established, encompassing astrocytes, microglia, and potentially oligodendrocyte progenitor cells (OPCs) - those that will interact with, and thereby directly influence, sensory afferent central terminals (Long et al., 2025).

Embryo Collection and Dissection

Initial embryo dissections were performed as described in Section 2.3.1. Spinal cords were gently removed from each pup using forceps, prior to DRG extraction, and transferred into 5 mL of fresh L-15 medium supplemented with 0.1% (m/v) BSA

and 1% (v/v) Penicillin-Streptomycin, and kept on ice.

Spinal Cord Dissociation and Cell Preparation

The L-15 solution, containing a minimum of six spinal cords, was transferred to a falcon tube and topped up to 10 mL with cold L-15 solution. Spinal cords were gently mechanically dissociated with a 10 mL stripette and kept on ice. The solution was centrifuged at 2500 x *g* for five minutes at 4°C and the supernatant discarded. The cell pellet was resuspended in fresh cold L-15 solution, passed through a 100 μm cell strainer (Falcon®, Corning) into a new falcon tube and centrifuged again at 2500 x *g* for five minutes at 4°C. The supernatant was discarded and the cell pellet resuspended in the desired volume of glial culture medium for seeding (1 mL per spinal cord): DMEM (21068-028, Gibco), 10% FBS, 1% GlutaMAX™, 1% Penicillin-Streptomycin. A cell count was performed before 1 mL of the cell suspension was seeded per T-25 flask, already containing 5 mL glial culture media (Figure 5.2). This is in line with one murine spinal cord per 25 cm^2 culture flask (Tamashiro, Dalgard, and Byrnes, 2012).

50 μL of cell suspension was seeded into the centre of PDMS rings for immunofluorescence, kept at 37°C and 5% CO_2 for two hours to attach, before the media was topped up to 200 μL.

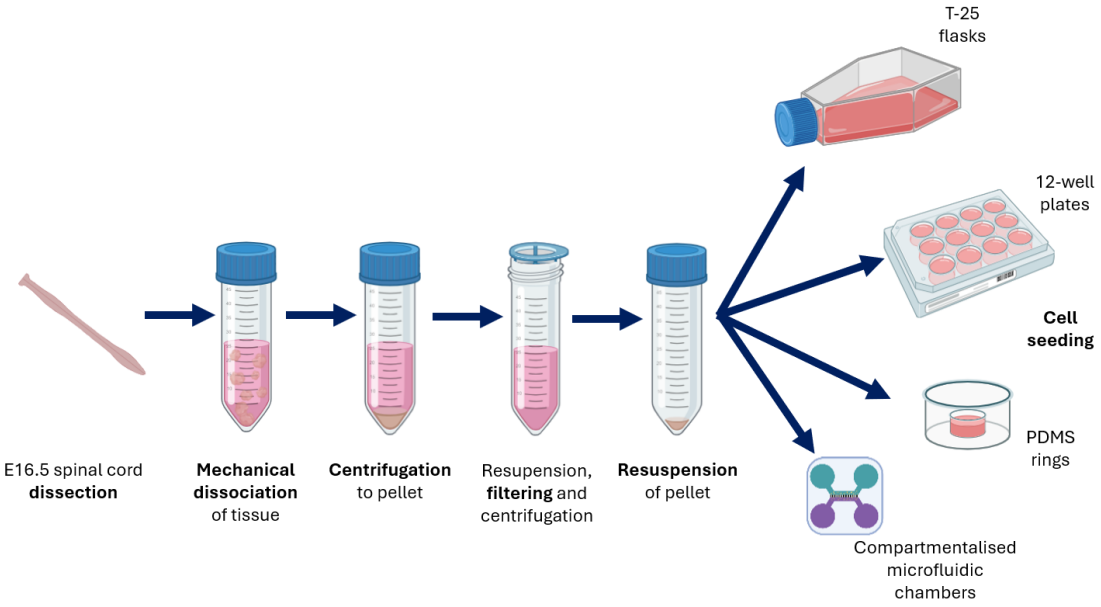


Figure 5.2. Protocol for the Culture of Mixed Glia from Embryonic Murine Spinal Cords. Spinal cords were gently removed from embryonic mice and mechanically disrupted in a falcon tube. After centrifugation to pellet the cells, they were resuspended and the suspension passed through a cell strainer to filter out debris. The suspension was centrifuged again and resuspended in cell seeding media. Cells were plated in T-25 cell culture flasks, 12-well plates, PDMS rings, or compartmentalised microfluidic chambers, depending on the experimental question. Created using BioRender™.

For co-culture with DRG sensory neurones, glial media was flushed through one channel and removed. 20 μL of glial cell suspension was added to each well on the same side of the compartmentalised microfluidic chamber. 200 μL culture medium was added to the empty side of the chamber to generate hydrostatic pressure, limiting glial migration and proliferation through the microgrooves to the other compartment. Cells were maintained at 37°C and 5% CO_2 for two hours before media was topped up to 100 μL (Figure 5.3).

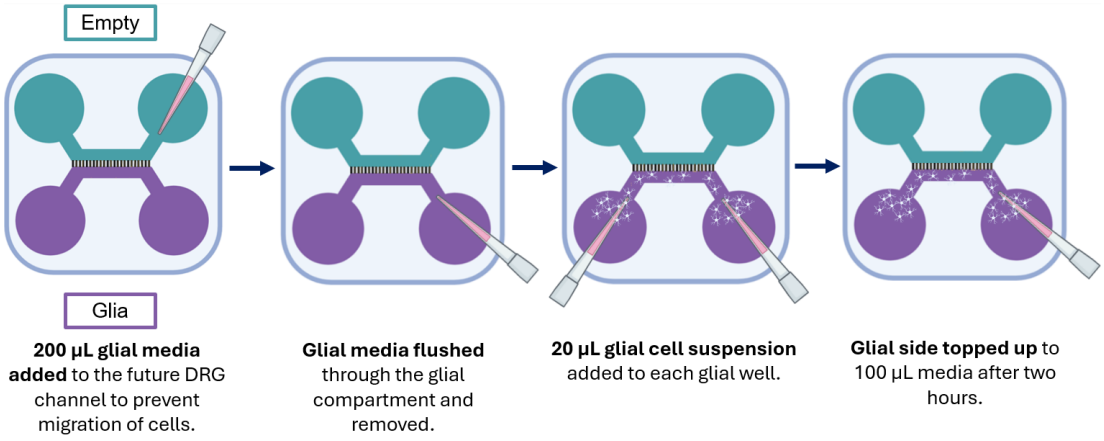


Figure 5.3. Schematic for Glial Culture in Preparation for Co-Culture with DRG Sensory Neurones. 200 μL glial culture medium was added to the empty side of the chamber to limit glial migration and proliferation through the microgrooves to the other compartment. Glial media was flushed through the other channel and removed. 20 μL of glial cell suspension was added to each well on the glial side of the compartmentalised microfluidic chamber. Cells were maintained at 37°C and 5% CO_2 for two hours before media was topped up to 100 μL. Created using BioRender™.

Glial Culture and Media

Mixed glia were cultured for 21 days, or until sufficiently confluent. Media was changed every 48-72 hours. At DIV21 (prior to treatment and EV collection), media was switched to serum-free (DMEM, 1% GlutaMAX™, 1% Penicillin-Streptomycin) for 24 hours to minimise FBS-derived EV contamination (Welsh et al., 2024).

Glia for co-cultures were cultured for ∼21 days, at which point media was removed from the opposite compartment and replaced with 0.1 mg/mL laminin (Section 2.3.2) for at least one hour. Media in the glial compartment was replaced with DRG media to encourage axon growth through the microgrooves. Following laminin removal, 10-15 DRGs were seeded and maintained at 37°C and 5% CO_2 . Two hours later, DRG media was topped up to 200 μL (Figure 5.4).

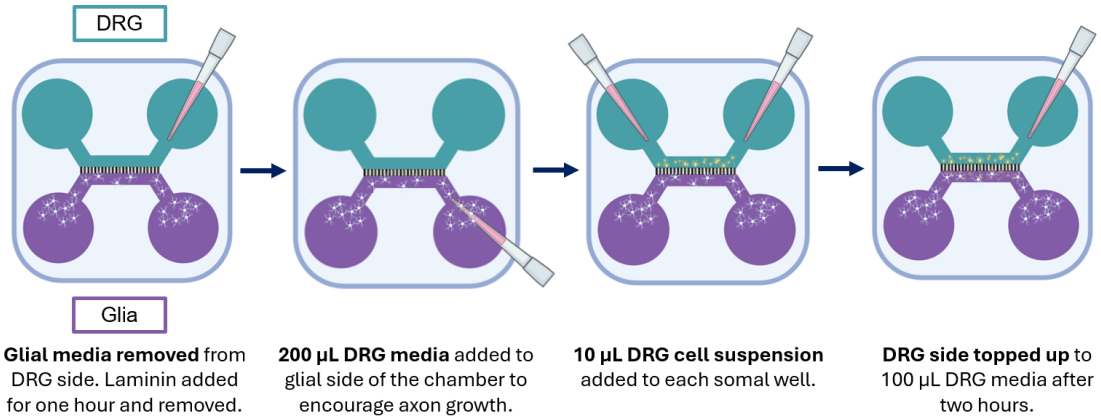


Figure 5.4. Schematic of DRG Addition for Co-Culture with Glia. Glia were cultured for ∼21 days, at which point media was removed from the opposite compartment and replaced with laminin for at least one hour. Following removal, 10-15 DRGs were seeded and allowed to grow through the microgrooves into the glial compartment. Created using BioRender™.

5.2.3 Mixed Glial Culture Optimisation

Culture Optimisation and Rationale

Given the variability in glial proliferation and yield under standard conditions, optimisation experiments were performed to identify culture conditions that maximised viability and reproducibility. To address this, various combinations of FBS concentration, substrate coating, and culture format were tested.

Serum and Extracellular Vesicle Considerations

Glia are proliferative cells, often requiring supplementation with serum *in vitro*, such as FBS, to promote survival and growth. However, serum is not an endogenously produced substance and has been reported to alter the morphology, reactivity, and function of glial cultures due to the presence of bioactive molecules not naturally found in the CNS (Subbiahanadar Chelladurai et al., 2021; White et al., 2024). Serum-free alternatives, including growth factor supplementation, have been explored to maintain glial cultures in a more physiological state (Bohlen et al., 2017).

To verify the viability and proliferative capacity of glial cultures, media supple-

mented with 10% FBS was initially used. However, for downstream EV isolation, this concentration was not feasible due to contamination from FBS-derived vesicles, which would interfere with accurate analysis of glial-derived EVs (Welsh et al., 2024). Attempts to reduce serum content to 0-2% FBS resulted in poor glial proliferation, failure to reach confluence, altered cellular composition - particularly a reduction in microglia - and reduced EV yield. As a result, cultures were maintained in 10% FBS until the start of the treatment protocol. At this point, for the different stages of the experimental protocol, media was replaced several times with serum-free medium to prevent contamination with residual FBS.

Cell Culture Material and Area

Initially, T-75s were used for mixed glial culture, but they were not reaching confluency and preferentially grew around the outside of the flask. T-25s were used for the rest of experimentation, with plenty of area for proliferation and the potential for a minimum of three flasks to be combined per treatment group to achieve a sufficient concentration of EVs.

Glass coverslips for immunofluorescence were tested but mixed glia would not attach to the glass, despite trials with coating (PLL and poly-D-lysine, PDL, P6407, Sigma-Aldrich). Cells were seeded into PDMS rings or compartmentalised microfluidic chambers attached directly to plastic nunc dishes, with no coating.

Culturing Isolated Microglia

Mixed glial cultures were maintained in T-25 flasks until DIV14. To isolate microglia, flasks were placed on an orbital shaker at 37°C and 5% CO_2 for two hours, facilitating the detachment of semi-adherent microglia. Dislodged microglia were collected and plated into 12-well plates with varying surface treatments (Figure 5.5) - PDL, PLL, or no coating - using microglial culture medium: DMEM, 10% (v/v) heat-inactivated horse serum (Gibco™), 1% (v/v) GlutaMAX™, 1% (v/v) Penicillin-Streptomycin. Although microglia were successfully dislodged, they failed to ad-

here under all conditions when transferred to 12-well plates, exhibited poor survival, and were therefore unsuitable for downstream experimentation.

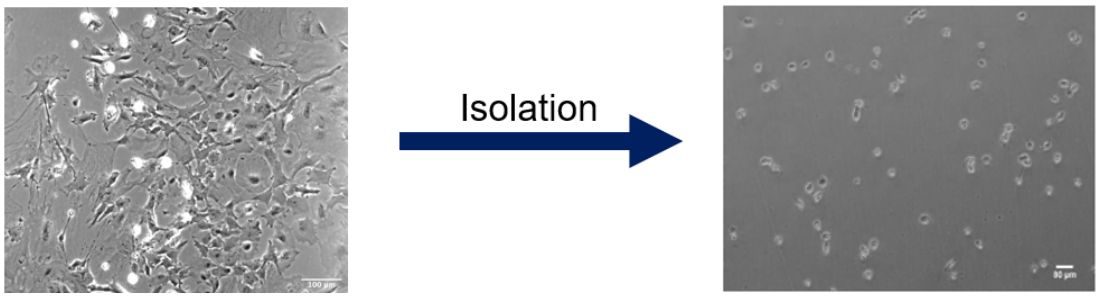


Figure 5.5. Brightfield Images of Microglia Isolated from Mixed Glial Culture. Mixed glial cells were isolated from embryonic day 16.5 mouse spinal cords and seeded into T-25 flasks (designated as DIV1). Microglia appear as bright, round cells on top of a layer of astrocytes. On DIV14, cultures were placed on an orbital shaker for two hours at 37°C and 5% CO_2 to detach semi-adherent microglia. Isolated microglia were transferred to 12-well plates. Scale bars 100 μm and 80 μm, respectively.

Summary of Optimisation

A summary of the optimisations described above is provided in Table 5.1.

Table 5.1. Optimisation of Mixed Glial Culture. Various conditions were tested to optimise culture success, cell proliferation, and suitability for downstream applications such as EV isolation and immunofluorescence. Optimisation combinations in green were used in experimentation. Abbreviations: MFC - microfluidic chamber, FBS - foetal bovine serum, HI - heat inactivated, EV - extracellular vesicle, PLL - poly-L-lysine, PDL - poly-D-lysine, PDMS - polydimethylsiloxane.

Serum (FBS)	Substrate / Coating	Culture Format	Culture Outcome	Notes
0%	Plastic, uncoated	T-25	No attachment or proliferation	Failed cultures
2%	Plastic, uncoated	T-25	Sparse growth	Low density, poor microglia yield, minimal EVs
10%	Glass coverslips, PLL/PDL	PDMS rings (nuncs)	No attachment or growth	Failed cultures
10%	Glass coverslips, uncoated	PDMS rings (nuncs)	No attachment or growth	Failed cultures
10%	**Plastic, uncoated**	**PDMS rings (nuncs)**	**Good proliferation**	**Successful; used for immunofluorescence and imaging**
10%	Plastic, uncoated	MFCs (nuncs); cells added to channel	Sparse growth	Little proliferation and migration within channel
10%	**Plastic, uncoated**	**MFCs (nuncs); cells added to well**	**Good proliferation**	**Used for co-culture; good adherence in channels. Did not succeed every prep**
10%	Plastic, uncoated	T-75	Patchy growth	Mainly growth around flask edges
10%	Uncoated	T-25	Consistent proliferation	Successful; good number of cells for EV isolation (combined $\geq$3 flasks per condition)
10% pre-treatment, then serum-free	**No coating**	**T-25**	**EV yield suitable for isolation**	**Used in EV experiments; FBS removed to prevent contamination**
10% HI horse serum	Attempted microglia isolation; PLL/ PDL coating	12-well (isolated microglia)	No attachment; few cells	Attempted microglia isolation unsuccessful

5.2.4 Brightfield Microscopy

Brightfield images were taken as described in Section 2.6.4 to compare control and cytokine-treated cultures, and glia cultured in FBS-supplemented medium versus serum-free.

5.2.5 Immunocytochemistry

Cells were fixed with 4% paraformaldehyde (w/v) once PDMS ring cultures reached confluence or when DRG axons had grown extensively into the glial compartment in co-cultures. The standard immunocytochemistry protocol was followed (Section 2.6); however, due to the absence of coverslips, all steps were performed directly in nunc dishes. At the primary antibody stage, an ImmEdge™ Hydrophobic Barrier Pen (Vector Laboratories) was used to create a barrier around the edge of the cell culture area to minimise antibody volume use. During antibody incubations, nunc dishes were placed directly into humidified chambers. 15 μL Vectashield® was applied to the cells and a coverslip gently lowered down onto the cells.

The ratio of glial subtypes in the mixed glial population was determined by immunocytochemistry. Microglia were labelled with Iba1 and astrocytes with GFAP (Table 2.2). Controls lacking primary antibody were performed to confirm selective binding of antibodies (Appendix Figure A1).

Cells were imaged at 10x or 20x, as described in Section 2.6.4. For each experimental condition, three dishes from separate biological replicates were analysed. From each dish, two randomly selected, non-overlapping fields of view (FOVs) were acquired to ensure representative sampling across the culture surface. Cell boundaries of microglia and astrocytes were manually traced in FIJI ImageJ (Schindelin et al., 2012) using the Freehand Selection Tool and each traced cell was saved as a region of interest (ROI).

For each FOV, the following parameters were quantified for microglia and astrocytes:

- Cell number
- Total cell area (sum of all ROIs per cell type)
- Average area per cell (mean ROI area per cell type)
- Percentage area of FOV (total area of a cell type divided by total FOV area)
- Cell number ratios (microglia:astrocytes based on ROI counts)
- Area ratios (microglia:astrocytes based on summed ROI areas)

5.2.6 Pro-inflammatory Stimulation with a Cytokine Cocktail

Stimulation of Mixed Glia

Mixed glia were cultured until DIV21, or until astrocytic confluence. Glial culture medium, which contained 10% FBS, was replaced with the serum-free version. The following day, half of the flasks of mixed glia were stimulated with an inflammatory cytokine cocktail in fresh serum-free culture medium: 3 ng/mL IL-1α (AF-200-01A, PeproTech®), 0.5 mg/mL TNF-α (AF-300-01A, PeproTech®) and 400 ng/mL C1q (C1740, Sigma-Aldrich) as used by Liddelow et al. (2017). The media in the remaining flasks was replaced with fresh serum-free medium containing no cytokines (control). This cytokine combination was chosen because it has been shown to reliably induce a neurotoxic A1 astrocyte phenotype in mixed glial cultures (Liddelow et al., 2017), while also directly activating microglia and promoting bidirectional astrocyte–microglia inflammatory signalling (Section 5.1.3).

After 24 hours, the media was replaced with fresh serum-free glial culture medium (without cytokines) and incubated for 48 hours to enable ample EV production (Figure 5.6). Driving this culture into an inflammatory state aimed to generate pathologically relevant EVs and characterise their biophysical and molecular signatures.

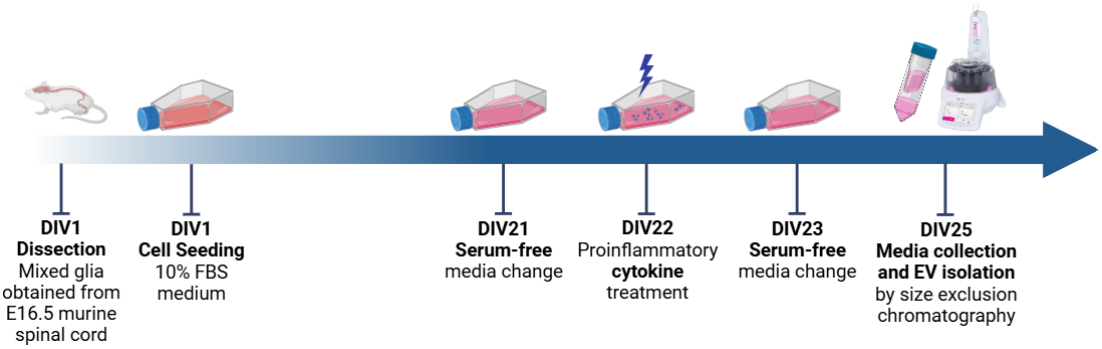


Figure 5.6. Mixed Glial Culture Timeline. Mixed glial cells were isolated from embryonic day 16.5 mouse spinal cords and seeded into T-25 flasks (designated as DIV1). On DIV21, or once cultures reached confluence, the glial culture medium was replaced with serum-free medium. After 24 hours, cells were either treated with a pro-inflammatory cytokine cocktail or maintained in fresh serum-free medium as a control. Following a further 24 hours, the treatment medium was removed and replaced with fresh serum-free medium. EVs were then allowed to accumulate in the medium over 48 hours, after which the media was collected for EV isolation. Images taken from BioRender™ and IZON Science Limited©.

Direct Stimulation of Sensory Neurones

To assess whether neuronal sensitisation was mediated specifically by glial-derived EVs rather than by soluble cytokines, the cytokine cocktail (at the same concentrations as above) was applied directly to DRG sensory neurones cultured in inverted chambers. After a 24-hour incubation, matching the conditions used for mixed glia or for sensory neurone incubation with glial-derived EVs (Section 5.2.12), neuronal responses were measured by calcium imaging.

5.2.7 Cell Lysate Collection

Once media was collected from the T-25s, mixed glial cultures were incubated with 1X trypsin-EDTA (T3924, Sigma) for five minutes at 37°C and 5% CO_2. Cells that remained attached were gently knocked off. Twice the volume of serum-free glial culture media was added to quench the trypsin activity.

The volume was collected and centrifuged at 210 x *g* for five minutes at RT to pellet cells and the supernatant discarded. The pellet was resuspended in 1 mL serum-free glial culture media, and a cell count performed (BioRad TC20®) with 0.4%

trypan blue solution (1:1 trypan blue:cell suspension, Gibco). The cell suspension was centrifuged again at 210 x *g* for five minutes at RT to re-pellet the cells and the supernatant removed. The cell pellet was washed with DPBS ($CaCl_2$/$MgCl_2$-free) and centrifuged for a further five minutes at 210 x *g* at RT. The supernatant was discarded and the cell lysates were snap frozen in liquid nitrogen, before storage at -80°C.

5.2.8 Extracellular Vesicle Isolation

Serum-free glial culture media containing EVs was collected from both control and cytokine-treated mixed glial cultures (pro-inflammatory stimulation in Section 5.2.6). Media was centrifuged at 530 x *g* for five minutes at RT to pellet cell debris and transferred to new falcon tubes. EVs were either immediately isolated or the media stored at 4°C for a maximum of three days prior to isolation.

Pooled culture media was transferred to a 10K molecular weight cut-off (MWCO) protein concentrator (Pierce™ Protein Concentrator polyethersulfone (PES), 88528 Thermo Fisher Scientific) for filtration and centrifuged at 3,600 x *g* at RT to a final volume of 500 μL. Extracellular vesicles were isolated using the Automatic Fraction Collector V2 (IZON Science Limited©), based on the principles of size exclusion chromatography (SEC). Gen 2 70 nm sepharose qEVoriginal columns (IZON Science Limited©) were used to maximise removal of Apolipoprotein B and other proteins, at the slight detriment to the yield of extracellular vesicles. DPBS ($CaCl_2$/$MgCl_2$-free) was used as the elution buffer, in accordance with the manufacturer's protocol to isolate small EVs <200 nm (and within the range considered to represent exosomes; Böing et al., 2014). SEC ensures minimal disturbance of vesicle size and content by avoiding ultracentifugation forces involved in alternative methodologies, thus preserving EV integrity and biological activity (Nordin et al., 2015).

Columns were washed and primed with DPBS ($CaCl_2$/$MgCl_2$-free) before the 500

μL sample was added to the top of the column. 2.5 mL buffer volume was eluted and discarded prior to fraction collection. Six 400 μL fractions were collected in Ultra High Recovery Microcentrifuge Tubes (Starlab), to minimise particle loss, and stored at -80°C until experimental use. Due to the molecular weight of protein, it is isolated in later fractions. To identify the protein elution factors, SDS-PAGE (sodium dodecyl sulfate-polyacrylamide gel electrophoresis) gels were used; 20 400 μL fractions were collected from control glial medium to ensure molecules of greater molecular weight, such as protein, were also isolated. Following isolation, columns were washed with 8.5 mL 0.5 M NaOH, then 17 mL DPBS ($CaCl_2$/$MgCl_2$-free) and used again for the next isolation or prepared for storage by flushing with 12 mL 0.05% (w/v) sodium azide, maintaining a volume in the top of the column. Columns were stored at RT.

In parallel, EV isolation was performed on cell-free media to generate a media control, as the isolation process itself may concentrate media components independently of vesicle content. Including this control is essential to account for any effects attributable to concentrated media rather than EVs.

5.2.9 Nanoparticle Tracking Analysis

Following EV isolation, NTA was used to quantify the size distribution and concentration of an EV sample. NTA was performed using the ZetaView® PMX 110 (Particle Metrix, Meerbusch, Germany). Pooled EV fractions (Fr) 1-3 were diluted 1:100 in DPBS ($CaCl_2$/$MgCl_2$-free).

The Brownian motion of EVs was tracked by laser light scattering over time to calculate particle size using the Stokes-Einstein equation to determine the translational diffusion constant. The parameters for all NTA measurements were as follows: sensitivity 85, shutter value 70 (corresponding to an exposure time of 15 ms) with a frame rate of 30 frames per second, set to high accuracy. Each sample was quantified for three cycles per 'experiment' and two independent runs performed

and averaged.

5.2.10 SDS-PAGE Gels to Determine Protein Elution Fractions

Different cell cultures produce variations in EVs and proteins by molecular weight and content, therefore the fraction content that results from SEC may also differ. SDS-PAGE gels were used to determine the fractions containing protein.

1.5 mm gel plates were washed with distilled water and then 70% ethanol. The gel casting stand was assembled and a 12% (w/v) acrylamide resolving gel was prepared (Table 5.2), adding ammonium persulfate (APS) and tetramethylethylenediamine (TEMED) to polymerise the gel just before pouring ($\sim$7 mL per mini gel). A layer of isopropanol (200 μL) was applied to the top of the gel to prevent any gel shrinkage and to create a level gel surface without bubbles. Following gel polymerisation, the isopropanol layer was rinsed off using distilled water. Any excess water was gently wicked away.

A 5% (w/v) acrylamide stacking gel (Table 5.2) was then prepared, adding APS and TEMED last, as previously described. 2 mL of stacking gel was added along the top of the resolving gel (up to the top of the plate) and the 1.5 mm combs inserted into the polymerising gel. Following polymerisation, the comb was gently removed from the gel and the wells rinsed with 1X Tris-Glycine-SDS solution (TGS) three times. Gels could be stored in their plates, with the comb in, at 4°C for up to a week, wrapped in saturated paper towel and then cling film.

Fresh 1X TGS was prepared from 10X (10X TGS: 0.25 M Tris, 1.92 M glycine and 1.0% (w/v) SDS), by diluting in dH_2O, and chilled. Samples were thawed on ice, before adding gel application buffer (GAB: 0.15 M Tris, 8 M urea, 2.5% (w/v) SDS, 20% (v/v) glycerol, 10% (v/v) 2-mercaptoethanol, 3% (w/v) DTT and 0.1% (w/v) bromophenol blue in dH_2O) at 1:5 (sample:GAB) and briefly vortexed. These samples were placed in a heat block at 90°C for 10 minutes and left to cool. Samples were spun at high speed for five minutes at RT.

Table 5.2. Composition of Resolving and Stacking Gels for SDS-PAGE. Volumes of reagents to produce four mini SDS-PAGE gels.

Reagent	12% acrylamide resolving gel	5% acrylamide stacking gel
30% (w/v) acrylamide solution	14 mL	2.55 mL
0.5 M Tris-HCl, pH 6.8	-	1.95 mL
1.5 M Tris-HCl, pH 8.8	8.75 mL	-
10% (w/v) SDS	350 μL	150 μL
10% (w/v) APS	175 μL	150 μL
TEMED	17.5 μL	15 μL
Distilled water	11.71 mL	10.2 mL
Total	**35 mL**	**15 mL**

Gels were inserted into the running apparatus (Mini-PROTEAN® 3, Bio-Rad) and the central chambers filled with chilled 1X TGS to check for leaks. The outer chamber was filled to 3/4 full and 50 μL of sample added per well. 10 μL Precision Plus Protein Dual Color Standard (BioRad) was added to one well per gel for molecular weight estimation. Any empty wells were loaded with 10 μL of GAB to prevent band distortion.

The power-pack was set to 125 V and run until the bottom bands neared the bottom of the gels (for $\sim$1.5 hours). Buffer was removed from the running apparatus and the gels gently removed. The stacking gel was carefully prised away, and the resolving gels were extracted. For protein fraction determination, proceed with the following steps; for Western blotting to identify EV markers, refer to the subsequent section (Section 5.2.11) .

Gels were placed on a rocker in Coomassie (50% (v/v) methanol, 20% (v/v) glacial acetic acid, 1.12% (w/v) Coomassie Brilliant Blue R-250 in dH_2O (Sigma)) for one hour at RT. Coomassie was removed and replaced with destain (10% (v/v) methanol, 10% (v/v) glacial acetic acid in dH_2O) overnight or until the bands were clearly visible in contrast to the rest of the gel, replacing the destain two-three times. Gels were imaged on a light-box qualitatively.

5.2.11 Western Blotting to Identify Extracellular Vesicle Markers

For EV markers, following completion of SDS-PAGE, the gel was transferred onto a nitrocellulose membrane (Amersham™ Protran® Western blotting membrane, 0.45 μm pore) using a standard wet-transfer system. Briefly, the gel was sandwiched between filter paper and the membrane, placed in a transfer tank containing chilled 1X blotting buffer (25 mM Tris, 192 mM glycine, 20% (v/v) methanol), and transferred for two hours at 80 V. Membranes were washed three times in Tris-buffered saline with 0.05% Tween-20 (TBS-T; 20 mM Tris, 150 mM NaCl, pH 7.5), then blocked in 5% milk-TBS-T (Marvel milk powder) for one hour at RT. Membranes were subsequently incubated with primary antibodies diluted in 5% milk-TBS-T overnight at 4°C (Table 5.3), washed again three times in TBS-T, and incubated with the appropriate secondary antibody in 5% milk-TBS-T for one hour.

Table 5.3. Antibodies Used for Western Blotting. All antibodies were diluted in 5% milk-TBS-T. Primary antibodies are indicated by a 1 and secondary antibodies by a 2.

Antibody	Dilution	Molecular Weight	1° or 2°	Species	Provider and Reference Code
anti-ALIX	1:1000	95 kDa	1	Rabbit	Abcam (ab186429)
anti-CD63	1:1000	25-35 kDa	1	Rabbit	Proteintech (25682-1-AP)
anti-CNX	1:10000	90 kDa	1	Goat	SICGEN (AB3747-200)
anti-FLOT-1	1:1000	47 kDa	1	Mouse	BDBiosciences (AB398139)
anti-mouse HRP	1:3000	-	2	Rabbit	Dako (PO260)
anti-rabbit HRP	1:3000	-	2	Swine	Dako (PO399)
anti-goat HRP	1:5000	-	2	Rabbit	Sigma (A5420)

The membrane was washed three times in TBS-T, incubated in enhanced chemiluminescence (ECL) solution for 30 seconds, and protected from light. Protein signals were detected by exposing the membrane to Amersham Hyperfilm® ECL

film for an appropriate duration. Multiple exposure times were tested to obtain the optimal image. Films were subsequently developed in Ilford PQ Universal developer (Ilford Photos, UK) until bands became visible, rinsed briefly in water, and fixed in Ilford Hypam fixer (Ilford Photos, UK).

5.2.12 Application of Glial-Derived Extracellular Vesicles to DRG Neuronal Cultures

EV fractions 1-3 were pooled and Pierce™ 10K MWCO Protein Concentrators PES (Thermo Fisher Scientific) were used to concentrate to 100 μL (12,000 x *g*) to reduce the DPBS volume administered to cells. $\sim$1.25 x 10^8 EVs in DRG complete media were added per well on DIV1. Brightfield images were acquired over a 24-hour period to monitor axon growth. Following this incubation, calcium imaging was performed to assess neuronal responsiveness (Figure 5.7).

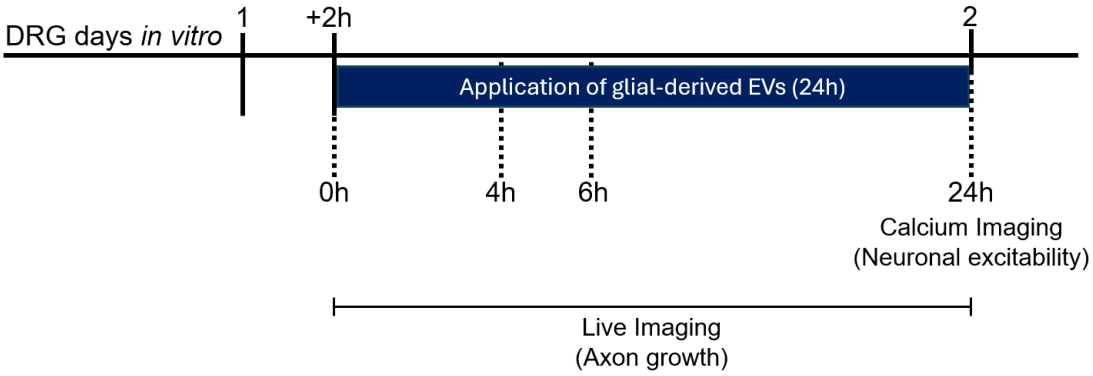


Figure 5.7. Timeline of Extracellular Vesicle Addition to DRG Sensory Neurone Cultures. Embryonic day E16.5 DRG sensory neurones were isolated and seeded in dissociated cultures at DIV1. Two hours after seeding, EVs derived from mixed glial cultures were applied to DRG cultures for 24 hours before calcium imaging to assess neuronal excitability. Live imaging of axonal outgrowth was performed at 0 hours, 4 hours, 6 hours and 24 hours following EV application.

5.2.13 Calcium Imaging in Microfluidic Chambers

Calcium imaging was performed according to the protocol described in Section 2.4. Dissociated cultures were imaged every 500 ms for three minutes. Fresh IB was applied to dissociated cultures prior to imaging and stimuli added directly to the buffer. The first stimulation was applied 30 seconds into recording with 30.5 μL

of capsaicin (final concentration 200 nM). The capsaicin response was recorded for 2.5 minutes before the IB was removed and replaced with fresh IB. After a 10-minute break, the same well was recorded from again using the same format of acquisition but with a stimulation of 24.8 μL KCl (final concentration 25 mM; Figure 5.8).

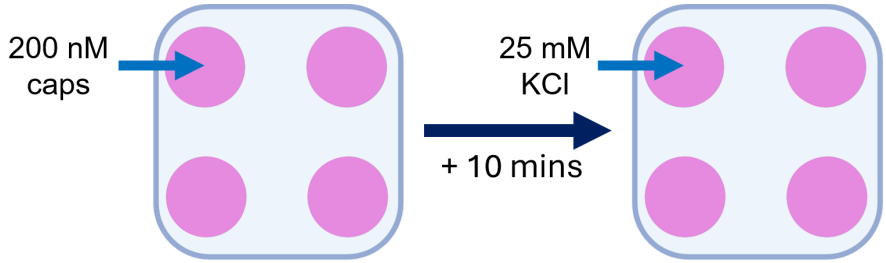


Figure 5.8. Calcium Imaging Stimulation Protocol for Inverted Chambers. Imaging buffer was replaced with fresh imaging buffer prior to beginning imaging. Cells were stimulated with 30.5 μL of capsaicin (final concentration 200 nM) and recorded for three minutes. 10 minutes after imaging ceased, the same well was stimulated with 24.8 μL KCl (final concentration 25 mM). Caps - capsaicin.

5.2.14 miRNA Power Inhibitors

A literature search using the terms 'glia', 'extracellular vesicles' and 'sequencing' was performed on PubMed to identify previous miRNA sequencing of pro-inflammatory microglia- and/or astrocyte-derived extracellular vesicle content from primary rodent glial culture. Two papers fit the criteria of using primary glial cultures and identifying miRNA transcripts encapsulated within the EVs (Chaudhuri et al., 2018; Prada et al., 2018). It is important to note that both papers utilised primary cells taken from Sprague-Dawley rats, with Prada et al. (2018), culturing glial cells from postnatal day two and Chaudhuri et al. (2018) culturing cells from embryonic rats. The cells cultured in these investigations are also embryonic, as early life cultures were ideal for comparison.

Although existing literature reported fold changes between treatment conditions, candidate selection in this study was based on any identified dysregulated miRNAs, irrespective of magnitude. Three target miRNA sequences were selected from the published datasets of EVs derived from primary microglia and astrocytes

under pro-inflammatory conditions for functional testing based on known roles and downstream targets (miR-142a-3p, miR-146a-5p, and miR-181a-5p).

miRCURY LNA miRNA Power Inhibitors (Qiagen), complementary to the mature miRNA sequences, were used to block miRNA activity by sequestering their target miRNA into highly stable heteroduplexes, preventing miRNA hybridisation. These inhibitors are designed for high affinity and nuclease resistance, and their chemical modifications enable efficient cellular uptake without the need for transfection reagents, minimising potential confounds. All selected inhibitors were compatible with murine (mmu) miRNA sequences, regardless of whether the human (hsa) variant was ordered (Appendix Table A4).

A miRCURY LNA miRNA Power Inhibitor Negative Control A (Qiagen) was used to confirm that observed phenotypes were due to specific antisense inhibition. This control oligonucleotide has a matching phosphorothioate backbone and less than 70% homology with any known cellular RNAs. Power inhibitors were reconstituted to 25 μM in DNase-free HyClone water, aliquoted, and stored at -20°C to minimise freeze-thaw cycles.

EVs were isolated from cytokine-treated or control mixed glial cultures and concentrated to a final volume of 100 μL, respectively. For each treatment condition, $\sim$1.7 x 10^8 EVs were mixed with either LNA Power Inhibitors or Negative Control A (final concentration: 100 nM; Lucci et al., 2020), and brought up to 300 μL with DRG complete media. This mixture was then distributed across wells, with 100 μL (containing $\sim$4.2 x 10^7 EVs) added per well of dissociated DRG neuronal cultures (three wells per treatment condition) a few hours after seeding (DIV1, Figure 5.9).

Prior to the main experiments, a pilot study was conducted to evaluate potential cytotoxic effects of the inhibitors and to confirm that the selected concentrations did not impact baseline excitability. Power Inhibitors were applied individually (100

nM) or in combination (33.33 nM each; total 100 nM) to dissociated DRG cultures. Negative Control A (100 nM) and DNAse-free HyClone water (vehicle control) were included for comparison. These preliminary tests indicated that the selected inhibitor concentrations were well tolerated under the culture conditions used and did not alter baseline excitability (Appendix Figure A2).

Around 20 hours post-inhibitor addition, calcium imaging was performed on the cells (Section 2.4 for protocol). 200 nM capsaicin was applied directly to the cells after 30 seconds (30.5 μL 850 nM added to 100 μL IB present on cells). Cells were imaged every 500 ms for a period of eight minutes.

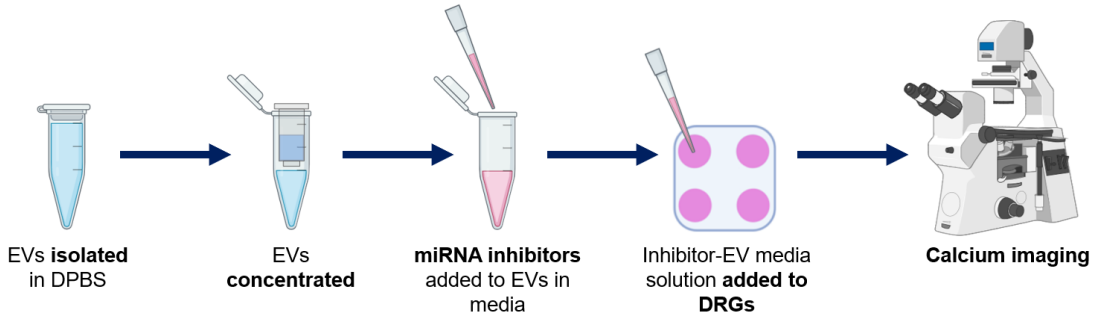


Figure 5.9. Protocol for miRNA Inhibitor-EV Addition to DRG Cultures. Extracellular vesicles were isolated from mixed glial cultures and concentrated to 100 μL. EVs were diluted in DRG complete media and miRNA LNA power inhibitors added to the solution (final concentration of 100 nM). The inhibitor-EV solution was then added to DRGs in inverted chambers, a few hours after seeding. 24 hours later, calcium imaging was performed, stimulating with 200 nM capsaicin. Created using BioRender™.

5.2.15 Pathway Enrichment Analysis

After observing a functional effect of miR-146a-5p, potential downstream targets that could be involved in the glial EV-induced miR-146a-5p-mediated neuronal sensitisation were investigated using pathway enrichment analyses.

Putative gene ontology targets of miR-146a-5p were predicted using miRDB (mirdb.org/ontology.html) for *Mus musculus* and *Homo sapien*. Gene IDs identified for *Mus musculus* were entered into the PANTHER Classification System (Version 19.0, pantherdb.org/webservices/go/overrep.jsp) and a statistical overrepresentation test

performed, selecting PANTHER GO-Slim Biological Processes as the annotation set and Fisher's exact as the test type. Only results with a False Discovery Rate (FDR) $p < 0.05$ were included in further analyses.

5.2.16 Statistical Analysis

Although multiple miRNA Power Inhibitors were tested simultaneously, data were analysed by comparing each miRNA inhibitor-treated group independently with the negative control. Comparisons between different miRNA inhibitor treatments were not performed, as the experimental aim was to assess the effect of individual miRNA inhibition relative to baseline, rather than to compare effects between miRNAs.

Statistical analyses were conducted according to the methods outlined in Chapter 2 (Section 2.7). For the experiments in this chapter, *t*-tests were used for comparisons between two groups. For comparisons involving three or more groups, one-way ANOVA with Tukey's multiple comparisons test was applied to normally distributed data, as determined by the Shapiro-Wilk normality test. Non-normally distributed data were analysed using a Kruskal-Wallis test followed by Dunn's multiple comparisons test. A p-value < 0.05 was considered statistically significant.

5.3 Results

5.3.1 Glial Cell Populations Are Heterogeneous

Mixed glial cultures derived from E16.5 murine spinal cord tissue exhibited diverse cell morphologies and marker expression profiles by DIV21. Brightfield and immunocytochemical analyses revealed distinct astrocytic and microglial populations under baseline and cytokine-treated conditions, with additional observations from DRG co-cultures.

Brightfield Imaging Reveals Glial Morphological Diversity

The general health, morphology, and confluency of glial cultures were assessed qualitatively by visual inspection using brightfield microscopy to ensure comparable cell density, morphology, and absence of overt stress or cell death prior to EV isolation. Mixed glial cultures contained astrocytes, microglia, and likely OPCs, consistent with the expected cellular diversity of spinal cord-derived preparations. While brightfield microscopy provides a useful overview of cell density and morphology, it does not allow definitive identification of glial subtypes, as many features overlap and marker expression is not visible. Therefore, cell type assignments were based on characteristic morphologies reported in the literature, with appropriate caveats.

Astrocytes typically formed an adherent layer of flattened cells, with rounded microglia semi-attached to the astrocytic surface (Figure 5.10B), consistent with previous descriptions by Park, Yu, and Dong (2024). Microglial density remained low early in culture, so the duration was extended to 21 days to promote proliferation and increase EV yield.

The variation in cell populations within a single culture is illustrated across the four panels of Figure 5.10 and reflects heterogeneity reported by other studies (Liu et al., 2015; Xu, Gou, and Dong, 2010). Within the same culture, ramified and amoeboid microglia coexisted, highlighting the morphological diversity of microglial activation states. In Figure 5.10A, OPCs are visible with their characteristic rounded somata and long, thin processes (Fan et al., 2014; Kim et al., 2024). Figure 5.10B shows rounded microglia growing atop a confluent astrocyte layer (Park, Yu, and Dong, 2024), while Figure 5.10C depicts a similar arrangement with reduced astrocyte confluency. Figure 5.10D demonstrates a more mixed population, with ramified microglia interspersed among astrocytes and OPCs.

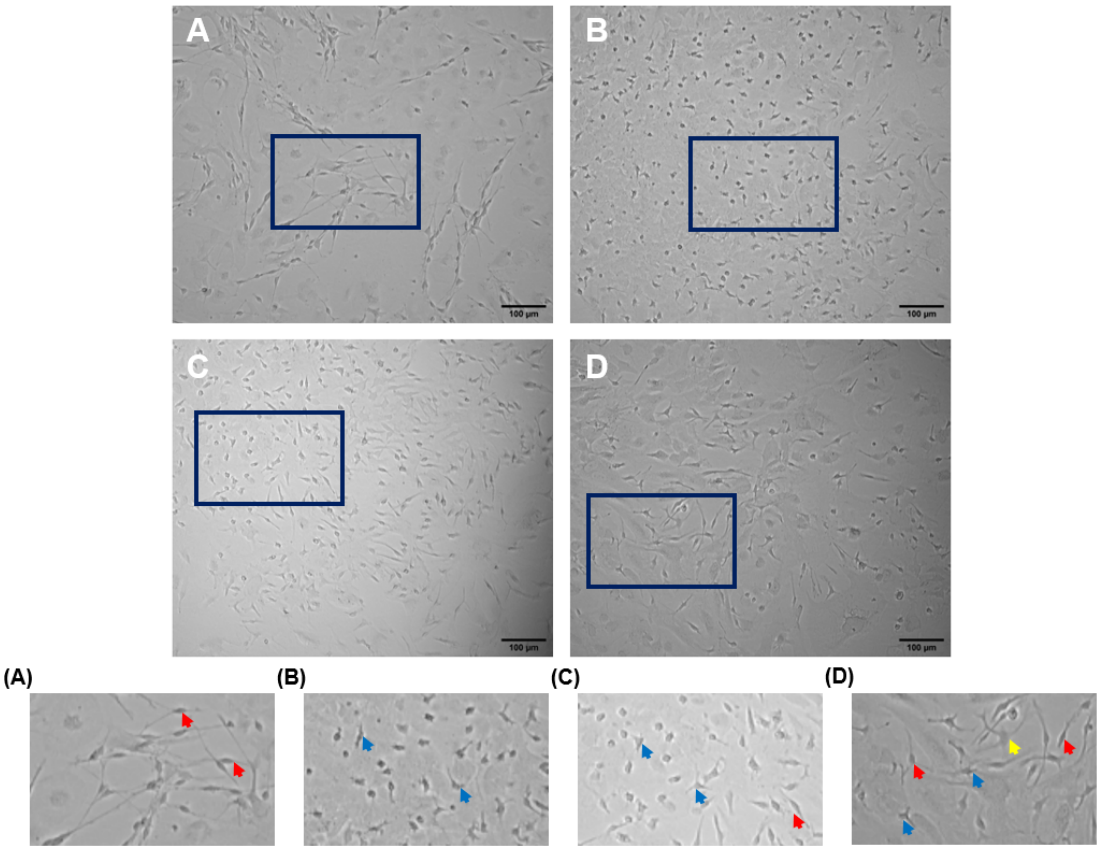


Figure 5.10. Different Glial Cell Growth Patterns Coexist in the Same Culture. Brightfield images of DIV21 mixed glia cultured in 10% FBS. Mixed glial cells were isolated from E16.5 mouse spinal cords, seeded into T-25 flasks (designated as DIV1), and cultured in media supplemented with 10% FBS until DIV21. Microglia semi-adhere to a layer of astrocytes. Heterogeneity within the cell population of a single culture is evident across the four panels, with representative regions enlarged and displayed below. **A -** Oligodendrocyte progenitor cells (OPCs) with rounded cell bodies and long, thin processes. **B -** Rounded microglia growing atop a layer of confluent astrocytes. **C -** A similar pattern to (B), but with reduced astrocyte confluency. **D -** A heterogeneous population featuring ramified microglia over astrocytes and interspersed OPCs.
Arrows indicate cell types: red - OPCs; blue - microglia; yellow - astrocytes. Brightfield images taken at 10x magnification, scale bar 100 μm.

Determination of Glial Cell Population Ratios via Immunocytochemistry

The ratio of microglia to astrocytes in mixed glial cultures was quantified by immunocytochemistry using Iba1 and GFAP antibodies, which label microglia and astrocytes, respectively (Figure 5.11). Attempts to identify OPCs using an Olig2 antibody were unsuccessful, likely due to antibody incompatibility or low antigen expression under the culture conditions. Consequently, OPCs were identified morphologically in brightfield images but could not be confirmed by immunostaining.

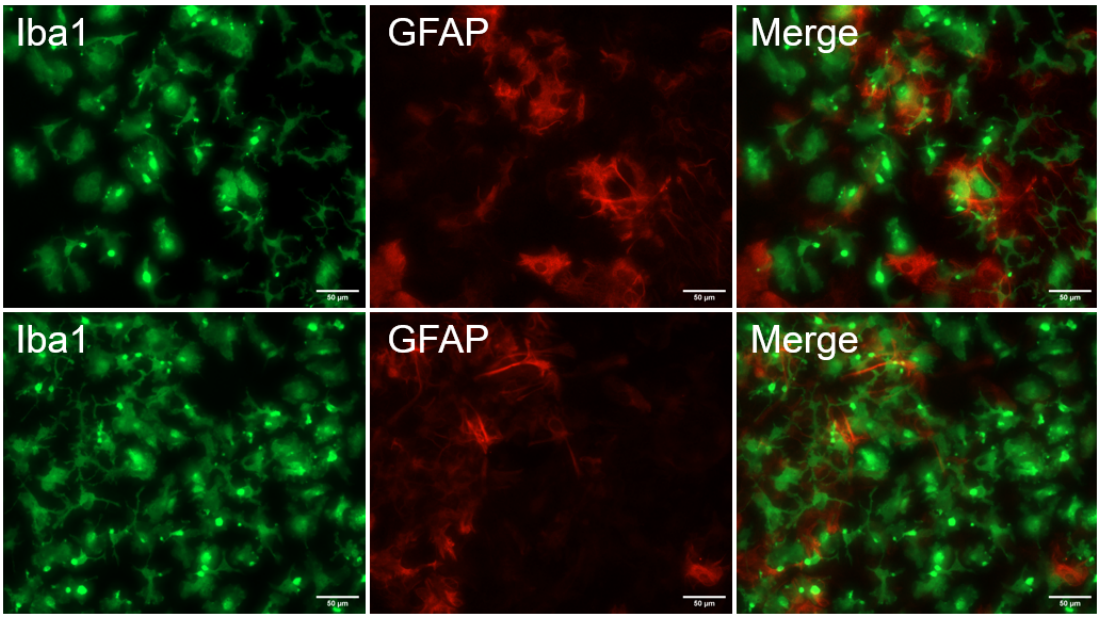


Figure 5.11. Immunocytochemistry of Mixed Glial Cultures Stained for Astrocytes and Microglia. Two representative examples of mixed glial cultures stained with antibodies against Iba1 (green, microglia marker, first column) and GFAP (red, astrocyte marker, second column); merged images are shown in the third column. Iba1-positive cells exhibit smaller, rounded morphologies with occasional fine processes, characteristic of microglia. GFAP-positive cells appear larger and stellate with elongated, filamentous processes, consistent with astrocytic morphology. Merged images demonstrate the coexistence of both astrocytes and microglia within the same culture. 20x images; scale bar 50 μm.

Quantification of glial cells in mixed cultures revealed that there were significantly more microglia (Iba1$^+$ cells) than astrocytes (GFAP$^+$ cells) (p = 0.0097, t-test; Figure 5.12A), with an average ratio of $\sim$3:1. The ratio of total stained area was 1.5:1, showing that microglia occupied a greater proportion of the field of view than astrocytes due to their higher abundance (Figure 5.12B). In contrast, when normalised to the average area per cell, the immunoreactive area of Iba1 signal was lower (0.6:1), indicating that astrocytes contributed a larger individual immunoreactive area (Figure 5.12C). Consequently, the percentage of the field of view occupied by each cell type reflected the higher abundance of microglia, with microglia contributing a greater proportion of the field than astrocytes due to their relative numbers, rather than differences in individual cell size (Figure 5.12D).

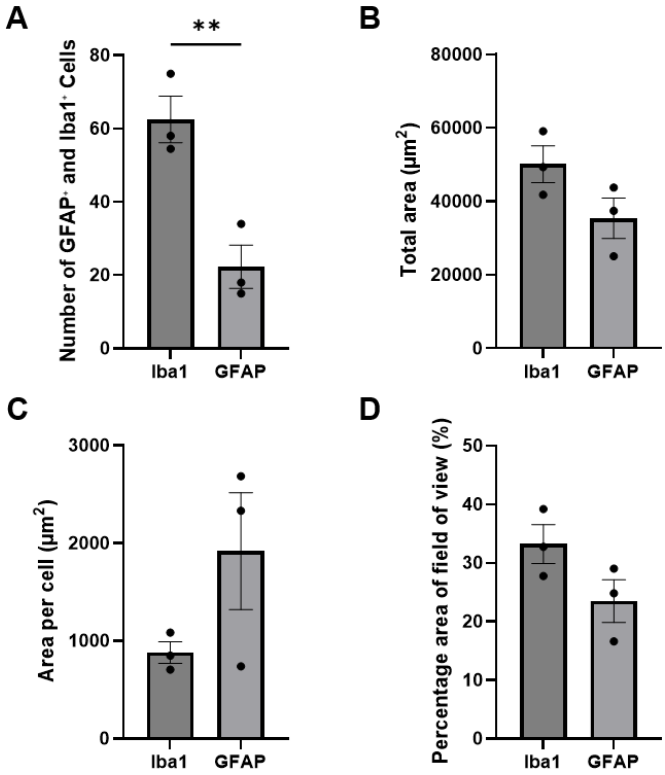


Figure 5.12. Quantification of GFAP⁺ and Iba1⁺ Cells. A - There were significantly more microglia (Iba1⁺ cells) than astrocytes (GFAP⁺ cells) in mixed glial cultures ($p = 0.0097$, *t*-test). **B -** Microglia occupied a greater total area than astrocytes, although this was not statistically significant. **C -** Astrocytes exhibited a larger average area per cell compared to microglia, but this was not significant. **D -** Microglia covered a greater percentage of the field of view than astrocytes, but this was not significant.
$N = 3$ biological replicates, $n = 2$ images per experiment; 36-107 Iba1⁺ cells per image; 11-35 GFAP⁺ cells per image. Data displayed as biological replicates; mean ± SEM. $p < 0.05$ was considered statistically significant.

Cytokine Stimulation Modified Glial Morphology

Upon pro-inflammatory stimulation with a cytokine cocktail (TNFα, IL-1β, C1q; Liddelow et al., 2017), microglia exhibited a more amoeboid morphology (Figure 5.13C-D) compared with control cultures (Figure 5.13A-B). However, changes in astrocyte morphology could not be reliably assessed by brightfield imaging.

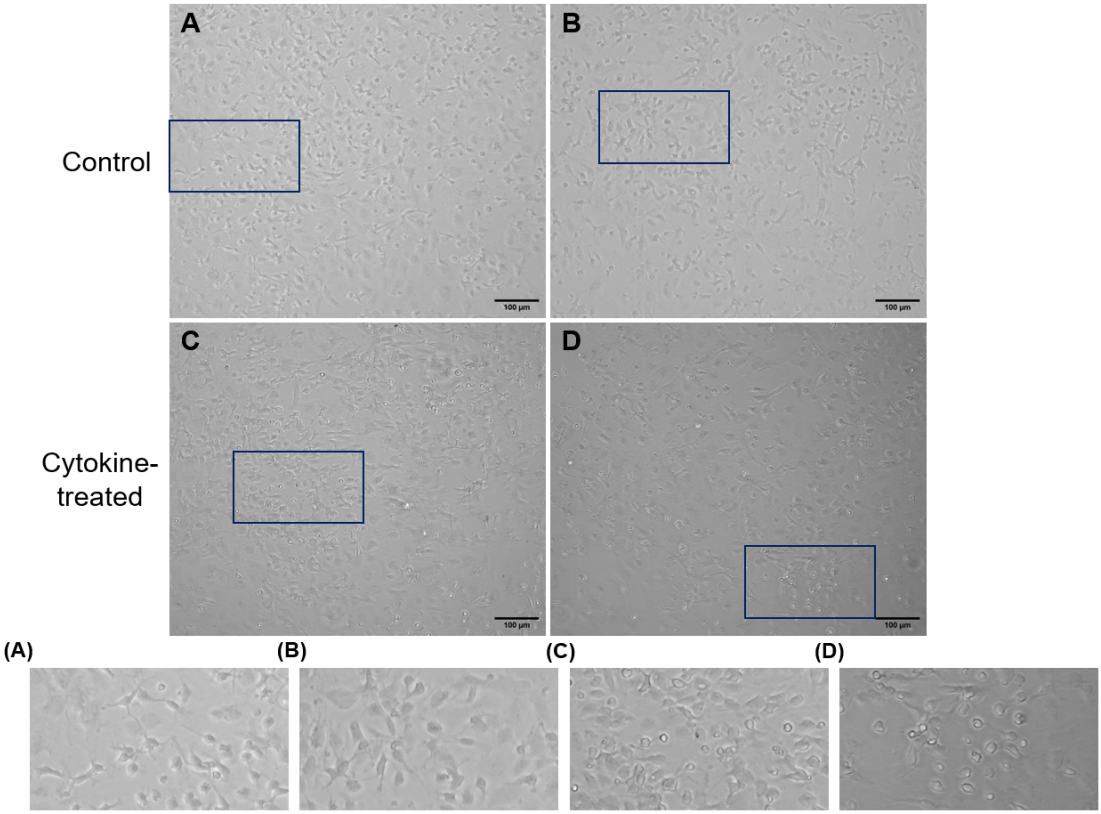


Figure 5.13. Morphological Comparison of Control versus Cytokine-Treated Mixed Glial Cultures. Representative brightfield microscopy images of mixed glial cultures taken 24 hours after cytokine treatment or in controls (media change only). The four panels have representative regions enlarged and displayed below. **A-B -** Representative images of control mixed glial cultures. Homeostatic microglia were more ramified, with branching processes. **C-D** Representative images of cytokine cocktail-treated mixed glial cultures. Activated microglia were amoeboid and had more retracted processes.
Images taken at 10x magnification; scale bar 100 μm.

Mixed Glia-DRG Co-Cultures

On DIV6 of DRG culture, brightfield images were captured to document axon-glia interactions (Figure 5.14). Co-cultures were immunolabelled with DAPI/βIII tubulin/Iba1 or DAPI/βIII tubulin/GFAP to distinguish neuronal and glial populations (Figure 5.15).

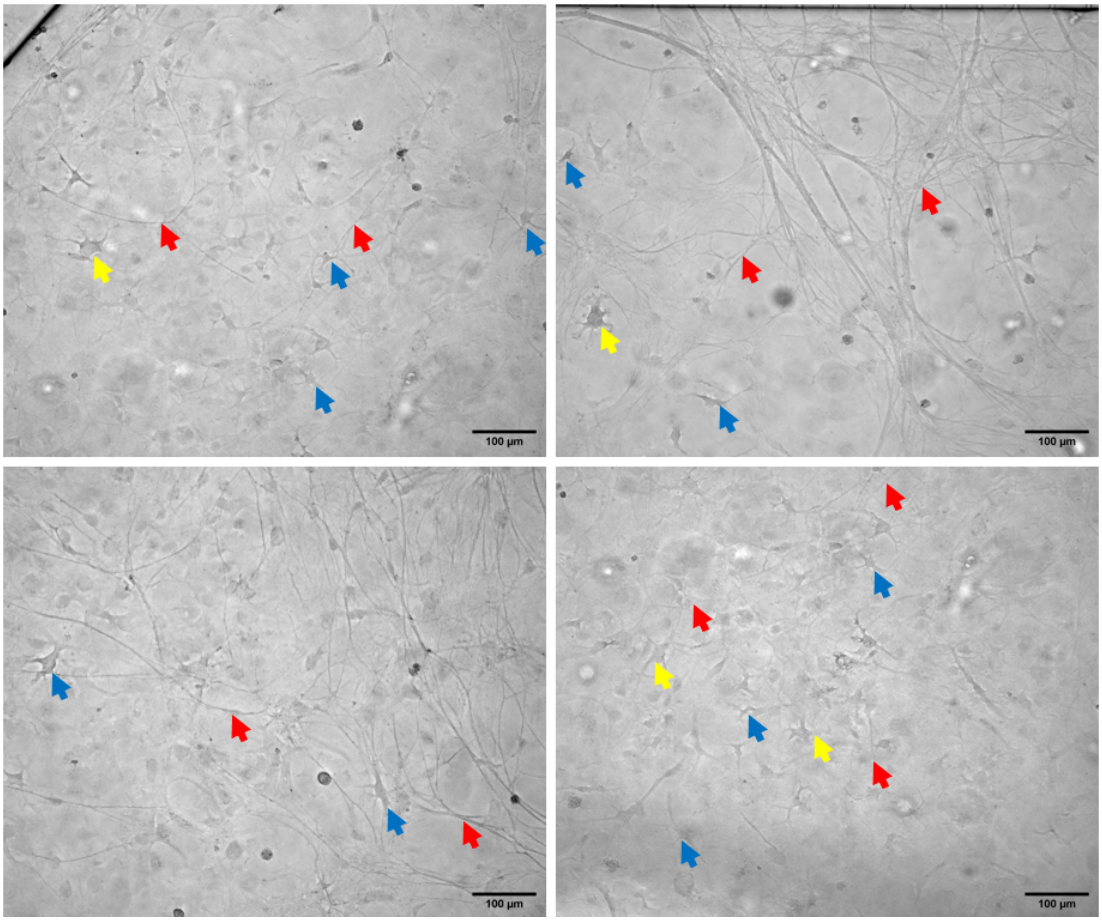


Figure 5.14. Representative Brightfield Images of Mixed Glia-DRG Co-Cultures. Mixed glia were cultured in compartmentalised microfluidic chambers until ∼DIV21 when DRG sensory neurones were seeded in the other compartment of the chamber. Axons projected from the DRG compartment into the glial region, traversing and overlaying glial cells rather than navigating around them (DIV6 DRG culture). Arrows indicate: axons (red), microglia (blue), and astrocytes (yellow). 10x images; scale bar 100 μm.

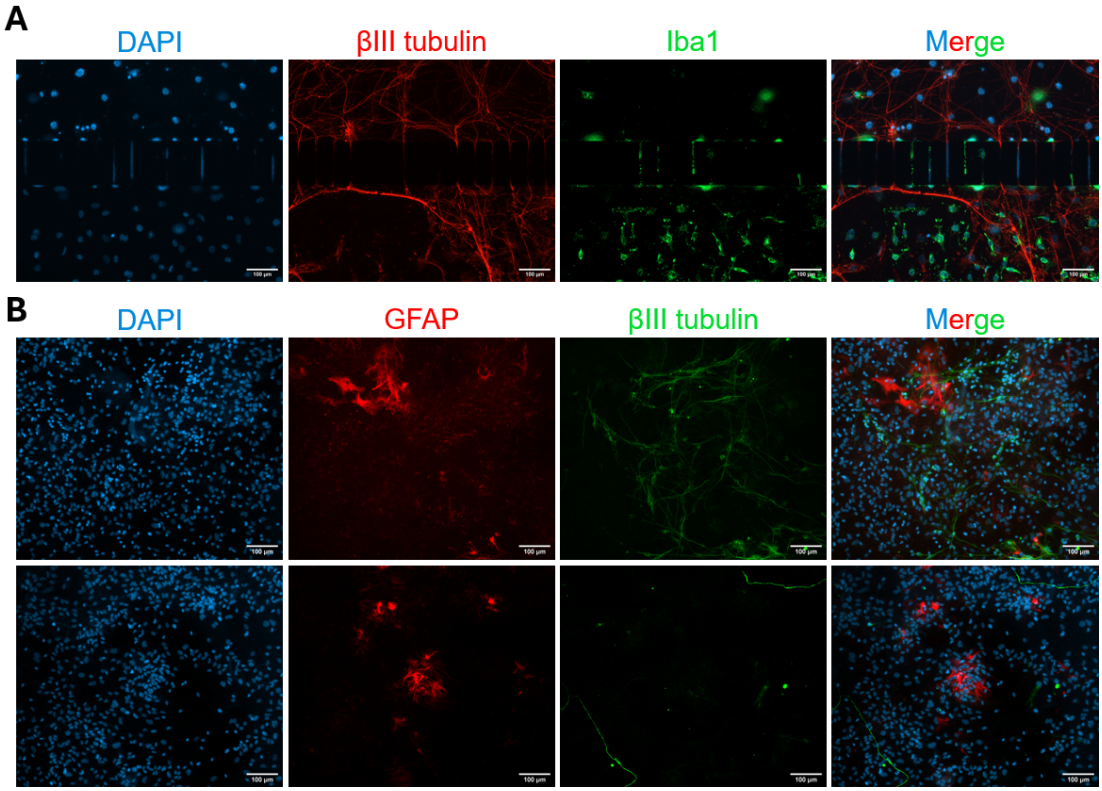


Figure 5.15. Immunocytochemistry of Mixed Glia-DRG Co-Cultures. Mixed glia were cultured in compartmentalised microfluidic chambers until ∼DIV21 when DRG sensory neurones were seeded in the other compartment of the chamber. DAPI (blue) identifies cell somata. **A -** βIII tubulin (red) indicates the cytoskeleton of cells of neuronal origin. Iba1 (green) marks microglia, some of which migrated to the DRG compartment, despite regular media changes. **B -** GFAP (red) shows astrocytes and βIII tubulin (green) marks neurones. 10x images; scale bar 100 μm.

5.3.2 Determination of Protein Fractions Following Size Exclusion Chromatography

Coomassie-stained SDS-PAGE gels were used to assess protein elution across size exclusion chromatography fractions. Media was collected from spinal cord-derived mixed glial cells, concentrated to 500 μL, and isolated into 20 fractions.

The first seven fractions contained no detectable free protein, as indicated by the absence of Coomassie staining (Figure 5.16); fractions 1-3 were designated as EV-rich, according to the isolator manufacturer (IZON Science Limited©) and NTA (Section 5.3.3), and therefore were used in subsequent functional experiments. Protein elution began at fraction 8, with substantial protein content observed in

fractions 12-18.

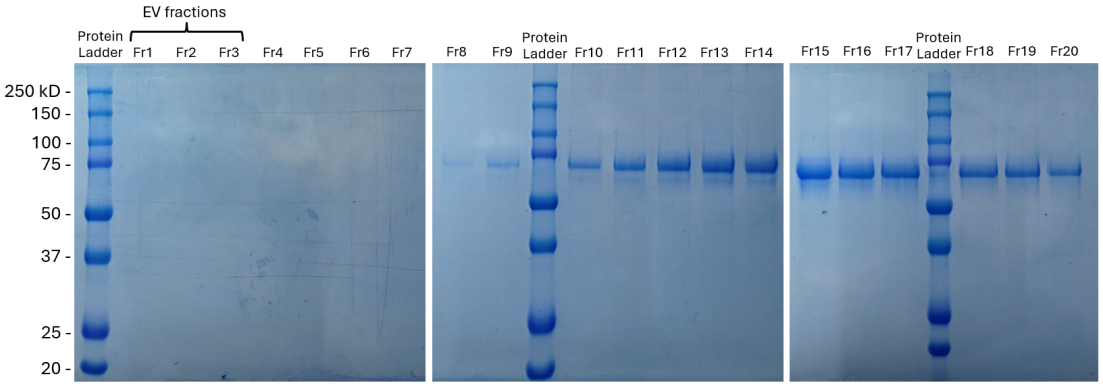


Figure 5.16. SDS-PAGE Gels of Fractions Isolated by Size Exclusion Chromatography from Mixed Glia Cell Culture Medium. Fractions 1 to 20 were collected, and 40 μL of each was mixed with 10 μL of gel application buffer. Protein content was assessed by Coomassie staining following SDS-PAGE. No visible protein was detected in early fractions (Fr1-7); protein elution began at Fr8, with the highest protein levels observed in Fr12-18.

5.3.3 Extracellular Vesicle Concentrations Determined by Nanoparticle Tracking Analysis

Following EV isolation, NTA was used to quantify the size distribution and concentration of EVs. The majority of the isolated EVs were <200 nm, consistent with SEC methods (Böing et al., 2014). Control EV samples (EV CTL) consistently exhibited higher particle concentrations than the cytokine-treated group (CytoG EVs) across much of the size distribution, with the most pronounced differences observed in the smaller size ranges where EVs are typically most abundant (Figure 5.17).

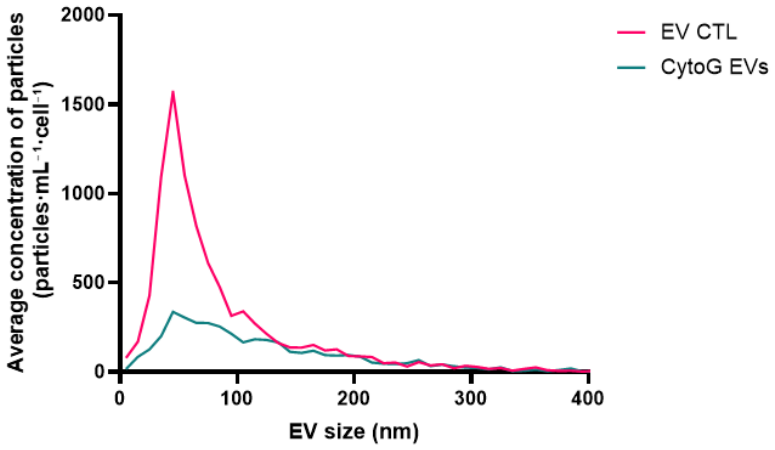


Figure 5.17. Average Size Distribution of Particles Normalised to Cell Count. EVs were isolated from mixed glia treated with a pro-inflammatory cytokine cocktail (CytoG EV) or from untreated control glia (EV CTL). Fractions 1-3 from each EV isolation were pooled, diluted 1:100 in DPBS, and the particle count within size bins was measured by NTA. EV CTL samples possessed a greater EV concentration than CytoG EV samples.
N = 5 biological replicates.

5.3.4 EV Markers Detected by Western Blot

Western blot analysis of EV-enriched fractions (Fr1-3) revealed robust detection of established EV markers ALG-2-interacting protein X (ALIX) and flotillin-1 (FLOT-1), alongside a substantial reduction in intracellular contaminants such as calnexin (CNX), in line with MISEV guidelines (Welsh et al., 2024).

FLOT-1 (∼47 kDa), a membrane-associated protein commonly enriched in EVs, was detectable at very low levels in individual fractions 1-3 but clearly enriched in the concentrated pool of Fr1-3. It was also present in the cell lysate but absent from the flow-through, indicating effective EV retention by the concentrator columns (Figure 5.18A). ALIX (∼95 kDa), an ESCRT (endosomal sorting complexes required for transport)-associated protein, was also clearly present in the concentrated EVs but not in the flow-through (Figure 5.18B), further confirming vesicle enrichment and isolation from the remaining media components. Two species of ALIX were identified in the cell lysate: the expected full-length protein at ∼95 kDa and an additional lower molecular weight band migrating just above 75 kDa. In contrast, only the full-length form of ALIX was detected in concentrated EV preparations. Both

FLOT-1 and ALIX fall within group 2 of MISEV-recommended EV markers: cytosolic proteins in EVs, specifically group 2a, denoting proteins with lipid or membrane protein-binding ability (Welsh et al., 2024).

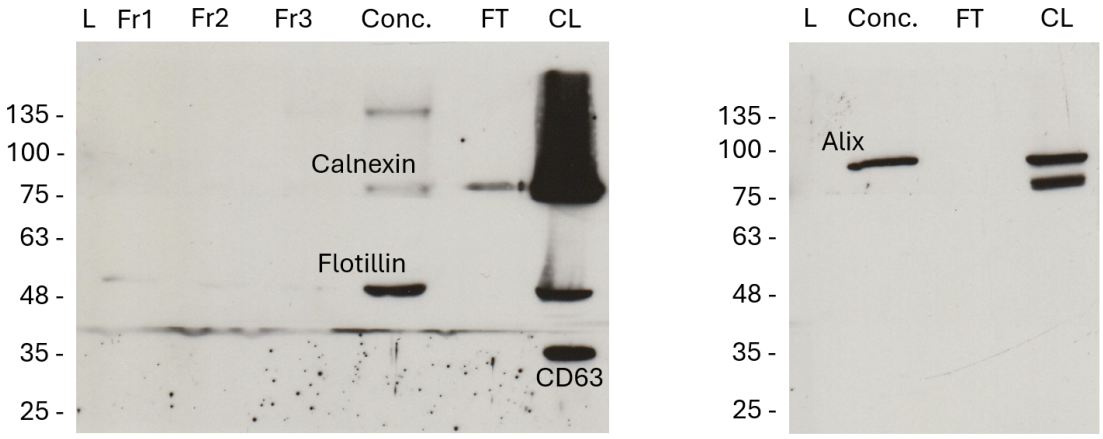


Figure 5.18. Western Blot Analysis of EV Markers Across Fractions from Size Exclusion Chromatography, Concentrated Pooled Fractions, Flow-Through, and Whole-Cell Lysate. A - FLOT-1 (∼47 kDa) was detected at very low levels in individual fractions and enriched in the concentrated EV sample. It was also present in the cell lysate but absent from the flow-through. CNX (∼90 kDa) was abundant in the cell lysate and more prominent in the flow-through than in the concentrated EV sample. CD63 (∼25-35 kDa) was not clearly detected in EV fractions but was observed in the cell lysate. **B -** Western blot of the same concentrated EV sample and flow-through using an anti-ALIX antibody. A clear ALIX band was observed in the EV sample but was absent in the flow-through. FT - flow-through, L - ladder, Fr - fraction, CL - cell lysate, Conc. - concentrated EV sample.

CD63 (∼25-35 kDa), a classical EV tetraspanin from group 1 (transmembrane or GPI-anchored proteins associated with plasma membrane and/or endosomes - specifically group 1a, multi-pass transmembrane proteins), was not detectable in the EV fractions - a diffuse, dot-like signal was observed around ∼35 kDa and below - but was clearly present as a discrete band in the cell lysate (Figure 5.18A). Finally, CNX (∼90 kDa), a marker of intracellular organelles, was abundant in the cell lysates at ∼90 kDa, accompanied by a higher molecular weight smear extending up to ∼135 kDa. The band was more prominent in the flow-through but was largely absent from the concentrated EV sample, with some smearing of CNX in the EV concentrated sample too. This supports a reduction in non-EV material (Figure 5.18A). CNX belongs to group 4c: transmembrane, lipid-bound, or soluble proteins associated with intracellular compartments other than the plasma membrane or

endosomes, such as the endoplasmic reticulum (Welsh et al., 2024).

5.3.5 Functional Effects of Glial-Derived Extracellular Vesicles on Neuronal Sensitisation

Subsequent experiments investigated whether extracellular vesicles derived from inflammatory glial cultures could functionally reprogramme sensory neurones, with neuronal excitability assessed as a readout of pro-nociceptive transformation.

Application of Glial-Derived Extracellular Vesicles to Sensory Neurones

EVs were isolated from control and cytokine-treated mixed glial cultures (Section 5.1.1) to assess their functional impact on sensory neurones. A media-only control was included to account for potential effects of concentrated media components. DRG neurones were exposed to EVs for 24 hours, and neuronal excitability was subsequently assessed via calcium imaging with capsaicin stimulation.

DRG neurones exhibited enhanced calcium responses following treatment with EVs derived from cytokine-stimulated glia, indicating a sensitising effect. Peak calcium responses across the three treatment groups: media control (Media CTL), EV control (EV CTL), and inflammatory EV (CytoG EVs) were compared; a significant overall effect was detected among the groups ($F(2, 6) = 19.96$, $p = 0.0022$, $R^2 = 0.8694$, one-way ANOVA). A significant increase in calcium transient peaks between the EV CTL and CytoG EV groups was revealed (mean difference = -0.06271, 95% CI [-0.09753, -0.02789], $p = 0.0036$, Tukey's post-hoc test), demonstrating that EVs derived from glia stimulated with inflammatory cytokines were able to sensitise DRG sensory neurones (Figure 5.19B). There was also a significant increase between the media CTL and CytoG EV treatment groups (mean difference = -0.06147, 95% CI [-0.09629, -0.02665], $p = 0.0039$).

The area under the stimulation response curves was compared across treatment groups to assess differences in neuronal excitability. The differences between the

area under the curve for the three groups yielded a borderline significant result (H = 5.600, p = 0.0500, Kruskal-Wallis; Figure 5.19C). There was a trend towards increased area under the curve in neurones treated with inflammatory EVs, though this did not reach statistical significance; comparisons showed no statistically significant differences between groups, although Media CTL vs. CytoG EVs was close (mean rank difference = -5.000, p = 0.0760; one-way ANOVA with Dunn's post-hoc test).

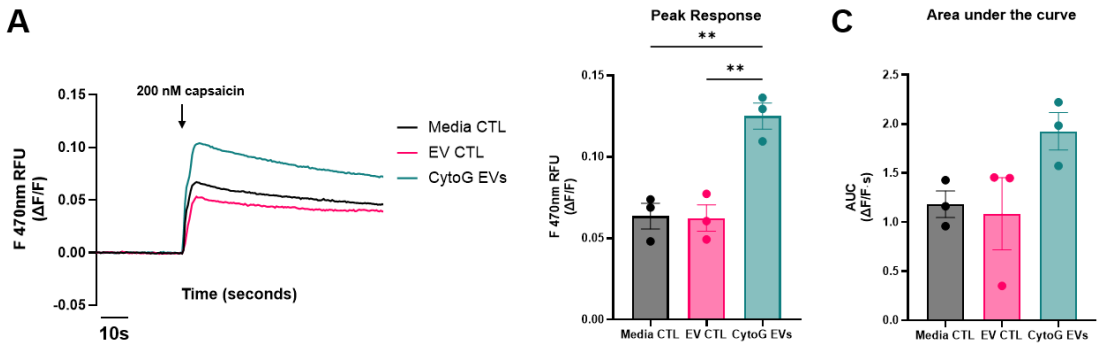


Figure 5.19. Extracellular Vesicles, Derived from Glia Stimulated with Pro-Inflammatory Cytokines, Sensitised DRG Sensory Neurones. A - Averaged calcium imaging traces (ΔF/F) from the somata of DRG sensory neurones treated with EVs derived from control glia (EV CTL), cytokine-treated glia (CytoG EVs), or cell-free media (Media CTL). 200 nM capsaicin was applied after 30 seconds. **B -** Quantification of peak calcium responses (ΔF/F, mean ± SEM). CytoG EVs displayed significantly increased calcium responses to capsaicin relative to EV CTL (p = 0.0036, Tukey's post-hoc test) and to media CTL (p = 0.0039, Tukey's post-hoc test). **C -** Area under the curve of the calcium trace (peak to 50 seconds; mean ± SEM) was increased in the CytoG-treated group relative to media CTL and EV CTL. No significant difference was found between groups (one-way ANOVA).
N = 3 biological replicates; $n \geq 2$ technical replicates; 10-144 cells per technical replicate. Data displayed as biological replicates. $p < 0.05$ was considered statistically significant.

Direct Application of Cytokines to Sensory Neurones

To determine whether neuronal sensitisation was mediated by glial-derived EVs rather than direct cytokine exposure, the pro-inflammatory cytokine cocktail was applied to sensory neurones, and calcium responses were compared to those elicited by EVs isolated from cytokine-stimulated glia. During calcium imaging, stimulation with 200 nM capsaicin revealed that direct cytokine treatment (Direct Cyto) did not elicit the same magnitude of calcium transients in neuronal somata

as CytoG EVs (Appendix Figure 5.20). Statistical analysis using one-way ANOVA confirmed significant differences among groups (F = 7.800, p = 0.0003, R^2 = 0.3372). Post-hoc tests revealed that CytoG EVs induced significantly larger calcium responses than Media CTL (mean difference = -0.05974, 95% CI: -0.09658 to -0.02290, p = 0.0005, Tukey's multiple comparisons test) and EV CTL (mean difference = -0.05182, 95% CI: -0.09000 to -0.01364, p = 0.0040), whereas Direct Cyto did not differ from Media CTL (mean difference = -0.002722, 95% CI: -0.04612 to 0.04068, p = 0.9983) or EV CTL (mean difference = 0.005201, 95% CI: -0.03934 to 0.04975, p = 0.9894). Comparison between CytoG EVs and Direct Cyto also revealed a significant difference (mean difference = 0.05702, 95% CI: 0.01309 to 0.1010, p = 0.0063), supporting the conclusion that neuronal sensitisation is mediated by glial-derived EVs rather than direct cytokine exposure.

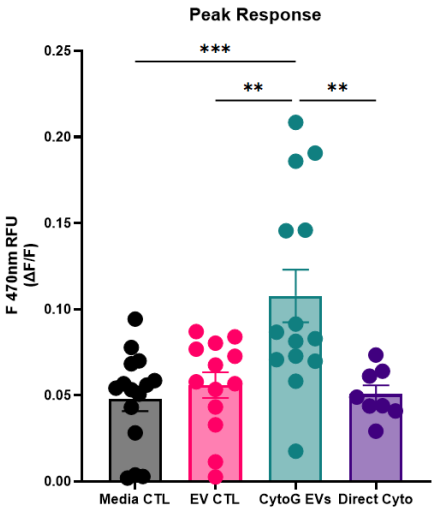


Figure 5.20. Extracellular Vesicles from Activated Glia Drive Enhanced DRG Sensitisation Relative to Cytokine Exposure Alone. Peak calcium responses (ΔF/F, mean ± SEM) in DRG sensory neurones treated directly with the cytokine cocktail (Direct Cyto) or with EVs derived from cytokine-treated glia (CytoG EVs). CytoG EV-treated neurones showed significantly increased responses compared to Media CTL (p = 0.0005, Tukey's multiple comparisons test) and EV CTL (p = 0.0040), whereas Direct Cyto-treated neurones were not significantly different from controls. Comparison between CytoG EVs and Direct Cyto also showed a significant increase (p = 0.0063).
N = 3 biological replicates; $n \geq 3$ technical replicates; 3-23 cells per technical replicate. Data displayed as technical replicates. $p < 0.05$ was considered statistically significant.

These investigations demonstrated the potential of inflammatory glial-derived EVs to induce neuronal sensitisation.

5.3.6 EV Functional Cargoes: Searching for miRNAs

Previous work has reported the role of miRNAs in the functional effects mediated by EVs, with glial-derived EVs a particular focus of research (Ahmad et al., 2022; Santiago et al., 2023; Zhu et al., 2025). Informed by literature-guided selection (Chaudhuri et al., 2018; Prada et al., 2018), the causal involvement of specific miRNAs in the observed phenotypes was tested through targeted manipulation and functional assessment. A Venn diagram was produced to discern overlaps between study datasets (Figure 5.21).

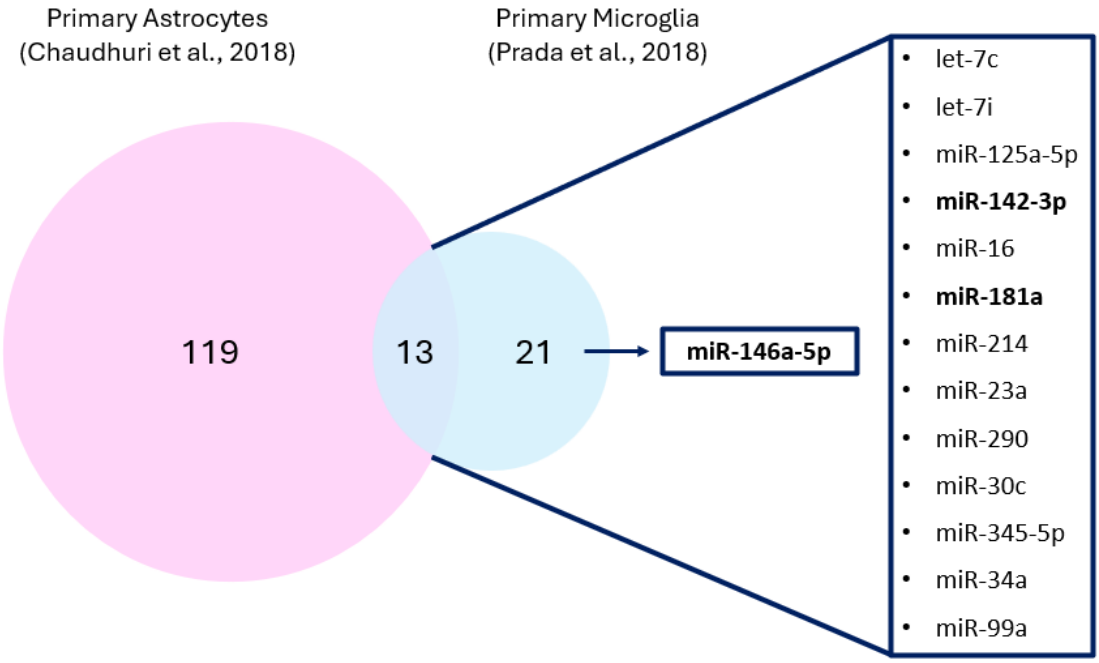


Figure 5.21. Venn Diagram of Dysregulated miRNA Transcripts Within Extracellular Vesicles Derived from Primary Glial Cultures Following Pro-Inflammatory Treatments in the Literature. A literature search identified two studies that cultured primary glia from rodents and profiled miRNA content within glial-derived extracellular vesicles. Thirteen shared transcripts are listed in the highlighted box adjacent to the Venn diagram. miR-146a-5p was uniquely identified in Prada et al. (2018).

The miRNAs that were present in both studies and their known functions are listed in Table 5.4 on the next page:

Table 5.4. Dysregulated miRNAs Identified in a Literature Search and their Known Functions. Transcripts in bold were selected for functional investigation. The transcript in italics was listed only in Prada et al. (2018).

miRNA	Role
let-7c	Overexpression causes deficits in neuronal morphology, electrical excitability, and synaptic transmission; reduction in spontaneous neuronal firing - likely to regulate neuronal differentiation and function (McGowan et al., 2018).
let-7i	Reduced in hippocampus and cortex of rat epilepsy models - involved in TLR4 regulatory pathway (Ou et al., 2022); reduces ischaemic injury and recovers motor function (Nguyen, Su, and Singh, 2018).
miR-125a-5p	Potential biomarker for mood disorders (Gecys et al., 2022); downregulated in some tumours; role in embryo development; activator of NF-κB (Potenza et al., 2017).
miR-142-3p	Implicated in the immune system and CNS (De Vito et al., 2022); vascular-inflammation axis (Roblain et al., 2021; Zhang et al., 2022); microglial recruitment and activation (Roblain et al., 2021); apoptosis and pro-inflammatory molecule expression (Glémain et al., 2022); aberrant expression in diseases (Boese et al., 2016; De Vito et al., 2022; Talebi et al., 2017; Tang et al., 2019; Pahlavan et al., 2020); increased after nerve injury (Ikuma et al., 2023); present in exosomes in diabetes (Guay et al., 2019).
miR-16	Role in neuronal cell apoptosis in Alzheimer's disease (Kim et al., 2020); upregulated in spinal cord injury rats (Zhao et al., 2024); overexpression retracts neurites and reduces branching in cultures of hippocampal neurones (Burak et al., 2018); role in inflammatory autoimmune diseases (Yan et al., 2019); contributes to therapeutic action of selective serotonin reuptake inhibitor antidepressants (Baudry et al., 2010).
miR-23a	Upregulation improved long-term neuronal function, reduced neurone apoptosis, and inhibited neuroinflammation in traumatic brain injury (Li et al., 2020); present in DRG neurones and taken up into macrophages, promoting inflammation and M1 polarisation via NF-κB activation – potential therapeutic target in spinal nerve injury-induced neuropathic pain (Zhang et al., 2021b).
miR-181a	Targets GluR2 (Prada et al., 2018); involved in neuronal degeneration (Stein et al., 2022), synaptic plasticity (Rodriguez-Ortiz et al., 2020), and endometriosis (Wright, Mitchell, and Santanam, 2017).
miR-214	Regulation of development - size and complexity increased with overexpression (Irie et al., 2016); highly expressed in neuronal progenitor cells and promotes neurogenesis (Shu et al., 2017); significantly upregulated in Parkinson's disease cell and animal models (Dong et al., 2024).

Continued on next page

Table 5.4 continued from previous page

miRNA	Role
miR-290	Mouse-specific microRNA cluster - regulation of a network of genes required for placental development, suggesting role in evolution of placental mammals (Paikari et al., 2017).
miR-30c	Regulates progression of Parkinson's disease (Zhang et al., 2021a); improves neuronal apoptosis and inflammatory response caused by cerebral ischaemia-reperfusion injury (Deng, Zeng, and Ding, 2024); stimulates formation of myelin sheath and promotes peripheral nerve regeneration (Yi et al., 2017); promotes nerve repair and neurogenesis in olfactory bulb and hippocampus, reduces inflammatory response via NF-κB suppression and oxidative stress reduction (Kumar and Li, 2023).
miR-345-5p	Induces inflammatory damage in hippocampal neurones by activating microglia (Liu et al., 2020).
miR-34a	Reducing miR-34a selectively enhances NMDAR-mediated synaptic transmission in adult hippocampus (Min et al., 2023); involved in DRG neurone damage and hyperglycaemia - suppresses axon growth in postnatal DRGs but promotes in adult (Jia et al., 2018); promotes neurogenesis (Morgado et al., 2015); associated with increased AD pathology via repression of genes for neuronal survival, synaptic plasticity, memory, Aβ clearance, mitochondrial functions, antioxidant defense, and energy metabolism (Bazrgar et al., 2021); regulates GABAergic neurotransmitter activity and behaviour in a context-dependent manner (Ielpo et al., 2023).
miR-99a	Overexpression in hippocampus leads to cognitive impairment (Hu et al., 2022); reduces neuronal damage following cerebral ischaemic reperfusion by regulating cell cycle progression and preventing apoptosis (Tao et al., 2015); increases cortical axon growth and regulates calcium oscillation frequency and synchronicity in cortical neurones (Mesquita-Ribeiro, 2019).
miR-146a-5p	*Involved in disease-related synaptic alterations, modulation of microglial inflammatory pathways, reduces dendritic spine density (Prada et al., 2018); biomarker for epilepsy (Omran et al., 2012), osteoarthritis (Liu, Lu, and Fu, 2022), and traumatic brain injury (Johnson et al., 2017).*

miR-142-3p, miR-146a-5p, and miR-181a were selected as potential candidates for mediating the EV-induced neuronal sensitisation, based on their previously identified roles, as listed in Table 5.4. Although it did not overlap with both datasets compared here, miR-146a-5p was chosen because it became the primary focus of the remainder of Prada et al. (2018), following its initial identification. In both studies, miR-181a was reported without specification of the mature isoform (-5p or -3p). To determine which to include in this study, additional literature was reviewed to select miR-181a-5p based on its functional relevance (Huang and Xu, 2020; Rodriguez-Ortiz et al., 2020).

5.3.7 miR-142-3p is Not Involved in Sensory Neurone Sensitisation via Glial-Derived Extracellular Vesicles

miRNA power inhibitors were co-applied with EVs, derived from either cytokine-stimulated or control glial cultures, to dissociated DRG sensory neurones for 24 hours. Functional changes were detected by measuring neuronal excitability with calcium imaging, stimulating with the nociceptive compound capsaicin.

To evaluate whether inflammatory EVs sensitise sensory neurones and whether this effect is mediated by miR-142-3p, calcium responses were compared across treatment groups:

- Negative control (NC) + CTL EV (negative control inhibitor with control EVs)
- NC + CYTO EV (negative control inhibitor with inflammatory EVs)
- miR-142-3p power inhibitor (142) + CTL EV (miR-142a-5p LNA power inhibitor with control EVs)
- 142 + CYTO EV (miR-142a-5p LNA power inhibitor with inflammatory EVs)

As expected, neurones treated with inflammatory EVs (and NC) showed increased calcium transients compared to those receiving control EVs (and NC), confirming the sensitising effect of inflammatory EVs and validating the assay system. Inhibi-

tion of miR-142-3p did not appear to block this effect: calcium responses in the 142 + CYTO EV group remained elevated relative to the 142 + CTL EV group, although this trend did not reach statistical significance relative to NC groups.

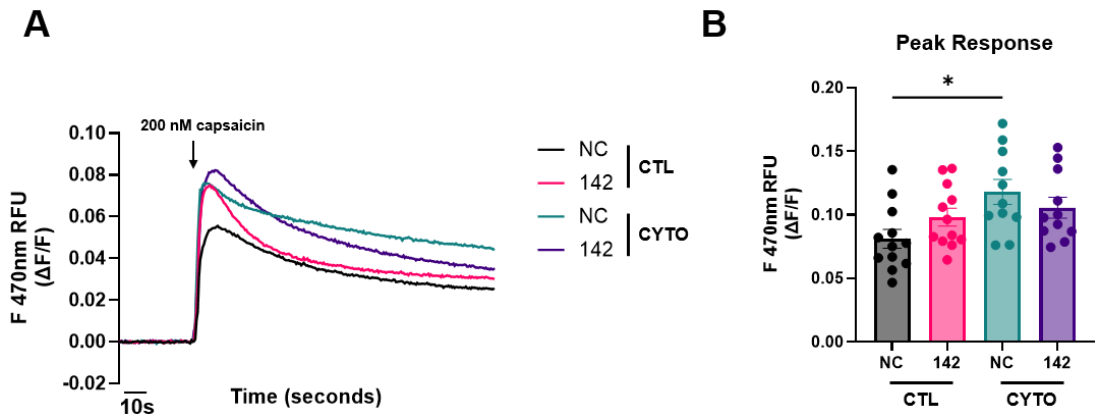


Figure 5.22. Inhibition of miR-142a-3p Does Not Affect the Glial EV-Induced Sensory Neurone Sensitisation. A - Averaged calcium imaging traces (ΔF/F) from the somata of DRG sensory neurones treated with EVs derived from control glia (CTL) or cytokine-treated glia (CYTO), alongside LNA Power Inhibitor targeting miR-142a-3p (142) or the negative control inhibitor (NC). **B -** Quantification of peak calcium responses (ΔF/F, mean ± SEM). Co-treatment with the miR-142a-3p inhibitor did not significantly alter the capsaicin-evoked calcium response in either the CTL or CYTO EV groups. However, there was a trend toward increased peak responses in both groups of neurones treated with miR-142a-3p inhibitor, compared to the NC + CTL EV group. A significant increase in calcium transients was observed in the NC + CYTO EV group compared to the NC + CTL EV group (p = 0.0126, Tukey's post-hoc test).
N = 4 biological replicates; $n \geq 2$ technical replicates; 7-53 cells per replicate. Data displayed as technical replicates. $p < 0.05$ was considered statistically significant.

Statistical analysis showed a significant overall difference in peak calcium responses among the four treatment groups ($F(3, 42) = 3.657$, $p = 0.0198$, $R^2 = 0.2071$, one-way ANOVA). Post-hoc testing confirmed a significant increase in calcium transients for NC + CYTO EV versus NC + CTL EV (mean difference = -0.03694, 95% CI [-0.06758, -0.006299], p = 0.0126, Tukey's post-hoc test), consistent with the sensitising effect of inflammatory EVs (Figure 5.22B), as in Section 5.3.5. No other pairwise comparisons achieved statistical significance; however, a modest increase in calcium transients was observed in several miR-142-3p inhibitor-treated groups, with the CYTO EV-treated group exhibiting a slightly greater effect. Together, these findings indicate that miR-142-3p inhibition does not prevent glial-derived inflam-

matory EV-induced sensitisation, suggesting that this miRNA is unlikely to be a key mediator in this pathway.

5.3.8 miR-181a-5p is Not Involved in Sensory Neurone Sensitisation via Glial-Derived Extracellular Vesicles

To assess whether miR-181a-5p contributes to the pro-nociceptive effects of inflammatory EVs, DRG sensory neurones in dissociated culture were co-treated for 24 hours with EVs derived from either cytokine-stimulated (inflammatory) or control glia, in the presence of either a miR-181a-5p inhibitor or a negative control inhibitor.

As expected, inflammatory EVs increased neuronal excitability compared to control EVs, confirming their sensitising effect. However, inhibition of miR-181a-5p did not significantly reduce this effect, although a slight trend toward reduced excitability was observed when neurones were treated with inflammatory EVs alongside the miR-181a-5p inhibitor.

Statistical analysis showed a significant overall difference in peak calcium responses among the four treatment groups (NC + CTL EV, NC + CYTO EV, 181 + CTL EV, and 181 + CYTO EV; $F(3, 43) = 3.517$, $p = 0.0229$, $R^2 = 0.1970$, one-way ANOVA). Post-hoc testing revealed a significant increase between the NC + CTL group and the NC + CYTO (mean difference = -0.03694, 95% CI [-0.06790, -0.005978], $p = 0.0137$, Tukey's post-hoc test; Figure 5.23B), which validated the sensitising effect of inflammatory EVs. No other pairwise comparisons reached significance. These results suggest that miR-181a-5p may have a limited or non-essential role in mediating EV-induced neuronal sensitisation.

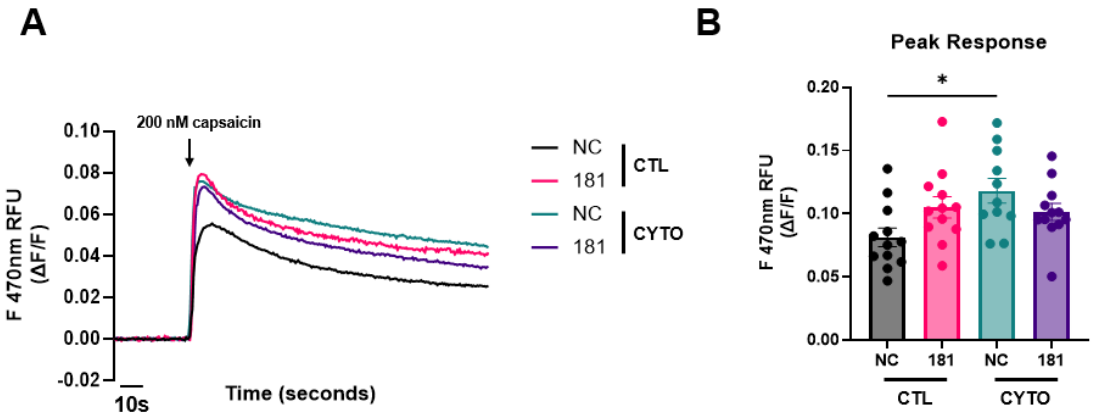


Figure 5.23. Inhibition of miR-181a-5p Does Not Affect the Glial EV-Induced Sensory Neurone Sensitisation. A - Averaged calcium imaging traces (ΔF/F) from the somata of DRG sensory neurones treated with EVs derived from control glia (CTL) or cytokine-treated glia (CYTO), and a LNA Power Inhibitor targeting miR-181a-5p (181) or negative control inhibitor (NC). **B -** Quantification of peak calcium responses (ΔF/F, mean ± SEM). Co-treatment with the miR-181a-5p inhibitor did not significantly alter the capsaicin-evoked calcium response in either the CTL or CYTO EV groups. However, there was a trend toward increased peak responses in both groups of neurones treated with miR-181a-5p inhibitor, compared to the NC + CTL EV group. A significant increase in calcium transients was observed in the NC + CYTO EV group compared to the NC + CTL EV group (p = 0.0137, Tukey's post-hoc test).
N = 4 biological replicates; $n \geq 3$ technical replicates; 7-58 cells per replicate. Data displayed as technical replicates. $p < 0.05$ was considered statistically significant.

5.3.9 miR-146a-5p Contributes to Sensory Neurone Sensitisation via Glial-Derived Extracellular Vesicles

As with the previous miRNAs, to assess whether miR-146a-5p contributes to the pro-nociceptive effects of inflammatory EVs, DRG sensory neurones in dissociated culture were treated for 24 hours with EVs derived from either cytokine-stimulated or control glia, in the presence of either a miR-146a-5p inhibitor or a negative control inhibitor.

As expected, inflammatory EVs increased calcium transients relative to control EVs, indicating enhanced neuronal excitability. In contrast, inhibition of miR-146a-5p abolished the sensitising effect of inflammatory EVs; neurones treated with the inhibitor alongside inflammatory EVs exhibited calcium responses comparable to those exposed to control EVs or to the negative control inhibitor with control

EVs.

Statistical analysis confirmed these effects: there was a significant overall difference among groups ($F(3, 43) = 4.388$, $p = 0.0088$, $R^2 = 0.2344$, one-way ANOVA). Post-hoc testing showed a significant increase in calcium transients in the NC + CYTO EV group compared to NC + CTL EV (mean difference = -0.03694, 95% CI [-0.06655, -0.007330], $p = 0.0092$, Tukey's post-hoc test). Importantly, responses in the 146 + CYTO EV group were significantly lower than in NC + CYTO EV (mean difference = 0.03112, 95% CI [0.001506, 0.06073], $p = 0.0361$) and were comparable to those of the 146 + CTL EV group (Figure 5.24B). The 146 + CTL EV group showed a near-significant decrease compared to the NC + CYTO EV group (mean difference = -0.005824, 95% CI [-0.03478, 0.02314], $p = 0.0515$). Taken together, these findings indicate that miR-146a-5p inhibition prevents the pro-nociceptive effects of inflammatory EVs on sensory neurones.

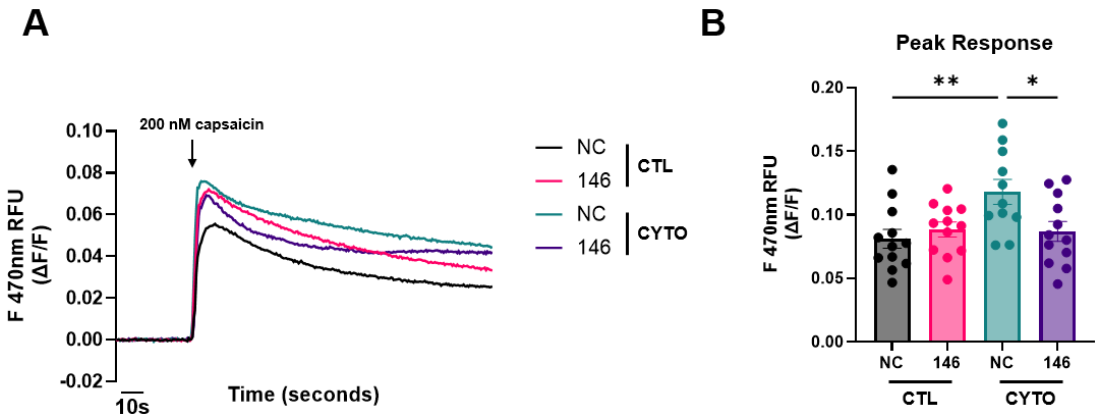


Figure 5.24. Inhibition of miR-146a-5p Prevented the Glial EV-Induced Sensory Neurone Sensitisation. A - Averaged calcium imaging traces (ΔF/F) from the somata of DRG sensory neurones treated with EVs derived from control glia (CTL) or cytokine-treated glia (CYTO), and a LNA Power Inhibitor targeting miR-146a-5p (146) or a negative control inhibitor (NC). **B -** Quantification of peak calcium responses (ΔF/F, mean ± SEM). A significant increase in calcium transients was observed in the NC + CYTO EV group compared to the NC + CTL EV group ($p = 0.0092$, Tukey's post-hoc test). Neurones administered with the miR-146a-5p inhibitor (CTL and CYTO EV groups) responded to capsaicin at a similar level as the NC + CTL EV-treated group. There was a significant decrease in calcium transients in 146 + CYTO EVs compared to NC + CYTO EVs ($p = 0.0361$).
$N = 4$ biological replicates; $n \geq 3$ technical replicates; 7-41 cells per replicate. Data displayed as technical replicates. $p < 0.05$ was considered statistically significant.

As a control experiment, inhibitors applied without EVs did not alter baseline ex-

citability, confirming they did not act independently (Appendix Figure A2). This control confirmed that the observed neuronal sensitisation required both the presence of EVs and their miRNA cargo, supporting a specific EV-mediated mechanism rather than a direct effect of the inhibitors.

These results indicate that miR-146a-5p is a critical mediator of glial-derived EV-induced neuronal sensitisation. Its inhibition blocked the excitability increase typically induced by the inflammatory EVs, supporting a model in which EV-associated miRNAs, rather than free inhibitors or cytokines, drive functional reprogramming of sensory neurones.

5.3.10 Downstream Targets of miR-146a-5p Differ Between Mouse and Human

To interrogate this miR-146a-5p-mediated mechanism further, downstream targets of miR-146a-5p were predicted using PANTHER. Despite strong species conservation of miR-146a-5p (Mao et al., 2023), only $\sim$21% of its predicted targets overlapped between mouse and human. The highest-ranked shared targets were *Traf6* and *Irak1*, reaffirming their central role in inflammatory signalling mediated by the NF-κB pathway (Hassan et al., 2024). However, other high-ranking targets, such as *Clasp1* or *Sort1*, were differently ranked between species, or were species-specific, such as *Sort1* and *Ppp1r11* (Tables 5.5 and 5.6), underscoring the need for human validation before translational application.

The genes listed in Table 5.5 represent the most highly predicted targets of miR-146a-5p in *Mus musculus*:

Table 5.5. The Top 10 Genes Predicted to be Targeted by miR-146a-5p in Mouse Compared to Human. Rank: gene position in the target list (1 = highest relevance). Target score: predictive confidence from 0 to 100 (100 = highest).

Gene	Rank Mouse	Rank Human	Target Score Mouse	Target Score Human
Traf6	1	1	100	100
Irak1	2	2	99	100
Clasp1	3	N/A	99	N/A
Esyt2	4	120	98	80
Numb	5	11	97	94
Sec23ip	6	3	96	99
Appl1	7	16	96	93
Med1	8	104	95	82
Kras	9	N/A	95	N/A
Nova1	10	4	94	98

The genes in Table 5.6 represent the remaining most highly predicted targets of miR-146a-5p in *Homo sapien* that are not conserved in *Mus musculus*, based on cross-species comparison:

Table 5.6. The Remaining Three Gene Targets of miR-146a-5p From the Top 10 In Humans. Rank: gene position in the target list (1 = highest relevance). Target score: predictive confidence from 0 to 100 (100 = highest).

Gene	Rank Mouse	Rank Human	Target Score Mouse	Target Score Human
Ppp1r11	243	5	64	97
Upp2	N/A	6	N/A	97
Wwc2	N/A	7	N/A	97
Bcorl1	30	8	89	96
Znf6	N/A	9	N/A	9
Sort1	218	10	66	95

5.3.11 Gene Set Enrichment Analysis Identified Downstream Gene Targets Associated with Neurotransmission

To explore the potential downstream mechanisms of miR-146a-5p, predicted murine gene targets were analysed using GO-Slim Biological Processes enrichment. This revealed significant overrepresentation of synaptic and neurotransmission-associated processes, including 'neurotransmitter secretion', 'signal release from synapse', 'signal release', and 'neurotransmitter transport' (fold enrichment $\sim$6.5-7.5; Table 5.7). In contrast, processes related to sensory perception and general nervous system function were markedly under-represented (fold enrichment < 0.01). An expanded table is included in the Appendix (Table A5).

Table 5.7. Biological Processes Predicted to be Targeted by miR-146a-5p. GO-Slim enrichment analysis was performed using the PANTHER classification system to identify biological processes associated with predicted miR-146a-5p targets. The table includes the following metrics: Reference Count - number of genes annotated to each GO term in the *Mus musculus* reference list; Observed Count - number of genes from the input list annotated to the term; Fold Enrichment (FE) - ratio of observed to expected counts; Direction (+/-) - indicates overrepresentation (+) or underrepresentation (-); Raw *p*-value - unadjusted significance from Fisher's Exact Test; and False Discovery Rate (FDR) - adjusted *p*-value accounting for multiple testing.

Process	Reference Count	Observed Count	FE	+/-	*p*-value	FDR
Neurotransmitter secretion	44	7	7.45	+	3.73E-05	1.98E-02
Signal release from synapse	44	7	7.45	+	3.73E-05	1.58E-02
Signal release	50	7	6.56	+	8.71E-05	2.64E-02
Biological regulation	6133	169	1.29	+	1.11E-04	2.61E-02
Neurotransmitter transport	50	7	6.56	+	8.71E-05	2.31E-02
Sensory perception of chemical stimulus	492	0	<0.01	-	4.53E-05	1.60E-02
Sensory perception	538	0	<0.01	-	1.34E-05	1.42E-02
Nervous system process	574	0	<0.01	-	6.05E-06	1.28E-02
System process	658	1	0.07	-	1.44E-05	1.02E-02

5.4 Discussion

5.4.1 Summary of Key Findings

I found that EVs, derived from mixed glia stimulated with pro-inflammatory cytokines, can robustly sensitise sensory neurones, highlighting a potential mechanism for central terminal sensory neurone sensitisation. My results support the growing view that EVs are not passive by-products but active agents of intercellular communication (Welsh et al., 2024; Paolicelli et al., 2022), capable of modulating neuronal excitability and neuroimmune responses (Datta Chaudhuri et al., 2020; Gabrielli et al., 2015; Li et al., 2017). This finding also aligns with emerging evidence that glial-derived EVs contribute to neuroinflammatory processes and pain signalling (Cheng, Xu, and Ma, 2022; Li et al., 2017; Warwick and Hanani, 2013).

To investigate the molecular drivers of glial EV-induced neuronal sensitisation, three miRNAs - miR-142-3p, miR-146a-5p, and miR-181a-5p - were selected based on their established roles in neuroinflammation and neuronal plasticity, as well as their encapsulation within EVs derived from primary glial cells (Chaudhuri et al., 2018; Prada et al., 2018). Among these, inhibition of miR-146a-5p consistently attenuated EV-induced sensitisation, indicating a dominant regulatory role in this process.

5.4.2 Glia-Neurone Communication via EVs in Neuroinflammation

Glial cells - including astrocytes, microglia, and oligodendrocytes - are central to CNS homeostasis and injury response. One key mechanism by which they influence neurones is through the release of EVs, which carry proteins, lipids, and RNA species capable of modulating neuronal function (Ahmad et al., 2022). The findings here demonstrate that EVs derived from cytokine-stimulated spinal cord glia

can induce sensitisation of DRG sensory neurones, supporting a model in which glial EVs actively contribute to pain hypersensitivity. Although EVs were secreted in lower quantities from control glia, they were applied to DRG cultures at equivalent concentrations, indicating that their cargo was sufficient to induce sensitisation in DRG neurones. Glial-derived EV-mediated sensitisation of sensory neurones aligns with studies showing that glial EVs can alter neuronal excitability, promote nociception, and modulate synaptic function. For example, astrocytes stimulated with ATP and IL-1β produced EVs that increased spike and burst activity in cortical neurones (Datta Chaudhuri et al., 2020). Similarly, microglia-derived EVs have been found to promote the excitation of neurones via enhancement of glutamatergic transmission and inhibition of GABAergic transmission (Gabrielli et al., 2015) and elicit considerable increases in spontaneous excitatory postsynaptic current frequency and amplitude (Li et al., 2017).

The control experiment, in which the cytokine cocktail was applied directly to sensory neurones, revealed a significant decrease in responsiveness, relative to CytoG EV-treated cells, suggesting that cytokines alone are not sufficient to account for the heightened effect. Furthermore, it is unlikely that soluble cytokines were co-isolated with EVs during size-exclusion chromatography, as the size of the proteins would be excluded from the EV fractions (as demonstrated by Western blot, Figure 5.18). Taken together, the robust sensitisation induced by CytoG EVs indicates that the heightened responsiveness is EV-mediated (Figure 5.20).

Importantly, the magnitude of DRG sensitisation observed in cultures treated solely with glial-derived EVs was substantially greater than that seen in cultures exposed to EVs alongside the miRNA power inhibitor (Figure 5.19 compared to Figure 5.20). This disparity likely reflects the experimental design: EVs isolated from a single biological replicate were divided across a larger number of technical replicates in the inhibitor condition, due to the increased complexity of the experimental set-up and the need to accommodate additional treatment groups and controls.

While these experiments used mixed glial cultures, which limits the ability to pinpoint the cellular origin of the EVs responsible for this effect, this approach preserved the natural interplay between glial subtypes and better reflected the *in vivo* neuroinflammatory environment. The incorporation of other immune cells, such as T-cells, would make this model even more physiological (Krames, 2014). Future studies should isolate EVs from individual glial populations to dissect their distinct contributions to central terminal sensitisation, although this presents technical challenges due to reduced EV yield. Alternatively, dual-marker analysis using flow cytometry could be used to identify the presence of cell-specific markers on single EVs (Inglis, Norris, and Danesh, 2015).

5.4.3 Extracellular Vesicle Uptake and Characterisation

Mechanisms of Glial EV Uptake by Sensory Neurones: An Open Question

The mechanism by which the sensory neurones internalised the glial EVs remains unclear. Known uptake pathways include clathrin-mediated endocytosis, macropinocytosis, and direct membrane fusion (as covered in Section 1.3.1.6; Teng and Fussenegger, 2021). Future experiments could utilise pharmacological inhibitors, such as dynasore (an endocytosis inhibitor; P. Jackson and R. Mesquita-Ribeiro, personal communication, 2023) or GW4869 (a neutral sphingomyelinase inhibitor, Yin et al., 2020), to investigate uptake and release pathways. Uptake could also be observed in real-time using fluorescent labels, such as DiD, which attach to EV membrane proteins (Welsh et al., 2024).

Marker Variability and the Limits of CD63 in Glial EV Characterisation

Regarding EV characterisation, CD63, a commonly used EV marker (Welsh et al., 2024), did not produce a clear signal in the Western blot in this study. The diffuse, dot-like pattern observed around $\sim$35 kDa may be attributable to antibody variability, poor transfer efficiency of this hydrophobic tetraspanin, or heterogeneity caused by differential glycosylation. Although CD63 is a widely cited exosome

marker, its detectability is highly variable and dependent on cell type, vesicle subtype, and detection method. For example, CD63 immunostaining in brain tissue has been described as ambiguous, with CD63-GFP reporter mice showing strong neuronal - but not glial - expression (Men et al., 2019). Similarly, a recent review confirmed that CD63 is not a consistent marker for astrocyte-derived EVs, and is insufficient on its own to characterise glial EVs (Sutter et al., 2024). Furthermore, the MISEV2023 guidelines explicitly recommend using multiple positive markers, including transmembrane proteins (e.g., tetraspanins) and cytosolic proteins (e.g., ALIX, TSG101, FLOT-1), without requiring that all be present in every sample (Welsh et al., 2024). In the dataset here, the presence of both ALIX and FLOT-1, provided evidence for EV enrichment from category 2 (cytosolic proteins in EVs). However, proof of a group 1 marker (transmembrane proteins) would be required to confirm, without doubt, the hallmarks of EVs - potentially CD9, CD81, or LAMP1. The substantial depletion of CNX from EV preparations further supported the purity of the isolated vesicles, consistent with its role as a negative marker for intracellular contamination (Welsh et al., 2024).

The appearance of a second, lower molecular weight ALIX band in cell lysates likely reflected a proteolytically cleaved form, consistent with reports of ALIX fragmentation during cellular stress or apoptosis (Maemoto et al., 2013). The band's absence in EVs suggests that these extracellular vesicles preferentially packaged the intact, full-length protein, supporting its well-established role in endosomal sorting and vesicle biogenesis (Teng and Fussenegger, 2021). As expected for a negative EV marker, CNX was not detected at high levels in vesicle preparations, indicating minimal contamination from intracellular organelles (Welsh et al., 2024). The higher molecular weight smear observed for CNX in cell lysates, and in the concentrated EV sample, is consistent with the extensive glycosylation and potential aggregation of this ER transmembrane chaperone (Lamriben et al., 2016).

Impact of Freeze-Thawing on EV Function

Despite rigorous EV characterisation, one limitation concerns the freeze-thawing of EV samples. Due to the nature of primary glial cultures, which require extended growth periods, and the need to synchronise EV application with DRG neurone readiness, it was not feasible to use freshly isolated EVs in experiments. Consequently, EVs were frozen post-collection and thawed once for functional use. While this approach minimised repeat freeze-thaw cycles, it is important to note that there is conflicting evidence regarding the impact of freeze-thawing on EV integrity, cargo stability, and functional potency. Membrane disruption, reduced EV yield, and altered bioactivity are potential concerns (Welsh et al., 2024). Future studies should explore the extent to which freeze-thawing affects glial-derived EV-mediated sensitisation. Preliminary observations support the view that freeze-thawing may not substantially alter EV function: one colleague reported that cortical-derived EVs retained their effect on axon growth following freeze-thawing, with no detectable difference compared to fresh preparations (R. Mesquita-Ribeiro, personal communication, September 15, 2025), while another found that both Neuro-2A-derived and cortical-derived EVs produced robust effects on axon growth post-thawing (P. Jackson, personal communication, September 15, 2025).

Non-Vesicular Components in Glial Secretomes

In addition to EVs, protein fractions (eluted later from the SEC column) in the culture media were identified by SDS-PAGE (Section 5.3.2), collected, and stored. Although not examined in the current study, these fractions may contain soluble glial-derived proteins capable of influencing sensory neurone sensitisation via non-vesicular mechanisms, independent of the EV-mediated pathways investigated. Future investigations should incorporate these protein fractions into functional assays to determine whether non-vesicular components also contribute to neuroimmune modulation.

5.4.4 miRNA-Mediated Sensitisation

Given the complex and heterogeneous nature of EV cargo (Welsh et al., 2024), identifying a single molecule responsible for a functional outcome is both challenging and highly significant. In this study, miR-146a-5p emerged as a key effector, with its inhibition consistently preventing EV-induced sensitisation of sensory neurones. This suggests a high degree of functional specificity and positions miR-146a-5p as a central mediator of glial EV-induced neuronal hyperexcitability.

This finding is relatively novel; few studies have reported miRNA-mediated changes in neuronal excitability or firing patterns and even fewer from miRNAs encapsulated in EVs. However, there is emerging evidence that other glial- or neurone-enriched miRNAs can influence neuronal activity, supporting the broader concept that small RNAs can dynamically tune neuronal responsiveness. For example, following inflammatory stimulation, astrocytes release EVs containing miRNAs that target proteins involved in neurotrophin signalling: miR-125a-5p and miR-16-5p target neurotrophic receptor tyrosine kinase 3 (NTRK3) and its downstream effector Bcl2, and their upregulation is associated with reduced spiking rates and burst activity in recipient neurones, indicative of decreased excitability (Chaudhuri et al., 2018). miR-16-5p has also been linked to neuroinflammatory processes (López-Cepeda et al., 2022). Similarly, miR-128 has been shown to suppress expression of ion channels and signalling components within the ERK2 network that regulates neuronal excitability, and this reduction in neurones leads to increased motor activity and spontaneous seizures culminating in fatal epilepsy (Tan et al., 2013). In contrast, overexpression of let-7c in human induced pluripotent stem cell (iPSC)-derived neurones resulted in a marked reduction in neuronal excitability: spontaneous action potential firing was strongly suppressed, the number of evoked action potentials in response to current injection was decreased, and the threshold to generate an action potential was increased, indicating that neurones required greater input to fire. Furthermore, let-7c overexpression reduced the frequency of

spontaneous excitatory postsynaptic currents, with some lines also showing decreased amplitude, consistent with weakened synaptic strength (McGowan et al., 2018). Conversely, miR-129-5p has been reported to enhance neuronal activity by increasing the weighted mean firing rate and the number of network bursts in neurone-astrocyte co-cultures (Kaurani et al., 2025). Within this emerging landscape, my findings extend the field by demonstrating that a glial EV-derived miRNA within EVs can act as a potent upstream driver of sensory neuronal sensitisation, directly linking glial inflammatory signalling to altered neuronal excitability.

5.4.5 miR-146a-5p as a Central Mediator of Glial EV-Induced Sensitisation

Context-Dependent Roles of miR-146a-5p in Neuroinflammation and Sensory Neuronal Excitability

Although inflammation and neuronal excitability are distinct processes, they intersect through convergent molecular pathways. My finding that glial-derived EVs, appearing to contain miR-146a-5p, drive a neuroinflammatory phenotype and sensitisation of sensory neurones, highlighting such a point of convergence (Figure 5.25). Although some literature reports anti-inflammatory or neuroprotective roles for miR-146a-5p, these studies typically involve different neuronal populations, delivery methods, or disease contexts; in the present study, the effect of glial EV-delivered miR-146a-5p on sensory neurones is specifically pro-nociceptive. In other neuronal contexts, miR-146a-5p has been shown to modulate excitability, but with variable effects depending on neuronal subtype and disease state. For example, exogenous overexpression of miR-146a-5p (microglia-derived), in hippocampal neurones has been shown to suppress neurogenesis and dampen spontaneous excitatory activity (Fan et al., 2022). However, this effect was observed in cortical neurones, specifically in relation to spontaneous discharge - a phenomenon characteristic of network-level activity within cortical circuits. While dis-

tinct from cortical dynamics, repeated or intense noxious stimulation can similarly induce repetitive firing and spontaneous action potential generation in sensory neurones, thereby amplifying nociceptive input. This parallel may render the observed effect relevant in the context of sensory processing (Section 1.3.1.3; Krames, 2014; Meng et al., 2016). Moreover, the study focused on excitatory neurones - a distinct subset with unique electrophysiological and molecular properties - highlighting that different neuronal populations may respond divergently to miRNA modulation and other molecular cues. In contrast, hyperexcitability and apoptosis of hippocampal neurones were induced in an oxidative stress-related study: miR-146a-5p exacerbated neuronal vulnerability by downregulating glycolysis and an apoptosis regulator (Lei et al., 2021). In addition, miR-146a-5p has been implicated as causative in epilepsy (Mao et al., 2023), and is also associated with neuronal hyperexcitability.

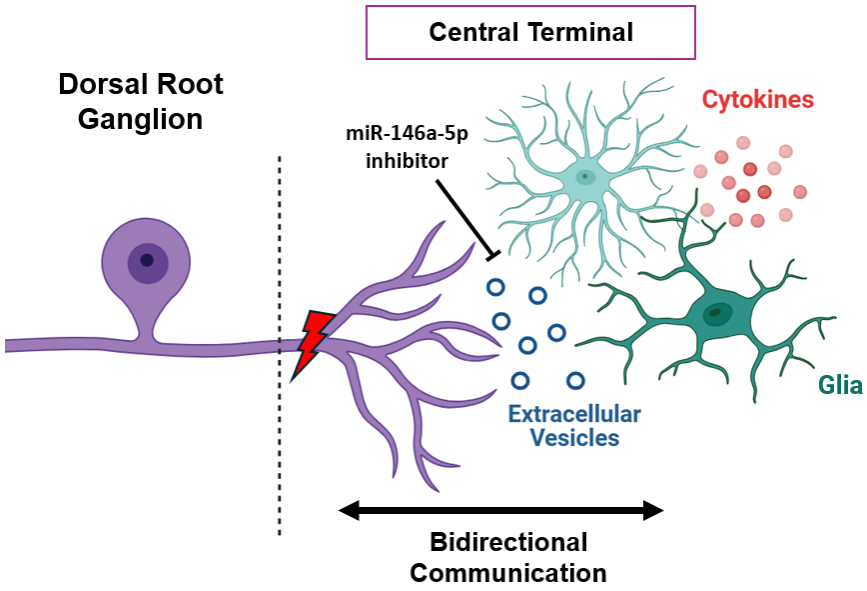


Figure 5.25. The Central Terminal Mechanism of Glial EV-Induced Neuronal Sensitisation. Glia become inflamed when cytokines are released at the central terminal of the sensory neurone. They release EV that contain cargo, some of which are pro-inflammatory. When these EVs are taken up by sensory neurones, the pro-inflammatory cargo is released and can exert its effects. miR-146a-5p was found to be involved in this inflammatory process; when a miR-146a-5p inhibitor was applied simultaneously with inflamed glial EVs, the sensitisation process was prevented. Created using BioRender™.

A growing body of evidence also links miR-146a-5p to persistent neuroinflammation and neuronal death, as well as synaptic and mitochondrial dysfunction (Long et al., 2025). Astrocyte-derived EVs enriched in miR-146a have been shown to induce IL-1β and COX-2 expression and promote apoptosis in recipient neurones in a TLR4-dependent manner (Ibáñez et al., 2019), providing direct evidence that glial EVs can deliver miR-146a to neurones and drive a neuroinflammatory phenotype. Elevated levels of this miRNA have also been associated with cognitive decline in Alzheimer's disease, partly through MAPK signalling and oxidative stress pathways (Cui et al., 2007; Zhan-qiang et al., 2023), and in ALS (Campos-Melo et al., 2013). Studies further support its role as a biomarker of pathological neuronal activity, with positive correlations between upregulated miR-146a and disease severity in epilepsy (Omran et al., 2012), osteoarthritis (Liu, Lu, and Fu, 2022), and traumatic brain injury (Johnson et al., 2017). Importantly, the direction of these effects may not always be consistent - Fan et al. (2020), Long et al. (2025) and Mao et al. (2023) highlight variability in miR-146a-5p function across disease types and stages, and via different downstream pathway activation, suggesting a context-dependent function. Within this landscape, my findings add a novel dimension by showing that glial-derived EVs deliver miR-146a-5p directly to sensory neurones, where it acts in a pro-inflammatory and algesic capacity. This provides mechanistic insight into how inflammatory glia can shape peripheral neuronal sensitisation, bridging miR-146a-5p's established roles in neuroinflammation with its emerging contributions to altered neuronal excitability.

In contrast, specifically in a pain and general inflammatory context, a substantial body of literature supports its analgesic properties: miR-146a-5p has been shown to attenuate neuropathic pain (Grace et al., 2018; Lu et al., 2015), suppress visceral hypersensitivity (Lu et al., 2018), and suppress rheumatoid arthritis (Pauley and Cha, 2011). Notably, when encapsulated within EVs, miR-146a-5p has also been reported to reduce airway inflammation (Liu et al., 2024), suggesting that its delivery mode may influence its functional outcome - many of these studies are

also in an *in vivo* context. In addition, miR-146a-5p may act in an anti-inflammatory manner on astrocytes and microglia (Lu et al., 2015; Long et al., 2025), but not on neurones, and may exert neuroprotective or damaging effects in cortical neurones (López-Cepeda et al., 2022), but enhance excitability in sensory neurones. This contextualisation within the literature underscores the mechanistic complexity, highlighting the influence of cellular context, disease state and progression, as well as the mode of miRNA delivery (Cui et al., 2010; Johnson et al., 2017; Liu, Lu, and Fu, 2022; Omran et al., 2012).

These findings contribute to the growing body of evidence supporting a pro-nociceptive role for miR-146a-5p in sensory neurones. Specifically, the data suggest that miR-146a-5p, when delivered via glial EVs, lowers the threshold for neuronal activation and enhances excitability. This encapsulated mode of delivery may confer increased miRNA stability and facilitate selective uptake by target neurones, bypassing intracellular degradation pathways and amplifying its functional impact. Such a mechanism positions glial EVs as active modulators of sensory neurone sensitisation, with miR-146a-5p acting as a key effector. Inhibition of miR-146a-5p likely restored the balance of pro-inflammatory signalling, potentially indirectly affecting downstream mediators, such as TRPV1, $Na_v1.8$, and ion channel trafficking, all known contributors to sensitisation (Jang, Kim, and Hwang, 2020). These findings underscore the importance of considering both molecular context and delivery modality when evaluating miRNA function, and highlight miR-146a-5p as a promising, albeit complex, target for therapeutic modulation in chronic pain.

Cell-Type Specificity of miR-142-3p: No Effect on Peripheral Neuronal Excitability

In contrast, miR-142-3p and miR-181a, despite being identified as dysregulated in EVs from inflammatory glia in previous studies (Chaudhuri et al., 2018; Prada et al., 2018), did not produce consistent functional changes in the system here. Prior work has shown that miR-142-3p is elevated in inflammatory diseases such as

multiple sclerosis, where it acts as a biomarker and contributes to pathology in glutamatergic neurones (De Vito et al., 2022). Its functional effects may therefore be more prominent in central excitatory networks than in peripheral sensory neurones. miR-142-3p has also been implicated in microglial recruitment and activation (Roblain et al., 2021), as well as in promoting neuronal death in inflammatory contexts (De Vito et al., 2022; Glémain et al., 2022), suggesting roles that are not limited to modulating excitability per se but extend to cell viability and immune-neural crosstalk. Moreover, while increased expression of miR-142-3p has been observed after peripheral nerve injury, this reflects release from damaged DRG neurones themselves rather than EV-mediated signalling between glia and neurones (Ikuma et al., 2023). Together, these findings suggest that the absence of sensitisation or hyperexcitability in this DRG model may reflect cell-type specificity, with miR-142-3p acting through pathways that are more relevant to glutamatergic CNS circuits, microglia, or endothelial interactions than to sensory neurone excitability. Alternatively, its abundance within EVs derived from mixed glial cultures may have been insufficient to trigger downstream changes in DRG firing properties. Future work combining single-cell transcriptomics with EV cargo profiling could help determine the precise cellular targets and context-dependent actions of this miRNA.

Challenges in miRNA Inhibitor Delivery: Implications for EV-Mediated Sensitisation

One limitation of the approach in this study is that miRNA inhibitors were co-applied directly to DRG neurones alongside EVs, rather than being pre-incubated with the vesicles. EVs could also alter recipient cell regulatory RNA expression, further contributing to the sensitising effect. While this design better models simultaneous neuronal exposure, it introduces uncertainty regarding inhibitor uptake and engagement with target miRNAs. An alternative approach was considered involving overnight incubation of EVs with the miRNA inhibitor, followed by re-isolation to remove unbound inhibitor prior to application to DRG neurones. However, this

strategy was ultimately not pursued due to concerns about EV loss during the additional processing steps, which would likely compromise the EV-mediated effect - particularly given the limited yield of EVs from the primary glial cultures.

While miR-146a-5p inhibition prevented EV-induced neuronal sensitisation, the effects could reflect either direct delivery of EV-encapsulated miRNA or modulation of endogenous miRNA in recipient neurones. Direct application of miR-146a-5p inhibitor without inflammatory stimulation had no effect, indicating that EV-mediated delivery in an inflammatory context is required. Nonetheless, the robust prevention of EV-induced sensitisation following miR-146a-5p inhibition highlights its central role and justifies closer examination of its predicted targets. Future studies could incorporate fluorescently labelled inhibitors to confirm neuronal uptake and intracellular localisation, or assess downstream target knockdown as a functional readout of engagement. Complementary strategies such as engineering inhibitor-containing EVs, or directly characterising EV miRNA cargo from the mixed glia, would provide valuable validation and more physiologically relevant insights.

5.4.6 Regulation of Neurotransmission-Associated Genes by miR-146a-5p

Following the identification of miR-146a-5p as a key mediator of EV-induced neuronal sensitisation, I next sought to investigate its potential molecular mechanisms and downstream targets. Bioinformatic prediction of high-confidence miR-146a-5p targets in *Mus musculus* was followed by GO enrichment analysis to identify functionally relevant pathways.

This analysis revealed significant enrichment of synaptic and neurotransmission-related processes, including 'neurotransmitter secretion', 'signal release from synapse', 'signal release', and 'neurotransmitter transport' (fold enrichment $\sim$6.5-7.5; Table 5.7). These processes are consistent with regulation of vesicle trafficking, transmitter handling, and neuronal communication. In contrast, GO terms related to

sensory perception and primary nervous system processes (e.g., 'sensory perception of chemical stimulus' and 'nervous system process') were markedly underrepresented (fold enrichment < 0.01), indicating that miR-146a-5p is unlikely to directly regulate canonical sensory transduction mechanisms such as ion channels or noxious stimulus receptors.

Although dissociated DRG cultures cannot form synapses with second-order neurones, they can form synaptic connections with each other (Bayat et al., 2021). Thus, enrichment for neurotransmission-related categories suggests that miR-146a-5p may disrupt homeostatic communication between sensory neurones. Such disruption could impair vesicle cycling and transmitter release, thereby promoting neuronal hyperexcitability and inflammatory signalling - hallmarks of sensitisation (Hehn, Baron, and Woolf, 2012). Consistent with this model, inhibition of miR-146a-5p prevented the EV-induced inflammatory response and preserved neuronal responsiveness, suggesting that blocking this miRNA releases repression on neurotransmission-associated genes, maintaining neuronal homeostasis.

5.4.7 Select Downstream Targets of miR-146a-5p Are Involved in Anti-Inflammatory Processes and Decrease Neuronal Excitability

In addition to GO pathway analysis linking neurotransmission, I identified a number of genes in the list of predicted miR-146a-5p targets with established roles in suppressing neuronal excitability and inflammation. As miRNAs act by downregulating their target transcripts, delivery of miR-146a-5p (for example via glial-derived EVs) would be expected to reduce the expression of these protective genes, thereby releasing restraints on excitability and promoting sensitisation. For instance, the potassium channel TREK-2 (*Kcnk10*) is selectively expressed in nociceptive neurones, and normally stabilises resting membrane potential and reduces excitability; its downregulation (for example by miR-146a-5p) has been shown to enhance neu-

ronal firing and contribute to pain hypersensitivity (Acosta et al., 2014; Messina, Peralta, and Acosta, 2022). The glutamate transporter EAAT2/GLT-1 (*Slc1a2*) is essential for maintaining low extracellular glutamate concentrations. Although predominantly expressed in astrocytes, silencing by miR-146a-5p would have direct consequences for neuronal function *in vivo*: reduced expression elevates extracellular glutamate, enhancing excitatory drive onto neurones and increasing susceptibility to hyperexcitability, enhanced synaptic transmission, and excitotoxicity (Morel et al., 2013). Other targets included negative regulators of kinase signalling, such as *Dusp16* and *Deptor*, which restrain pro-inflammatory JNK/p38 MAPK and mTOR pathways, respectively. Inhibition of these proteins would be expected to enhance neuronal responsiveness by increasing excitatory ion channel expression, receptor trafficking, and pro-inflammatory mediator production, thereby potentiating synaptic signalling (Catena and Fanciulli, 2017; Niedzielska et al., 2014; Zhang et al., 2015). In sensory neurones, such changes could contribute to hyperexcitability and sensitisation, consistent with established mechanisms of nociceptor modulation and inflammatory or neuropathic pain.

A second cluster of predicted targets were associated with anti-inflammatory or neuroprotective functions. Genes such as *Axl* contribute to the suppression of pro-inflammatory signalling (Wu, McBride, and Zhang, 2018). Signalling molecules, such as *ErbB4*, have further been implicated in maintaining neuronal stability, modulating pain and reducing hyperexcitability in pathological states. *ErbB4* is a receptor tyrosine kinase that plays a crucial role in sensory neurones; conditional knockout results in reduced pain hypersensitivity in inflammatory pain models. Gene expression analyses indicated that *ErbB4*-mediated regulation involves the calcium signalling pathway, which is vital for maintaining neuronal excitability and synaptic plasticity (Guo et al., 2024). Neurotrophic factors, such as *Gdnf*, support neuronal survival, stabilise ion channel expression, and maintain normal excitability - suppressing *Gdnf* leads to increased sensory neurone excitability and heightened pain sensitivity via enhanced expression of excitatory ion channels (Yuan et al.,

2022).

As mentioned in the previous section, this contrasts with reports in hippocampal neurones where miR-146a-5p can reduce spontaneous activity (Fan et al., 2022). There are also many downstream targets involved in pro-inflammatory processes, such as *Traf6* and *Irak1* (Hassan et al., 2024). Such opposing roles likely reflect cell type- and context-specific targeting: in excitatory cortical or hippocampal neurones, suppression of innate immune mediators may limit hyperactivity, whereas in peripheral sensory neurones, enrichment of miR-146a-5p in inflamed glial EVs may preferentially silence protective targets, thereby driving pro-algesic signalling. This context dependence provides an important framework for interpreting the gene ontology analysis and experimental findings.

Taken together, these predictions support a model in which glial-derived EVs containing miR-146a-5p may drive EV-induced neuronal sensitisation by repressing genes involved in neuronal communication, as well as genes that normally restrain excitability and inflammation. Thus, the pro-algesic action of miR-146a-5p may derive from a dual mechanism: positive regulation of neurotransmission alongside the suppression of protective, homeostatic pathways. This provides a coherent explanation for the experimental finding that blocking miR-146a-5p prevented EV-induced sensitisation: by preserving the expression of transcripts that normally suppress neuronal excitability and inflammation, inhibitor treatment reverses the pro-nociceptive influence of glial EV cargo. In order to test this, rescue experiments could be performed, for example using siRNA-mediated knockdowns against the genes listed above, to determine which are functionally involved in the miRNA-mediated increase in neuronal excitation.

5.4.8 Interspecies Variation

Species-specific differences in miR-146a-5p target profiles further complicate translational applications. While *Traf6* and *Irak1* are conserved targets, others such as

Clasp1 and *Kras* differ between mouse and human. This underscores the need for human validation of miRNA targets before clinical translation.

These findings suggest that although miR-146a-5p could contribute to EV-induced sensitisation in both species, the specific downstream mechanisms may differ. Although the GO data from the human gene list strongly supports that miR-146a-5p targets key regulators of neurotransmission - processes that are central to maintaining neuronal function and excitability, the mouse gene list indicates the targeting of neurotransmitter release and synapse function. By repressing these processes, the miRNA promotes a pro-inflammatory, pro-sensitisation phenotype when delivered via glial EVs.

My results support a model in which miR-146a-5p, delivered to DRG neurones via glial-derived EVs, contributes to peripheral sensitisation by repressing genes involved in neurotransmission. This repression may promote neuronal hyperexcitability, creating a permissive environment for sustained nociceptive signalling. Rather than directly modulating sensory receptor function, miR-146a-5p appears to influence downstream excitability and inflammatory signalling pathways that amplify pain transmission.

Confirming these pathways at different developmental stages, as well as *in vivo* - for example through EV injection studies or transgenic mouse models - will be essential to fully understand the clinical relevance of this pathway in chronic pain. However, given the species-specific differences in predicted target profiles, future work requires validation of key human targets which may reduce the translational relevance. Nevertheless, miR-146a-5p represents a promising therapeutic target to counteract inflammation-induced neuronal sensitisation.

5.4.9 Conclusions

This work identifies glial-derived EVs as active drivers of sensory neurone sensitisation and highlights miR-146a-5p as a mediator of this process. By showing that

inhibition of miR-146a-5p is sufficient to rescue the sensitising effect of inflamed glial EVs, these findings reveal a novel mechanism through which miRNAs disrupt neuronal homeostasis. Rather than directly altering sensory transduction, miR-146a-5p appears to dysregulate the normal control of excitability, tipping neurones into a hyper-responsive state.

To refine mechanistic understanding, future work should:

- Isolate EVs from individual glial subtypes.
- Further characterise EVs via RNA-Seq/proteomics, TEM imaging, and testing freeze-thawing effects.
- Validate miR-146a-5p in *in vivo* models.
- Investigate EV uptake pathways using live-cell fluorescent imaging and uptake inhibitors.
- Use protein fractions in functional assays.

From a translational perspective, miR-146a-5p represents a promising therapeutic target for preventing or reversing pathological neuronal sensitisation. Engineered EVs could ultimately be harnessed to deliver anti-inflammatory cargo or block pronociceptive signals, offering a novel route for disease modification in chronic pain. Testing these strategies in rodent models and transgenic systems will be crucial for evaluating their potential to shift the neuroinflammatory response toward resilience and recovery.

Chapter 6

General Discussion and Future Work

6.1 Compartmentalised Mechanisms of Pain Sensitisation

Pain arising from inflammation can be persistent and difficult to treat, in part because it involves complex neuroimmune communication across multiple compartments of the sensory nervous system, which remains incompletely understood (Middleton et al., 2021; Staud, 2013). Pain perception is further shaped by individual psychological and social factors (Brewer and Baccei, 2020; Cohen, Vase, and Hooten, 2021; Zimmer et al., 2022), with current analgesics offering limited efficacy and frequently inducing off-target effects (Li, Angst, and Clark, 2001; Mercadante, Arcuri, and Santoni, 2019; NICE, 2021; Reisine and Pasternak, 1996). Consequently, chronic pain imposes a substantial socioeconomic burden through both healthcare costs and lost productivity (Brewer and Baccei, 2020).

Despite extensive study, most research has treated sensory neurones as morphologically and functionally uniform cells, overlooking the spatial compartmentalisation of their long axons, somata, and terminals (Atmaramani et al., 2021; Tsantoulas et al., 2013). This has limited our understanding of how local inflammatory signals can trigger widespread changes in neuronal function. In this thesis, I addressed this gap by combining compartmentalised and dissociated primary sensory neurone cultures with transcriptomic analysis and functional manipulation using siRNA, miRNA power inhibitors, and EV treatments. The goal was to uncover compartment-specific mechanisms of neuronal sensitisation that could be targeted for more precise and effective pain therapies.

My findings reveal that inflammatory signals at both peripheral and central terminals drive long-lasting changes in sensory neurone excitability via spatially localised and molecularly distinct pathways. More broadly, this work demonstrates that DRG neurones integrate information across complex spatiotemporal domains, relying on local translation, cell-cell communication, and microenvironmental cues to shape their functional responses. These insights not only advance our understanding of pain pathogenesis but also highlight new molecular targets for spatially

tailored therapeutic intervention.

6.2 Spatially Distinct Transcriptomic Responses to PGE_2

PGE_2 is a well-established pro-inflammatory mediator that acts directly on sensory neurones via EP receptors to increase their excitability (Jang, Kim, and Hwang, 2020). Although EP receptors are expressed on both axons and somata of nociceptive sensory neurones (Kimourtzis et al., 2024; St-Jacques and Ma, 2013; Woodhams et al., 2007), most previous studies have used whole-cell PGE_2 application (Gu, Kwong, and Lee, 2003; Lopshire and Nicol, 1997; Wei et al., 2024) and short incubation times (Gu, Kwong, and Lee, 2003; Kimourtzis et al., 2024; Lopshire and Nicol, 1997; Moriyama et al., 2005; Rangwani, 2018; Southall and Vasko, 2001; St-Jacques and Ma, 2013; Vasko, Campbell, and Waite, 1994; Wei et al., 2024), overlooking the spatial specificity and temporal persistence of exposure to PGE_2 *in vivo*. In Chapter 3, I addressed this gap by applying PGE_2, for a prolonged period of time, exclusively to the distal axons of DRG sensory neurones cultured in compartmentalised microfluidic chambers, thereby mimicking a persistent, peripheral inflammatory insult while isolating the site of stimulation.

This approach revealed that local activation of EP receptors at the axon terminal is sufficient to induce sensitisation at the soma, consistent with a model of retrograde signalling from the periphery to the cell body (Clark et al., 2018). These findings provide direct functional evidence that spatially restricted PGE_2 signalling can drive long-range changes, as demonstrated in previous studies (Ben-Yaakov et al., 2012; Clark et al., 2018; Hanz et al., 2003; Kar et al., 2013; Lucci et al., 2020), pointing to possible local translation or trafficking. Preliminary evidence suggested that EP_4 was involved in this sensitisation effect, supported by the literature (Kimourtzis et al., 2024; Southall and Vasko, 2001; St-Jacques and Ma, 2013). To confirm TRPV1-dependence, immunocytochemistry for protein expression and $TRPV1^{-/-}$ mice could be used to assess if the effects are abolished. More broadly, this work highlights the utility of combining dissociated and compartmen-

talised neuronal culture systems to probe distinct subcellular compartments, depending on the experimental question, and underscores the importance of incorporating spatial resolution into studies of inflammatory sensitisation (Gale et al., 2022). By modelling localised signalling events and testing candidate pathways under controlled conditions, these systems offer a powerful translational platform for validating mechanisms that may drive pain processing in intact organisms.

Transcriptomic profiling of axons following PGE_2 treatment revealed widespread changes in gene expression, including the upregulation of transcripts involved in inflammatory signalling and receptor and ligand activity (Arendt-Tranholm, 2022; Pope et al., 2025). These findings support the idea that axons are not passive conduits but actively respond to extracellular cues through compartmentalised gene regulation (Gale et al., 2022; Holt, Martin, and Schuman, 2019). Among the transcripts elevated in the axonal compartment was *Tnfrsf12a*, a receptor that has only recently been linked to pain in two *in vivo* studies (Huang et al., 2019; Huang et al., 2025), and its role in nociceptive neurones at the subcellular level remains unexplored. Although *Tnfrsf12a* is known to be upregulated in inflammatory conditions and in whole DRG tissue *in vivo* (Huang et al., 2019; Huang et al., 2025; Inta et al., 2008; Tanabe et al., 2003; Potrovita et al., 2004), its localisation within axons and its functional impact on neuronal excitability had not been characterised.

Building on these observations, in Chapter 4 I wanted to demonstrate that *Tnfrsf12a* was functionally relevant in sensory neurone sensitisation. siRNA-mediated knockdown of *Tnfrsf12a* reduced TRPV1-mediated calcium responses to capsaicin, indicating that TNFRSF12A is not only present in nociceptive neurones (Huang et al., 2019; Tanabe et al., 2003) but also functionally required for sensitisation. These results suggest that TNFRSF12A may act as a convergence point for inflammatory signals within sensory neurones.

These findings have important implications for understanding how inflammatory signals originating in the periphery influence neuronal excitability at the cell body,

shaping nociceptive output. They suggest that the peripheral axon is not merely a site of stimulus detection, but a critical initiator of long-range signalling events that contribute to persistent sensitisation (Ferrari et al., 2013; Ferrari, Bogen, and Levine, 2014; Gale et al., 2022). The identification of *Tnfrsf12a* as an axonally enriched transcript, that functionally contributes to TRPV1-mediated responses, highlights how specific molecular mediators can translate local inflammatory stimuli into broader changes in excitability. Its axonal localisation and necessity for sensitisation make TNFRSF12A a compelling candidate for therapeutic targeting in chronic inflammatory pain.

While siRNA knockdown implicates TNFRSF12A in sensitisation, the downstream signalling pathways linking local receptor activation to somatic excitability remain to be defined. Future studies could leverage compartmentalised cultures alongside transcriptomic or proteomic profiling to identify axonally initiated cascades downstream of TNFRSF12A, including the involvement of NF-κB and MAPK pathways. Functional interrogation - via targeted knockdown, pharmacological inhibition, or overexpression of candidate effectors - may reveal how receptor-mediated signalling alters intrinsic membrane properties and action potential firing. Investigating TWEAK ligand levels will also be key to clarifying TNFRSF12A's role in peripheral sensitisation and its therapeutic relevance.

Together, these results underscore the value of spatially compartmentalised models in pain research, as conventional dissociated cultures may obscure directional communication and the contributions of axonally localised signalling molecules (Giorgi et al., 2023; Kimourtzis et al., 2024; Tsantoulas et al., 2013). Importantly, this work offers a translational framework for identifying therapeutic targets that act at the level of the peripheral axon - where early intervention could prevent the propagation of sensitising signals to the soma and central terminals. By pinpointing molecules such as TNFRSF12A that mediate axon-initiated excitability changes, future therapies may selectively disrupt maladaptive signalling before it culminates

in chronic pain, enabling more precise modulation of pain pathways with reduced off-target effects.

6.3 Glial-Derived EVs Contribute to Central Terminal Sensitisation

Sensory neurone sensitisation does not occur in isolation, but within a dynamic microenvironment shaped by glial cells, extracellular signals, and intercellular communication. Rather than adopting a soma-centric view, the next chapter explored glia-neurone communication within a spatially complex and interactive cellular landscape where astrocytes, microglia, and neurones exchange information through vesicle-mediated mechanisms (Ahmad et al., 2022; Prada et al., 2018; Zhu et al., 2025). By investigating the interactions between mixed glia and DRG neurones, in Chapter 5 I aimed to contribute to a broader understanding of how localised signalling environments shape neuronal responsiveness and plasticity within the nervous system.

Glial cells in the spinal cord are established contributors to central sensitisation (Latremoliere and Woolf, 2009), yet the mechanisms by which they communicate with sensory neurones remain incompletely understood. EVs are emerging as a key mode of glia-neurone communication, but their role in driving neuronal sensitisation during inflammation is still largely unexplored (Ahmad et al., 2022). Many studies use isolated glial populations (Chaudhuri et al., 2018; Prada et al., 2018), but mixed glial cultures more closely recapitulate the *in vivo* environment, allowing interactions between astrocytes, microglia, and oligodendrocytes to modulate each other's behaviour (Ahmad et al., 2022; Liddelow et al., 2017). Whether EVs alone can induce sensitisation remains an emerging area of investigation (Datta Chaudhuri et al., 2020; Gabrielli et al., 2015; Li et al., 2017).

To address these gaps, I applied EVs derived from cytokine-stimulated (Liddelow et al., 2017), spinal-derived mixed glial cultures to DRG sensory neurones. These

EVs were sufficient to induce sensitisation, and further investigation identified miR-146a-5p as a critical mediator: inhibition of this miRNA prevented EV-induced increases in neuronal excitability. This demonstrates a vesicle-mediated pathway by which glia can influence sensory neurone function, potentially contributing to the transition from acute to chronic pain (Kaurani et al., 2025; López-Cepeda et al., 2022; Tan et al., 2013). Interestingly, although miR-146a-5p is generally described as an anti-inflammatory regulator (Grace et al., 2018; Liu et al., 2024; Lu et al., 2015; Lu et al., 2018; Pauley and Cha, 2011), its pro-nociceptive effect here reflects the context- and cell-type specificity of miRNA action, likely through suppression of anti-nociceptive or cytoskeletal regulatory genes. This role is also supported by involvement in hyperexcitability (Fan et al., 2022; Lei et al., 2021; Mao et al., 2023), pro-inflammatory processes (Ibáñez et al., 2019; Johnson et al., 2017; Liu, Lu, and Fu, 2022; Long et al., 2025), and its variable effects between disease types and stages, and via different downstream pathway activation (Fan et al., 2020; Long et al., 2025; Mao et al., 2023).

GO analysis of predicted miR-146a-5p targets in *Mus musculus* further supports a pro-nociceptive mechanism. Targets were enriched in neurotransmission-related processes ('neurotransmitter secretion', 'signal release from synapse', 'neurotransmitter transport') while categories such as 'sensory perception' and general nervous system processes were under-represented. Some predicted targets have established roles in restraining excitability and inflammation, including potassium channel TREK-2, the glutamate transporter EAAT2/GLT-1, negative regulators of kinase signalling (*Dusp16*, *Deptor*), anti-inflammatory gene *Axl*, and neurotrophic signalling molecules (GDNF, ErbB4; Acosta et al., 2014; Catena and Fanciulli, 2017; Guo et al., 2024; Messina, Peralta, and Acosta, 2022; Morel et al., 2013; Niedzielska et al., 2014; Wu, McBride, and Zhang, 2018; Yuan et al., 2022; Zhang et al., 2015). Suppression of these protective targets, alongside a strong association with synaptic and neurotransmission-related processes, provides a coherent explanation for the observed pro-algesic effect of glial EV-derived miR-146a-

5p.

These results reveal a novel mechanism of glia-neurone communication, whereby EVs deliver miRNAs that modulate central terminal excitability. They underscore the importance of cellular context in interpreting miRNA function: targets known to suppress activity in hippocampal neurones (Fan et al., 2022) may be differentially regulated in sensory neurones, or miR-146a-5p may exhibit preferential binding to alternative downstream targets depending on neurone type - potentially shifting miR-146a-5p's role from anti-inflammatory to pro-nociceptive. Species conservation is another key consideration, as several predicted miR-146a-5p targets were not equally conserved between mouse and human, suggesting functional outcomes may vary across systems. Future studies should employ human iPSC-derived neurones and test causality by rescuing the effects of miR-146a-5p inhibition by suppressing downstream targets. Complementary approaches could include blocking EV uptake with reuptake inhibitors or using compartmentalised cultures to distinguish axonal versus somatic effects. Ultimately, *in vivo* validation will be critical to determine whether this mechanism contributes to nociceptive processing in the intact nervous system. If confirmed, this pathway could offer new therapeutic avenues for targeting chronic pain at the level of glia-neurone interactions.

6.4 Considerations for Future Experimental Design

While this thesis provides novel insights into subcellular mechanisms of neuronal sensitisation, future studies could build on these findings by incorporating systems of greater cellular and architectural complexity. Isolated *in vitro* models offer powerful tools for dissecting compartment-specific mechanisms, but complementary approaches, including co-culture systems, 3D environments, and *in vivo* validation, will be essential for translating these insights into broader neurobiological contexts (Chrysostomidou, Cooper, and Weir, 2021; Caparaso, Redwine, and Wachs, 2023; Fan et al., 2014).

6.4.1 Primary Neurone Cultures

Experiments were conducted in primary sensory neurone monocultures, which enabled precise interrogation of neurone-intrinsic mechanisms. To further explore cell-cell interactions that contribute to peripheral and central sensitisation, future studies could incorporate satellite glia, immune cells, and vascular elements known to modulate nociceptive signalling *in vivo* (Dubin and Patapoutian, 2010; Krames, 2015). Additionally, transitioning from two-dimensional cultures to three-dimensional hydrogels may improve structural fidelity and axonal outgrowth, though optimisation for calcium imaging would be required due to altered diffusion kinetics (Caparaso, Redwine, and Wachs, 2023).

6.4.2 Embryonic Cultures

Embryonic DRG neurones offer high yield, viability, and tractability, making them well-suited for mechanistic studies of axonal regulation. While postnatal experience is required for full circuit maturation (Sections 1.9.2 and 1.3.1), transcriptomic comparisons suggest that most axonal mRNAs identified in E16.5 neurones are also present in adult DRG neurones (Pope et al., 2025). Future work could complement these findings with postnatal or adult cultures to assess developmental regulation and validate compartment-specific mechanisms across maturation stages (Owen and Egerton, 2012).

6.4.3 Compartmentalised Microfluidic Cultures

Microfluidic chambers enabled precise spatial manipulation of neuronal compartments and facilitated studies of retrograde and anterograde signalling (Clark et al., 2018; Cox et al., 2008; Kimourtzis et al., 2024; Lucci et al., 2020; Pope et al., 2025). While highly effective for modelling directional signalling, these systems present technical considerations that can inform future optimisation:

- Seeding cells into narrow channels requires precision, and uneven distribu-

tion may affect consistency. Seeding at an angle under a microscope improves control and could enhance reproducibility across experiments.

- Axonal outgrowth across channels varies, particularly for small subpopulations such as TRPV1$^+$ nociceptive neurones. Future studies may benefit from enrichment protocols or tailored growth factor gradients to increase the pool of analysable cells (Atmaramani et al., 2021; Giorgi et al., 2023).

- Fluid flow within the device can introduce mechanical artefacts during imaging or media changes. While flow controls confirmed minimal pressure-induced calcium transients in this study, automated pipetting systems could further reduce variability and improve consistency.

- PDMS-based devices promote rapid water loss, risking osmolarity fluctuations in low-volume chambers (Halldorsson et al., 2015). Frequent media changes mitigated this effect, though they would have introduced mechanical stress. Future designs using alternative materials or humidity-controlled environments may improve cell viability and reduce handling burden.

6.4.4 Calcium Imaging as a Functional Readout

Calcium imaging provided a robust, compartment-resolved proxy for neuronal excitability (Atmaramani et al., 2021), but it has several inherent limitations. Calcium transients are slower than membrane potential changes and therefore cannot capture the precise timing of action potentials. Fluorescence intensity reflects intracellular calcium levels rather than direct electrical activity, meaning that changes in signal amplitude may not scale linearly with neuronal firing (Quicke, Howe, and Foust, 2023). Additionally, calcium responses can be influenced by receptor expression, compartmental distribution and prior stimulation, which can lead to desensitisation or tachyphylaxis, particularly during repeated agonist applications (Lawrence et al., 2021). However, Clark et al. (2018) showed that repeat stimulation every five minutes with KCl did not induce desensitisation or tachyphy-

laxis, indicating that the stimulation protocol used here is acceptable. To complement this approach, future studies could integrate patch-clamp electrophysiology for single-cell resolution, microelectrode arrays for network-level activity, and voltage-sensitive dyes for spatiotemporal mapping (Bayat et al., 2021; Kimourtzis et al., 2024; McGowan et al., 2018). Each method offers distinct advantages and trade-offs in resolution, coverage, and invasiveness. Combining these tools with genetic and pharmacological manipulation will further refine our understanding of excitability dynamics across compartments.

6.4.5 Retrograde vs Anterograde Signalling and Terminal Modelling

Compartmentalised cultures enabled modelling of peripheral and central terminals, though simplifications were necessary. Two-channel chambers were used instead of three-channel designs, requiring careful interpretation of terminal identity. In these experiments, peripheral terminals were modelled by seeding neurones in one compartment and applying inflammatory stimuli (PGE_2) to the distal axonal compartment, mimicking peripheral exposure. Central terminals were modelled by applying spinal cord-derived glial EVs to DRGs, reflecting the anatomical orientation of DRG neurones projecting centrally into the dorsal horn. While this approach provides a tractable framework for studying directional signalling, future studies could incorporate tri-compartmental systems or retrograde tracers to more precisely validate terminal-specific responses. Nonetheless, the observed retrograde signalling from peripheral axons to soma and EV-mediated central terminal sensitisation underscore the utility of these models in dissecting spatially distinct mechanisms of neuronal plasticity.

6.5 Future Directions

While the experimental systems used in this thesis provided valuable insight into subcellular mechanisms of neuronal sensitisation, there are several areas for fur-

ther investigation. Investigating downstream signalling cascades activated by peripheral EP receptor or TNFRSF12A receptor stimulation, and validating the targets of glial EV-derived miR-146a-5p in sensory neurones, would clarify the molecular underpinnings of compartment-specific sensitisation. Integrating additional cell types and direct electrophysiological measurements could increase physiological relevance and allow more precise characterisation of excitability changes. Moreover, extending these findings to human iPSC-derived sensory neurones or *in vivo* models would test the translational potential of compartment-targeted interventions. By addressing these questions, future studies can build on the framework established here to further elucidate the mechanisms of inflammatory pain and identify strategies for targeted, subcellular-level therapeutic modulation. Future directions are summarised below.

Downstream Signalling Pathways

- Extend *Tnfrsf12a* siRNA incubation to achieve more complete knockdown, with the addition of pro-inflammatoy PGE_2.
- Confirm TNFRSF12A protein reduction via Western blot or immunocytochemistry.
- For TNFRSF12A, quantify TWEAK ligand levels, determine downstream effectors (such as NF-κB and MAPK pathways), and assess how these pathways converge on TRPV1 and other excitability regulators.
- Use an siRNA-based approach to perform rescue experiments, selectively knocking down candidate genes to identify which are functionally required for the miR-146a-5p-driven increase in neuronal excitability.
- Perform immunocytochemistry for quantification of other EP receptors and TRPV1 levels in PGE_2 experiments.

Mechanistic Elucidation of EV-Mediated Sensitisation

- Perform further characterisation: TEM, proteomics, freeze-thawing investiga-

tions, EVs from individual glia.

- Pre-incubate EVs with miRNA inhibitors, re-isolate, and apply to DRGs to confirm that the miRNAs are encapsulated and delivered to neurones within the vesicles.
- Assess the contribution of other EV cargo (proteins, lipids, additional miRNAs) to reveal potential combinatorial effects on neuronal excitability and central sensitisation.

Advanced Culture Models

- Use compartmentalised chambers to localise glial EV exposure, adding physiological complexity and resolving terminal-specific effects.
- Use retrograde tracers to selectively label neurones with axons that have crossed into the distal compartment, confirming terminal identity and enabling targeted analysis of compartment-specific responses.
- Incorporate satellite glia in DRG cultures to provide a more physiologically relevant environment for exploring neuronal responses to inflammatory signalling.
- Use three-channel compartmentalised microfluidic chambers, placing sensory neurones centrally and macrophages and mixed glia in separate lateral compartments, to better replicate physiological neuroimmune architecture.
- Investigate EV uptake mechanisms by using inhibitors and fluorescent labels.

Electrophysiological and Imaging Approaches

- Complement calcium imaging with patch-clamp electrophysiology or voltage-sensitive dyes to allow direct measurement of action potential generation and intrinsic membrane properties, providing a more detailed picture of sensitisation.

Traditional and Alternative Models

- Use iPSC-derived human sensory neurones to test whether the compartment-specific mechanisms and miRNA-mediated effects identified in mouse DRG cultures are conserved in humans.
- Investigate the *in vivo* relevance of glial EV-mediated sensitisation, for example via targeted delivery of miRNA inhibitors in animal models of inflammatory pain.
- Inject *Tnfrsf12a* siRNA into rodent models of PGE_2-induced models of pain.
- Create $TRPV1^{-/-}$ cells, or animal models, to determine if the effects of PGE_2 and *Tnfrsf12a* are TRPV1-dependent.

By addressing these questions, future research can build upon the framework established here to elucidate the cellular and molecular basis of inflammatory pain, with the goal of developing compartment-targeted therapeutics that minimise systemic side effects.

6.6 Thesis Conclusions

Together, these studies support a multi-compartmental, multi-modal view of sensory neurone sensitisation, revealing how spatially distinct signalling pathways converge to shape neuronal excitability. The mechanisms uncovered - local translation, EV-mediated communication, and compartment-specific transcriptomic regulation - likely extend beyond sensory neurones to inform broader principles of nervous system communication.

At the peripheral terminal, PGE_2 stimulation not only sensitised TRPV1 channels locally but also induced long-term somatic changes through retrograde signalling and local translation. TNFRSF12A emerged as a mediator of these effects, potentially linking extracellular inflammation with intracellular pathways that regulate neuronal excitability. At the central terminal, glial-derived EVs delivered regulatory miRNAs, notably miR-146a-5p, which modified neuronal function without re-

quiring direct cell-cell contact. Each mechanism operated within a distinct spatial domain - the soma, peripheral axons, and central terminals - yet converged on a common functional outcome: heightened responsiveness to noxious input (Figure 6.1).

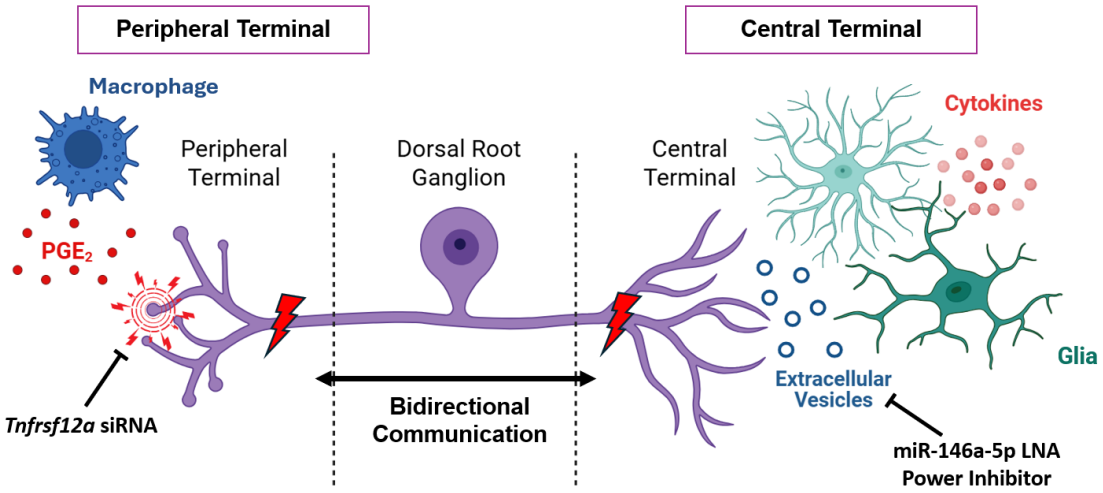


Figure 6.1. Bidirectional Modulation of Sensory Neurone Sensitisation via Peripheral and Central Terminals. PGE_2, released by local immune cells such as macrophages following tissue injury, was applied to axon terminals of sensory neurones cultured in compartmentalised microfluidic devices. Calcium imaging demonstrated sensitisation both locally at the axon terminal and retrogradely at the soma, indicative of an axon-initiated inflammatory signal. This sensitisation was dependent on capsaicin-sensitive TRPV1 channels. Glia became inflamed upon cytokine stimulation at the central terminal of sensory neurones, leading to the secretion of EVs containing pro-inflammatory cargo. Uptake of these EVs by sensory neurones enhanced neuronal excitability, indicating a contribution to sensitisation. Notably, application of a miR-146a-5p inhibitor alongside glial EVs prevented this sensitisation, highlighting miR-146a-5p's critical role in modulating this inflammatory process. Created using BioRender™.

These findings highlight the importance of spatiotemporal and compartmentalised processes in nervous system communication. Local translation, EV signalling, and domain-specific transcriptomic regulation allow neurones to adapt dynamically to their microenvironment through decentralised mechanisms of excitability and plasticity (Ahmad et al., 2022; Ferrari et al., 2013; Gale et al., 2022; Holt, Martin, and Schuman, 2019). Within this context, subcellular experimental models - including microfluidic chambers and targeted siRNA approaches - proved invaluable for dissecting the spatial mechanisms of pain signalling. While *in vivo* models remain essential for capturing whole-organism behaviour, *in vitro* systems enabled fine-

grained resolution of the cellular and molecular dynamics that drive sensitisation (Chrysostomidou, Cooper, and Weir, 2021).

The identification of *Tnfrsf12a* and miR-146a-5p as spatially restricted regulators of excitability provides new opportunities for compartment-targeted analgesia, potentially avoiding the systemic side-effects of current pain treatments (Mercadante, Arcuri, and Santoni, 2019). Future work should define the downstream targets of miR-146a-5p in neurones, map the signalling cascades activated by TNFRSF12A, and explore how these compartment-specific pathways interact under conditions of persistent inflammation or neuropathic injury. By integrating transcriptomics, functional imaging, and compartment-specific manipulation, this thesis establishes a framework for uncovering both cell-intrinsic and cell-extrinsic drivers of chronic pain.

In summary, this work provides novel insight into the compartment-specific mechanisms of inflammatory sensitisation in primary sensory neurones. Using dissociated and compartmentalised DRG cultures, transcriptomic profiling, and functional manipulation with siRNA, miRNA inhibitors, and glial-derived EVs, I demonstrate that inflammatory signals at both peripheral and central terminals induce long-lasting, spatially localised changes in neuronal excitability. These findings advance both fundamental neuroscience and translational pain research by clarifying how compartment-specific signalling shapes sensitisation and by laying the groundwork for targeted therapies with improved efficacy and reduced systemic side-effects.

Chapter 7

Appendix

Table A1. siRNA Sequences Used for Knockdown.

Target	Sequences
Tnfrsf12a	F 5'-GACCTCGACAAGTGCATGGA and R 3'-GCCAAAACCAGGACCAGACT
siRNA control non-targeting pool	UGGUUUACAUGUCGACUAA, UGGUUUACAUGUUUUCUGA, UGGUUUACAUGUUUUCCUA, UGGUUUACAUGUUGUGUGA

Table A2. Primers Used for Quantitative Real-Time PCR.

Gene	Forward Primer	Reverse Primer
Tnfrsf12a	5'-GACCTCGACAAGTGCATGGA	5'-GCCAAAACCAGGACCAGACT
Gapdh	5'-AAGAAGGTGGTGAAGCAGGC	5'-ATCGAAGGTGGAAGAGTGGG
Ube2	5'-TGCCTGAGATTGCTCGGATCT	5'-TCGCATACTTCTGAGTCCAATCC

Table A3. Primers Used for qPCR Validation of Transcriptomic Targets. Primer sequences used by the collaborator to assess *Tnfrsf12a* expression following transcriptomic analysis. *Gapdh* used as the housekeeper gene.

Gene	Forward Primer	Reverse Primer
Gapdh	5'-AAGAAGGTGGTGAAGCAGGC	5'-ATCGAAGGTGGAAGAGTGGG
Tnfrsf12a	5'-CATGGACTGCGCTTCTTGTC	5'-CAGTCTCCTCTATGGGGGTAGT

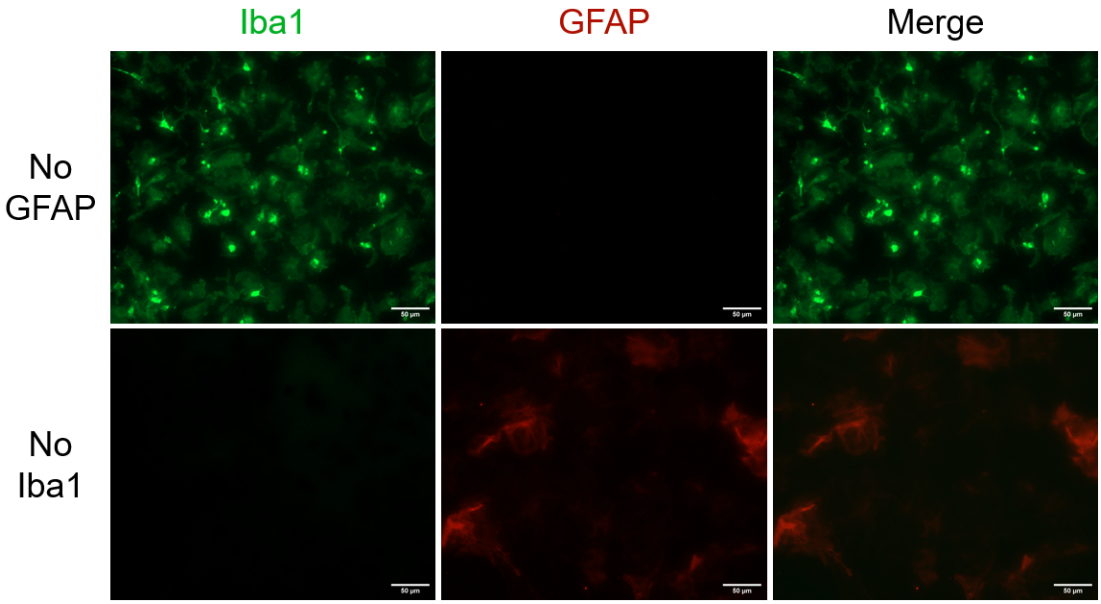


Figure A1. Controls Lacking Primary Antibody for Immunocytochemistry of Mixed Glial Cultures. Cells were stained with antibodies against Iba1 (microglia marker, first column) and GFAP (astrocyte marker, second column); merged images are shown in the third column. The top row represents the no GFAP primary antibody control, where only Iba1 primary antibody was included. The bottom row represents the no Iba1 primary antibody control, where only GFAP primary antibody was included. In both controls, omission of one primary antibody confirmed that secondary antibodies did not produce non-specific signal. 20x images; scale bar 50 μm.

Table A4. miRNA Power Inhibitor Sequences. Three miRNA targets were identified through a literature search, and Locked Nucleic Acid Power Inhibitors specific to these targets were purchased, along with a Negative Control A.

miRNA	Sequence	Reference Code	Accession Number
mmu-miR-142a-3p	CCATAAAGTAGGAAACACT	Y104100268-DDA	MIMAT0000155
hsa-miR-146a-5p	ACCCATGGAATTCAGTTCTC	Y104100676-DDA	MIMAT0000449
hsa-miR-181a-5p	ACTCACCGACAGCGTTGAATG	Y104101132-DDA	MIMAT0000256
Negative Control A	TAACACGTCTATACGCCCA	Y100199006-DDA	

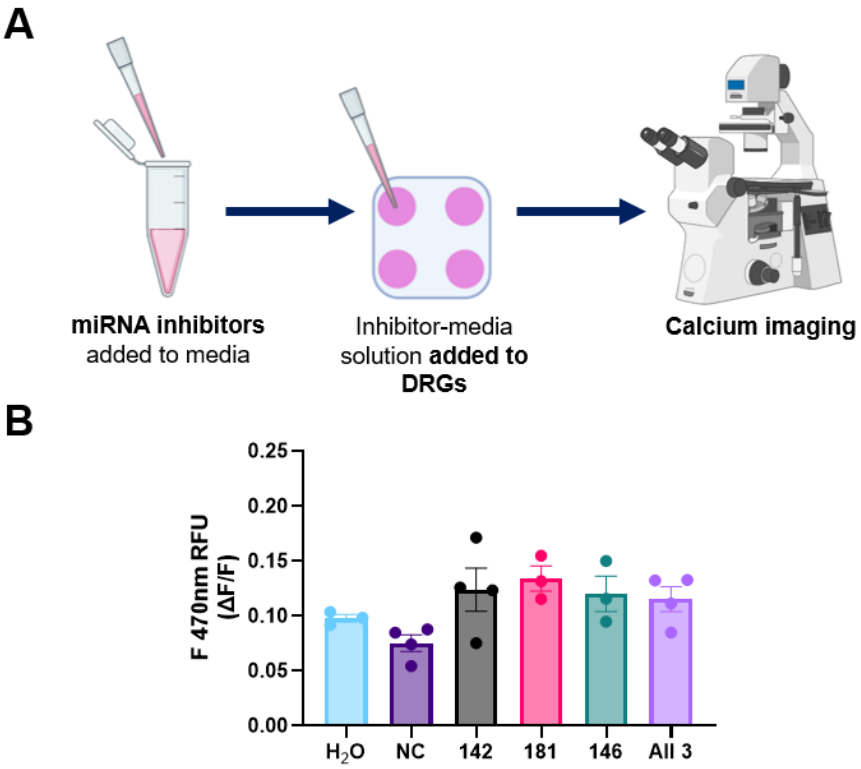


Figure A2. miRNAs Added Alone Did Not Affect Neuronal Excitability. A - Pilot protocol for miRNA inhibitor addition to DRG cultures alone. miRNA LNA power inhibitors were added to DRG complete media (final concentration of 100 nM). Negative control power inhibitor (NC) and dH_2O were used as controls. The inhibitor-media solution was then added to DRGs in inverted chambers, a few hours after seeding. 24 hours later, calcium imaging was performed, stimulating with 200 nM capsaicin. Created using BioRender. **B -** Quantification of peak calcium responses ($\Delta F/F$, mean ± SEM) in response to 200 nM capsaicin during calcium imaging. No significant difference was found between groups.
$N = 1$ biological replicate; $n \geq 3$ technical replicates. Data displayed as technical replicates. $p < 0.05$ was considered statistically significant.

Table A5. Expanded Biological Process Enrichment for miR-146a-5p Targets (Including Reference and Expected Counts.) GO-Slim enrichment analysis was performed using the PANTHER classification system to identify biological processes associated with predicted miR-146a-5p targets. The table includes the following metrics: Reference Count - number of genes annotated to each GO term in the Mus musculus reference list; Observed Count - number of genes from the input list annotated to the term; Expected Count - number of genes expected by chance; Fold Enrichment (FE) - ratio of observed to expected counts; Direction (+/-) - indicates overrepresentation (+) or underrepresentation (-); Raw *p*-value - unadjusted significance from Fisher's Exact Test; and False Discovery Rate (FDR) - adjusted *p*-value accounting for multiple testing.

Process	Reference Count	Observed Count	Expected Count	FE	+/-	p-value	FDR
Neurotransmitter secretion	44	7	0.94	7.45	+	3.73E-05	1.98E-02
Signal release from synapse	44	7	0.94	7.45	+	3.73E-05	1.58E-02
Signal release	50	7	1.07	6.56	+	8.71E-05	2.64E-02
Biological regulation	6133	169	130.88	1.29	+	1.11E-04	2.61E-02
Neurotransmitter transport	50	7	1.07	6.56	+	8.71E-05	2.31E-02
Sensory perception of chemical stimulus	492	0	10.50	<0.01	-	4.53E-05	1.60E-02
Sensory perception	538	0	11.48	<0.01	-	1.34E-05	1.42E-02
Nervous system process	574	0	12.25	<0.01	-	6.05E-06	1.28E-02
System process	658	1	14.04	0.07	-	1.44E-05	1.02E-02

PIPS Reflection Statement

Note to examiners:

This statement is included as an appendix to the thesis in order that the thesis accurately captures the PhD training experienced by the candidate as a BBSRC Doctoral Training Partnership student.

The Professional Internship for PhD Students (PIPS) is a compulsory 3-month placement which must be undertaken by DTP students. It is usually centred on a specific project and this reflective statement is designed to capture the skills development which has taken place during the student's placement and the impact on their career plans it has had.

PIPS Reflective Statement:

I undertook a three-month research placement at Medicines Discovery Catapult (MDC), based at Alderley Park in Macclesfield. I worked as an intern within the neurobiology team, gaining invaluable exposure to industry-led translational neuroscience. This experience significantly broadened my understanding of how cross-disciplinary research is applied in a commercial context and helped me develop a range of technical and professional skills that will shape my future career choices.

One of the main projects I contributed to involved working alongside a bioinformatician to develop a Python-based analysis pipeline for high-throughput calcium imaging. This introduced me to large-scale data acquisition and the importance of automated analysis in an industry setting. Another major focus of my placement was culturing and differentiating iPSC-derived sensory neurones and microglia, which were purchased from a range of commercial suppliers. I had previously worked with primary sensory neurones, but working with iPSC-derived cells required learning new protocols and understanding the variability between cell lines and about donor backgrounds. The team was investigating which iPSC lines most

closely resembled primary sensory neurones in terms of receptor presentation and responsiveness during calcium imaging. I contributed to experiments involving the stimulation of these cells with a range of agonists to assess their functional properties. This required precise planning, familiarity with cell handling over a multi-week differentiation period, and coordination with other team members to manage multiple overlapping time-points. Learning to work with iPSCs deepened my appreciation of their potential in modelling disease-relevant phenotypes.

A particularly exciting part of the placement involved using a different kind of microfluidic platform to model the spread of pathogenic proteins *in vitro* - specifically focusing on tau protein seeding, a hallmark of several neurodegenerative diseases. These platforms allowed the team to track the spatial spread of tau aggregates between connected compartments. I was involved in preparing and seeding these devices, immunostaining, and imaging using confocal microscopy, a technique I had not previously used. This hands-on work with cutting-edge platforms gave me practical insight into how complex biological processes like protein aggregation and transmission can be studied in a controlled environment, and it provided a useful point of comparison to the more acute pain models I typically work with in academia.

In addition to these technical projects, I fully immersed myself in the collaborative culture at MDC. I regularly attended cross-speciality lab meetings, project progress reviews, company-wide all-hands meetings (including one hosted at Jodrell Bank Observatory), and funding update sessions. Being present in these meetings gave me a much clearer sense of how project milestones are tracked in industry, how funding impacts scientific direction, and how different scientific and business teams work together to drive research developments. I was also given the opportunity to present my own work at one of the neurobiology team's cross-speciality meetings, which helped me practice pitching technical results to colleagues from other disciplines, a skill that is essential in both academia and industry.

A major highlight of the placement was the small team environment I worked in. Working in such a close-knit team allowed me to build strong professional relationships quickly, and I learned a great deal from observing how colleagues approached experimental troubleshooting, data interpretation, and collaborative problem-solving. I also benefitted from frequent team meetings; my colleagues were generous with feedback and encouraged me to take ownership of my aspects of the projects. This mentorship was especially helpful when navigating new techniques, and it helped me become more confident in asking questions and proposing ideas.

More broadly, the placement offered a unique window into the culture and values of industry-based research. It was fascinating to see how different specialisms - from molecular biology to data science - worked together under one roof to achieve a shared translational goal to deliver results for collaborators and clients. Witnessing this first-hand prompted me to reflect on the kind of work environment I enjoy, and it has led me to seriously consider industry as a potential career path after my PhD. I appreciated the pace of progress, the emphasis on application, and the opportunity to work across disciplinary boundaries in a more structured framework.

In summary, this internship was an incredibly valuable and formative experience. I gained new technical skills, such as iPSC differentiation, confocal microscopy, and microfluidic modelling, as well as soft skills in teamwork, scientific communication, and collaborative planning. I developed a better understanding of the strategic and commercial drivers behind translational neuroscience research and saw how scientific projects evolve in a cross-functional industrial setting. Most importantly, I left the placement feeling inspired by the potential of collaborative research to make real-world impact and motivated to explore how I can apply my own scientific training in similar environments in the future.

Bibliography

Acosta, Cristian et al. (2014). "TREK2 expressed selectively in IB4-binding C-fiber nociceptors hyperpolarizes their membrane potentials and limits spontaneous pain". In: *Journal of Neuroscience* 34.4, pp. 1494–1509. ISSN: 02706474. DOI: 10.1523/JNEUROSCI.4528-13.2014.

Ahmad, Shahzad et al. (2022). "Role of Extracellular Vesicles in Glia-Neuron Intercellular Communication". In: *Frontiers in Molecular Neuroscience* 15. ISSN: 16625099. DOI: 10.3389/fnmol.2022.844194.

Aley, Kochuvelikakam O and Jon D Levine (1999). *Role of Protein Kinase A in the Maintenance of Inflammatory Pain*. Tech. rep.

Amir, Ron, Martin Michaelis, and Marshall Devor (1999). "Membrane Potential Oscillations in Dorsal Root Ganglion Neurons: Role in Normal Electrogenesis and Neuropathic Pain". In: *The Journal of Neuroscience* 19.19, pp. 8589–8596.

Arendt-Tranholm, Asta (2022). "Axonal mRNA localisation and the development of peripheral sensitisation in vitro." PhD thesis. University of Nottingham. URL: https://eprints.nottingham.ac.uk/id/eprint/71713.

Atmaramani, Rahul et al. (2021). "Investigating the function of adult drg neuron axons using an in vitro microfluidic culture system". In: *Micromachines* 12.11. ISSN: 2072666X. DOI: 10.3390/mi12111317.

Baron, Michael J and Paul W McDonald (2006). "Significant pain reduction in chronic pain patients after detoxification from high-dose opioids". In: *J Opioid Manag* 2.5.

Bartel, David P (2004). "MicroRNAs: Genomics, Biogenesis, Mechanism, and Function". In: *Cell* 116, pp. 281–297. DOI: 10.1016/s0092-8674(04)00045-5.

Baudry, Anne et al. (2010). "MiR-16 Targets the Serotonin Transporter: A New Facet for Adaptive Responses to Antidepressants". In: *Science* 329.5784, pp. 1537–1541. ISSN: 00368075. DOI: 10.1126/science.1193692.

Baufeld, Caroline et al. (2018). *Differential contribution of microglia and monocytes in neurodegenerative diseases*. DOI: 10.1007/s00702-017-1795-7.

Bayat, F. Kemal et al. (2021). "Adult mouse dorsal root ganglia neurons form aberrant glutamatergic connections in dissociated cultures". In: *PLoS ONE* 16.3 March. ISSN: 19326203. DOI: 10.1371/journal.pone.0246924.

Bazrgar, Maryam et al. (2021). *The role of microRNA-34 family in Alzheimer's disease: A potential molecular link between neurodegeneration and metabolic disorders*. DOI: 10.1016/j.phrs.2021.105805.

Becker, C. et al. (2010). "mRNA and microRNA quality control for RT-qPCR analysis". In: *Methods* 50.4, pp. 237–243. ISSN: 10462023. DOI: 10.1016/j.ymeth.2010.01.010.

Ben-Yaakov, Keren et al. (2012). "Axonal transcription factors signal retrogradely in lesioned peripheral nerve". In: *EMBO Journal* 31.6, pp. 1350–1363. ISSN: 02614189. DOI: 10.1038/emboj.2011.494.

Berntson, Lillemor et al. (Jan. 2024). "Blood brain barrier permeability and astrocyte-derived extracellular vesicles in children with juvenile idiopathic arthritis: a cross-sectional study". In: *Pediatric Rheumatology* 22.1. ISSN: 15460096. DOI: 10.1186/s12969-024-00984-2.

Berta, Temugin et al. (2017). "Targeting dorsal root ganglia and primary sensory neurons for the treatment of chronic pain". In: *Expert Opinion on Therapeutic Targets* 21.7, pp. 695–703. ISSN: 17447631. DOI: 10.1080/14728222.2017.1328057.

Bindu, Samik, Somnath Mazumder, and Uday Bandyopadhyay (2020). *Non-steroidal anti-inflammatory drugs (NSAIDs) and organ damage: A current perspective*. DOI: 10.1016/j.bcp.2020.114147.

Biringer, Roger G (2012). "A Review of Prostanoid Receptors: Expression, Characterization, Regulation, and Mechanism of Action". In: *Journal of Cell Communication and Signaling* 15, pp. 155–184. DOI: 10.1007/s12079-020-00585-0/Published. URL: https://gpcrdb.org,.

Blanco-Colio, Luis M. (2014). "TWEAK/Fn14 axis: A promising target for the treatment of cardiovascular diseases". In: *Frontiers in Immunology* 5.JAN. ISSN: 16643224. DOI: 10.3389/fimmu.2014.00003.

Boese, Amrit S. et al. (2016). "MicroRNA abundance is altered in synaptoneurosomes during prion disease". In: *Molecular and Cellular Neuroscience* 71, pp. 13–24. ISSN: 10959327. DOI: 10.1016/j.mcn.2015.12.001.

Bohlen, Christopher J. et al. (2017). "Diverse Requirements for Microglial Survival, Specification, and Function Revealed by Defined-Medium Cultures". In: *Neuron* 94.4, pp. 759–773. ISSN: 10974199. DOI: 10.1016/j.neuron.2017.04.043.

Böing, Anita N. et al. (2014). "Single-step isolation of extracellular vesicles by size-exclusion chromatography". In: *Journal of Extracellular Vesicles* 3.1. ISSN: 20013078. DOI: 10.3402/jev.v3.23430.

Bouskila, Yona and Hugh Bostock (1998). *Modulation of Voltage-Activated Calcium Currents by Mechanical Stimulation in Rat Sensory Neurons*. Tech. rep.

Brás, João Paulo et al. (2020). "TNF-alpha-induced microglia activation requires miR-342: impact on NF-kB signaling and neurotoxicity". In: *Cell Death and Disease* 11.6. ISSN: 20414889. DOI: 10.1038/s41419-020-2626-6.

Brewer, Chelsie L. and Mark L. Baccei (2020). "The development of pain circuits and unique effects of neonatal injury". In: *Journal of Neural Transmission* 127.4, pp. 467–479. ISSN: 14351463. DOI: 10.1007/s00702-019-02059-z.

Burak, Kristyn et al. (2018). "MicroRNA-16 targets mRNA involved in neurite extension and branching in hippocampal neurons during presymptomatic prion disease". In: *Neurobiology of Disease* 112, pp. 1–13. ISSN: 1095953X. DOI: 10.1016/j.nbd.2017.12.011.

Burkly, Linda C. (2014). "TWEAK/Fn14 axis: The current paradigm of tissue injury-inducible function in the midst of complexities". In: *Seminars in Immunology* 26.3, pp. 229–236. ISSN: 10963618. DOI: 10.1016/j.smim.2014.02.006.

Burkly, Linda C., Jennifer S. Michaelson, and Timothy S. Zheng (2011). "TWEAK/Fn14 pathway: An immunological switch for shaping tissue responses". In: *Immunological Reviews* 244.1, pp. 99–114. ISSN: 01052896. DOI: 10.1111/j.1600-065X.2011.01054.x.

Burkly, Linda C. et al. (2007). *TWEAKing tissue remodeling by a multifunctional cytokine: Role of TWEAK/Fn14 pathway in health and disease*. DOI: 10.1016/j.cyto.2007.09.007.

Campos-Melo, Danae et al. (2013). "Altered microRNA expression profile in amyotrophic lateral sclerosis: A role in the regulation of NFL mRNA levels". In: *Molecular Brain* 6.1. ISSN: 17566606. DOI: 10.1186/1756-6606-6-26.

Caparaso, Sydney M., Adan L. Redwine, and Rebecca A. Wachs (2023). "Engineering a multicompartment in vitro model for dorsal root ganglia phenotypic assessment". In: *Journal of Biomedical Materials Research - Part B Applied Biomaterials* 111.11, pp. 1903–1920. ISSN: 15524981. DOI: 10.1002/jbm.b.35294.

Carlson, Jonathan D. et al. (2007). "Sensitization of pain-modulating neurons in the rostral ventromedial medulla after peripheral nerve injury". In: *Journal of Neuroscience* 27.48, pp. 13222–13231. ISSN: 02706474. DOI: 10.1523/JNEUROSCI.3715-07.2007.

Catena, Valeria and Maurizio Fanciulli (2017). *Deptor: Not only a mTOR inhibitor*. DOI: 10.1186/s13046-016-0484-y.

Caterina, Michael J et al. (1997). "The capsaicin receptor: a heat-activated ion channel in the pain pathway". In: *Nature* 389, pp. 816–824. DOI: 10.1038/39807.

Cavanaugh, Daniel J. et al. (July 2011). "Restriction of transient receptor potential vanilloid-1 to the peptidergic subset of primary afferent neurons follows its developmental downregulation in nonpeptidergic neurons". In: *Journal of Neuroscience* 31.28, pp. 10119–10127. ISSN: 02706474. DOI: 10.1523/JNEUROSCI.1299-11.2011.

Chaudhuri, Amrita Datta et al. (2018). "TNFα and IL-1β modify the miRNA cargo of astrocyte shed extracellular vesicles to regulate neurotrophic signaling in neurons article". In: *Cell Death and Disease* 9.3. ISSN: 20414889. DOI: 10.1038/s41419-018-0369-4.

Chen, Isaac and Forshing Lui (2023). "Neuroanatomy, Neuron Action Potential." In: *In: StatPearls [Internet].* Treasure Island (FL): StatPearls Publishing.

Chen, Xiaojie, Kimberly Tanner, and Jon D Levine (1999). "Mechanical sensitization of cutaneous C-fiber nociceptors by prostaglandin E 2 in the rat". In: *Neuroscience Letters*, pp. 105–108.

Chen, Yiwei et al. (2025a). "Identification of WDR74 and TNFRSF12A as biomarkers for early osteoarthritis using machine learning and immunohistochemistry". In: *Frontiers in Immunology* 16, p. 1517646. ISSN: 16643224. DOI: 10.3389/fimmu.2025.1517646.

Chen, Zixin et al. (2025b). "Kirenol relieves rheumatoid arthritis by targeting the TWEAK/Fn14 pathway". In: *International Journal of Molecular Medicine* 56.4. ISSN: 1791244X. DOI: 10.3892/ijmm.2025.5586.

Cheng, Tong, Zhongling Xu, and Xiaqing Ma (2022). "The role of astrocytes in neuropathic pain". In: *Frontiers in Molecular Neuroscience* 15. ISSN: 16625099. DOI: 10.3389/fnmol.2022.1007889.

Christopher, Josie A. et al. (2022). "Subcellular Transcriptomics and Proteomics: A Comparative Methods Review". In: *Molecular and Cellular Proteomics* 21.2. ISSN: 15359484. DOI: 10.1016/J.MCPRO.2021.100186.

Chrysostomidou, Lina, Andrew H. Cooper, and Greg A. Weir (2021). "Cellular models of pain: New technologies and their potential to progress preclinical research". In: *Neurobiology of Pain* 10. ISSN: 2452073X. DOI: 10.1016/j.ynpai.2021.100063.

Clark, Alex J. et al. (2018). "Functional imaging in microfluidic chambers reveals sensory neuron sensitivity is differentially regulated between neuronal regions". In: *Pain* 159.7, pp. 1413–1425. ISSN: 18726623. DOI: 10.1097/j.pain.0000000000001145.

Clarke, Benjamin E. et al. (2019). "Regional differences in the inflammatory and heat shock response in glia: implications for ALS". In: *Cell Stress and Chaperones* 24.5, pp. 857–870. ISSN: 14661268. DOI: 10.1007/s12192-019-01005-y.

Clegg, R and D Hughes (2022). *Chronic pain: the "unbearable" condition affecting one in four*.

Cohen, Steven P, Lene Vase, and William M Hooten (2021). "Chronic pain: an update on burden, best practices, and new advances". In: *The Lancet* 397, pp. 2082–2097. URL: www.thelancet.com.

Colvin, Lesley A., Fiona Bull, and Tim G. Hales (Apr. 2019). *Perioperative opioid analgesia—when is enough too much? A review of opioid-induced tolerance and hyperalgesia*. DOI: 10.1016/S0140-6736(19)30430-1.

Cox, Llewellyn J. et al. (2008). "Intra-axonal translation and retrograde trafficking of CREB promotes neuronal survival". In: *Nature Cell Biology* 10.2, pp. 149–159. ISSN: 14657392. DOI: 10.1038/ncb1677.

Cui, Bianxiao et al. (2007). "One at a time, live tracking of NGF axonal transport using quantum dots". In: *Proc. Natl. Acad. Sci.* 104.34, pp. 13666–13671. DOI: 10.1073/pnas.0706192104. URL: www.pnas.org/cgi/content/full/.

Cui, Jian Guo et al. (2010). "Differential regulation of Interleukin-1 Receptor-associated Kinase-1 (IRAK-1) and IRAK-2 by microRNA-146a and NF-κB in stressed human astroglial cells and in Alzheimer disease". In: *Journal of Biological Chemistry* 285.50, pp. 38951–38960. ISSN: 00219258. DOI: 10.1074/jbc.M110.178848.

Dajas-Bailador, Federico et al. (2012). "MicroRNA-9 regulates axon extension and branching by targeting Map1b in mouse cortical neurons". In: *Nature Neuroscience* 15.5, pp. 697–699. ISSN: 10976256. DOI: 10.1038/nn.3082.

Dalla Costa, Irene et al. (Feb. 2021). *The functional organization of axonal mRNA transport and translation*. DOI: 10.1038/s41583-020-00407-7.

Datta Chaudhuri, Amrita et al. (2020). "Stimulus-dependent modifications in astrocyte-derived extracellular vesicle cargo regulate neuronal excitability". In: *GLIA* 68.1, pp. 128–144. ISSN: 10981136. DOI: 10.1002/glia.23708.

De Vito, Francesca et al. (2022). "MiR-142-3p regulates synaptopathy-driven disease progression in multiple sclerosis". In: *Neuropathology and Applied Neurobiology* 48.2. ISSN: 13652990. DOI: 10.1111/nan.12765.

Deng, Xinbo, Ying Zeng, and Dan Ding (2024). "MiR-30c-5p-Targeted Regulation of GNAI2 Improves Neural Function Injury and Inflammation in Cerebral Ischemia-Reperfusion Injury". In: *Applied Biochemistry and Biotechnology* 196.8, pp. 5235–5248. ISSN: 15590291. DOI: 10.1007/s12010-023-04802-5.

Díaz-Muñoz, Manuel D. et al. (2010). "Coordinated up-regulation of cyclooxygenase-2 and microsomal prostaglandin E synthase 1 transcription by nuclear factor kappa B and early growth response-1 in macrophages". In: *Cellular Signalling* 22.10, pp. 1427–1436. ISSN: 08986568. DOI: 10.1016/j.cellsig.2010.05.011.

Dong, Hui et al. (2024). "miR-214-3p promotes the pathogenesis of Parkinson's disease by inhibiting autophagy". In: *Biomedicine and Pharmacotherapy* 171. ISSN: 19506007. DOI: 10.1016/j.biopha.2024.116123.

Dubin, Adrienne E. and Ardem Patapoutian (2010). "Nociceptors: The sensors of the pain pathway". In: *Journal of Clinical Investigation* 120.11, pp. 3760–3772. ISSN: 00219738. DOI: 10.1172/JCI42843.

Durur, Devrim Yagmur et al. (June 2022). "Alteration of miRNAs in Small Neuron-Derived Extracellular Vesicles of Alzheimer's Disease Patients and the Effect of Extracellular Vesicles on Microglial Immune Responses". In: *Journal of Molecular Neuroscience* 72.6, pp. 1182–1194. ISSN: 15591166. DOI: 10.1007/s12031-022-02012-y.

England, S, S Bevan, and R J Docherty (1996). *PGE2 modulates the tetrodotoxin-resistant sodium current in neonatal rat dorsal root ganglion neurones via the cyclic AMP-protein kinase A cascade*. Tech. rep. 2, pp. 429–440.

Esposito, Michael F. et al. (2019). "Unique Characteristics of the Dorsal Root Ganglion as a Target for Neuromodulation". In: *Pain Medicine* 20, S23–S30. ISSN: 15264637. DOI: 10.1093/pm/pnz012.

Fan, Chun Ling et al. (2014). "Effect of type-2 astrocytes on the viability of dorsal root ganglion neurons and length of neuronal processes". In: *Neural Regeneration Research* 9.2, pp. 119–128. ISSN: 18767958. DOI: 10.4103/1673-5374.125339.

Fan, Cuiqin et al. (2022). "Microglia secrete miR-146a-5p-containing exosomes to regulate neurogenesis in depression". In: *Molecular Therapy* 30.3, pp. 1300–1314. ISSN: 15250024. DOI: 10.1016/j.ymthe.2021.11.006.

Fan, Weihao et al. (2020). "MicroRNA-146a Is a Wide-Reaching Neuroinflammatory Regulator and Potential Treatment Target in Neurological Diseases". In: *Frontiers in Molecular Neuroscience* 13. ISSN: 16625099. DOI: 10.3389/fnmol.2020.00090.

Fazal, Furqan M. and Howard Y. Chang (2019). "Subcellular spatial transcriptomes: Emerging frontier for understanding gene regulation". In: *Cold Spring Harbor Symposia on Quantitative Biology* 84, pp. 31–45. ISSN: 19434456. DOI: 10.1101/sqb.2019.84.040352.

Ferrari, Luiz F., Oliver Bogen, and Jon D. Levine (2014). "Second messengers mediating the expression of neuroplasticity in a model of chronic pain in the rat". In: *Journal of Pain* 15.3, pp. 312–320. ISSN: 15265900. DOI: 10.1016/j.jpain.2013.12.005.

Ferrari, Luiz F. et al. (2013). "Peripheral administration of translation inhibitors reverses increased hyperalgesia in a model of chronic pain in the rat". In: *Journal of Pain* 14.7, pp. 731–738. ISSN: 15265900. DOI: 10.1016/j.jpain.2013.01.779.

Ferrea, E. et al. (2012). "Large-scale, high-resolution electrophysiological imaging of field potentials in brain slices with microelectronic multielectrode arrays". In: *Frontiers in Neural Circuits* NOV, pp. 1–14. ISSN: 16625110. DOI: 10.3389/fncir.2012.00080.

Ferreira, S. H., S. Moncada, and J. R. Vane (1974). "Prostaglandins and the mechanism of analgesia produced by aspirin like drugs". In: *Annals of the Royal College of Surgeons of England* 55.6, p. 287. ISSN: 00358843. DOI: 10.1111/j.1476-5381.1997.tb06823.x.

Fiorin, Fernando da Silva and Caroline Cunha do Espírito Santo (2025). "The Potential Roles of Astrocytes and Microglia in the Spinal Cord and Brain After Spinal Cord Injury". In: *Neuroglia* 6.1. ISSN: 25716980. DOI: 10.3390/neuroglia6010012.

Gabrielli, Martina et al. (2015). "Active endocannabinoids are secreted on extracellular membrane vesicles". In: *EMBO reports* 16.2, pp. 213–220. ISSN: 1469-221X. DOI: 10.15252/embr.201439668.

Gale, Jenna R. et al. (2022). "Local translation in primary afferents and its contribution to pain". In: *Pain* 163.12, pp. 2302–2314. ISSN: 0304-3959. DOI: 10.1097/j.pain.0000000000002658.

Gecys, Dovydas et al. (2022). “Circulating hsa-let-7e-5p and hsa-miR-125a-5p as Possible Biomarkers in the Diagnosis of Major Depression and Bipolar Disorders”. In: *Disease Markers* 2022. ISSN: 18758630. DOI: 10.1155/2022/3004338.

Giorgi, Simona et al. (2023). “Compartmentalized primary cultures of dorsal root ganglion neurons to model peripheral pathophysiological conditions”. In: *Molecular Pain* 19. ISSN: 17448069. DOI: 10.1177/17448069231197102.

Glémain, Alexandre et al. (2022). “Neutrophil-derived extracellular vesicles induce endothelial inflammation and damage through the transfer of miRNAs”. In: *Journal of Autoimmunity* 129. ISSN: 10959157. DOI: 10.1016/j.jaut.2022.102826.

Gold, Michael S, Jon D Levine, and Ana M Correa (1998). “Modulation of TTX-R I Na by PKC and PKA and Their Role in PGE 2-Induced Sensitization of Rat Sensory Neurons In Vitro”. In: *The Journal of Neuroscience* 18.24, pp. 10345–10355.

Goldberg, Daniel S. and Summer J. McGee (2011). “Pain as a global public health priority”. In: *BMC Public Health* 11. ISSN: 14712458. DOI: 10.1186/1471-2458-11-770.

Grace, Peter M. et al. (2018). “MicroRNA-124 and microRNA-146a both attenuate persistent neuropathic pain induced by morphine in male rats”. In: *Brain Research* 1692, pp. 9–11. ISSN: 18726240. DOI: 10.1016/j.brainres.2018.04.038.

Grider, Michael H., Rishita Jessu, and Rian Kabir (2023). “Physiology, Action Potential”. In: *In: StatPearls [Internet]*. Treasure Island (FL): StatPearls Publishing.

Gu, Qihai, Kevin Kwong, and Lu Yuan Lee (2003). “Ca2+ transient evoked by chemical stimulation is enhanced by PGE2 in vagal sensory neurons: Role of cAMP/PKA signaling pathway”. In: *Journal of Neurophysiology* 89.4, pp. 1985–1993. ISSN: 00223077. DOI: 10.1152/jn.00748.2002.

Guay, Claudiane et al. (2019). “Lymphocyte-Derived Exosomal MicroRNAs Promote Pancreatic β Cell Death and May Contribute to Type 1 Diabetes Development”. In: *Cell Metabolism* 29.2, pp. 348–361. ISSN: 19327420. DOI: 10.1016/j.cmet.2018.09.011.

Gumy, Laura F. et al. (2011). “Transcriptome analysis of embryonic and adult sensory axons reveals changes in mRNA repertoire localization”. In: *RNA* 17.1, pp. 85–98. ISSN: 13558382. DOI: 10.1261/rna.2386111.

Guo, Ran et al. (2019). “Pain regulation by gut microbiota: molecular mechanisms and therapeutic potential”. In: *British Journal of Anaesthesia* 123.5, pp. 637–654. ISSN: 14716771. DOI: 10.1016/j.bja.2019.07.026.

Guo, Zhongxin et al. (2024). “Tyrosine Kinase Receptor ErbB4 in Advillin-Positive Neurons Contributes to Inflammatory Pain Hypersensitivity in Mouse DRG”. In: *Aging and Disease* 15.6, pp. 2799–2812. ISSN: 21525250. DOI: 10.14336/AD.2023.1110.

Halldorsson, Skarphedinn et al. (2015). “Advantages and challenges of microfluidic cell culture in polydimethylsiloxane devices”. In: *Biosensors and Bioelectronics* 63, pp. 218–231. ISSN: 18734235. DOI: 10.1016/j.bios.2014.07.029.

Han, Jin et al. (2022). “DICAM in the Extracellular Vesicles from Astrocytes Attenuates Microglia Activation and Neuroinflammation”. In: *Cells* 11.19. ISSN: 20734409. DOI: 10.3390/cells11192977.

Hanz, Shlomit et al. (2003). “Axoplasmic Importins Enable Retrograde Injury Signaling in Lesioned Nerve”. In: *Neuron* 40.6, pp. 1095–1104. DOI: 10.1016/S0896âĂŠ6273(03)00770âĂŠ0. URL: http://www.neuron.org/cgi/content/full/40/6/1095/DC1.

Hassan, Mubashir et al. (2024). *Therapeutic Implication of miRNAs as an Active Regulatory Player in the Management of Pain: A Review*. DOI: 10.3390/genes15081003.

Hathway, G. J. et al. (2009). “The changing balance of brainstem-spinal cord modulation of pain processing over the first weeks of rat postnatal life”. In: *Journal of Physiology* 587.12, pp. 2927–2935. ISSN: 00223751. DOI: 10.1113/jphysiol.2008.168013.

Hehn, Christian A. von, Ralf Baron, and Clifford J. Woolf (2012). “Deconstructing the Neuropathic Pain Phenotype to Reveal Neural Mechanisms”. In: *Neuron* 73.4, pp. 638–652. ISSN: 08966273. DOI: 10.1016/j.neuron.2012.02.008.

Hengst, Ulrich et al. (2006). “Functional and selective RNA interference in developing axons and growth cones”. In: *Journal of Neuroscience* 26.21, pp. 5727–5732. ISSN: 02706474. DOI: 10.1523/JNEUROSCI.5229-05.2006.

Hilger, Daniel, Matthieu Masureel, and Brian K. Kobilka (2018). “Structure and dynamics of GPCR signaling complexes”. In: *Nature Structural and Molecular Biology* 25.1, pp. 4–12. ISSN: 15459985. DOI: 10.1038/s41594-017-0011-7.

Ho, Idy H.T. et al. (2020). “Spinal microglia-neuron interactions in chronic pain”. In: *Journal of Leukocyte Biology* 108.5, pp. 1575–1592. ISSN: 19383673. DOI: 10.1002/JLB.3MR0520-695R.

Holt, Christine E., Kelsey C. Martin, and Erin M. Schuman (2019). *Local translation in neurons: visualization and function*. DOI: 10.1038/s41594-019-0263-5.

Hu, Yue et al. (2022). “Overexpression of miR-99a in hippocampus leads to impairment of reversal learning in mice”. In: *Behavioural Brain Research* 416. ISSN: 18727549. DOI: 10.1016/j.bbr.2021.113542.

Hua, Xiao Ying et al. (Nov. 2005). “Intrathecal minocycline attenuates peripheral inflammation-induced hyperalgesia by inhibiting p38 MAPK in spinal microglia”. In: *European Journal of Neuroscience* 22.10, pp. 2431–2440. ISSN: 0953816X. DOI: 10.1111/j.1460-9568.2005.04451.x.

Huang, Li Na et al. (2019). “Fn14 Participates in Neuropathic Pain Through NF-κB Pathway in Primary Sensory Neurons”. In: *Molecular Neurobiology* 56.10, pp. 7085–7096. ISSN: 15591182. DOI: 10.1007/s12035-019-1545-y.

Huang, Tianfeng et al. (2025). “The Cytidine N-Acetyltransferase NAT10 Promotes Thalamus Hemorrhage-Induced Central Poststroke Pain by Stabilizing Fn14 Expression in Thalamic Neurons”. In: *Molecular Neurobiology* 62.3, pp. 3276–3292. ISSN: 0893-7648. DOI: 10.1007/s12035-024-04454-4. URL: https://link.springer.com/10.1007/s12035-024-04454-4.

Huang, Zheng and Hang Xu (2020). “MicroRNA-181a-5p regulates inflammatory response of macrophages in sepsis”. In: *Open Medicine (Poland)* 14.1, pp. 899–908. ISSN: 23915463. DOI: 10.1515/med-2019-0106.

Ibáñez, Francesc et al. (2019). “TLR4 participates in the transmission of ethanol-induced neuroinflammation via astrocyte-derived extracellular vesicles”. In: *Journal of Neuroinflammation* 16.1. ISSN: 17422094. DOI: 10.1186/s12974-019-1529-x.

Ielpo, Donald et al. (2023). “GABAergic miR-34a regulates Dorsal Raphè inhibitory transmission in response to aversive, but not rewarding, stimuli”. In: *Proceedings of the National Academy of Sciences of the United States of America* 120.32. ISSN: 10916490. DOI: 10.1073/pnas.2301730120.

Ikuma, Yuko et al. (2023). “Increased extracellular release of microRNAs from dorsal root ganglion cells in a rat model of neuropathic pain caused by peripheral nerve injury”. In: *PLOS ONE* 18.1, e0280425. ISSN: 1932-6203. DOI: 10.1371/journal.pone.0280425.

Inglis, Heather, Philip Norris, and Ali Danesh (2015). “Techniques for the analysis of extracellular vesicles using flow cytometry”. In: *Journal of Visualized Experiments* 2015.97. ISSN: 1940087X. DOI: 10.3791/52484.

Inta, Ioana et al. (2008). “Induction of the cytokine TWEAK and its receptor Fn14 in ischemic stroke”. In: *Journal of the Neurological Sciences* 275, pp. 117–120. ISSN: 0022510X. DOI: 10.1016/j.jns.2008.08.005.

Irie, Koichiro et al. (2016). “MicroRNA-214 promotes dendritic development by targeting the schizophrenia-associated gene quaking (Qki)”. In: *Journal of Biological Chemistry* 291.26, pp. 13891–13904. ISSN: 1083351X. DOI: 10.1074/jbc.M115.705749.

St-Jacques, B and W Ma (2014). “Peripheral prostaglandin E2 prolongs the sensitization of nociceptive dorsal root ganglion neurons possibly by facilitating the synthesis and anterograde axonal trafficking of EP4 receptors”. In: *Experimental Neurology*, pp. 354–366. DOI: 10.1016/j.expneurol.2014.05.028.

St-Jacques, Bruno and Weiya Ma (2013). “Prostaglandin E2/EP4 signalling facilitates EP4 receptor externalization in primary sensory neurons in vitro and in vivo”. In: *Pain* 154.2, pp. 313–323. ISSN: 18726623. DOI: 10.1016/j.pain.2012.11.005.

Jang, In Jeong et al. (2017). “Acute inflammation reveals GABAA receptor-mediated nociception in mouse dorsal root ganglion neurons via PGE2 receptor 4 signaling”. In: *Physiological Reports* 5.8. ISSN: 2051817X. DOI: 10.14814/phy2.13178.

Jang, Yongwoo, Minseok Kim, and Sun Wook Hwang (2020). “Molecular mechanisms underlying the actions of arachidonic acid-derived prostaglandins on peripheral nociception”. In: *Journal of Neuroinflammation* 17.1. ISSN: 17422094. DOI: 10.1186/s12974-020-1703-1.

Ji, Ru-Rong et al. (2002). “p38 MAPK Activation by NGF in Primary Sensory Neurons after Inflammation Increases TRPV1 Levels and Maintains Heat Hyperalgesia”. In: *Neuron* 36, pp. 57–68.

Jia, Longfei et al. (2018). “MiR-34a Regulates Axonal Growth of Dorsal Root Ganglia Neurons by Targeting FOXP2 and VAT1 in Postnatal and Adult Mouse”. In: *Molecular Neurobiology* 55.12, pp. 9089–9099. ISSN: 15591182. DOI: 10.1007/s12035-018-1047-3.

Johansson, Torbjörn, Shuh Narumiya, and Hanns Ulrich Zeilhofer (May 2011). “Contribution of peripheral versus central EP1 prostaglandin receptors to inflammatory pain”. In: *Neuroscience Letters* 495.2, pp. 98–101. ISSN: 03043940. DOI: 10.1016/j.neulet.2011.03.046.

Johnson, David et al. (2017). “Acute and subacute microRNA dysregulation is associated with cytokine responses in the rodent model of penetrating ballistic-like brain injury”. In: *Journal of Trauma and Acute Care Surgery* 83.1, S145–S149. ISSN: 21630763. DOI: 10.1097/TA.0000000000001475.

Joseph, E. K. and J. D. Levine (2010). “Hyperalgesic priming is restricted to isolectin B4-positive nociceptors”. In: *Neuroscience* 169.1, pp. 431–435. ISSN: 03064522. DOI: 10.1016/j.neuroscience.2010.04.082.

Kar, Amar N. et al. (2013). “Intra-axonal synthesis of eukaryotic translation initiation factors regulates local protein synthesis and axon growth in rat sympathetic neurons”. In: *Journal of Neuroscience* 33.17, pp. 7165–7174. ISSN: 02706474. DOI: 10.1523/JNEUROSCI.2040-12.2013.

Kassuya, C. A.L. et al. (2007). “Intraplantar PGE2 causes nociceptive behaviour and mechanical allodynia: The role of prostanoid e receptors and protein kinases”. In: *British Journal of Pharmacology* 150.6, pp. 727–737. ISSN: 00071188. DOI: 10.1038/sj.bjp.0707149.

Kaur, Indu Pal and Gaurav Sharma (2012). “siRNA A New Approach to Target Neuropathic Pain”. In: *Biodrugs* 26.6, pp. 401–412.

Kaurani, Lalit et al. (2025). “A role for astrocytic miR-129-5p in frontotemporal dementia”. In: *Translational Psychiatry* 15.1. ISSN: 21583188. DOI: 10.1038/s41398-025-03338-y.

Kawahara, Kohichi et al. (2015). *Prostaglandin E2-induced inflammation: Relevance of prostaglandin e receptors*. DOI: 10.1016/j.bbalip.2014.07.008.

Khadria, Anjul (2022). *Tools to measure membrane potential of neurons*. DOI: 10.1016/j.bj.2022.05.007.

Kim, Hanki et al. (2024). “Protocol for the acquisition and maturation of oligodendrocytes from neonatal rodent brains”. In: *STAR Protocols* 5.4. ISSN: 26661667. DOI: 10.1016/j.xpro.2024.103327.

Kim, Yeong Jin et al. (2020). “miR-16-5p is upregulated by amyloid β deposition in Alzheimer’s disease models and induces neuronal cell apoptosis through direct targeting and suppression of BCL-2”. In: *Experimental Gerontology* 136. ISSN: 18736815. DOI: 10.1016/j.exger.2020.110954.

Kim, Yong Ho et al. (2012). “TRPV1 in GABAergic Interneurons Mediates Neuropathic Mechanical Allodynia and Disinhibition of the Nociceptive Circuitry in the Spinal Cord”. In: *Neuron* 74.4, pp. 640–647. ISSN: 08966273. DOI: 10.1016/j.neuron.2012.02.039.

Kimourtzis, Georgios et al. (2024). “Prostaglandin E2 depolarises sensory axons in vitro in an ANO1 and Nav1.8 dependent manner”. In: *Scientific Reports* 14.1. ISSN: 20452322. DOI: 10.1038/s41598-024-67793-1.

Kong, Erliang et al. (2024). “Microglial exosome miR-124-3p in hippocampus alleviates cognitive impairment induced by postoperative pain in elderly mice”. In: *Journal of Cellular and Molecular Medicine* 28.3. ISSN: 15821838. DOI: 10.1111/jcmm.18090.

Kong, Xiaoli et al. (2019). “TNF-α regulates microglial activation via the NF-κB signaling pathway in systemic lupus erythematosus with depression”. In: *International Journal of Biological Macromolecules* 125, pp. 892–900. ISSN: 18790003. DOI: 10.1016/j.ijbiomac.2018.12.146.

Koppers, Max et al. (2024). “Axonal endoplasmic reticulum tubules control local translation via P180/RRBP1-mediated ribosome interactions”. In: *Developmental Cell* 59.16, pp. 2053–2068. ISSN: 18781551. DOI: 10.1016/j.devcel.2024.05.005.

Koralewska, Natalia et al. (2024). “Short 2-O-methyl/LNA oligomers as highly-selective inhibitors of miRNA production in vitro and in vivo”. In: *Nucleic Acids Research* 52.10, pp. 5804–5824. ISSN: 13624962. DOI: 10.1093/nar/gkae284.

Krames, Elliot S (2014). “The Role of the Dorsal Root Ganglion in the Development of Neuropathic Pain”. In: *Pain Medicine* 15, pp. 1669–1685. URL: http://www.csus.edu/.

– (2015). “The dorsal root ganglion in chronic pain and as a target for neuromodulation: A review”. In: *Neuromodulation* 18.1, pp. 24–32. ISSN: 15251403. DOI: 10.1111/ner.12247.

Kras, Jeffrey V., Ling Dong, and Beth A. Winkelstein (2013). “The prostaglandin E2 receptor, EP2, is upregulated in the dorsal root ganglion after painful cervical facet joint injury in the rat”. In: *Spine* 38.3, pp. 217–222. ISSN: 03622436. DOI: 10.1097/BRS.0b013e3182685ba1.

Kringel, Dario and Jörn Lötsch (2025). “Knowledge of the genetics of human pain gained over the last decade from next-generation sequencing”. In: *Pharmacological Research* 214. ISSN: 10961186. DOI: 10.1016/j.phrs.2025.107667.

Kügelgen, Nicolai von and Marina Chekulaeva (2020). *Conservation of a core neurite transcriptome across neuronal types and species*. DOI: 10.1002/wrna.1590.

Kumar, Manish and Guohong Li (2023). *Emerging Role of MicroRNA-30c in Neurological Disorders*. DOI: 10.3390/ijms24010037.

Kwon, Hyuk Sung and Seong Ho Koh (2020). *Neuroinflammation in neurodegenerative disorders: the roles of microglia and astrocytes*. DOI: 10.1186/s40035-020-00221-2.

Lamriben, Lydia et al. (2016). “N-Glycan-based ER Molecular Chaperone and Protein Quality Control System: The Calnexin Binding Cycle”. In: *Traffic* 17.4, pp. 308–326. ISSN: 16000854. DOI: 10.1111/tra.12358.

Latremoliere, Alban and Clifford J. Woolf (2009). *Central Sensitization: A Generator of Pain Hypersensitivity by Central Neural Plasticity*. DOI: 10.1016/j.jpain.2009.06.012.

Lawrence, Gary W. et al. (2021). “Population coding of capsaicin concentration by sensory neurons revealed using Ca2+ imaging of dorsal root ganglia explants from adult pirt-GCaMP3 mouse”. In: *Cellular Physiology and Biochemistry* 55.4, pp. 428–448. ISSN: 14219778. DOI: 10.33594/000000394.

Lawrence, Jill M. et al. (2023). “Roles of neuropathology-associated reactive astrocytes: a systematic review”. In: *Acta Neuropathologica Communications* 11.1. ISSN: 20515960. DOI: 10.1186/s40478-023-01526-9.

Lechner, Stefan G. et al. (2009). “Developmental waves of mechanosensitivity acquisition in sensory neuron subtypes during embryonic development”. In: *EMBO Journal* 28.10, pp. 1479–1491. ISSN: 02614189. DOI: 10.1038/emboj.2009.73.

Lei, Bo et al. (2021). “NF-κB-Induced Upregulation of miR-146a-5p Promoted Hippocampal Neuronal Oxidative Stress and Pyroptosis via TIGAR in a Model of Alzheimer’s Disease”. In: *Frontiers in Cellular Neuroscience* 15. ISSN: 16625102. DOI: 10.3389/fncel.2021.653881.

Li, Jian et al. (2017). “Microvesicles shed from microglia activated by the P2X7-p38 pathway are involved in neuropathic pain induced by spinal nerve ligation in rats”. In: *Purinergic Signalling* 13.1, pp. 13–26. ISSN: 15739546. DOI: 10.1007/s11302-016-9537-0.

Li, Xiangqi, Martin S Angst, and J David Clark (2001). *Opioid-Induced Hyperalgesia and Incisional Pain*. Tech. rep., pp. 204–209.

Li, Zhikun et al. (2020). “MicroRNA-23a-3p improves traumatic brain injury through modulating the neurological apoptosis and inflammation response in mice”. In: *Cell Cycle* 19.1, pp. 24–38. ISSN: 15514005. DOI: 10.1080/15384101.2019.1691763.

Liang, Zhi et al. (2020). “A transcriptional toolbox for exploring peripheral neuroimmune interactions”. In: *Pain* 161.9, pp. 2089–2106. ISSN: 18726623. DOI: 10.1097/j.pain.0000000000001914.

Liddelow, Shane A. et al. (2017). “Neurotoxic reactive astrocytes are induced by activated microglia”. In: *Nature* 541.7638, pp. 481–487. ISSN: 14764687. DOI: 10.1038/nature21029.

Lin, C-R et al. (2006). “Prostaglandin E2 Receptor EP4 Contributes to Inflammatory Pain Hypersensitivity”. In: *Journal of Pharmacology and Experimental Therapeutics* 319.3, pp. 1096–1103. DOI: 10.1124/jpet.106.105569.

Linley, John E. et al. (2010). *Understanding inflammatory pain: Ion channels contributing to acute and chronic nociception*. DOI: 10.1007/s00424-010-0784-6.

Liu, Jia Neng, Song Lu, and Chang Ma Fu (2022). “MiR-146a expression profiles in osteoarthritis in different tissue sources: a meta-analysis of observational studies”. In: *Journal of Orthopaedic Surgery and Research* 17.1. ISSN: 1749799X. DOI: 10.1186/s13018-022-02989-7.

Liu, Jiaxi et al. (2024). “MiR-146a-5p engineered hucMSC-derived extracellular vesicles attenuate Dermatophagoides farinae-induced allergic airway epithelial cell inflammation”. In: *Frontiers in Immunology* 15. ISSN: 16643224. DOI: 10.3389/fimmu.2024.1443166.

Liu, Li et al. (2025). “TWEAK-Fn14 signaling protects mice from pulmonary fibrosis by inhibiting fibroblast activation and recruiting pro-regenerative macrophages”. In: *Cell Reports* 44.2. ISSN: 22111247. DOI: 10.1016/j.celrep.2024.115220.

Liu, Rui et al. (2015). “A cortical astrocyte subpopulation inhibits axon growth in vitro and in vivo”. In: *Molecular medicine reports* 12.2, pp. 2598–2606. ISSN: 17913004. DOI: 10.3892/mmr.2015.3702.

Liu, Xiaoyu and Ning Quan (2018). “Microglia and CNS interleukin-1: Beyond immunological concepts”. In: *Frontiers in Neurology* 9.JAN. ISSN: 16642295. DOI: 10.3389/fneur.2018.00008.

Liu, Yulan et al. (2020). “MicroRNA-345-5p regulates depression by targeting suppressor of cytokine signaling 1”. In: *Brain and Behavior* 10.9. ISSN: 21623279. DOI: 10.1002/brb3.1653.

Liu, Zhen, Alhousseynou Sall, and Decheng Yang (2008). *MicroRNA: An emerging therapeutic target and intervention tool*. DOI: 10.3390/ijms9060978.

Livak, Kenneth J. and Thomas D. Schmittgen (2001). “Analysis of relative gene expression data using real-time quantitative PCR and the 2-$\Delta\Delta$CT method”. In: *Methods* 25.4, pp. 402–408. ISSN: 10462023. DOI: 10.1006/meth.2001.1262.

Lock, Jeffrey T., Ian Parker, and Ian F. Smith (2015). “A comparison of fluorescent Ca2+ indicators for imaging local Ca2+ signals in cultured cells”. In: *Cell Calcium* 58.6, pp. 638–648. ISSN: 15321991. DOI: 10.1016/j.ceca.2015.10.003.

Long, Yunfan et al. (2025). “The complex effects of miR-146a in the pathogenesis of Alzheimer’s disease”. In: *Neural Regeneration Research* 20.5, pp. 1309–1323. ISSN: 1673-5374. DOI: 10.4103/nrr.nrr-d-23-01566.

Lopes, Cátia D.F., José C. Mateus, and Paulo Aguiar (2018). “Interfacing microfluidics with microelectrode arrays for studying neuronal communication and axonal signal propagation”. In: *Journal of Visualized Experiments* 2018.142. ISSN: 1940087X. DOI: 10.3791/58878.

López-Cepeda, Leonardo et al. (2022). “Modulation of Small RNA Signatures by Astrocytes on Early Neurodegeneration Stages; Implications for Biomarker Discovery”. In: *Life* 12.11, p. 1720. ISSN: 20751729. DOI: 10.3390/life12111720.

Lopshire, J C and G D Nicol (1997). “Activation and Recovery of the PGE 2-Mediated Sensitization of the Capsaicin Response in Rat Sensory Neurons”. In: *Journal of Neurophysiology* 78.6, pp. 3154–3164. DOI: 10.1152/jn.1997.78.6.3154.

Loreto, A and J Gilley (2020). “Axon Degeneration Assays in Superior Cervical Ganglion Explant Cultures”. In: *Axon Degeneration; Methods and Protocols*. Ed. by Elisabetta Babetto. Vol. 2143. New York: Humana Press. URL: http://www.springer.com/series/7651.

Lu, Ying et al. (2015). “MicroRNA-146a-5p attenuates neuropathic pain via suppressing TRAF6 signaling in the spinal cord”. In: *Brain, Behavior, and Immunity* 49, pp. 119–129. ISSN: 10902139. DOI: 10.1016/j.bbi.2015.04.018.

Lu, Ying et al. (2018). “MicroRNA-146a-5p attenuates visceral hypersensitivity through targeting chemokine CCL8 in the spinal cord in a mouse model of colitis”. In: *Brain Research Bulletin* 139, pp. 235–242. ISSN: 18732747. DOI: 10.1016/j.brainresbull.2018.03.007.

Lucci, Cristiano et al. (2020). “Spatiotemporal regulation of GSK3β levels by miRNA-26a controls axon development in cortical neurons”. In: *Development* 147.3. ISSN: 14779129. DOI: 10.1242/dev.180232.

Luo, Qing Qing et al. (2024). “ZBTB20 mediates stress-induced visceral hypersensitivity via activating the NF-κB/transient receptor potential channel pathway”. In: *Neurogastroenterology and Motility* 36.2. ISSN: 13652982. DOI: 10.1111/nmo.14718.

Ma, Junxuan et al. (2021). “In vitro model to investigate communication between dorsal root ganglion and spinal cord glia”. In: *International Journal of Molecular Sciences* 22.18. ISSN: 14220067. DOI: 10.3390/ijms22189725.

Ma, Limin et al. (2024). “Neuronal small extracellular vesicles carrying miR-181c-5p contribute to the pathogenesis of epilepsy by regulating the protein kinase C-δ/glutamate transporter-1 axis in astrocytes”. In: *GLIA* 72.6, pp. 1082–1095. ISSN: 10981136. DOI: 10.1002/glia.24517.

Ma, Rong, Naseer A. Kutchy, and Guoku Hu (2021). “Astrocyte-Derived Extracellular Vesicle–Mediated Activation of Primary Ciliary Signaling Contributes to the Development of Morphine Tolerance”. In: *Biological Psychiatry* 90.8, pp. 575–585. ISSN: 18732402. DOI: 10.1016/j.biopsych.2021.06.009.

Ma, W and B St-Jacques (2018). “Signalling transduction events involved in agonist-induced PGE2/EP4 receptor externalization in cultured rat dorsal root ganglion neurons”. In: *European Journal of Pain* 22.5, pp. 845–861. DOI: 10.1002/ejp.1172.

Ma, W. et al. (2016). “Stimulating TRPV1 externalization and synthesis in dorsal root ganglion neurons contributes to PGE2 potentiation of TRPV1 activity and nociceptor sensitization”. In: *European Journal of Pain (United Kingdom)* 21.4, pp. 575–593. ISSN: 15322149. DOI: 10.1002/ejp.959.

Ma, Weiya (2010). “Chronic prostaglandin E2 treatment induces the synthesis of the pain-related peptide substance P and calcitonin gene-related peptide in cultured sensory ganglion explants”. In: *Journal of Neurochemistry* 115.2, pp. 363–372. ISSN: 00223042. DOI: 10.1111/j.1471-4159.2010.06927.x.

Maday, Sandra et al. (2014). *Axonal Transport: Cargo-Specific Mechanisms of Motility and Regulation*. DOI: 10.1016/j.neuron.2014.10.019.

Maemoto, Yuki et al. (2013). “Analysis of limited proteolytic activity of calpain-7 using non-physiological substrates in mammalian cells”. In: *FEBS Journal* 280.11, pp. 2594–2607. ISSN: 1742464X. DOI: 10.1111/febs.12243.

Malty, Ramy Habashy et al. (2016). “Long-term exposure to PGE2 causes homologous desensitization of receptor-mediated activation of protein kinase A”. In: *Journal of Neuroinflammation* 13. ISSN: 17422094. DOI: 10.1186/s12974-016-0645-0.

Mao, Shiqi et al. (2023). “Dysregulation of miR-146a: a causative factor in epilepsy pathogenesis, diagnosis, and prognosis”. In: *Frontiers in Neurology* 14. ISSN: 16642295. DOI: 10.3389/fneur.2023.1094709.

Maqbool, Ayesha et al. (2013). “Sustained, neuron-specific IKK/NF-κB activation generates a selective neuroinflammatory response promoting local neurodegeneration with aging”. In: *Molecular Neurodegeneration* 8.1. ISSN: 17501326. DOI: 10.1186/1750-1326-8-40.

Marton, Soledad et al. (2023). “SOD1G93A Astrocyte-Derived Extracellular Vesicles Induce Motor Neuron Death by a miRNA-155-5p-Mediated Mechanism”. In: *ASN Neuro* 15. ISSN: 17590914. DOI: 10.1177/17590914231197527.

Mattson, Mark R. (2007). *Calcium and neurodegeneration*. DOI: 10.1111/j.1474-9726.2007.00275.x.

McGowan, Heather et al. (2018). “hsa-let-7c miRNA Regulates Synaptic and Neuronal Function in Human Neurons”. In: *Frontiers in Synaptic Neuroscience* 10. ISSN: 16633563. DOI: 10.3389/fnsyn.2018.00019.

Melli, Giorgia and Ahmet Höke (2009). *Dorsal root ganglia sensory neuronal cultures: A tool for drug discovery for peripheral neuropathies*. DOI: 10.1517/17460440903266829.

Men, Yuqin et al. (2019). “Exosome reporter mice reveal the involvement of exosomes in mediating neuron to astroglia communication in the CNS”. In: *Nature Communications* 10. ISSN: 20411723. DOI: 10.1038/s41467-019-11534-w.

Meng, Jianghui et al. (2016). “TNFα induces co-trafficking of TRPV1/TRPA1 in VAMP1-containing vesicles to the plasmalemma via Munc18-1/syntaxin1/SNAP-25 mediated fusion”. In: *Scientific Reports* 6. ISSN: 20452322. DOI: 10.1038/srep21226.

Mercadante, Sebastiano, Edoardo Arcuri, and Angela Santoni (2019). “Opioid-Induced Tolerance and Hyperalgesia”. In: *CNS Drugs* 33.10, pp. 943–955. ISSN: 11791934. DOI: 10.1007/s40263-019-00660-0.

Merianda, Tanuja T. et al. (2009). “A functional equivalent of endoplasmic reticulum and Golgi in axons for secretion of locally synthesized proteins”. In: *Molecular and Cellular Neuroscience* 40.2, pp. 128–142. ISSN: 10447431. DOI: 10.1016/j.mcn.2008.09.008.

Mesquita-Ribeiro, Raquel (2019). “Axonal microRNAs in cortical neuronal development and network connectivity”. PhD thesis. Nottingham: University of Nottingham.

Mesquita-Ribeiro, Raquel et al. (2021). “Distinct small non-coding RNA landscape in the axons and released extracellular vesicles of developing primary cortical neurons and the axoplasm of adult nerves”. In: *RNA Biology* 18.S2, pp. 832–855. ISSN: 15558584. DOI: 10.1080/15476286.2021.2000792.

Messina, Diego N., Emanuel D. Peralta, and Cristian G. Acosta (2022). “Glial-derived neurotrophic factor regulates the expression of TREK2 in rat primary sensory neurons leading to attenuation of axotomy-induced neuropathic pain”. In: *Experimental Neurology* 357. ISSN: 10902430. DOI: 10.1016/j.expneurol.2022.114190.

Middleton, Steven J. et al. (2021). “Studying human nociceptors: From fundamentals to clinic”. In: *Brain* 144.5, pp. 1312–1335. ISSN: 14602156. DOI: 10.1093/brain/awab048.

Min, Xia et al. (2023). “miR-34a regulates silent synapse and synaptic plasticity in mature hippocampus”. In: *Progress in Neurobiology* 222. ISSN: 18735118. DOI: 10.1016/j.pneurobio.2023.102404.

Minami, Toshiaki et al. (1999). “Involvement of primary afferent C-fibres in touch-evoked pain (allodynia) induced by prostaglandin E2”. In: *European Journal of Neuroscience* 11.6, pp. 1849–1856. ISSN: 0953816X. DOI: 10.1046/j.1460-9568.1999.00602.x.

Morchio, Martina et al. (2023). “The Role of miRNAs in Neuropathic Pain”. In: *Biomedicines* 11.3. ISSN: 22279059. DOI: 10.3390/biomedicines11030775.

Morel, Lydie et al. (2013). “Neuronal exosomal mirna-dependent translational regulation of astroglial glutamate transporter glt1”. In: *Journal of Biological Chemistry* 288.10, pp. 7105–7116. ISSN: 00219258. DOI: 10.1074/jbc.M112.410944.

Morgado, Ana L. et al. (2015). “MicroRNA-34a Modulates Neural Stem Cell Differentiation by Regulating Expression of Synaptic and Autophagic Proteins”. In: *Molecular Neurobiology* 51.3, pp. 1168–1183. ISSN: 15591182. DOI: 10.1007/s12035-014-8794-6.

Morimoto, Kazushi et al. (2014). “Prostaglandin E2–EP3 Signaling Induces Inflammatory Swelling by Mast Cell Activation”. In: *The Journal of Immunology* 192.3, pp. 1130–1137. ISSN: 0022-1767. DOI: 10.4049/jimmunol.1300290.

Moriyama, Tomoko et al. (2005). “Sensitization of TRPV1 by EP1 and IP reveals peripheral nociceptive mechanism of prostaglandins”. In: *Molecular Pain* 1. ISSN: 17448069. DOI: 10.1186/1744-8069-1-3.

Mundy, William R., Nicholas M. Radio, and Theresa M. Freudenrich (2010). “Neuronal models for evaluation of proliferation in vitro using high content screening”. In: *Toxicology* 270.2-3, pp. 121–130. ISSN: 0300483X. DOI: 10.1016/j.tox.2010.02.004.

Nagahisa, A. and T. Okumura (2017). “Pharmacology of grapiprant, a novel EP4 antagonist: receptor binding, efficacy in a rodent postoperative pain model, and a dose estimation for controlling pain in dogs”. In: *Journal of Veterinary Pharmacology and Therapeutics* 40.3, pp. 285–292. ISSN: 13652885. DOI: 10.1111/jvp.12349.

Nagano, Seiichi and Toshiyuki Araki (2021). *Axonal Transport and Local Translation of mRNA in Neurodegenerative Diseases*. DOI: 10.3389/fnmol.2021.697973.

Nazeri, Arash et al. (2014). “A further TWEAK to multiple sclerosis pathophysiology”. In: *Molecular Neurobiology* 49.1, pp. 78–87. ISSN: 15591182. DOI: 10.1007/s12035-013-8490-y.

Nguyen, Trinh, Chang Su, and Meharvan Singh (2018). “Let-7i inhibition enhances progesterone-induced functional recovery in a mouse model of ischemia”. In: *Proceedings of the National Academy of Sciences of the United States of America* 115.41, E9668–E9677. ISSN: 10916490. DOI: 10.1073/pnas.1803384115.

NHS Digital (2017). “Health Survey for England 2017”. In: *National Statistics*.

NICE (2021). *Chronic pain (primary and secondary) in over 16s: assessment of all chronic pain and management of chronic primary pain*. Tech. rep. URL: https://www.nice.org.uk/guidance/ng193.

Niedzielska, Magdalena et al. (2014). “Gene trap mice reveal an essential function of dual specificity phosphatase Dusp16/MKP-7 in perinatal survival and regulation of toll-like receptor (TLR)-induced cytokine production”. In: *Journal of Biological Chemistry* 289.4, pp. 2112–2126. ISSN: 00219258. DOI: 10.1074/jbc.M113.535245.

Nordin, Joel Z. et al. (2015). “Ultrafiltration with size-exclusion liquid chromatography for high yield isolation of extracellular vesicles preserving intact biophysical and functional properties”. In: *Nanomedicine: Nanotechnology, Biology, and Medicine* 11.4, pp. 879–883. ISSN: 15499642. DOI: 10.1016/j.nano.2015.01.003.

Oida, Hiroji et al. (1995). “In situ hybridization studies of prostacyclin receptor mRNA expression in various mouse organs”. In: *British Journal of Pharmacology* 116.7, pp. 2828–2837. ISSN: 14765381. DOI: 10.1111/j.1476-5381.1995.tb15933.x.

Omran, Ahmed et al. (2012). “Interleukin-1β and microRNA-146a in an immature rat model and children with mesial temporal lobe epilepsy”. In: *Epilepsia* 53.7, pp. 1215–1224. ISSN: 00139580. DOI: 10.1111/j.1528-1167.2012.03540.x.

Osteen, Jeremiah D. et al. (2025). “Pharmacology and Mechanism of Action of Suzetrigine, a Potent and Selective NaV1.8 Pain Signal Inhibitor for the Treatment of Moderate to Severe Pain”. In: *Pain and Therapy*. ISSN: 2193651X. DOI: 10.1007/s40122-024-00697-0.

Ou, Shu et al. (2022). “miRNA-let-7i modulates status epilepticus via the TLR4 pathway”. In: *Acta Epileptologica* 4.1. ISSN: 25244434. DOI: 10.1186/s42494-022-00085-1.

Owen, Davina E. and Julie Egerton (2012). “Culture of dissociated sensory neurons from dorsal root ganglia of postnatal and adult rats”. In: *Methods in Molecular Biology* 846, pp. 179–187. ISSN: 10643745. DOI: 10.1007/978-1-61779-536-7{_}16.

Pahlavan, Yasamin et al. (2020). *Prominent roles of microRNA-142 in cancer*. DOI: 10.1016/j.prp.2020.153220.

Paikari, Alireza et al. (2017). “The eutheria-specific miR-290 cluster modulates placental growth and maternal-fetal transport”. In: *Development (Cambridge)* 144.20, pp. 3731–3743. ISSN: 14779129. DOI: 10.1242/dev.151654.

Paolicelli, Rosa C et al. (2022). “Defining Microglial States and Nomenclature: A Roadmap to 2030”. In: *Cell Sneak Peek*. DOI: 10.2139/ssrn.4065080. URL: https://ssrn.com/abstract=4065080.

Paredes, R. Madelaine et al. (2008). “Chemical calcium indicators”. In: *Methods* 46.3, pp. 143–151. ISSN: 10462023. DOI: 10.1016/j.ymeth.2008.09.025.

Park, Jean Y., Michael H. Pillinger, and Steven B. Abramson (2006). “Prostaglandin E2 synthesis and secretion: The role of PGE2 synthases”. In: *Clinical Immunology* 119.3, pp. 229–240. ISSN: 15216616. DOI: 10.1016/j.clim.2006.01.016.

Park, Jian, Ruoqi Yu, and Yifei Dong (July 2024). “Generating and Co-culturing Murine Primary Microglia and Cortical Neurons”. In: *Journal of visualized experiments : JoVE* 209. ISSN: 1940087X. DOI: 10.3791/67078.

Pauley, Kaleb M. and Seunghee Cha (2011). “miRNA-146a in rheumatoid arthritis: A new therapeutic strategy”. In: *Immunotherapy* 3.7, pp. 829–831. ISSN: 1750743X. DOI: 10.2217/imt.11.70.

Peng, Dong et al. (2022). “Extracellular vesicles derived from astrocyte-treated with haFGF14-154 attenuate Alzheimer phenotype in AD mice”. In: *Theranostics* 12.9, pp. 3862–3881. ISSN: 18387640. DOI: 10.7150/THNO.70951.

Petersen, Cecilia et al. (2005). “The p38 MAPK pathway mediates interleukin-1-induced Sertoli cell proliferation”. In: *Cytokine* 32.1, pp. 51–59. ISSN: 10434666. DOI: 10.1016/j.cyto.2005.07.014.

Pope, Rebecca et al. (2025). *Conserved Axonal Transcriptome Dynamics Underlie PGE-Induced Sensitisation and Identify Tnfrsf12a /Fn14 as a Regulator of Neuronal Excitability in DRG Neurons*. DOI: 10.1101/2025.09.02.673723. URL: http://biorxiv.org/lookup/doi/10.1101/2025.09.02.673723.

Potenza, Nicoletta et al. (2017). “Molecular mechanisms governing microRNA-125a expression in human hepatocellular carcinoma cells”. In: *Scientific Reports* 7. ISSN: 20452322. DOI: 10.1038/s41598-017-11418-3.

Potrovita, Ioana et al. (2004). “Tumor necrosis factor-like weak inducer of apoptosis-induced neurodegeneration”. In: *Journal of Neuroscience* 24.38, pp. 8237–8244. ISSN: 02706474. DOI: 10.1523/JNEUROSCI.1089-04.2004.

Prada, Ilaria et al. (2018). “Glia-to-neuron transfer of miRNAs via extracellular vesicles: a new mechanism underlying inflammation-induced synaptic alterations”. In: *Acta Neuropathologica* 135.4, pp. 529–550. ISSN: 14320533. DOI: 10.1007/s00401-017-1803-x.

Qi, Zheng et al. (2023). “M1-Type Microglia-Derived Extracellular Vesicles Overexpressing IL-1R1 Promote Postoperative Cognitive Dysfunction by Regulating Neuronal Inflammation”. In: *Inflammation* 46.6, pp. 2254–2269. ISSN: 15732576. DOI: 10.1007/s10753-023-01875-6.

Quicke, Peter, Carmel L. Howe, and Amanda J. Foust (2023). “Balancing the Fluorescence Imaging Budget for All-Optical Neurophysiology Experiments”. In: *All-Optical Methods to Study Neuronal Function*. Vol. 191. New York: Humana Press Inc. Chap. Chapter 2, pp. 49–74. DOI: 10.1007/978-1-0716-2764-8{_}2.

Raffaeli, William and Elisa Arnaudo (2017). “Pain as a disease: An overview”. In: *Journal of Pain Research* 10, pp. 2003–2008. ISSN: 11787090. DOI: 10.2147/JPR.S138864.

Raja, Srinivasa N. et al. (2020). *The revised International Association for the Study of Pain definition of pain: concepts, challenges, and compromises*. DOI: 10.1097/j.pain.0000000000001939.

Rangwani, Natasha R (2018). “A Microfluidic Approach to Investigate Changes in Functional Properties of Nociceptive Axons Underlying Inflammatory Pain States”. PhD thesis. London: King’s

College London, pp. 118–119. URL: https://kclpure.kcl.ac.uk/ws/portalfiles/portal/95697711/2018_Rangwani_Natasha_0909323_ethesis.pdf.

Ray, Pradipta et al. (2018). "Comparative transcriptome profiling of the human and mouse dorsal root ganglia: An RNA-seq-based resource for pain and sensory neuroscience research". In: *Pain* 159.7, pp. 1325–1345. ISSN: 18726623. DOI: 10.1097/j.pain.0000000000001217.

Redpath, Paula et al. (2023). "Guided Self-Help for People with Chronic Pain: Integrated Care in a Public Tertiary Pain Clinic—A Pilot Study". In: *Pain and Therapy* 12.2, pp. 449–460. ISSN: 2193651X. DOI: 10.1007/s40122-022-00464-z.

Reichling, David B. and Jon D. Levine (2009). *Critical role of nociceptor plasticity in chronic pain*. DOI: 10.1016/j.tins.2009.07.007.

Reisine, T and G Pasternak (1996). "Opioid analgesics and antagonists". In: *Gilman A.G Hardman J.G Limbird L.E Goodman & Gilman's The pharmacological basis of therapeutics*. 9th. New York: McGraw-Hill, pp. 521–555.

Rexed, Bror (1952). "The cytoarchitectonic organization of the spinal cord in the cat". In: *Journal of Comparative Neurology* 96.3, pp. 415–495. ISSN: 10969861. DOI: 10.1002/cne.900960303.

Rice, Andrew S.C., Blair H. Smith, and Fiona M. Blyth (Apr. 2016). "Pain and the global burden of disease". In: *Pain* 157.4, pp. 791–796. ISSN: 18726623. DOI: 10.1097/j.pain.0000000000000454.

Roblain, Quentin et al. (2021). "Intravitreal injection of anti-miRs against miR-142-3p reduces angiogenesis and microglia activation in a mouse model of laser-induced choroidal neovascularization". In: *Aging* 13.9. DOI: 10.18632/aging.203035.

Rodriguez-Ortiz, Carlos J. et al. (2020). "miR-181a negatively modulates synaptic plasticity in hippocampal cultures and its inhibition rescues memory deficits in a mouse model of Alzheimer's disease". In: *Aging Cell* 19.3. ISSN: 14749726. DOI: 10.1111/acel.13118.

Saito, Shigeru and Claire T. Saito (2025). "Evolution of Temperature Receptors and Their Roles in Sensory Diversification and Adaptation". In: *Zoological science* 42.1. ISSN: 02890003. DOI: 10.2108/zs240060.

Samidurai, Manikandan et al. (2020). "Tumor Necrosis Factor-Like Weak Inducer of Apoptosis (TWEAK) Enhances Activation of STAT3/NLRC4 Inflammasome Signaling Axis through PKCδ in Astrocytes: Implications for Parkinson's Disease". In: *Cells* 9.8, pp. 1–35. ISSN: 20734409. DOI: 10.3390/cells9081831.

Santiago, Juliet V. et al. (2023). *Identification of state-specific proteomic and transcriptomic signatures of microglia-derived extracellular vesicles*. DOI: 10.1101/2023.07.28.551012. URL: http://biorxiv.org/lookup/doi/10.1101/2023.07.28.551012.

Sasaki, Yukio (2020). *Local translation in growth cones and presynapses, two axonal compartments for local neuronal functions*. DOI: 10.3390/biom10050668.

Schindelin, J et al. (2012). "Fiji: an open-source platform for biological-image analysis." In: *Nature Methods* 9.7, pp. 676–682.

Schwaller, Fred and Maria Fitzgerald (2014). "The consequences of pain in early life: Injury-induced plasticity in developing pain pathways". In: *European Journal of Neuroscience* 39.3, pp. 344–352. ISSN: 0953816X. DOI: 10.1111/ejn.12414.

Sekiguchi, Fumiko et al. (2013). "AKAP-dependent sensitization of Cav3.2 channels via the EP 4 receptor/cAMP pathway mediates PGE2-induced mechanical hyperalgesia". In: *British Journal of Pharmacology* 168.3, pp. 734–745. ISSN: 00071188. DOI: 10.1111/j.1476-5381.2012.02174.x.

Shannonhouse, John et al. (2023). "In Vivo Calcium Imaging of Neuronal Ensembles in Networks of Primary Sensory Neurons in Intact Dorsal Root Ganglia". In: *Journal of Visualized Experiments* 192.192, e64826. ISSN: 1940-087X. DOI: 10.3791/64826.

Shu, Pengcheng et al. (2017). "MicroRNA-214 modulates neural progenitor cell differentiation by targeting Quaking during cerebral cortex development". In: *Scientific Reports* 7.1. ISSN: 20452322. DOI: 10.1038/s41598-017-08450-8.

Silverman, Sean M. et al. (2016). "C1q propagates microglial activation and neurodegeneration in the visual axis following retinal ischemia/reperfusion injury". In: *Molecular Neurodegeneration* 11.1. ISSN: 17501326. DOI: 10.1186/s13024-016-0089-0.

Sörnmo, Leif and Pablo Laguna (2005). "The Electroencephalogram—A Brief Background". In: *Bioelectrical Signal Processing in Cardiac and Neurological Applications*. Ed. by Leif Sörnmo and Pablo Laguna. Academic Press, pp. 25–53.

Southall, M. D. and M. R. Vasko (2001). “Prostaglandin Receptor Subtypes, EP3C and EP4, Mediate the Prostaglandin E2-induced cAMP Production and Sensitization of Sensory Neurons”. In: *Journal of Biological Chemistry* 276.19, pp. 16083–16091. ISSN: 00219258. DOI: 10.1074/jbc.M011408200.

Souza, Guilherme R. et al. (2013). “Fractalkine mediates inflammatory pain through activation of satellite glial cells”. In: *Proceedings of the National Academy of Sciences of the United States of America* 110.27, pp. 11193–11198. ISSN: 00278424. DOI: 10.1073/pnas.1307445110.

Staedtler, Ellen S. et al. (2024). “The μ-opioid receptor differentiates two distinct human nociceptive populations relevant to clinical pain”. In: *Cell reports. Medicine* 5.10, p. 101788. ISSN: 26663791. DOI: 10.1016/j.xcrm.2024.101788.

Staud, Roland (2013). *The important role of CNS facilitation and inhibition for chronic pain*. DOI: 10.2217/ijr.13.57.

Stein, Colleen S. et al. (2022). “Modulation of miR-181 influences dopaminergic neuronal degeneration in a mouse model of Parkinson’s disease”. In: *Molecular Therapy Nucleic Acids* 28, pp. 1–15. ISSN: 21622531. DOI: 10.1016/j.omtn.2022.02.007.

Stelt, Mario van der et al. (2005). “Anandamide acts as an intracellular messenger amplifying Ca2+ influx via TRPV1 channels”. In: *EMBO Journal* 24.17, pp. 3026–3037. ISSN: 14602075. DOI: 10.1038/sj.emboj.7600784.

Stucky, C L et al. (1996). “Prostaglandin E2 Increases the Proportion of Neonatal Rat Dorsal Root Ganglion Neurons That Respond to Bradykinin”. In: *Neuroscience* 74.4, pp. 1111–1123. DOI: 10.1016/0306-4522(96)00264-3.

Su, Yeu Shiuan et al. (2016). “Serotonin Receptor 2B Mediates Mechanical Hyperalgesia by Regulating Transient Receptor Potential Vanilloid 1”. In: *Journal of Molecular Neuroscience* 59.1, pp. 113–125. ISSN: 15591166. DOI: 10.1007/s12031-015-0693-4.

Subbiahanadar Chelladurai, Karthikeyan et al. (Aug. 2021). *Alternative to FBS in animal cell culture - An overview and future perspective*. DOI: 10.1016/j.heliyon.2021.e07686.

Suntres, Zacharias E et al. (2013). “Therapeutic Uses of Exosomes”. In: *Journal of Circulating Biomarkers* 1. DOI: 10.5772/56522.

Sutter, Pearl A. et al. (2024). “Emerging Role of Astrocyte-Derived Extracellular Vesicles as Active Participants in CNS Neuroimmune Responses”. In: *Immunological Investigations* 53.1, pp. 26–39. ISSN: 15324311. DOI: 10.1080/08820139.2023.2281621.

Taiwo, Y 0 and J D Levine (1990). *Direct Cutaneous Hyperalgesia Induced by Adenosine*. Tech. rep. 3, pp. 757–762.

Talebi, Farideh et al. (2017). “MicroRNA-142 regulates inflammation and T cell differentiation in an animal model of multiple sclerosis”. In: *Journal of Neuroinflammation* 14.1. ISSN: 17422094. DOI: 10.1186/s12974-017-0832-7.

Tamashiro, Tami T., Clifton Lee Dalgard, and Kimberly R. Byrnes (2012). “Primary microglia isolation from mixed glial cell cultures of neonatal rat brain tissue”. In: *Journal of Visualized Experiments*. ISSN: 1940087X. DOI: 10.3791/3814.

Tan, Chan Lek et al. (2013). “MicroRNA-128 governs neuronal excitability and motor behavior in mice”. In: *Science* 342.6163, pp. 1254–1258. ISSN: 10959203. DOI: 10.1126/science.1244193.

Tanabe, Katsuhisa et al. (2003). “Fibroblast Growth Factor-Inducible-14 Is Induced in Axotomized Neurons and Promotes Neurite Outgrowth”. In: *The Journal of Neuroscience* 23.29, pp. 9675–9686. DOI: 10.1523/JNEUROSCI.23-29-09675.2003.

Tang, Qian jie et al. (2019). “Plasma miR-142 predicts major adverse cardiovascular events as an intermediate biomarker of dual antiplatelet therapy”. In: *Acta Pharmacologica Sinica* 40.2, pp. 208–215. ISSN: 17457254. DOI: 10.1038/s41401-018-0041-7.

Tao, Zhen et al. (2015). “Neuroprotective effect of microRNA-99a against focal cerebral ischemia-reperfusion injury in mice”. In: *Journal of the Neurological Sciences* 355.1-2, pp. 113–119. ISSN: 18785883. DOI: 10.1016/j.jns.2015.05.036.

Teng, Fei and Martin Fussenegger (2021). “Shedding Light on Extracellular Vesicle Biogenesis and Bioengineering”. In: *Advanced Science* 8.1. ISSN: 21983844. DOI: 10.1002/advs.202003505.

Thermo Fisher Scientific (2011). *Fluo Calcium Indicators*. Tech. rep.

Thomas, D. et al. (2000). “A comparison of fluorescent Ca2+ indicator properties and their use in measuring elementary and global Ca2+ signals”. In: *Cell Calcium* 28.4, pp. 213–223. ISSN: 01434160. DOI: 10.1054/ceca.2000.0152.

Tominaga, Makoto et al. (1998). “The Cloned Capsaicin Receptor Integrates Multiple Pain-Producing Stimuli”. In: *Neuron* 21, pp. 531–543. DOI: 10.1016/s0896-6273(00)80564-4.

Treede, Rolf Detlef et al. (2015). *A classification of chronic pain for ICD-11*. DOI: 10.1097/j.pain.0000000000000160.

Tsantoulas, Christoforos et al. (2013). “Probing functional properties of nociceptive axons using a microfluidic culture system”. In: *PLoS ONE* 8.11. ISSN: 19326203. DOI: 10.1371/journal.pone.0080722.

Tsuge, Kyoshiro et al. (2019). *Molecular mechanisms underlying prostaglandin E2-exacerbated inflammation and immune diseases*. DOI: 10.1093/intimm/dxz021.

Tushev, Georgi et al. (2018). “Alternative 3 UTRs Modify the Localization, Regulatory Potential, Stability, and Plasticity of mRNAs in Neuronal Compartments”. In: *Neuron* 98.3, pp. 495–511. ISSN: 10974199. DOI: 10.1016/j.neuron.2018.03.030.

Unsain, Nicolas et al. (2014). “Production and Isolation of Axons from Sensory Neurons for Biochemical Analysis Using Porous Filters”. In: *Journal of Visualized Experiments* 89, e51795. ISSN: 1940-087X. DOI: 10.3791/51795.

Usachev, Yuriy M. and Stanley A. Thayer (1999). “Ca2+ influx in resting rat sensory neurones that regulates and is regulated by ryanodine-sensitive Ca2+ stores”. In: *Journal of Physiology* 519.1, pp. 115–130.

Vane, John R et al. (1994). “Inducible isoforms of cyclooxygenase and nitric-oxide synthase in inflammation”. In: *Proc. Nad. Acad. Sci. USA* 91, pp. 2046–2050.

Varcianna, André et al. (2019). “Micro-RNAs secreted through astrocyte-derived extracellular vesicles cause neuronal network degeneration in C9orf72 ALS”. In: *EBioMedicine* 40, pp. 626–635. ISSN: 23523964. DOI: 10.1016/j.ebiom.2018.11.067.

Vasko, M R, W B Campbell, and K J Waite (1994). *Prostaglandin E2 Enhances Bradykinin-stimulated Release of Neuropeptides from Rat Sensory Neurons in Culture*. Tech. rep., pp. 4987–4997.

Vogel, Christine and Edward M. Marcotte (2012). “Insights into the regulation of protein abundance from proteomic and transcriptomic analyses”. In: *Nature Reviews Genetics* 13.4, pp. 227–232. ISSN: 14710056. DOI: 10.1038/nrg3185.

Walters, Edgar T. and Amanda C. De C. Williams (2019). “Evolution of mechanisms and behaviour important for pain”. In: *Philosophical Transactions of the Royal Society B: Biological Sciences* 374.1785. ISSN: 14712970. DOI: 10.1098/rstb.2019.0275.

Wang, Congying, Guang Wen Li, and Li Yen Mae Huang (2007). “Prostaglandin E2 potentiation of P2X3 receptor mediated currents in dorsal root ganglion neurons”. In: *Molecular Pain* 3. ISSN: 17448069. DOI: 10.1186/1744-8069-3-22.

Wang, Kaikai et al. (2021). “Single-cell transcriptomic analysis of somatosensory neurons uncovers temporal development of neuropathic pain”. In: *Cell Research* 31.8, pp. 904–918. ISSN: 17487838. DOI: 10.1038/s41422-021-00479-9.

Wang, Zheyin et al. (2020). “Baicalin prevents the up-regulation of TRPV1 in dorsal root ganglion and attenuates chronic neuropathic pain”. In: *Veterinary Medicine and Science* 6.4, pp. 1034–1040. ISSN: 20531095. DOI: 10.1002/vms3.318.

Wangzhou, Andi et al. (2020). “Pharmacological target-focused transcriptomic analysis of native vs cultured human and mouse dorsal root ganglia”. In: *Pain* 161.7, pp. 1497–1517. ISSN: 18726623. DOI: 10.1097/j.pain.0000000000001866.

Warwick, R. A. and M. Hanani (2013). “The contribution of satellite glial cells to chemotherapy-induced neuropathic pain”. In: *European Journal of Pain (United Kingdom)* 17.4, pp. 571–580. ISSN: 10903801. DOI: 10.1002/j.1532-2149.2012.00219.x.

Webb, Carly M and Charlotte E Steeds (2022). “The anatomy and physiology of pain”. In: *Clinics in Integrated Care* 14, p. 100115. DOI: 10.1016/j.intcar.2022.100115.

Wei, Dongyu et al. (2024). “PGE2 potentiates Orai1-mediated calcium entry contributing to peripheral sensitization.” In: *Journal of Neuroscience* 44.1. ISSN: 15292401. DOI: 10.1523/JNEUROSCI.0329-23.2023.

Welsh, Joshua A. et al. (2024). “Minimal information for studies of extracellular vesicles (MISEV2023): From basic to advanced approaches”. In: *Journal of Extracellular Vesicles* 13.2. ISSN: 20013078. DOI: 10.1002/jev2.12404.

White, Katherine E. et al. (2024). “A convenient model of serum-induced reactivity of human astrocytes to investigate astrocyte-derived extracellular vesicles”. In: *Frontiers in Cellular Neuroscience* 18. ISSN: 16625102. DOI: 10.3389/fncel.2024.1414142.

Willis, Dianna E and Jeffery L Twiss (2011). “Profiling Axonal mRNA Transport”. In: *Methods in Molecular Biology* 714, pp. 335–352. ISSN: 19406029. DOI: 10.1007/978-1-61779-005-8{_}21.

Willis, William D. (2009). *The role of TRPV1 receptors in pain evoked by noxious thermal and chemical stimuli*. DOI: 10.1007/s00221-009-1760-2.

Winkles, Jeffrey A. (2008). *The TWEAK-Fn14 cytokine-receptor axis: Discovery, biology and therapeutic targeting*. DOI: 10.1038/nrd2488.

Woodhams, Peter L. et al. (2007). “Localisation and modulation of prostanoid receptors EP1 and EP4 in the rat chronic constriction injury model of neuropathic pain”. In: *European Journal of Pain* 11.6, pp. 605–613. ISSN: 10903801. DOI: 10.1016/j.ejpain.2006.09.005.

Woolf, Clifford J. and Qiufu Ma (2007). “Nociceptors-Noxious Stimulus Detectors”. In: *Neuron* 55.3, pp. 353–364. ISSN: 08966273. DOI: 10.1016/j.neuron.2007.07.016.

Wright, Kristeena Ray, Brenda Mitchell, and Nalini Santanam (2017). “Redox regulation of microRNAs in endometriosis-associated pain”. In: *Redox Biology* 12, pp. 956–966. ISSN: 22132317. DOI: 10.1016/j.redox.2017.04.037.

Wu, Guangyong, D. W. McBride, and John H. Zhang (2018). “Axl activation attenuates neuroinflammation by inhibiting the TLR/TRAF/NF-κB pathway after MCAO in rats”. In: *Neurobiology of Disease* 110, pp. 59–67. ISSN: 1095953X. DOI: 10.1016/j.nbd.2017.11.009.

Wu, Wei et al. (2021). “Neuronal enhancers are hotspots for DNA single-strand break repair”. In: *Nature* 593.7859, pp. 440–444. ISSN: 14764687. DOI: 10.1038/s41586-021-03468-5.

Wu, Yumei et al. (2017). “Contacts between the endoplasmic reticulum and other membranes in neurons”. In: *Proceedings of the National Academy of Sciences of the United States of America* 114.24, E4859–E4867. ISSN: 10916490. DOI: 10.1073/pnas.1701078114.

Xin, Danqing et al. (2024). “MiR-100-5p-rich small extracellular vesicles from activated neuron to aggravate microglial activation and neuronal activity after stroke”. In: *Journal of Nanobiotechnology* 22.1. ISSN: 14773155. DOI: 10.1186/s12951-024-02782-0.

Xing, Yinghao et al. (2024). “Dorsal root ganglion-derived exosomes deteriorate neuropathic pain by activating microglia via the microRNA-16-5p/HECTD1/HSP90 axis”. In: *Biological Research* 57.1. ISSN: 07176287. DOI: 10.1186/s40659-024-00513-1.

Xu, Han peng, Lin Gou, and Hong Wei Dong (2010). “Study glial cell heterogeneity influence on axon growth using a new coculture method”. In: *Journal of Visualized Experiments* 43. ISSN: 1940087X. DOI: 10.3791/2111.

Xu, Peng et al. (2020). “A Systematic Way to Infer the Regulation Relations of miRNAs on Target Genes and Critical miRNAs in Cancers”. In: *Frontiers in Genetics* 11. ISSN: 16648021. DOI: 10.3389/fgene.2020.00278.

Xu, Qiu, Gai Fan, and Su Shao (2025). “Role of TNFRSF12A in cell proliferation, apoptosis, and proinflammatory cytokine expression by regulating the MAPK and NF-κB pathways in thyroid cancer cells”. In: *Cytokine* 186, p. 156841. ISSN: 10960023. DOI: 10.1016/j.cyto.2024.156841.

Xuan, Fang Ling et al. (2019). “Differences of Microglia in the Brain and the Spinal Cord”. In: *Frontiers in Cellular Neuroscience* 13. ISSN: 16625102. DOI: 10.3389/fncel.2019.00504.

Yam, Mun Fei et al. (2018). “General pathways of pain sensation and the major neurotransmitters involved in pain regulation”. In: *International Journal of Molecular Sciences* 19.8. ISSN: 14220067. DOI: 10.3390/ijms19082164.

Yan, Lan et al. (2019). *The role of microRNA-16 in the pathogenesis of autoimmune diseases: A comprehensive review*. DOI: 10.1016/j.biopha.2019.01.044.

Yao, Chengcan and Shuh Narumiya (2019). “Prostaglandin-cytokine crosstalk in chronic inflammation”. In: *British Journal of Pharmacology* 176.3, pp. 337–354. ISSN: 14765381. DOI: 10.1111/bph.14530.

Yi, Sheng et al. (2017). “MiR-30c promotes Schwann cell remyelination following peripheral nerve injury”. In: *Neural Regeneration Research* 12.10, pp. 1708–1714. ISSN: 18767958. DOI: 10.4103/1673-5374.217351.

Yin, Kathleen, Gregory J. Baillie, and Irina Vetter (2016). “Neuronal cell lines as model dorsal root ganglion neurons: A transcriptomic comparison”. In: *Molecular Pain* 12. ISSN: 17448069. DOI: 10.1177/1744806916646111.

Yin, Zhenyu et al. (2020). “Neuron-derived exosomes with high miR-21-5p expression promoted polarization of M1 microglia in culture”. In: *Brain, Behavior, and Immunity* 83, pp. 270–282. ISSN: 10902139. DOI: 10.1016/j.bbi.2019.11.004.

You, Changhui et al. (2025). “LncRNA 4933431K23Rik modulate microglial phenotype via inhibiting miR-10a-5p in spinal cord injury induced neuropathic pain”. In: *Scientific Reports* 15.1. ISSN: 20452322. DOI: 10.1038/s41598-025-91021-z.

Yuan, Zhu Lin et al. (2022). “Activation of GDNF-ERK-Runx1 signaling contributes to P2X3R gene transcription and bone cancer pain”. In: *iScience* 25.9. ISSN: 25890042. DOI: 10.1016/j.isci.2022.104936.

Zeisel, Amit et al. (2018). “Molecular Architecture of the Mouse Nervous System”. In: *Cell* 174.4, pp. 999–1014. ISSN: 10974172. DOI: 10.1016/j.cell.2018.06.021.

Zhan, Yang et al. (2014). “Deficient neuron-microglia signaling results in impaired functional brain connectivity and social behavior”. In: *Nature Neuroscience* 17.3, pp. 400–406. ISSN: 10976256. DOI: 10.1038/nn.3641.

Zhan-qiang, H. et al. (2023). “miR-146a aggravates cognitive impairment and Alzheimer disease-like pathology by triggering oxidative stress through MAPK signaling”. In: *Neurologia* 38.7, pp. 486–494. ISSN: 15781968. DOI: 10.1016/j.nrl.2020.12.006.

Zhang, Bing Yu et al. (2020). “Alpha-lipoic acid downregulates TRPV1 receptor via NF-κB and attenuates neuropathic pain in rats with diabetes”. In: *CNS Neuroscience and Therapeutics* 26.7, pp. 762–772. ISSN: 17555949. DOI: 10.1111/cns.13303.

Zhang, Li et al. (2021a). “MiR-30c-5p/ATG5 Axis Regulates the Progression of Parkinson’s Disease”. In: *Frontiers in Cellular Neuroscience* 15. ISSN: 16625102. DOI: 10.3389/fncel.2021.644507.

Zhang, Rui et al. (2022). “A Potential Target for Diabetic Vascular Damage: High Glucose-Induced Monocyte Extracellular Vesicles Impair Endothelial Cells by Delivering miR-142-5p”. In: *Frontiers in Bioengineering and Biotechnology* 10. ISSN: 22964185. DOI: 10.3389/fbioe.2022.913791.

Zhang, Xiaoyu et al. (2023). *Advances in the role and mechanism of miRNA in inflammatory pain*. DOI: 10.1016/j.biopha.2023.114463.

Zhang, Yamei et al. (2021b). “Extracellular vesicle-encapsulated microRNA-23a from dorsal root ganglia neurons binds to A20 and promotes inflammatory macrophage polarization following peripheral nerve injury”. In: 13.5, pp. 6752–6764. DOI: 10.18632/aging.202532.

Zhang, Yongliang et al. (2015). “MAPK Phosphatase 7 Regulates T Cell Differentiation via Inhibiting ERK-Mediated IL-2 Expression”. In: *The Journal of Immunology* 194.7, pp. 3088–3095. ISSN: 0022-1767. DOI: 10.4049/jimmunol.1402638.

Zhao, Liping et al. (2023). “Satellite glial cell-secreted exosomes after in-vitro oxaliplatin treatment presents a pro-nociceptive effect for dorsal root ganglion neurons and induce mechanical hypersensitivity in naïve mice”. In: *Molecular and Cellular Neuroscience* 126. ISSN: 10959327. DOI: 10.1016/j.mcn.2023.103881.

Zhao, Qian-Cheng et al. (2024). “Enhancement of miR-16-5p on spinal cord injury-induced neuron apoptosis and inflammatory response through inactivating ERK1/2 pathway”. In: *Journal of Neurosurgical Sciences* 68.1. ISSN: 03905616. DOI: 10.23736/S0390-5616.20.04880-8.

Zheng, Timothy S. and Linda C. Burkly (2008). “No end in site: TWEAK/Fn14 activation and autoimmunity associated- end-organ pathologies”. In: *Journal of Leukocyte Biology* 84.2, pp. 338–347. ISSN: 0741-5400. DOI: 10.1189/jlb.0308165.

Zhou, Yi Mei et al. (2019). “Enhancement of acid-sensing ion channel activity by prostaglandin E2 in rat dorsal root ganglion neurons”. In: *Brain Research* 1724. ISSN: 18726240. DOI: 10.1016/j.brainres.2019.146442.

Zhu, Zhenghuan et al. (2025). “The role of astrocyte-derived extracellular vesicles in cellular microenvironment remodeling after spinal cord injury: A study based on quantitative proteomics

analysis". In: *Experimental Neurology* 391. ISSN: 10902430. DOI: 10.1016/j.expneurol.2025.115321.

Zimmer, Zachary et al. (2022). "A global study of pain prevalence across 52 countries: Examining the role of country-level contextual factors". In: *Pain* 163.9, pp. 1740–1750. ISSN: 18726623. DOI: 10.1097/j.pain.0000000000002557.